THE CATALYTIC REDUCTION OF NITRIC OXIDE OVER COPPER DOPED ALUMINOSILICATES

By

Gerard Hwang

Submitted to the University of Cape Town

in fulfilment of the requirements for the degree of

MASTER OF SCIENCE

Department of Chemical Engineering
University of Cape Town
Rondebosch
Cape Town
Republic of South Africa

February 1993

ACKNOWLEDGEMENTS

To my supervisor, Doctor James Petrie who devoutly believes that possession is nine tenths of the law: Jim, thanks for helping me to learn.

I would like to thank the staff, research assistants and fellow postgraduate students at the Department of Chemical Engineering who have all readily offered advice and assistance, in particular, Dr Jack Fletcher, Dr Klaus Möller, Leslie, "Tigs" and Andrew.

Mr Chris Wozniak of the Energy Research Institute was more than generous in assistance and his help is very much appreciated.

Most of all, my thanks to my family.

"Though this be madness, yet there is method in't."
Polonius

(Hamlet, Prince of Denmark - Act II, Scene II)

SYNOPSIS

With the object of greater energy efficiency, a role has been identified for a facility capable of the simultaneous removal of NOx, SO_2 and particulates from flue gas at high temperature. This project forms the initial phase of the development of such a high temperature flue gas cleaning facility and is limited to the study of catalytic NOx reduction over aluminosilicates.

A copper ion-exchanged zeolite (Cu-ZSM-5) and copper oxide were studied as catalysts for the Selective Catalytic Reduction (SCR) of nitric oxide in the temperature range 250-530°C. Ammonia was employed as the reducing agent. The intention of this investigation was to work towards an examination of the potential for obtaining an active SCR catalyst by doping amorphous aluminosilicate fibres (which are used as high temperature particulate filters), with copper.

The direct decomposition of nitric oxide over Cu-ZSM-5 was investigated in order to validate the experimental rig and procedures by duplicating published results. An activation energy of 29 kcal/mol was determined and a reaction order with respect to nitric oxide of 1.2 was obtained at 500°C. Both values compare well with published data.

Cu-ZSM-5, CuO supported on silicalite and CuO physically blended with the fibrous aluminosilicate were investigated as SCR catalysts. It was found that:

The rate of the SCR reaction was three orders of magnitude higher than the rate of the direct decomposition reaction over Cu-ZSM-5.

CuO supported on silicalite yielded higher reaction rates than unsupported CuO and the rates of the former approached those for the reaction over Cu-ZSM-5.

An activation energy of 14 kcal/mol was obtained for the SCR reaction over Cu-ZSM-5 and a value of 9 kcal/mol was obtained for reaction over CuO (supported and unsupported).

The ability of supported CuO to catalyse the SCR reaction at a rate comparable to that found with Cu-ZSM-5 suggests that the use of CuO should be investigated further, both in its own right as a NOx reducing catalyst since little has been published in this regard, and as a simultaneous NOx/SO_2 removal sorbent/catalyst.

The intrinsic catalytic activity of copper oxide and the success with which it has been dispersed/supported on the porous silicalite structure, suggests that a suitably active SCR catalyst form may be obtained if a high dispersion of copper oxide may be achieved on the non-porous aluminosilicate fibres.

TABLE OF CONTENTS

LIST OF FIGURES

LIST OF TABLES

1. INTRODUCTION

Nitric oxide and nitrogen dioxide (together known as "NOx") produced during the combustion of fossil fuels are toxic and are environmental pollutants. NOx is a precursor to acid rain, contributes to photochemical smog and as an environmental pollutant, it is considered amongst the most severe forms alongside sulphur oxides (SOx), carbon monoxide and particulate emissions.

Initial concern with acid rain was primarily directed solely at SO_2 emissions with the result that these emissions have been reduced while NOx emissions continue to increase, particularly from motor vehicles. These trends are shown in Figure 1.1 which emphasizes the need to implement NOx control (Boer *et al.*, 1990).

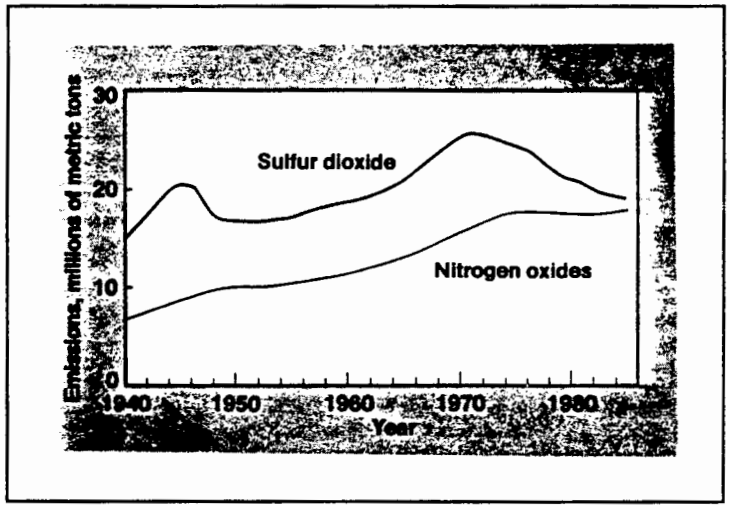

***Figure 1.1** Emissions of acid rain precursors (Boer et al.*, 1990)

This introductory chapter discusses the sources of NOx, NOx treatment techniques, the most effective NOx reduction method, process considerations and presents justification for the experimental programme to be carried out.

1.1. SOURCES OF NOx

The two main sources of NOx in the lower atmosphere are the combustion of fossil fuels and the burning of biomass as shown in Table 1.1. Other notable sources are: nitrogen fixation by lightning and volcanic activity, the oxidation of tropospheric ammonia, the influx of NO from the stratosphere and ammonia oxidation from the decomposition of proteins (Bosch and Janssen, 1988).

Table 1.1 Sources of global NOx (Bosch and Janssen, 1988)

SOURCE	*CONTRIBUTION(%)*
Combustion of fossil fuels	*28.5 - 44*
Biomass burning	*40 - 57*
Lightning	*8 - 8.5*
Stratosphere	*3 - 4.5*
Ammonia oxidation	*1.5 - 5*

Table 1.2 Sources of man-made NOx emissions in the U.S., 1985. (Boer et al., 1990).

SOURCE	*CONTRIBUTION(%)*
Utilities	*33*
Highway vehicles	*33*
Other transport (air/rail/water/off-road)	*10*
Industrial	*20*
Other	*4*

Industrial and domestic burning of fossil fuels including that for transportation are the most significant sources of man-made NOx and Table 1.2 gives estimates of various sources in the USA at 1985. A third was produced by cars, another third through power generation and a significant fraction produced by industrial processes.

1.2. NOx EMISSIONS IN SOUTH AFRICA AND EMISSION STANDARDS

Table 1.3 gives an indication of the scale of NOx produced in the eastern Transvaal, which is a high density industrial region characterized by coal combustion, synthetic fuel production and metallurgical processes.

The largest contributor of NOx is the electricity supply authority, Eskom, which has 10 power stations in this region. Els (1987) estimated NOx emissions from power stations contributed over 90% to the total NOx produced in the eastern Transvaal.

It is interesting to note that in South Africa, SO_2 emissions are nearly three times those of NOx, in contrast with the trend displayed in Figure 1.1 for the USA, indicating the present lack of SO_2 control in this country. The extent of NOx emissions from local sources other than power generation has not been quantified.

Table 1.3 Atmospheric pollutants in the eastern Transvaal Highveld at 1987 (Tyson et al., 1988)

POLLUTANT	*TONS/YEAR*
Particulates	*374 692*
Sulphur dioxide	*1 038 556*
Nitrogen oxides	*355 246*
Carbon monoxide	*399 574*
Hydrocarbons	*276 503*
Carbon dioxide	*123 605 162*

The United States of America, Germany, Japan and Sweden are among the few countries which have legislated limiting values of NOx emissions (Bosch and Janssen, 1988).

South Africa has no absolute statutory limits. However, each industrial activity is licensed under the Pollution Act of 1956 to ensure a given performance level. When comparing current NOx emission levels from an Eskom power plant with international emission targets (Table 1.4), it is clear that South Africa lags behind in NOx control.

German standards for NOx emissions from coal fired power plants, are as low as 100 ppm in the stack or 0.16 lbs per million Btu of generated electrical power. This is twice as stringent as Japanese standards and about 4 times more stringent than USA standards at 1990 (Boer *et al.*, 1990).

***Table 1.4** Comparison of emissions targets for new power plant and current Eskom emission levels (Petrie et al., 1992)*

	NOx (mg Nm^{-3})
Australia	*500*
Germany	*200*
Japan	*411*
UK	*best practicable means*
USA	*475-620*
Eskom (existing emissions)	*600-700*

The annual mean ambient NOx concentration in the eastern Transvaal is of the order of 34 $\mu g.m^{-3}$ (Turner, 1990). In comparison, annual average rural European NOx levels between 10-40 $\mu g.m^{-3}$ have been measured and urban and industrial ambient levels have reached 200 $\mu g.m^{-3}$ (Wellburn, 1985).

1.3. TYPES OF NOx

NOx produced in the combustion process can be considered as being of three types: thermal NOx, fuel NOx and prompt NOx.

1) Thermal NOx is produced by the fixation of atmospheric nitrogen at high temperatures (of the order of 1300°C) with the following two reactions occurring under oxygen rich conditions (Zeldovich, 1946):

$$\begin{aligned} O + N_2 &\rightleftharpoons NO + N \\ N + O_2 &\rightleftharpoons NO + O \end{aligned} \qquad (1.1)$$

As cited by Bosch and Janssen, Glick *et al.* (1957) determined an exponential rate dependence on temperature for the formation of NO from these two reactions.

2) Fuel NOx is produced by the oxidation of nitrogen containing compounds in the fuel. In their review, Bosch and Janssen (1988) noted the Fenimore Mechanism (Fenimore, 1972)

which describes the attack of organic nitrogen containing compounds by OH^- radicals in a scheme proposed as:

$$\text{N-complex} + OH^- \rightleftharpoons NO + \text{other products} \qquad (1.2)$$

3) Prompt NOx results from the oxidation of HCN to NO. The HCN is formed in the reaction of nitrogen radicals and hydrocarbons. The production of prompt NOx is said to be significant only in very fuel-rich flames (Fenimore, 1971).

Figure 1.2 taken from Bosch and Janssen (1988) shows the extent of the three modes of NOx formation as a function of temperature in a coal fired furnace, and shows the strong dependence of the formation of thermal NOx on temperature.

NOx produced by spark ignition engines is entirely Thermal NOx since gasoline contains essentially no chemically bound nitrogen (Lyon and Hardy, 1986). Fuel NOx however, contributes the largest NOx fraction in coal and oil fired furnaces (Figure 1.2) which typically operate at around 1300°C.

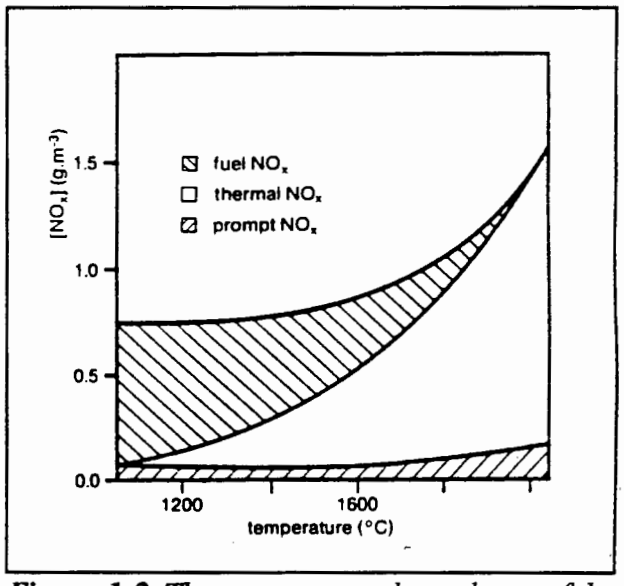

***Figure 1.2** The temperature dependence of the three sources of NOx from a coal fired furnace (Sigal, 1983)*

1.4. THE EFFECTS OF NOx

The role of NO_2 in initiating the formation of photochemical smog (also known as "brown haze") is described by the reaction:

$$NO_2 + h\nu \rightarrow NO + O \qquad (1.3)$$

where nitrogen dioxide produces nitric oxide and monatomic oxygen with the aid of light of wavelength 392 nm (Masterton and Slowinski, 1977).

The reactive oxygen atoms then react with oxygen molecules to produce ozone according to the scheme:

$$O + O_2 \rightarrow O_3 \qquad (1.4)$$

Ozone is a major component of photochemical smog. The oxygen atom and ozone react with olefins, yielding a variety of products such as alcohols, ketones and aldehydes eg. formaldehyde

and acrolein. Unsaturated hydrocarbons also react directly with either NO or NO_2 to produce compounds such as methyl nitrate and peroxyacetyl nitrate (PAN). Both are principal constituents of photochemical smog and are eye irritants (Masterton and Slowinski, 1977).

Ozone also reacts with NO to produce NO_2 by the reaction

$$NO + O_3 \rightharpoonup NO_2 + O_2 \qquad (1.5)$$

which perpetuates the "smog reaction cycle" initiated by reaction (1.3) (Sienko and Plane, 1979).

Acid rain is produced from nitrous and nitric acid formed in the reaction of NOx with photochemically generated radicals (Bosch and Janssen, 1988):

$$\begin{aligned} NO + OH^- &\rightharpoonup HNO_2 \\ NO_2 + OH^- &\rightharpoonup HNO_3 \end{aligned} \qquad (1.6)$$

Normal rainfall has a pH of 5.6 as a result of carbon dioxide in the atmosphere. In a local context, sulphur and nitrogen oxide emissions in the eastern Transvaal has produced rainfall with direct pH measurements in the range 3.9 to 4.6 (Bosman, 1990). Acidic deposition is quantified more reliably by considering the contribution of both wet and dry deposition to groundwater acidity which has been measured at pH values less than 3.5 (Bosman, 1987).

Inhalation of large amounts of NOx has oxygen deprivation effects similar to those caused by carbon monoxide - NO attaches to haemoglobin. The USA air quality standard is 0.240 $mg.m^{-3}$ (117 ppb) and concentrations of 0.3 $mg.m^{-3}$ (146 ppb) are considered highly dangerous, leading to permanent health damage (Bosch and Janssen, 1988). In comparison to the magnitude of the concentrations tolerable to humans, point source emissions from operations such as Eskom's coal fired furnaces emit stack gas with NOx concentrations of 600-700 mg. Nm^{-3} (Table 1.4). At the same time, it should be noted that the annual mean ambient concentration in the Eastern Transvaal is of the order of 0.034 mg Nm^{-3} (refer to section 1.2).

As a matter of interest, humans have a threshold of 0.12 ppm for the detection of the chlorine-like odour of NO_2.

1.5. NOx CONTROL TECHNIQUES

The three modes of NOx formation *viz*, thermal, fuel and prompt NOx suggest, of themselves, methods of reducing NOx formation in each instance. Thermal NOx may be controlled by reducing peak combustion temperature, fuel NOx is reduced by eliminating as far as possible,

nitrogen containing species in the fuel and prompt NOx may be inhibited by avoiding fuel rich conditions.

A scheme of various de-NOx techniques is shown in Figure 1.3. A distinction is made between combustion modification which is aimed at limiting the amount of NOx produced during combustion and flue gas treatment, subsequent to NOx formation. Thus, combustion control is considered to be a primary method and post-combustion control (flue gas treatment), a secondary method of NOx removal.

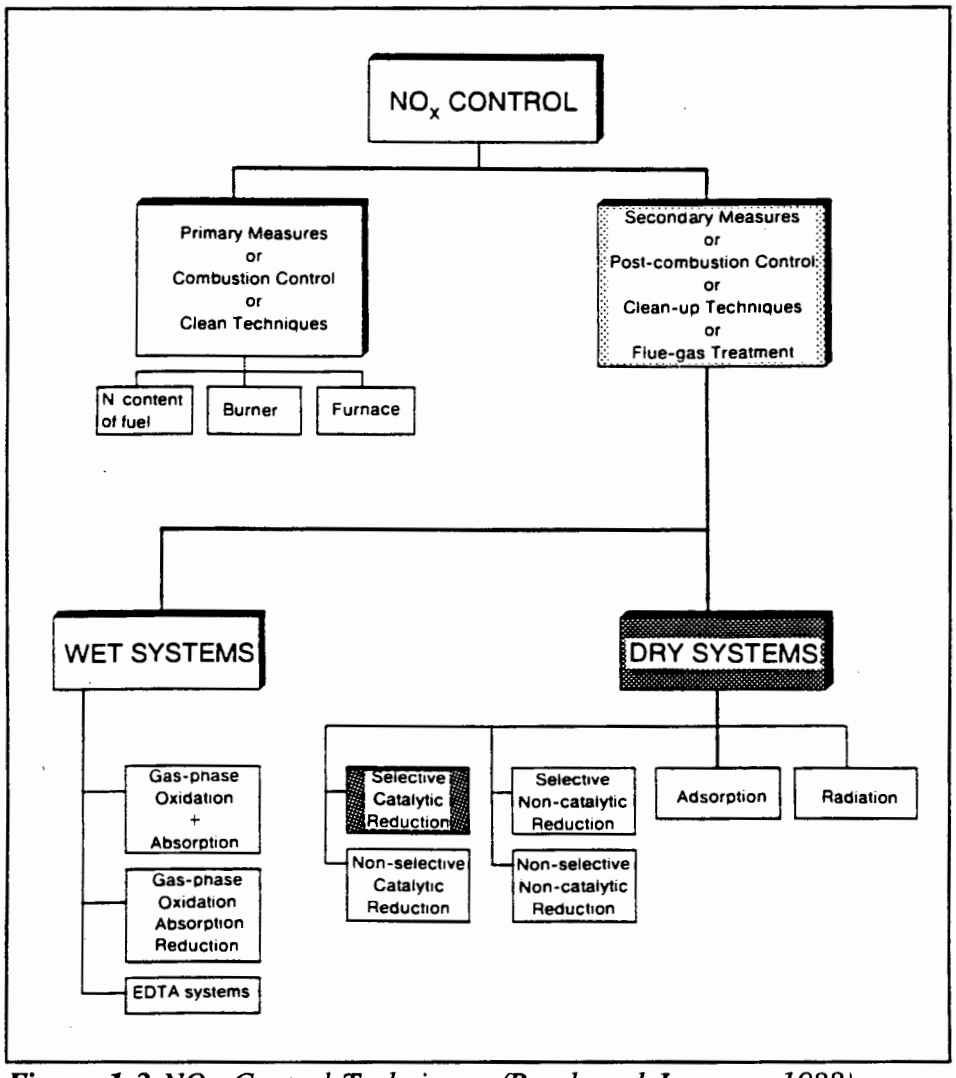

***Figure 1.3** NOx Control Techniques (Bosch and Janssen, 1988)*

Although NOx from spark ignition engines is Thermal NOx, a lower combustion temperature is not easily achieved if satisfactory operation is to be maintained and emission of other pollutants is to be controlled. However, Thermal NOx from stationary sources may be controlled by combustion modification techniques which are described below. Notwithstanding a reduction in thermal NOx formation, the effectiveness of combustion modification for the control of fuel

NOx is limited (Lyon and Hardy, 1986). Hence, post combustion facilities are required to treat these emissions.

1.5.1. PRIMARY MEASURES

Combustion control is implemented by modifying furnace operating conditions or the combustion hardware and is essentially aimed at controlling Thermal NOx formation. The objectives of such a control strategy are to:

- decrease the amount of oxygen available at peak temperature
- reduce the maximum temperature and residence time

The various methods of implementing this strategy include:

1) Injecting water or steam to lower the temperature.

2) Flue gas recirculation (FGR) - which involves returning a portion of the flue gas to the flame in order to lower the temperature.

3) Low excess firing air - is applied to oil and gas burners. The amount of oxygen supplied to the flame is restricted. This could result in flame instability, smoke formation and the formation of CO from incomplete combustion.

4) Furnace/Burner design - Staged combustion control is applied to coal, liquid or gaseous fuels. The combustion process is separated into multiple stages with varying amounts of combustible air. Two methods are noted: over fired air (OFA) and in-furnace reduction (IFR). In reducing zones (lean in oxygen) hydrocarbon radicals from the fuel reduce NOx to nitrogen. Over fired air is then introduced above the reducing zone, completing combustion. The reducing zone can adversely affect flame stability.

   Low NOx burners operate on the same principle; air required for complete combustion is added stagewise, creating reducing zones where NOx is reduced and oxidizing zones where the remaining fuel is combusted. Staged combustion burners are suitable for all fuels including pulverized coal. Low NOx burners may effect 40-65% NOx reduction over conventional oil and gas burners (Pruce, 1981).

   These techniques may be combined eg. low NOx burners may be applied with low excess air, two stage combustion and flue gas recirculation; IFR may be combined with two stage combustion.

1.5.2. SECONDARY MEASURES

As displayed in Figure 1.3, flue gas treatment is effected either by liquid absorption (wet methods) or either of homogeneous or gas/solid catalysis (dry methods). Other dry methods are also shown.

Wet systems - Absorption

Unlike the "dry methods", scrubbing invariably entails the simultaneous removal of NOx and SOx. Although such a liquid process is inherently attractive by virtue of efficient mass transfer afforded by the extended gas/liquid interface, two drawbacks are noted in absorption processes:

1) the insolubility of NO in aqueous solutions requires oxidation to NO_2 prior to absorption.
2) the need to dispose of nitrate and nitrite by-products which pose significant problems for biological waste treatment.

Two types of wet simultaneous methods are noted: oxidation/reduction and complex absorption.

The first approach involves oxidation of NO to NO_2 with ozone or ClO_2 and subsequent scrubbing in solutions of NaOH, NH_3 or CaO (Bosch and Janssen, 1988). In the second approach, SO_2 and NOx can be removed simultaneously by absorption in an iron(II) ethylenediamine tetraacetate solution.

Wet methods have not been used in large scale applications and require further improvements (Bosch and Janssen, 1988). Unlike SCR for NOx removal, wet processes dominate flue gas desulphurization (FGD) techniques (Nakatsuji and Miyamoto, 1991).

Dry systems

The catalytic decomposition of nitric oxide to nitrogen and oxygen is an ideal route to NOx abatement. In such a process, NOx is converted in a single step, without the aid of co-reactants and produces no harmful by-products. Various metal oxides have been used to catalyse this reaction, but to date, copper ion exchanged ZSM-5 has been shown to be the most active (Iwamoto and Hamada, 1991c). Even the activity of Cu-ZSM-5 is not sufficiently high for commercial use (Iwamoto and Hamada, 1991c), with the result that the direct decomposition reaction has not found large scale application. The direct decomposition reaction is discussed in the literature review presented in Chapter 2.

A number of materials such as activated charcoal, molecular sieves, chemically treated aluminas and molecular sieves possess high adsorption capacities for SO_2. However, no suitable sorbents have been found to selectively remove NO at high temperature with sufficient loading capacities. Adsorption techniques have not been economically viable in applications such as coal combustion processes because of the large volumes of gas to be treated. Large adsorption beds are required and considerable energy must be expended to regenerate the sorbents (Paplawski and Pence, 1989).

Radiation, selective catalytic, non-selective catalytic and selective non-catalytic reduction of NOx which use reducing agents such as ammonia, have been shown to be commercially viable methods of NOx reduction and are discussed below.

1) Radiation - the electron beam process

This dry scrubber is able to remove SO_2 and NOx simultaneously. Flue gas is cooled to 70-120°C and ammonia is introduced. Bombardment of the gas mixture with electrons produces O, OH and HO_2 radicals which react with SO_2 and NO to yield sulphuric and nitric acids. Neutralization of the acids by reactions with ammonia yields NH_4NO_3 and $(NH_4)_2SO_4$ (Suzuki *et al.*, 1980; Iwamoto and Hamada, 1991c)

Up to 70% NOx and 40% SO_2 removal is achieved by this dry method (Bosch and Janssen, 1988).

This technique incurs the penalty of the cost of the energy required to generate the electron beam.

2) Non-selective catalytic reduction (NSCR)

In this technique, a reducing agent such as methane is introduced in excess of that required for combustion with the available oxygen. Nitric oxide is then reduced by the excess methane over a noble metal catalyst at approximately 450°C (Necker, 1985). Since the method is non-selective, large quantities of reducing agent are required. Another drawback is the corrosiveness of the high temperature oxygen deficient flue gas.

3) Selective non-catalytic reduction (SNCR)

In "Thermal DeNOx" (Lyon, 1975), ammonia is used to selectively reduce NO to N_2 in the presence of oxygen in a temperature window of 900-1100°C and NOx reductions from 65% up

to 90% have been reported (Lyon, 1987). Dean *et al.* (1985) modelled the process by the complex set of reactions displayed in Figure 1.4.

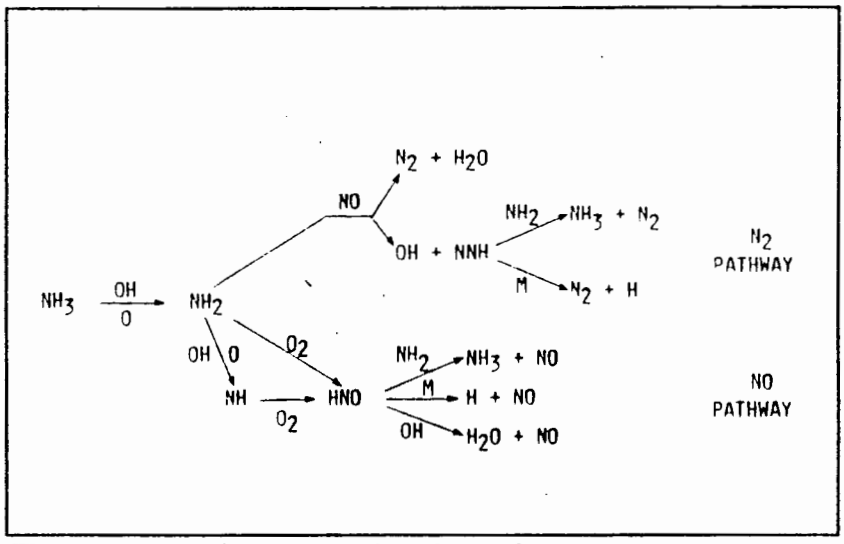

***Figure 1.1** Mechanism of the Thermal DeNOx reaction (Lyon and Hardy, 1986)*

Although Bosch and Janssen (1988) and more recently, Nakajima (1991) described this process as being unsuitable for reasons including:

- low NOx reduction levels
- the requirement for a high NH_3:NOx ratio, giving rise to salt formation, NH_3 adsorption onto flyash and ammonia slip (commercial specifications for ammonia leakage are often less than 5 ppm (Byrne *et al.*, 1992)),

evidence given by the patent holder, Richard Lyon, displays the merits of this process in specific applications and its marked cost effectiveness in comparison with catalytic reduction. For initial NOx levels of 300 and 600 ppm from a 500 MW boiler, Thermal DeNOx costs $ 0.57/lb and $ 0.41/lb NOx removed respectively while the costs for catalytic reduction were $ 2.43/lb and $ 1.54 (Lyon, 1987).

The narrow temperature windows for this process are shown in Figure 1.5. The conversion profiles show a sharp decrease in NO conversion on either side of an optimum temperature. Above the optimum temperature, the decrease was ascribed to the formation of NO from ammonia oxidation and below this, to kinetic limitations. Lyon and Hardy (1986) have shown that the optimum temperature can be adjusted by the addition of hydrogen, allowing the process to be matched to a particular application.

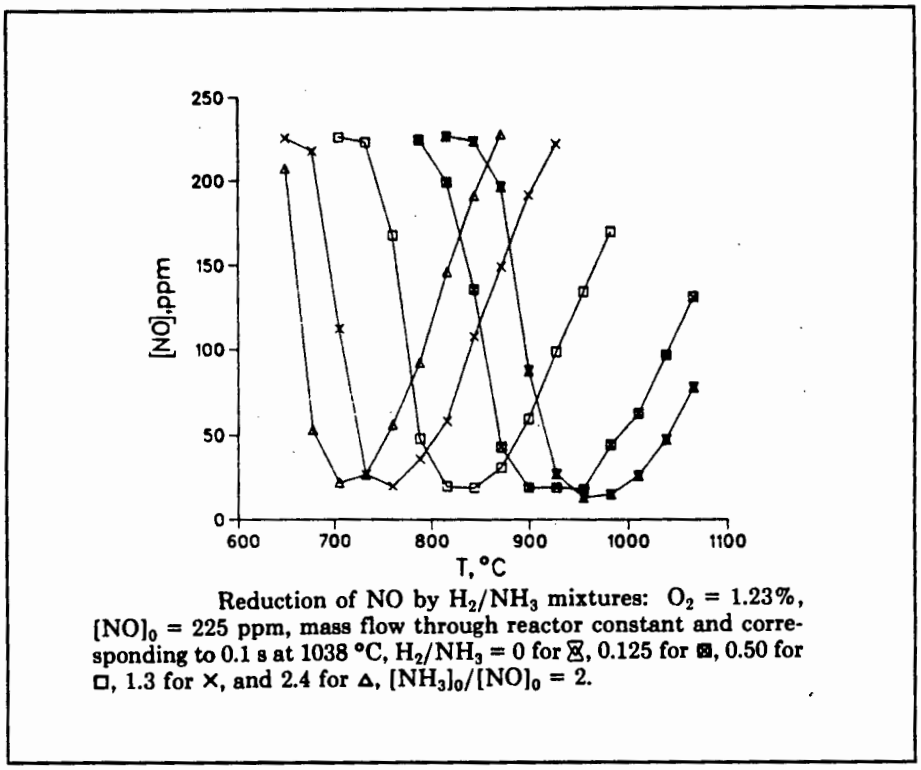

Reduction of NO by H_2/NH_3 mixtures: O_2 = 1.23%, $[NO]_0$ = 225 ppm, mass flow through reactor constant and corresponding to 0.1 s at 1038 °C, H_2/NH_3 = 0 for ⧖, 0.125 for ▣, 0.50 for □, 1.3 for ×, and 2.4 for △, $[NH_3]_0/[NO]_0$ = 2.

***Figure 1.5** Reduction of NO by Thermal DeNOx (Lyon and Hardy, 1986)*

4) Selective catalytic reduction (SCR)

This method makes use of ammonia (and other reducing agents) to reduce NOx to nitrogen and water over a solid catalyst at much lower temperatures (150-500°C) than those found in the non-catalytic Thermal DeNOx Process (Lyon, 1975). SCR is the most well developed and widely used catalytic NOx removal technique for power plant flue gas and typically yields 80-90% NOx conversion which is higher than any other commercially proven technique (Boer *et al.*, 1990). The reaction of NO with ammonia in the presence of oxygen has been described by Hirsch (1982), as:

$$4NO + 4NH_3 + O_2 \rightarrow 4N_2 + 6H_2O \qquad (1.7)$$

Reducing agents such as CO, H_2, CH_4 and other hydrocarbons have been used in place of ammonia but are less selective, reacting with oxygen in the flue gas as well as the NOx (Bosch and Janssen, 1988).

The optimum operating temperatures for SCR are determined by the relative rates of the de-NOx reaction and the ammonia oxidation reaction, similar to the temperature effect on Thermal DeNOx. The optima vary over different catalysts, yielding operating curves similar to those shown in Figure 1.6.

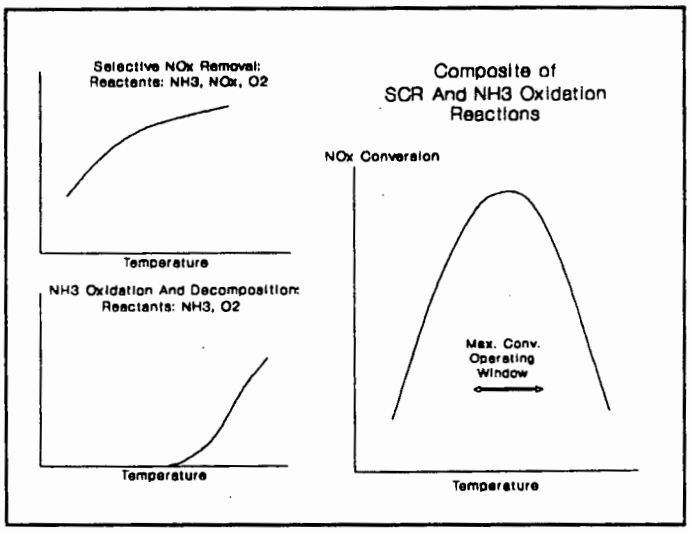

***Figure 1.6** Competing reactions in the SCR of NOx (Byrne et al., 1992)*

Traditionally, the most successful catalysts have been of two types: inorganic oxides and platinum group metals. More recently, transition metal containing zeolites have been used commercially.

The various types of catalysts and the limits of their operating temperature ranges are discussed in more detail in section 1.6 and a detailed assessment is presented in Chapter 2.

1.5.3. EVALUATION OF CONTROL TECHNIQUES

In comparing primary and secondary control techniques, combustion control is more cost effective and is also more energy efficient. The advantages of dry over wet systems are: lower capital investment, lower operating costs, greater simplicity and less generation of waste products (Bosch and Janssen, 1988).

Table 1.5 lists removal efficiencies of commercially significant de-NOx methods and shows that flue gas cleaning effects a greater degree of NOx removal than combustion control methods - the inability of combustion modification to reduce fuel NOx (refer Section 1.5) now becomes more apparent. Further, Table 1.5 shows that selective catalytic reduction (SCR) can be as effective as wet scrubbing. SCR has the principal advantage of all dry systems which have no liquid effluent penalty. Depending on the location of the facility, SCR may incur less energy penalty than wet systems since the operating temperatures (200-500°C) are far higher than those applicable to liquid absorption systems (100°C) which requires reheating of the flue gas prior to exhausting through the stack. The location of the SCR unit in relation to the combustion chamber and the stack is discussed in more detail in Section 1.6.

Table 1.5 Comparison of efficiencies of NOx removal techniques (taken from Bosch and Janssen, 1987)

	levels of NO_x reduction (%)		
	coal	oil	gas
COMBUSTION MODIFICATION			
Low excess air	5-20	5-20	5-20
Flue-gas recirculation	-	15-20	45-75
Staged combustion	-	20-40	25-45
Low-NO_x Burners	25-60	20-50	20-50
Water/steam injection	-	10-50	-
FLUE-GAS DENITRIFICATION			
dry process:			
Selective catalytic reduction	70-90	70-90	70-90
Selective non-catalytic reduction	40-60	40-70	40-70
Activated carbon	-	-	-
wet process:			
Chemical scrubbing	90	90	90

Boer *et al.* (1990) have described SCR having a NOx removal efficiency higher than any other commercially proven technology and described SCR as "the best developed and most widely used catalytic NOx removal technique for power plant stack gas." As an added attraction, this facility can be easily retrofitted. With this premise, a more detailed look at SCR technology follows in Section 1.6.

Just as various combustion modifications may be combined, it is possible to combine flue gas NOx removal units with combustion control. Figure 1.7 illustrates how low-NOx burners may be used in conjunction with two-stage combustion, in-furnace reduction and either selective non-catalytic reduction located immediately ahead of the economizer or selective catalytic reduction placed after the economizer. It is pertinent to note the temperatures at which the various techniques operate.

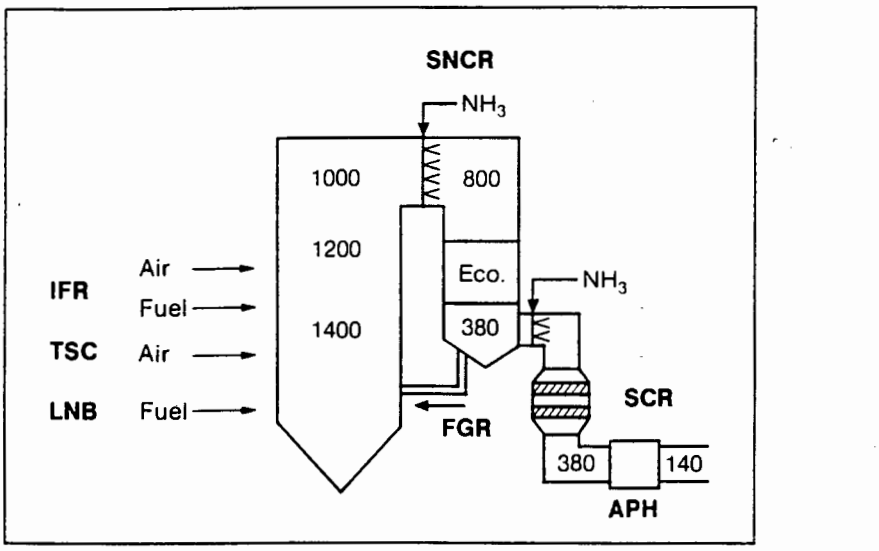

NO_x-abatement methods for utility boilers
LNB: Low-NO_x Burner; TSC: Two-Stage Combustion; IFR: In-Furnace Reduction; FGR: Flue-Gas Recirculation; SNCR: Selective Non-Catalytic Reduction; SCR: Selective Catalytic Reduction; Eco: the Economizer; and APH: Air PreHeater. The numbers indicate the temperatures of the gas in °C

***Figure 1.7** SCR combined with combustion modifications (Ando, 1985; taken from Bosch and Janssen, 1988)*

1.6. SCR PROCESS CONSIDERATIONS

1.6.1. SCR LOCATION

Figure 1.8 shows a number of possible configurations for post combustion de-NOx facilities. Selective non-catalytic reduction takes place within the combustion chamber while the remaining flue gas treatment (SCR, absorption, electron beam process) operations are placed downstream of the boiler economizer. Flue gas temperatures relevant to the unit locations are also shown.

Processes are described as being low- or high-dust applications depending on the location of the de-NOx facility with respect to a particulate removal unit. Low dust de-NOx systems are located downstream of devices such as electrostatic precipitators (ESP) or fabric filters which remove particulates from the flue gas.

Many early de-NOx installations were placed downstream of particulate traps and flue gas desulphurization (FGD) facilities (so called "clean gas" systems) to prevent abrasion and plugging of the catalyst by flyash and to prevent SO_2 poisoning and the formation of ammonium salts; an attendant problem with the reaction of ammonia with SO_2 and SO_3. Since FGD is effected mostly by wet methods (absorption) an energy penalty was incurred upon reheating the flue gas to the temperature required for SCR.

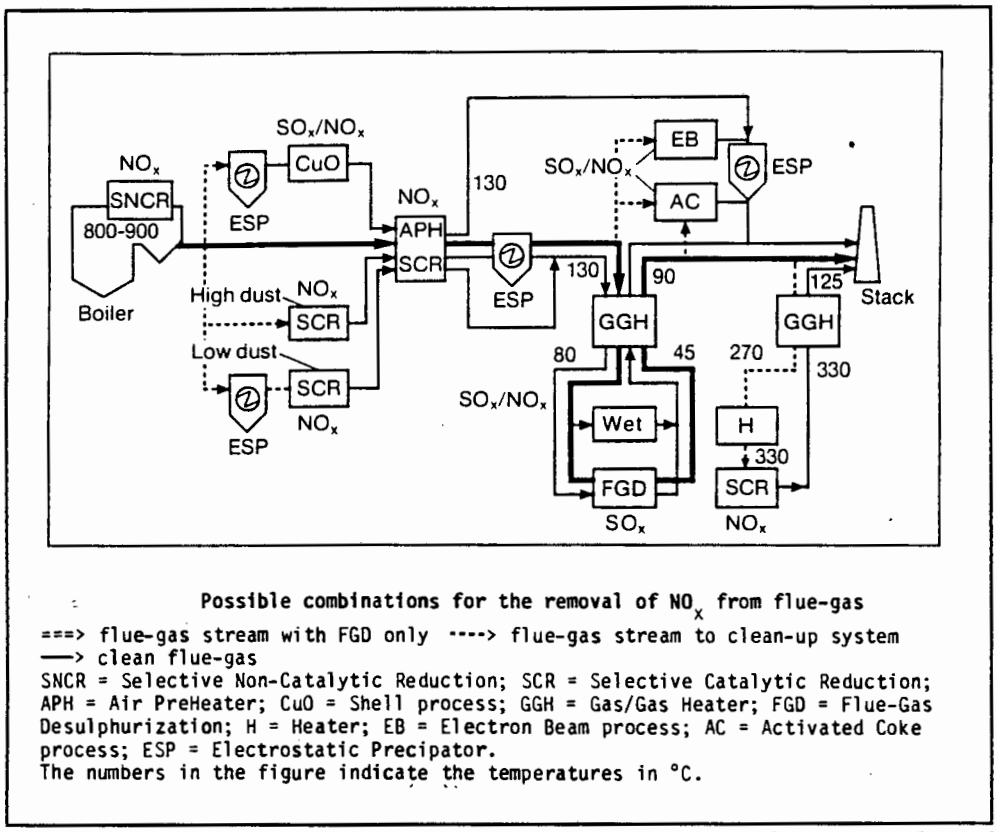

***Figure 1.8** Possible configurations for NOx removal facilities (Bosch and Janssen, 1988)*

Catalysts resistant to SO_2 poisoning have since been discovered (most based on TiO_2), allowing NOx removal facilities to be installed upstream of FGD units with the benefit of not having to reheat flue gas from a low temperature process such as SO_2 absorption.

Catalyst supports have been developed to withstand the adverse conditions of flyash abrasion and catalyst plugging, allowing SCR catalysts to be used in high dust applications. The incentive for locating any flue gas cleaning process within or immediately downstream of the combustion chamber in a high dust application, is energy efficiency.

1.6.2. CATALYST FORM

Catalyst supports have been designed to overcome dust clogging problems and maintain sufficiently high surface areas in high dust regions. The result is the development of ceramic monoliths, the plate form and the metal monolith which are illustrated in Figure 1.9.

Ceramic monoliths, commonly used for metal oxides, are comprised of square channels 3 -7 mm in width, forming a typically rectangular block of cells 15 cm on a side and 50-100 cm in length. The monolith is extruded from paste, cut, dried, activated, packed in steel frames of

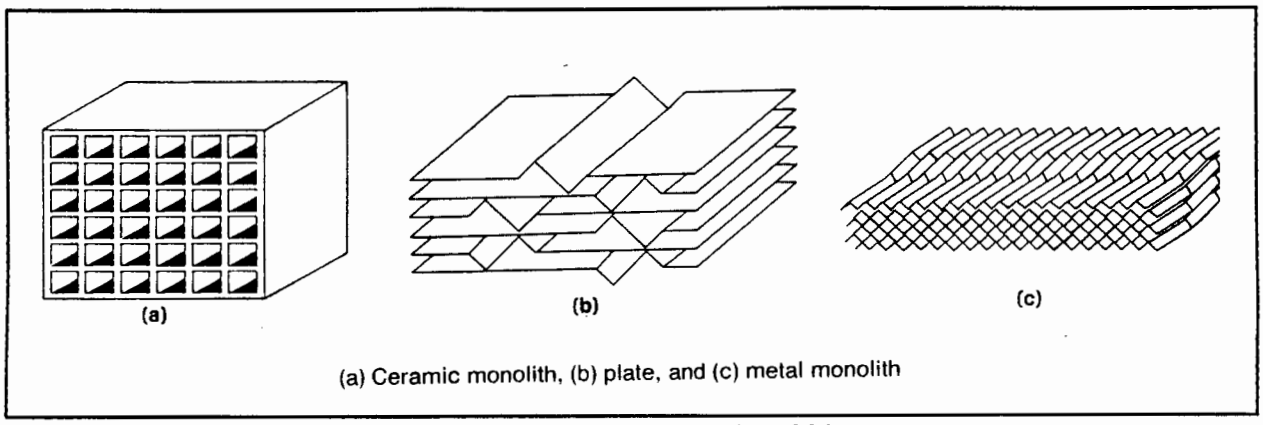

Figure 1.9 SCR catalyst support geometries (Boer et al., 1990)

about 1 m^3 and stacked in a reactor. Extruded monoliths have become the dominant form of SCR catalysts (Boer *et al.*, 1990).

The second catalyst format is the plate. Paste is applied to metal screens or grids which are bent to form dividers. The units are dried, activated and stacked.

Metal monoliths, are especially appropriate for the support of noble metals in gas turbine applications. Corrugated metal sheets are coated with a thin layer of an oxide support impregnated with noble metals. The sheets are folded to form 1 mm channels and placed in a metal frame up to 70 cm square and 15 cm deep in the direction of gas flow. Frames may be placed side to side in a larger frame and assembled into units as large as 12 m^2, still only 8-15 cm deep with the advantage of a low pressure drop which is vital for this application (Boer *et al.*, 1990). For each megawatt of electric power generating capacity, about 1-1.5 m^3 of catalyst is required and the pressure drop through the catalyst elements is typically a few inches of water (Boer *et al.*, 1990).

Notwithstanding the ability of catalysts to operate under high dust conditions, low dust positions allow extended catalyst life and permit the use of catalyst support structures with smaller channels, yielding increased catalytic activity per unit volume of reactor volume (Boer *et al.*, 1990).

1.6.3. SCR PROCESS ECONOMICS

An indication of the costs associated with a SCR unit is shown in Table 1.6.

Catalyst costs account for approximately 50% of the SCR expenditure, demonstrating that significant cost reductions can be gained through catalyst improvement. The high catalyst cost demands a suitable lifespan and design goals may be 3,5 or even 10 years (Boer *et al.*, 1990).

The cost of ammonia is typically 5-10% of the operating costs of the SCR process (Boer *et al.*, 1990).

Boer *et al.* (1990) evaluated the process economics of SCR, comparing costs of first and second generation catalyst systems and related these to the cost of generated electricity. Considering a 50% increase in activity offered by Grace's[1] *SYNOX* catalyst over a first generation catalyst, the increase in the cost of electricity was projected at 3-4% compared with 5% for the first generation catalyst.

Table 1.6 Levelized busbar cost breakdown of SCR in 1988(Boer et al., 1990)

Variable operating costs	
Catalyst replacement	34%
Ammonia	5%
Power	7%
Fixed operating and maintenance costs	
Maintenance labor	11%
Administrative	8%
Capital charges	
Catalyst first fill	14%
Ancillary equipment	21%

The results of a more authoritative and recent survey[2] conducted by the Organization for Economic Cooperation and Development (OECD) using cost data from developed countries in the western world, indicated that the levelized annual cost of SCR translated to a 9% increase in the cost of generated electricity. The OECD report also indicated that the incorporation of SCR added 6% to the base capital cost of a plant, this figure being less than half of the additional 15% increase incurred by the installation of FGD equipment (Petrie *et al.*, 1992).

1.7. SCR CATALYSTS

Many catalyst compositions have been tested for the SCR of NOx but metal oxides and noble metals are the most commonly encountered SCR catalysts (Boer *et al.*, 1990). Zeolites have been employed on a smaller scale.

Table 1.7 records the chronological development of commercial SCR catalysts.

While the noble metal catalysts, platinum and Pt-Rh are intrinsically more active than the oxides, they are less selective and are used at lower temperatures (240-280°C). Noble metals are deactivated by oxygen chemisorption at high temperature (Kiovsky *et al.*, 1980).

[1] W.R. Grace & Co., New York, N.Y.

[2] "Emission controls in electricity generation and industry", OECD/International Energy Agency (1988)

The noble metals are prone to SO_2 poisoning and are therefore usually not considered for coal or oil fired furnaces. However, they are suited to applications such as co-generation turbines fired by clean gas (Boer *et al.*, 1990).

Metal oxide catalysts are typically composed of titania supported vanadia. Vanadium pentoxide resists sulphur poisoning but catalyses the oxidation of SO_2 to SO_3 and is expensive (Kiovsky *et al.*, 1980). TiO_2 also imparts resistance to SO_2 poisoning and titania-based catalysts are probably the most widely used SCR catalysts (Kiovsky *et al.*, 1980; Nakajima, 1991). Additional activity can be gained by promoting with other oxides such as tungsten and molybdenum (Nakajima, 1991).

Table 1.7 Chronology of SCR catalyst development (Boer et al., 1990)

Catalyst type	Key components	Year
Noble metal	Pt, Pd, Ru/Al_2O_3	1959
Metal oxide	Fe_2O_3/Cr_2O_3	1965
Metal oxide	$V_2O_5/MoO_3/WO_3/Al_2O_3$	1966
Metal oxide	V_2O_5/TiO_2	1973
Metal oxide	$V_2O_5/MoO_3/WO_3/TiO_2$	1973
Mixed oxide	$V_2O_5/WO_3/TiO_2$-SiO_2	1976
Zeolite	Synthetic mordenite	1978
Noble metal (metal monolith)	Pt/Al_2O_3	1989
Metal oxide (ceramic monolith)	$V_2O_5/TiO_2/SiO_2$	1989

Fe_2O_3 , iron oxide mixtures with other oxides and copper oxide have also been used as SCR catalysts, supported on Al_2O_3 or SiO_2-Al_2O_3.

The metal oxide catalysts are generally effective in the temperature range 300-400°C (Boer *et al.*, 1990; Nakajima, 1991).

Hydrogen mordenites were used as SCR catalysts in the late 1970's (Table 1.7), but more recently, the discovery of the activity of copper containing ZSM-5 for the direct decomposition of nitric oxide has resulted in renewed interest in zeolites. In the last two years an iron containing zeolite, "ZNX" manufactured by Engelhard Corporation has been installed in four commercial applications in the USA (Byrne *et al.*, 1992).

The most significant advantage of the zeolite catalyst "ZNX", is the large and high temperature operating window (350-550°C) which can be seen in Figure 1.10. The activity of the zeolite is compared with a noble metal and a vanadium catalyst and the activity of the latter, can be seen to decrease above 400°C. Thus, zeolites are suitable for use at higher temperatures than vanadium based catalysts.

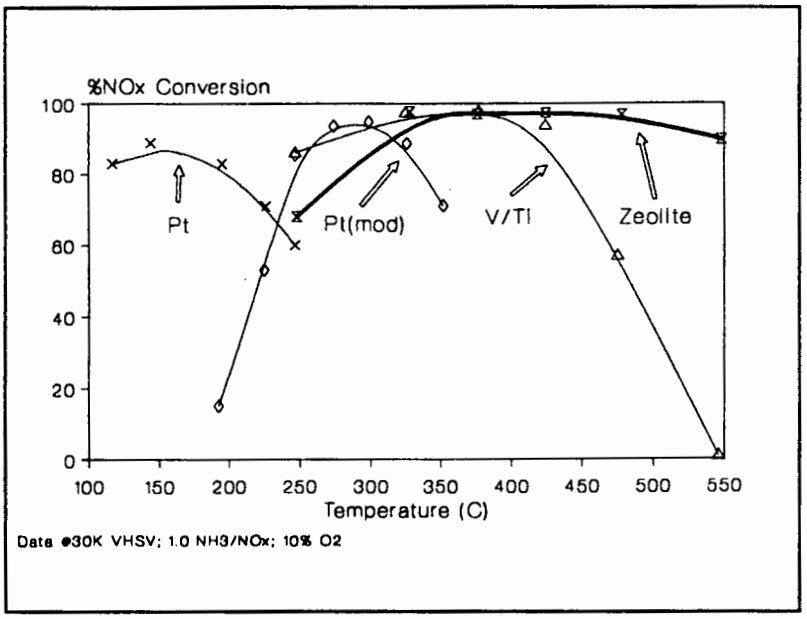

***Figure 1.10** Temperature windows for various SCR catalysts (Byrne et al., 1992)*

1.8. SIMULTANEOUS SO_2/NOx REMOVAL

As already discussed in Section 1.5.2., the simultaneous removal of SO_2 and NOx can be effected by liquid absorption. However, low operating temperatures are imposed by the boiling points of the scrubbing solutions, requiring the cooling and subsequent re-heating of flue gas, thereby incurring energy penalties (refer to process considerations - section 1.6.1.). The attendant problems of waste disposal have also been discussed in section 1.5.2. Thus, a role exists for a dry, high temperature, simultaneous SOx/NOx removal system.

Few methods of dry, simultaneous SO_2/NOx removal have been noted.

As early as 1964, Shell developed a process using CuO/Al_2O_3 for simultaneous SO_2 and NOx removal (Siddiqi and Tenini, 1981). Copper oxide acted as a sorbent for SO_2, resulting in the formation of copper sulphate which catalysed the reduction of NOx with ammonia.

More recently, Paplawski and Pence (1989) investigated the use of iron and copper doped mordenite for such a dual-function flue gas treatment process at 400°C, and were able to achieve 80% NOx removal and 90% SO_2 removal.

Both of these reaction systems differ from the SCR systems described in the preceding paragraphs, by the need to regenerate the catalyst after reaction with SO_2.

The ability to remove both SO_2 and NOx in a single operation may be more cost effective and efficient than two separate processes, and the need for a high temperature process (for energy efficiency), warrants further investigation of a dual-function catalyst.

1.9. HIGH TEMPERATURE FLUE GAS CLEANING

Besides NOx and SO_2, particulate removal is required in furnaces fired by fossil fuels. Electrostatic precipitators and fabric filters are often used. However, fabric filters are not used above 300°C and conventional ESPs are typically operated in a temperature window of 250°C (recent developments have extended this range to 450°C).

Barrier filtration by rigid porous ceramic materials has been shown to be effective to temperatures up to 1100°C (Chang *et al.*, 1986), allowing gas cleaning to be effected at high temperature and resulting in greater energy efficiency.

These ceramic materials which are able to withstand high temperatures, present an opportunity to incorporate the removal of all three of the major pollutants *viz*, SO_2, NOx and particulates, into a single operation, if they are also catalytically active.

Considering the benefits of dry over wet NOx removal systems, the need for the removal of SOx, NOx and particulates and the energy efficiency offered by high temperature applications, a clear role exists for a high temperature, multi-functional flue gas treatment facility. Not least, higher reaction rates offered by the influence of temperature on reaction kinetics would permit less catalyst to be used, resulting in smaller reactor bed volumes (Byrne *et al.*, 1992).

1.10. RATIONALE AND RESEARCH OBJECTIVES

Selective catalytic reduction has been shown to be the most effective method of NOx removal. Present SCR systems operate at 300-400°C and new catalyst designs are required if SCR is to be effected at higher temperatures to realize greater energy efficiency.

The thermal stability of zeolites makes them suitable candidates for high temperature applications, and recent studies with metal containing zeolites have shown them to be effective SCR catalysts at high temperature.

Copper doped zeolites have been used for the direct decomposition and SCR of nitric oxide and in addition, copper oxide and copper exchanged catalysts have also been employed for simultaneous SO_2/NOx removal.

Consequently, the primary objective of the study is to investigate the use of :
1) a copper doped zeolite and
2) copper oxide
as NOx reduction catalysts in order to gain a better understanding of the function of copper and the role, if any, of the zeolite framework. A further objective is to use the knowledge gained in the assessment of the above two catalysts, to design a catalytically active ceramic filter, to effect the high temperature, simultaneous removal of NOx and particulates.

ZSM-5 was chosen as an appropriate zeolite to investigate because it has been shown to be the most effective decomposition catalyst and has also been found to catalyse the SCR of NOx. Furthermore, this zeolite was selected on the basis of in-house synthesis and characterization skills developed at the department of Chemical Engineering at UCT.

Two catalytic NOx reduction reactions are to be investigated. They are:
1) direct decomposition and
2) selective reduction with ammonia.

The decomposition reaction is to be investigated as a means of validating the experimental procedures (by duplicating published results). A more comprehensive set of tests is envisaged for the SCR work, since it is the primary focus of this investigation.

The catalytic activity for the SCR reaction is to be investigated by varying the following parameters:
1) temperature
2) feed flowrate
3) reactant concentrations

Further details of the specific experimental runs are discussed in Chapter 3.

1.11. THESIS SCOPE AND LAYOUT

This work forms the initial phase of the development of a simultaneous SO_2/NOx/particulate removal process and addresses NOx removal with copper doped aluminosilicates.

Nitric oxide decomposition and its SCR with ammonia over Cu-ZSM-5 are investigated. The catalytic activity of CuO for SCR is examined and specifically, copper oxide dispersed on silicalite and aluminosilicate fibre are investigated.

In Chapter 2, the chemistry and thermodynamics of NOx are covered and an introduction to the structure and properties of zeolites is presented. This is followed by a review of nitric oxide

reduction studies with zeolites and copper oxide and covers the direct decomposition reaction as well as SCR.

Design and setup of the experimental work are detailed in Chapter 3. This chapter includes a description of catalyst preparation and characterization, the equipment used in the reaction studies, experimental procedures and analytical tools and techniques.

Results of the experimental phase are recorded and discussed in Chapter 4. This section covers the investigation of the direct decomposition of NO over Cu-ZSM-5 and the study of SCR (with ammonia) over Cu-ZSM-5 and CuO dispersed on silicalite and amorphous aluminosilicate fibres.

Finally, conclusions derived from the experimental program are presented in Chapter 5 and recommendations for further work are offered.

2. A LITERATURE REVIEW

2.1. INTRODUCTION

In the discussion of NOx reduction processes presented in Chapter 1, Selective Catalytic Reduction was noted as the most effective method for stationary source NOx abatement. With the premise of greater energy efficiency, a niche for a high temperature, tri-functional flue gas cleaning system was identified. Also, zeolites and CuO were identified as potential candidates for high temperature NOx reducing catalysts. On this basis, available literature on the use of these two types of catalysts for catalytic NOx reduction are examined.

In order to understand NOx reduction, the chemistry and thermodynamics of NOx are first investigated. Thereafter, properties of zeolites are discussed with attention focused on factors which affect zeolite chemistry. The remainder of the literature review concentrates on the reactions and catalysts of interest *i.e.*, the direct decomposition reaction, the SCR reaction and the catalysts: zeolites and copper oxide.

The literature was analyzed with the objectives of gaining an understanding of the function of the catalysts, determining the factors which affect catalytic activity, establishing some yardsticks with which to evaluate SCR catalysts and to describe selection criteria for these catalysts.

2.2. CHEMISTRY AND THERMODYNAMICS OF NOx

Nitrogen forms covalent bonds with oxygen, yielding seven known oxides: NO, NO_2 , NO_3 , N_2O, N_2O_3 , N_2O_4 and N_2O_5. NOx found in flue gases is comprised mainly of nitric oxide, (90-95%) with the remainder being NO_2 (Bosch and Janssen, 1988), making nitric oxide the subject of NOx removal investigations. Kiel *et al.* (1992) have cited Montgomery *et al.* (1989) and Muzio *et al.* (1989) as having determined that nitrous oxide is not a substantial component of flue gas NOx.

Table 2.1 shows the oxidation states of nitrogen in the corresponding oxides.

There are essentially two routes to eliminate NOx. It can be oxidized to nitrate/nitrite compounds or it can be reduced to nitrogen. Clearly, an ideal path for NOx removal would be the direct decomposition to nitrogen and oxygen without the aid of any reducing agents or generating nitrogen compounds to be disposed of or which require further treatment.

Commercial implementation of this direct decomposition reaction has been limited by the low reaction rate obtained over available catalysts or the need to regenerate catalysts which are oxidized through this reaction. Thus, the aid of a reducing agent such as ammonia is employed,

yielding reaction rates which make SCR commercially viable.

Table 2.1 The oxidation states of nitrogen (Nakajima, 1991)

SPECIES	OXIDATION STATE OF NITROGEN
N_2O_5	+5
NO_2	+4
N_2O_3	+3
NO	+2
N_2O	+1
N_2	0
NH_3	-3

Nitric oxide and ammonia react according to the stoichiometry described by (Bosch and Janssen, 1988; Hirsch, 1982; Nakatsuji and Miyamoto, 1991; Nakajima, 1991):

$$6NO + 4NH_3 \rightharpoonup 5N_2 + 6H_2O \qquad (2.1)$$

In the presence of oxygen, the overall stoichiometry is (Bosch and Janssen, 1988; Hirsch, 1982; Nakatsuji and Miyamoto, 1991; Nakajima, 1991):

$$4NO + 4NH_3 + O_2 \rightharpoonup 4N_2 + 6H_2O \qquad \Delta H_0 = -1631 \text{ kJ} \qquad (2.2)$$

and describes the SCR of nitric oxide with ammonia.

Ammonia is oxidized at high temperature to produce nitrogen and nitric oxide in the following reactions (Bosch and Janssen, 1988):

$$4NH_3 + 3O_2 \rightharpoonup 2N_2 + 6H_2O \qquad \Delta H_0 = -1296 \text{ kJ} \qquad (2.3)$$

$$4NH_3 + 5O_2 \rightharpoonup 4NO + 6H_2O \qquad \Delta H_0 = -907 \text{ kJ} \qquad (2.4)$$

The oxidation to nitric oxide is the reaction referred to in Section 1.5.2. and in Figure 1.6., the extent of which determines the optimum operating temperature for SCR over a particular catalyst - at high temperatures ammonia is oxidised to nitric oxide rather than being consumed in the reaction to reduce NOx.

Although nitrous oxide can be produced from the reaction of ammonia/oxygen and nitric oxide (Bosch and Janssen, 1988), these reactions have not been noted as having significant roles in the SCR process:

$$8NO + 2NH_3 \rightleftharpoons 5N_2O + 3H_2O \qquad \Delta H_0 = -950\ kJ$$
$$4NO + 4NH_3 + 3O_2 \rightleftharpoons 4N_2O + 6H_2O \qquad \Delta H_0 = -1304\ kJ \qquad (2.5)$$
$$2NH_3 + 2O_2 \rightleftharpoons N_2O + 3H_2O \qquad \Delta H_0 = -553\ kJ$$

It has been proposed that the "SCR reactions" involving NO_2 are:

$$6NO_2 + 8NH_3 \rightleftharpoons 7N_2 + 12H_2O \qquad (2.6)$$

$$NO + NO_2 + 2NH_3 \rightleftharpoons 2N_2 + 3H_2O \qquad (2.7)$$

and

$$8NO + 4NO_2 + 8NH_3 + O_2 \rightleftharpoons 12N_2 + 18H_2O \qquad (2.8)$$

with reactions (2.6) and (2.7) occurring in the absence of oxygen (Hirsch, 1982; Nakatsuji and Miyamoto, 1991) and reaction (2.8) taking place with oxygen (Nakatsuji and Miyamoto, 1991). Nakatsuji and Miyamoto (1991) were the only source of equation (2.8) which, in order to balance, requires a stoichiometric co-efficient of 12 for ammonia, rather than "8" indicated above.

Although no catalyst or conditions were specified, the same authors described the relative rates of the reactions as being: (2.8) > (2.2) > (2.7) >> (2.6) > (2.1).

It can be seen from the negative standard heats of reaction shown for the stoichiometries listed above, that the NOx reduction and ammonia oxidation reactions are all exothermic. Since the heat of reaction is not required to be supplied, a process advantage is gained in terms of energy efficiency.

The reduction of nitric oxide with ammonia and oxygen is thermodynamically favourable to temperatures well over 1300°C (a typical furnace operating temperature). This is evident in Figures 2.1, 2.2, and 2.3 which show that this is the true for all the stoichiometries listed and indicate that any limitations would thus be kinetic and not thermodynamic.

The equilibrium constants were calculated by the method described by Smith and Van Ness (1987) with data taken from the same source. The calculations are shown in Appendix 1.

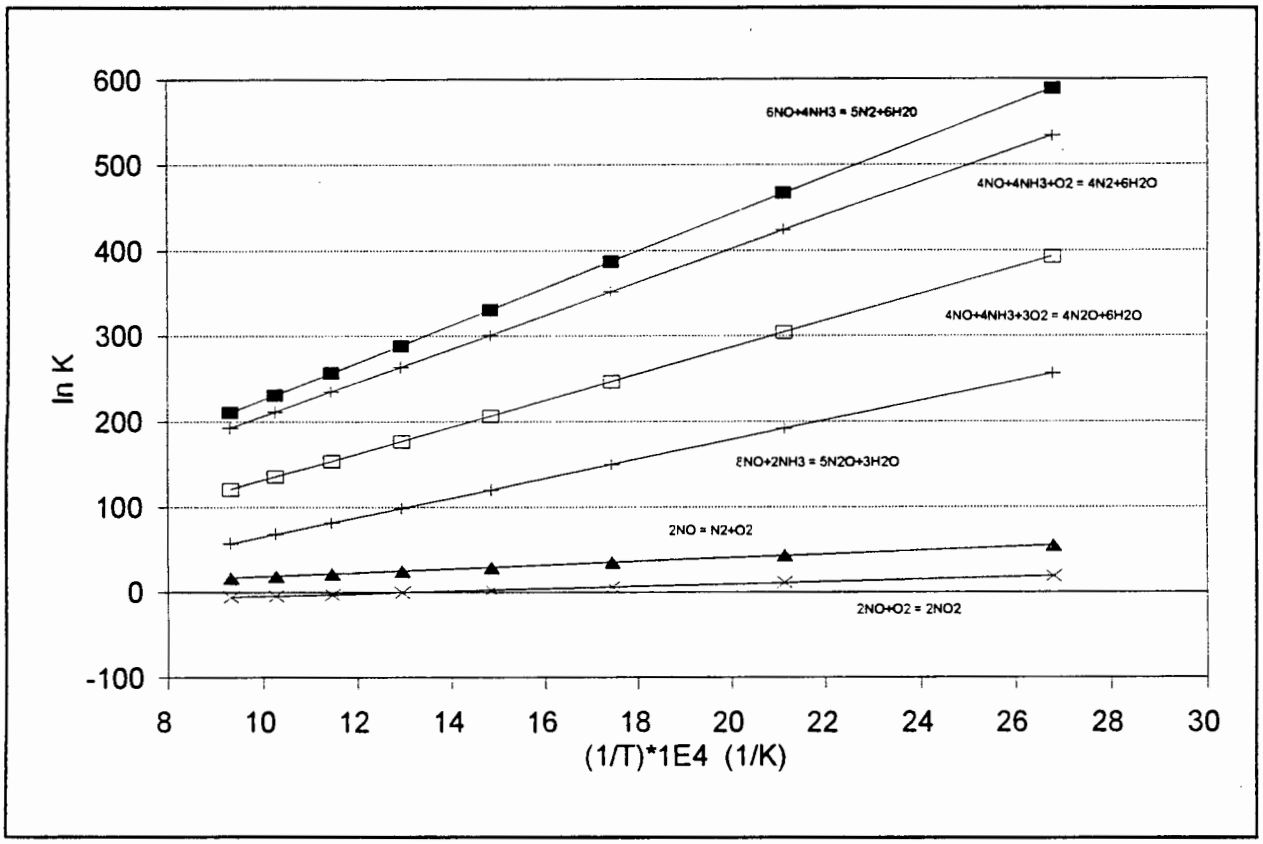

Figure 2.1 Equilibrium constants for NOx reactions (I)

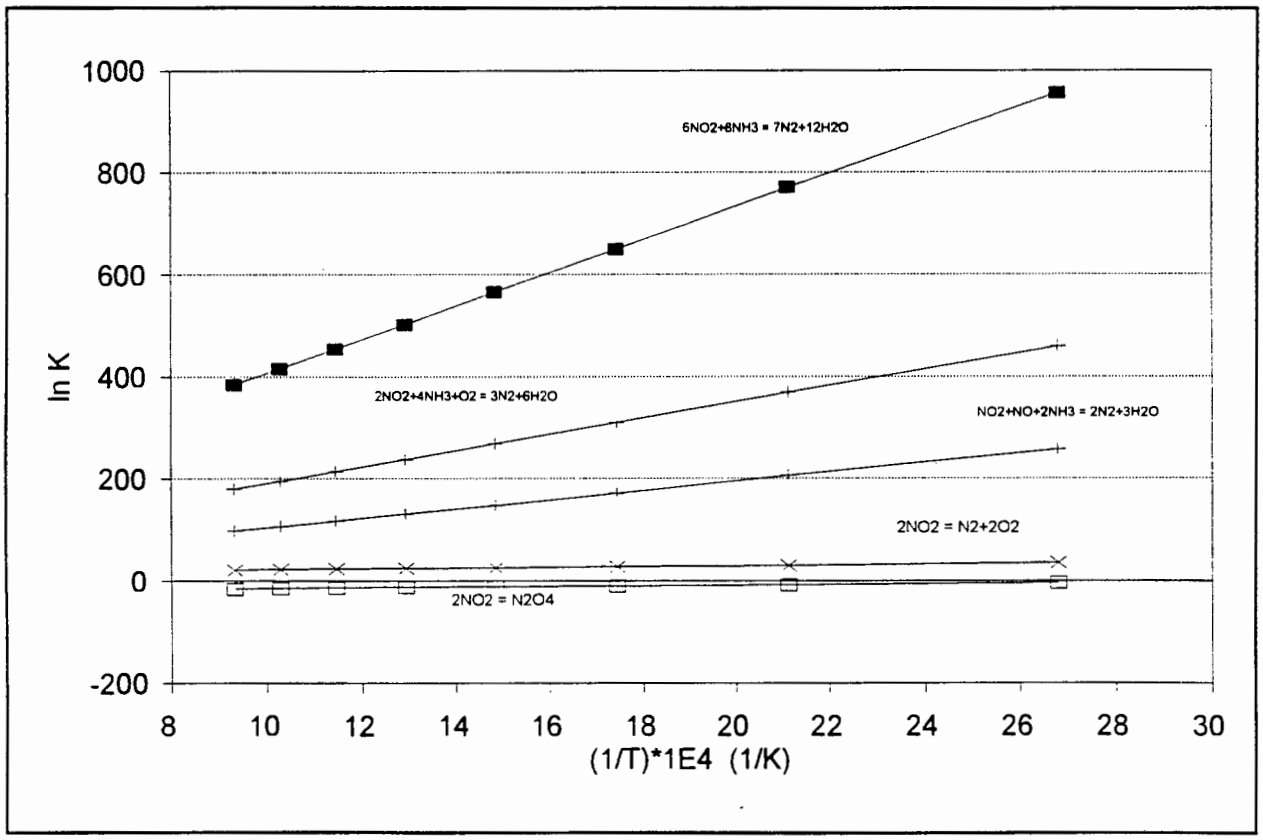

Figure 2.2 Equilibrium constants for NOx reactions (II)

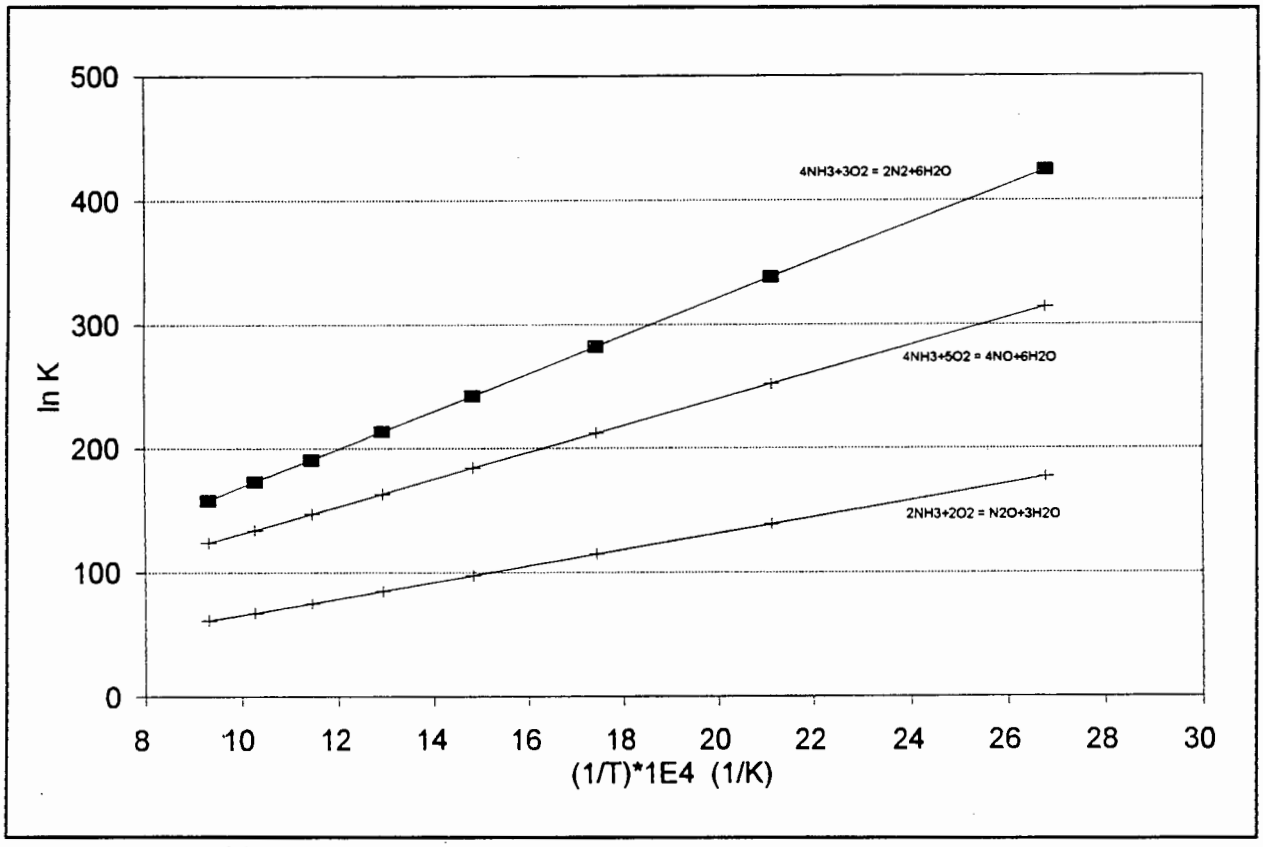

Figure 2.3 Equilibrium constants for NOx reactions (III)

This draws the examination of NOx chemistry and thermodynamics to a close. Zeolite composition, nomenclature, structure and chemistry are now investigated to develop an understanding of their use in NOx reduction and to reveal factors which may affect catalytic activity.

2.3. ASPECTS OF ZEOLITE PROPERTIES AND CHARACTERISTICS

2.3.1 INTRODUCTION

Zeolites are hydrated crystalline aluminosilicates having a 3-dimensional network of TO_4 tetrahedra, where "T" is a silicon or aluminium atom. These tetrahedra form a framework of uniform channels and cavities of molecular dimensions (Dyer, 1988).

An isolated SiO_4 entity would have a charge of -4 since Si has a valency of +4 while each oxygen anion carries a -2 charge. However, since two "T" atoms are bridged by an oxygen atom which shares electron density with each, a framework SiO_4 unit is neutral. Hence, a pure SiO_2 framework does not contain any charge (Davis, 1991).

Oxygen atoms which are tetrahedrally co-ordinated to an aluminium atom, result in a net -1 charge since aluminium has a valency of 3. Thus, when the Si and Al tetrahedra are connected in an aluminosilicate framework, there is a net negative charge associated with each Al atom. This negative charge is balanced by cations to give electrical neutrality. These cations are typically group IA and IIA elements such as sodium, potassium, magnesium and calcium (Davis, 1991).

Among other purposes, zeolites are employed as desiccants, ion exchange materials and catalysts.

They are useful as desiccants by virtue of being hydrophillic and containing large void fractions within the framework to accommodate the adsorbed water. This phenomenon gave rise to the word "zeolite", which is of Greek origin and translates as "boiling stones" which was an allusion to the visible loss of water which was noted when natural zeolites were heated (Dyer, 1988).

The charge balancing cations often have a high degree of mobility which gives rise to facile ion exchange and zeolites have been modified by ion exchange for specific catalytic action (Dyer, 1988). If H^+ is the charge balancing cation, then a solid acid is produced. As already mentioned in Chapter 1, the acid form of mordenites (H-mordenites) has been employed for SCR of NOx. Acid catalysts have been used in alkylation, cracking, paraffin isomerization, methanation, the conversion of methanol to gasoline and many other reactions (Kirk-Othmer, 1981).

Basic catalysts such as the sodium or calcium forms of zeolite-X and -Y have been used in reactions involving H_2S, such as the conversion of furan to thiophene, and reactions such as isopropanol dehydration and the alkylation of toluene and other aromatics with methanol (Barthomeuf, 1991).

Zeolites are known and employed as molecular sieves on the basis of their ability to selectively, with respect to effective molecular dimensions, allow the passage of molecules through the apertures created by the framework (Dyer, 1988). This, along with the catalytic action of zeolites, gives rise to the concept of "shape selective catalysis". Reactant selectivity results from restrictions of reactant molecules and similarly, product selectivity is determined by the passage of products through the channels. Stereospecificity of products may be possible if the space within the zeolite is not sufficiently large to accommodate the larger of several possible transition state intermediates (Davis, 1991)

2.3.2. ZEOLITE CLASSIFICATION

The simplest classification of zeolite frameworks is based on 8 recurring structural sub-units referred to as "secondary building units" (sbus). The units are defined by the size and orientation of the tetrahedra which form distinct "oxygen windows". All zeolites frameworks may be described by a combination of these sbus which are shown below in Figure 2.4 .

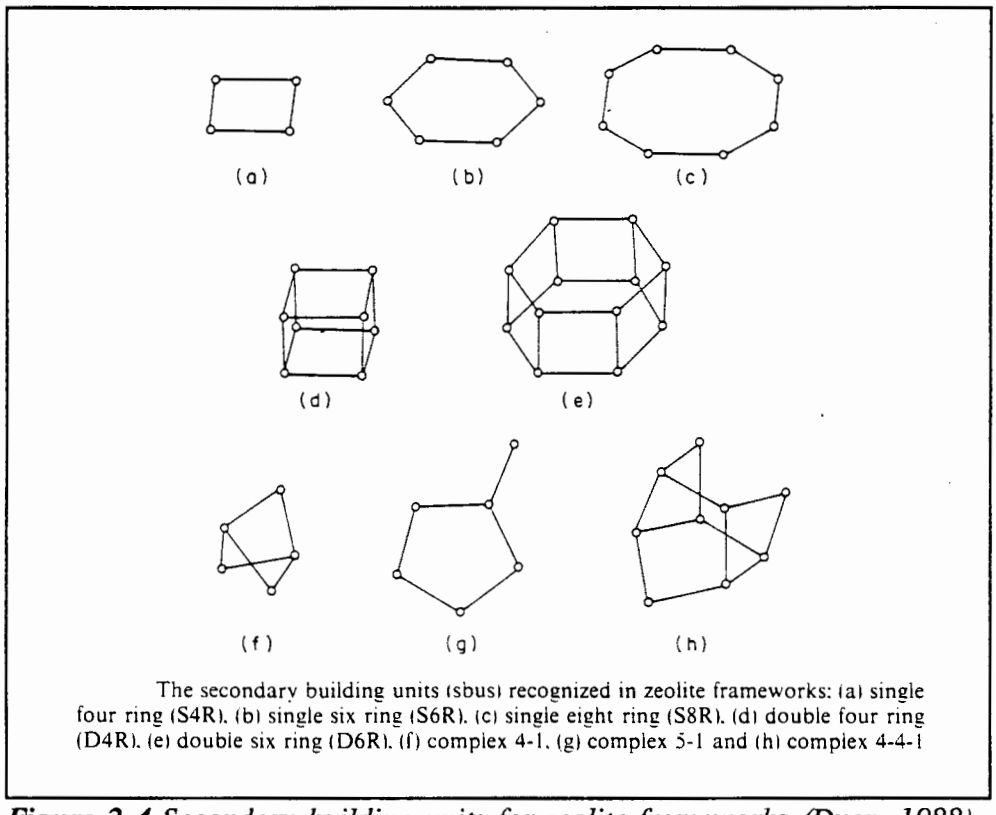

The secondary building units (sbus) recognized in zeolite frameworks: (a) single four ring (S4R), (b) single six ring (S6R), (c) single eight ring (S8R), (d) double four ring (D4R), (e) double six ring (D6R), (f) complex 4-1, (g) complex 5-1 and (h) complex 4-4-1

***Figure 2.4** Secondary building units for zeolite frameworks (Dyer, 1988)*

Figure 2.5 shows how the tetrahedra are arranged in the "single four ring" (S4R) and "single six ring" (S6R) sbu's. In Figure 2.5a, the oxygen atoms which link the tetrahedra and form the square "single four ring " are clearly shown.

Zeolites have also been classified by mnemonic codes of their various structure types (IUPAC nomenclature). Zeolite-Y belongs to the Faujasite family coded as "FAU" while mordenite is referred to as "MOR" and ZSM-5, as "MFI" for Mobil Five, the code used by the developers of ZSM-5 at Mobil (Dyer, 1988).

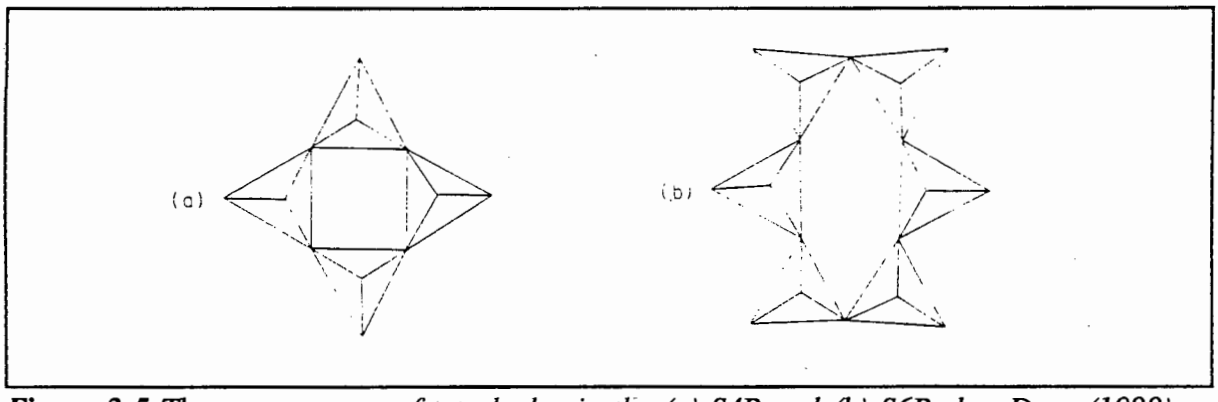

***Figure 2.5** The arrangement of tetrahedra in the (a) S4R and (b) S6R sbu, Dyer (1988).*

2.3.3. ZEOLITE STRUCTURE

The structural formula of a zeolite is based on the crystal unit cell represented by :

$$M_{\frac{x}{n}}[(AlO_4)_x(SiO_4)_y].w\ H_2O \qquad (2.9)$$

where n is the valence of cation M, w is the number of water molecules per unit cell and x and y are the total number of tetrahedra per unit cell .

Three zeolites in particular, have been used for NOx reduction, zeolite-Y, mordenite and ZSM-5 and details of their structures are given below.

Zeolite-Y is known as a large pore zeolite, ZSM-5 is known as a medium pore zeolite and the synthetic mordenite, Zeolon 900 which has been widely used (manufactured by Norton Company), is characterized as a large port zeolite with 0.8 nm pores (Kirk-Othmer, 1981).

ZSM-5

Structure type: MFI
Structure based on 5-1 sbu
Typical unit cell formula: $Na_n[(AlO_2)_n(SiO_2)_{(96-n)}].16H_2O$ $(n \sim 3)$

The 5-1 sbus are linked into a chain, giving ZSM-5 a 3-dimensional pore structure enclosed by 10-membered oxygen rings which form two pore systems (Figure 2.6). One consists of sinusoidal channels of near circular cross-section (0.54 * 0.56 nm) and another of straight channels of elliptical shape (0.51 * 0.56 nm). All intersections are of the same size (Dyer, 1988).

Silicalite, a molecular sieve, is topologically similar to ZSM-5. Its framework is also constituted from 5-1 sbus and silicalite possesses the same 3-dimensional pore configuration as ZSM-5. However, silicalite is composed only of SiO_4 tetrahedra and since it contains no aluminium and hence, no exchangeable metal cations, it is by definition no a zeolite (Kirk-Othmer, 1981).

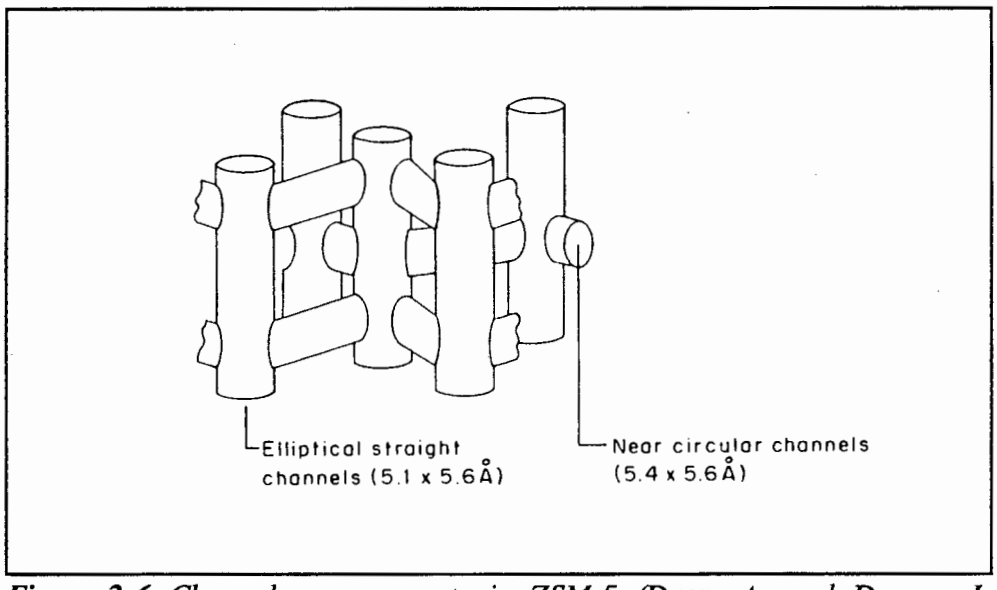

***Figure 2.6** Channel arrangements in ZSM-5 (Dyer, A. and Dwyer, J. (1984), taken from Dwyer (1988))*

Mordenite

Structure type: MOR
Structure based on 5-1 sbu
Typical unit cell formula: $Na_8[(AlO_2)_8(SiO_2)_{40}].24H_2O$

In mordenite, the 5-1 units are linked into a series of chains joined together to form two major (non-intersecting parallel) channels; one restricted by 12-membered oxygen rings (0.67 * 0.7 nm) and the other by 8-membered oxygen rings (0.29 * 0.57 nm) (Dyer, 1988).

While there are side pockets with openings between 0.387 and 0.472 nm, no diffusion occurs between the channels.

Zeolite-Y

Structure type: FAU
Structure based on D6R
Typical unit cell formula: $Na_{56}[(AlO_2)_{56}(SiO_2)_{136}].250H_2O$

Zeolite-X and -Y and natural faujasite are isostructural. However, zeolite-Y has a lower Al content than zeolite-X and thus, contains fewer cations and more water molecules.

The synthetic zeolites -X and -Y (and faujasite) can be viewed as being composed of three polyhedral cavities:

i) hexagonal prisms (ie. a D6R),
ii) Sodalite or Beta cages which are cubooctahedra and
iii) type II 26 hedrons (alpha cages) (Dyer,1988).

The truncated octahedra (Beta cages) of diameter 0.65 nm are arranged tetrahedrally, being joined to each other by their hexagonal faces (S6R) (see Figure 2.7). Thus, they form a hexagonal prism or D6R between them. The enclosed cavity created by the joined sodalite cages and D6R's forms the alpha cage. These supercages are 1.3 nm in diameter, and each is entered by a 12-membered ring, 0.8 nm in diameter which is the largest pore known in zeolites (Kirk-Othmer, 1981).

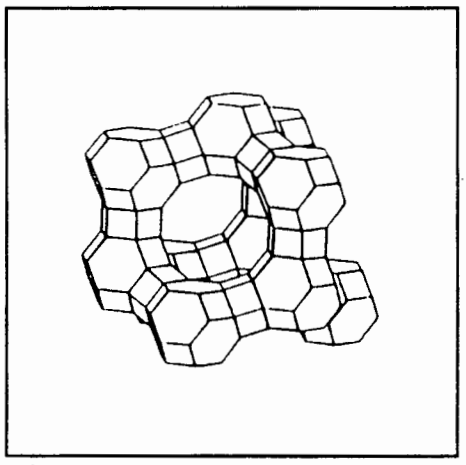

Figure 2.7 Zeolite-Y

Accessibility of gas molecules

Oxygen windows formed by S4R's and S5R's cannot be transversed by guest molecules and the S6R's (270 pm) only by the smallest. While effective window sizes are influenced by cations in the framework, the S8R (0.430 nm), S10R and S12R (0.770 nm) have the greatest influence

on the sieving action. A comparison of the sizes of all the gas molecules listed in Table 2.2, with zeolite pore apertures, reveals that the gases are easily permitted into the pores of ZSM-5, mordenite and zeolite-Y (kinetic diameters for NO, N_2O and NO_2 not available).

Table 2.2 *Lennard-Jones kinetic diameters of probe molecules (Van Hooff and Roelofsen, 1991)*

MOLECULE	*DIAMETER (nm)*
He	*0.260*
NH_3	*0.260*
H_2O	*0.265*
H_2	*0.289*
CO_2	*0.330*
Ar	*0.340*
O_2	*0.346*
SO_2	*0.360*
N_2	*0.364*
CO	*0.376*
CH_4	*0.380*

2.3.4. EXTRAFRAMEWORK SITES IN ZEOLITES

Cations such as sodium and other charge balancing metal ions contained within the zeolite structure are located at positions outside of the framework formed by the "TO_4" tetrahedra. These extra-framework sites have been extensively studied in zeolite-Y and mordenite while only two sites have been localized in ZSM-5. These two sites can be seen in Figure 2.8 taken from the compilation of extra framework sites by Mortier (1982). Eight cation sites have been identified and listed for mordenite (Figure 2.9) and 16 extraframework sites are listed for zeolite-Y (Figure 2.10).

Many factors influence the occupation of particular sites in any zeolite *e.g.*, water content, the nature of the cation and framework charge (Dyer, 1988).

2.3.5. ZEOLITE ACIDITY

Bronsted and Lewis acid sites are encountered in zeolites.

Bronsted acid sites are hydroxyl groups constituted by the attachment of protons to framework oxygen atoms. They may be formed by introducing ammonium ions through ion exchange, which leaves protons attached to the framework after ammonia is driven off by calcination at high temperature (Kirk-Othmer, 1981). These protons are mobile and may be transferred from oxygen to oxygen atom (Barthomeuf, 1989).

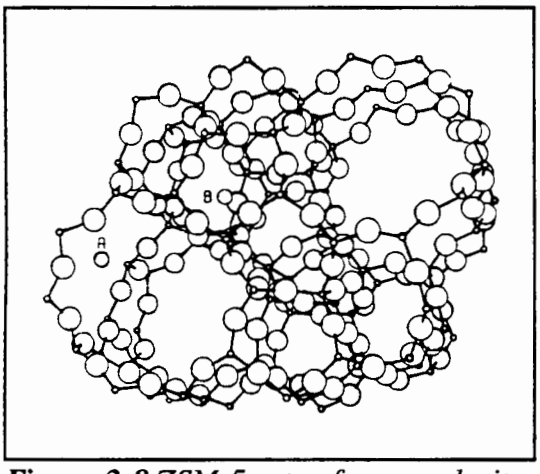

Figure 2.8 ZSM-5 extra-framework sites (Mortier, 1982)

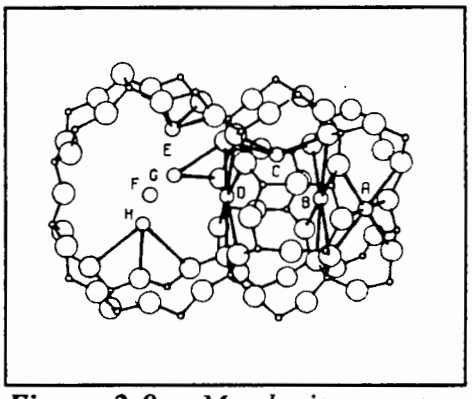

Figure 2.9 Mordenite extra-framework sites (Mortier, 1982)

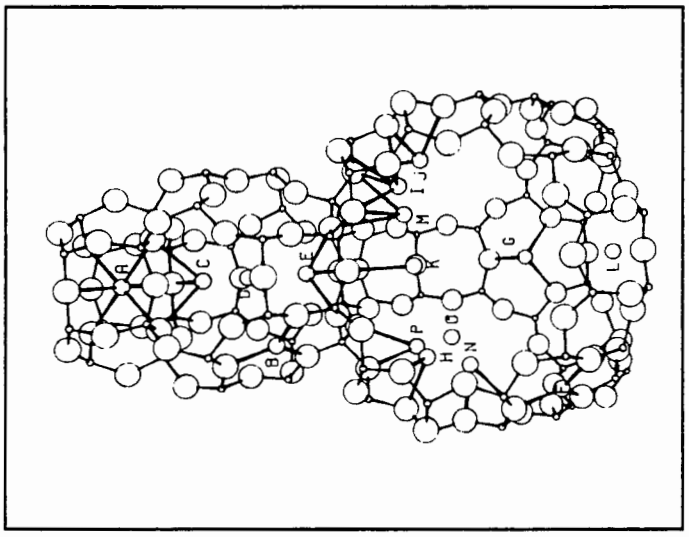

Figure 2.10 Zeolite-Y extra-framework sites (Mortier, 1982)

Since the number of exchanged ammonium ions is determined by the number of AlO_4^- tetrahedra in the framework which require charge balancing, the acidity is dictated by the aluminium content.

It is accepted that Bronsted acid site strengths increase as zeolite Al content decreases. Acid site strength can for example be decreased by exchanging the protons with metallic cations - the strongest sites being exchanged first (Barthomeuf, 1991).

It was thought that Lewis acid sites are formed by the process of dehydroxylation, producing a trigonal aluminium atom and a positively charged silicon atom when two hydroxyl groups are lost at elevated temperatures. Recent evidence suggests that the Lewis sites are generated by the formation of hexacoordinated aluminium atoms at extra-framework cationic positions (Kirk-Othmer, 1981).

2.3.6. THERMAL STABILITY

Collapse of the zeolite structure does not represent a true melting point but a gradual degradation dependent on factors (other than temperature), such as the presence of water vapour, the nature and number of metal cations and possibly other factors. For instance, it has been shown that greater thermal stability accompanies an increase in framework Si:Al ratio (McDaniel and Maher, 1976).

No standard procedure exists for quantifying thermal stability and as an indication of this, the collapse of Na-Y (Si:Al=5 to 6) was determined by Bremer *et al.* (1973) to be 920°C, 870°C by Ambs and Flank (1969) (both by differential thermal analysis), and 700°C by McDaniel and Maher in a muffle furnace (as cited by McDaniel and Maher, 1976).

A table drawn up by Breck (1984) lists a zeolite-Y of Si:Al=2.5 showing no structural change upon heating up to 760°C. An exotherm (recorded by differential thermal analysis) accompanied structural breakdown at 793°C leaving an amorphous residue at 800°C. With mordenite, no change was observed to 800°C with the exotherm appearing at temperatures above 1000°C. Mordenite is probably the most stable zeolite and this property has been attributed to the prevalence of 5-rings in the framework structure (Breck, 1984). ZSM-5 which can be found with high Si:Al ratios (eg 60 and higher) and whose framework is also built upon the five-ring, would presumably possess a similar resistance to thermal destruction.

2.3.7. EXCHANGE OF COPPER IONS INTO ZEOLITES

Cations have been introduced into zeolites by ion exchange to modify their catalytic or molecular sieving properties and virtually every cationic form of the elements in the periodic table has been introduced into a zeolite framework (Dyer, 1988).

Ion exchange can be achieved by slurrying a zeolite in an aqueous solution of the desired metal salt, typically a nitrate. The un-exchanged zeolites are usually in the sodium or ammonium form (Nicolaides *et al.*, 1991).

Kucherov and Slinkin (1986) have described another method of ion exchange *viz*, solid state reaction. This was achieved by heating mixtures of copper compounds such as CuO with H-mordenite and H-ZSM-5 at 520-800°C. The copper ions were found to have taken up the same positions which would have been occupied by ions introduced through liquid phase ion exchange. The Bronsted acid sites were a pre-requisite for this solid state ion exchange reaction. In H-ZSM-5, the majority of Cu(II) was located as isolated, coordinatevely unsaturated, covalent-bonded ions.

Hamada *et al.* (1990b) investigated the form of the copper species in ZSM-5 exchanged with copper acetate and determined that they were essentially atomically dispersed Cu(II) ions contained in the zeolite cages. The copper species were more ionic than CuO and were not in the form of CuO, Cu_2O, Cu metal, $Cu(OAc)_2.H_2O$ or $Cu(OH)_2$ clusters. This was true for the fresh, calcined and used catalyst. Choi *et al.* (1991) examined Cu-mordenite and also observed that a fresh catalyst contained monomolecular Cu(II) species co-ordinated to oxygen which were unlike either CuO or Cu_2O.

In order to comply with the requirement for framework charge balancing, the exchange capacity of a zeolite is dependent on its aluminium content. Ion exchange capacity can be described in units of milli equivalents per gram or alternatively, percentage exchange (as described by among others, Iwamoto *et al.* (1991b) and Sato *et al.* (1991)), is calculated by considering the number of cations required to balance the charge of the AlO_4^- tetrahedra. Hence, using Cu^{2+} as an example:

$$\%Cu^{2+}\ \text{exchange} = \frac{2.\text{moles of } Cu^{2+}}{\text{moles of Al}}.100 \qquad (2.10)$$

Factors which may affect selectivity and the degree of ion exchange include the size and charge of the ion, temperature and solution concentration (Kirk-Othmer, 1981). Since ion exchange is an equilibrium process, solution concentration affects the degree of exchange. The extent of ion exchange with respect to time and temperature in zeolite-X is illustrated in Figure 2.11 below.

The stability of particular sites in the cavities of the faujasite type structure is evident from the effect of temperature.

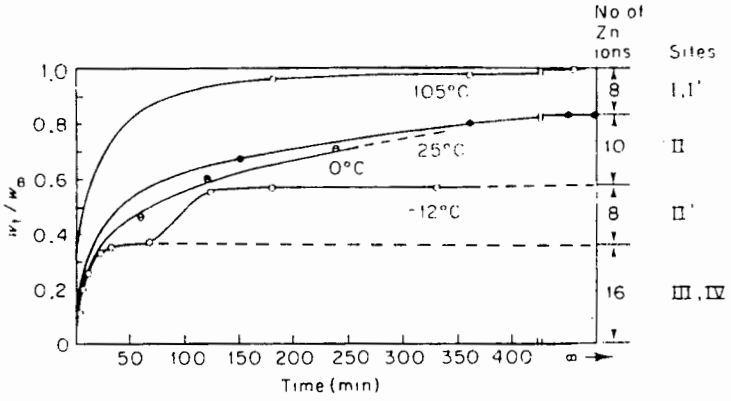

Fractional attainment of equilibrium (W_t/W_∞) for the self-exchange of Zn^{2+} in zeolite X at different temperatures. Figures on the righthand axis show numbers of Zn^{2+} (radiolabelled) ions replaced and related to their suggested sites within the X framework

***Figure 2.11** The effect of temperature and time on ion exchange in zeolite-X (Dyer, 1988)*

The phenomenon of non-stoichiometric exchange

It has been found that an amount of copper greater than that required for achieving charge neutrality in the zeolite framework may be introduced into the structure ie., greater than 100% exchange as calculated by equation (2.10). This phenomenon has been observed by Iwamoto (1991d) in copper exchanged ZSM-5 and by Schoonheydt *et al.* (1976) in Zeolite-Y. The significance of "excess" ion exchange lies in the state and location of these ions and their role in catalytic NOx reduction.

Schoonheydt *et al.* (1976) attributed the excess or non-stoichiometric copper to the formation of polynuclear cation complexes of the type $M_x(OH)^{+2x-y}$. This occurred when ion exchange took place at a pH where hydrolysis of the transition metal could be expected and this phenomenon was likely to occur with copper. However, Li and Hall (1991) have cited Woolery *et al.* (1986) as having reported that internal silanols are responsible for this phenomenon of excess cation exchange in ZSM-5.

2.3.8. CONCLUDING REMARKS

This concludes the discussion of the structure and properties of zeolites. With the understanding of the chemistry and thermodynamics of NOx and the knowledge of the ion exchange process, the location of the ions at extra framework positions, zeolite pore structure and pore diameters, the use of zeolites in catalytic studies is now discussed.

2.4. THE DIRECT DECOMPOSITION OF NO OVER COPPER EXCHANGED ZEOLITES

2.4.1. INTRODUCTION

The direct decomposition of nitric oxide to nitrogen and oxygen is described by the reaction:

$$NO \rightarrow \frac{1}{2}N_2 + \frac{1}{2}O_2 \qquad (2.11)$$

Early NO decomposition catalysts were either noble metals or metal oxides (Iwamoto and Hamada, 1991c). The low activity of a number of catalysts for NOx reduction was attributed to the strong adsorption of oxygen which was produced from the decomposition reaction of NO - oxygen adsorption poisoned the active sites. The reduced forms of these catalysts (polyvalent state of metals) were rapidly oxidized by NO with the release of nitrogen but not of oxygen and subsequent reduction of the catalyst was necessary to restore the catalytic activity (Iwamoto *et al.*, 1986; Li and Hall, 1991)

Winter (1971) studied 40 metallic oxides for the decomposition of NO and the effect of oxygen in all cases was to retard decomposition by competing for the same sites (as described by Bosch and Janssen, 1988). Amirnazmi *et al.* (1973) investigated the use of copper oxide as a direct decomposition catalyst. They found it to be less active than cobalt oxide (Co_3O_4), which had been shown to be an active decomposition catalyst.

More recently perovskite-type oxides and copper zeolites have been used to catalyse the decomposition reaction without deactivation. According to Iwamoto and Hamada (1991c), copper zeolites have to date, been shown to be those most active catalysts for the nitric oxide decomposition reaction. Iwamoto (1991a) has ranked decomposition catalysts in the following reactivity order:

$$\text{Cu-ZSM-5} > \text{Ag-}Co_3O_4 > Pt/Al_2O_3 > \text{Y-Ba-Cu-O/MgO}$$

The use of copper ion exchanged ZSM-5 will now be discussed in detail, in light of its superior performance as a decomposition catalyst. The stoichiometry of the reaction, factors affecting the reaction rate and the reaction mechanism are discussed. The work of three central personalities will become apparent in the discussion of the direct decomposition studies. They are: W.K. Hall, Y. Li and M Iwamoto.

2.4.2. THE CATALYTIC SIGNIFICANCE OF COPPER

The catalytic nature of the reaction over Cu-ZSM-5 was noted by Iwamoto and Hamada (1991c) who found no decomposition in the absence of catalyst. Temperature programmed desorption (TPD) studies led Li and Armor (1991) to conclude that NO adsorption and the decomposition reaction are associated with copper sites - no nitric oxide adsorbed onto Na-ZSM-5 and no decomposition was detected in the absence of copper.

Odenbrand *et al.* (1989) found no direct decomposition of NO to nitrogen and oxygen over H-mordenite between 150 and 410°C while both Li and Hall (1991) and Iwamoto *et al.* (1986) showed that Cu-mordenite is active for this reaction.

In conflict with the above observations however, Mastikhin and Filimonova (1992) recorded nitric oxide decomposition over Na-ZSM-5 and H-ZSM-5 using ^{15}N NMR. Although weak and significantly less than that over Na-ZSM-5 and H-ZSM-5, perceptible activity was even observed over silicalite. Thus, although these metal free materials may not possess suitably high levels of activity, they are nevertheless catalytically active.

2.4.3. REACTION STOICHIOMETRY

Li and Hall (1990) observed that reaction of NO over Cu-ZSM-5 resulted in the following species in the product stream: oxygen, nitrogen, nitric oxide, nitrogen dioxide and nitrous oxide. However, both Li and Hall (1990) and Iwamoto *et al.* (1991d) noted the absence of nitrous oxide at steady state reaction above 400°C. Subsequent work by Li and Armor (1992) has shown the high efficiency of Cu-ZSM-5 in decomposing N_2O - complete conversion was obtained at 400°C.

Li and Hall (1990) completed a mass balance over their reaction system and determined that the decomposition reaction was intrinsically stoichiometric as described by equation (2.11). They were able to achieve complete conversion of NO to nitrogen (100% N_2 yield[3]) over Cu-ZSM-5-12-140[4] at 500°C. Less than 100% nitrogen yield which observed in other experimental runs, was attributed to the formation of NO_2 through the reaction of oxygen produced in the decomposition reaction and unconverted NO. This oxidation reaction was not catalysed by the Cu-ZSM-5, but was a homogeneous gas phase reaction which occurred downstream of the reactor at low temperature.

---

[3] Yield defined as: Fraction of reactant (NO) converted to a specific product (N_2) (Smith, 1981).

[4] Designation: (Metal) - (Zeolite type) - (Si:Al ratio) - (% ion exchange)

Cognizance of the oxidation reaction should be taken in experimental and analytical procedures, since it is not a catalytic reaction and takes place upon contact of nitric oxide and oxygen. For this reason the kinetics of this oxidation reaction was investigated.

The homogeneous gas phase reaction of nitric oxide and oxygen

The equilibrium constant for the NO oxidation reaction:

$$NO + \frac{1}{2}O_2 \rightleftharpoons NO_2 \qquad (2.12)$$

favours the forward reaction at low temperatures, as displayed by the labelled graph in Figure 2.1. Below 150°C, almost all NO reacts to yield NO_2 if allowed sufficient time (Kirk-Othmer, 1981).

Although the mechanism of the oxidation reaction remains controversial, it is generally accepted that the rate can be described by a third order process (England and Corcoran, 1975) of the form:

$$\frac{d(P_{NO})}{dt} = - k (P_{NO})^2 (P_{O_2}) \qquad (2.13)$$

England and Corcoran (1975) investigated the oxidation of NO at conditions similar to those prevailing in the atmosphere i.e., ppm concentrations of NO and percent concentrations of oxygen between 25 and 50°C and atmospheric pressure. A rate constant of $1.46*10^4$ $l^2mol^{-2}sec^{-1}$ was determined at 25°C and an activation energy of -1.197 kcal was calculated for $2NO + O_2 = 2NO_2$. The rate constant was found to decrease with increasing temperature and it was shown that the presence of water did not affect the rate of gas phase NO oxidation.

Taking note of the third order kinetics, Li and Hall (1990) have suggested that the rate of oxidation should probably remain low if the concentration of NO is low i.e., ppm levels. In addition, according to the equilibrium constant, a high temperature would retard the reaction.

2.4.4. THE EFFECT OF ZEOLITE STRUCTURE

Li and Hall (1991) determined turnover frequencies (TOF)[5] for Cu-zeolite-Y which were 1 to 2 orders of magnitude lower than that of Cu-ZSM-5 (see Figure 2.12). Cu-ZSM-5 was also found to give higher TOFs than mordenite (The mordenite used had a Si:Al ratio of 5 while the

[5] The number of NO molecules converted to N_2 per second per Cu ion

ZSM-5 had Si:Al ratios of 20 and more - this effect of zeolite aluminium content is discussed in Section 2.4.6. below). The large pores which exist in zeolite-Y would suggest that pore diameter is not the determining factor for catalytic activity in zeolites. However, pore structure could affect the accessibility of gas molecules since ZSM-5 has a 3-dimensional pore structure while the channels in mordenite only extend in 1-dimension. In addition to the orientation and shape of the zeolite channels, one would intuitively consider the location of the exchanged cations and the stability of particular sites to affect catalytic activity.

Iwamoto *et al.* (1986) suggested that zeolite structure was not the determining factor in zeolite activity but rather, the aluminium content was. A more elaborate explanation was later offered (Iwamoto, 1991a), which separated the influence of the zeolite structure on the "effectiveness" of Cu^{2+} ions from the influence of framework aluminium on those copper ions which were considered to be accessible and "effective". Employing temperature programmed desorption (TPD) of nitric oxide, Kagawa *et al.* (1980) suggested that 85-95% of Cu^{2+} ions exchanged into ferrierite and ZSM-5 were active for NO adsorption while only 40-45% of the copper ions in L-type and mordenite were useful (Iwamoto 1991a).

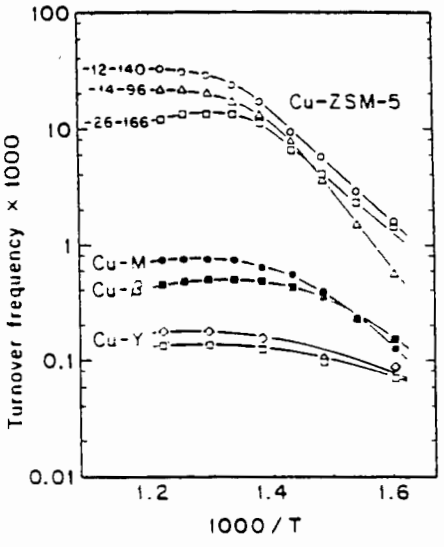

Arrhenius plots for NO decomposition over Cu-zeolites. The inlet concentration of NO was 4% in He. The total pressure was 1 atm. The turnover frequency is defined as the number of NO molecules converted to N_2 per second per Cu ion.

***Figure 2.12** Arrhenius plots for NO decomposition (Li and Hall, 1991)*

In the interpretation of Figure 2.13, Iwamoto *et al.* (1986) proposed that the NO conversion above 30% Cu^{2+}- exchange in zeolite-Y corresponded to the filling of supercage extraframework sites. In contrast with this, the steady increase in conversion over mordenite and ZSM-5 at lower copper exchange levels was taken as an indication that the catalytically active copper sites were located in positions which were all equally accessible/utilized in the decomposition reaction.

Two explanations were offered for the sigmoidal conversion versus exchange graph for NO conversion over Cu-ZSM-5 (Figure 2.13). Firstly, only particular sites were active for the decomposition reaction and these would only be filled by copper ions at sufficiently high exchange levels. The second suggestion was that two adjacent active sites were required for NO decomposition and this was only attained with sufficiently high copper contents.

This copper-pair concept may possibly be linked to the results of gravimetric studies by Li and Hall (1991). Their study indicated a redox capacity of 0.5 oxygen atoms per copper on Cu-ZSM-5, suggesting that adjacent Cu atoms are bridged by an oxygen atom. Although this bridging may be easily visualized in a structure such as zeolite-Y which has a high aluminium content and many extraframework sites which may be occupied, the high Si:Al ratios of ZSM-5 present a difficulty in this interpretation. In spite of this, the presence of Cu^{+}-Cu^{+} dimers as reported by Iwamoto *et al.* (1991d) and the suggestion of the Cu^{+}-O^{-}-Cu^{+} species as the active sites for the NO decomposition, were consistent with Li and Hall's findings.

2.4.5. THE EFFECT OF COPPER CONCENTRATION

Increasing the copper content of a particular zeolite has been shown to enhance its specific activity (measured as TOF) for the NO reduction reaction (Li and Hall, 1991). This again serves as evidence that the reaction is associated with copper sites. The effect of copper concentration on NO conversion is shown in Figure 2.13 for ZSM-5, mordenite, zeolite-X and -Y (Iwamoto *et al.*, 1986).

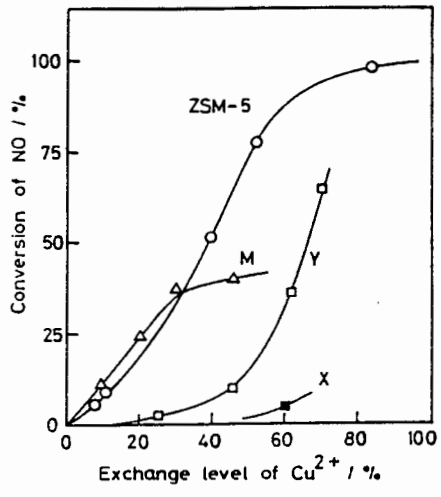

Influence of the exchange level of cupric ions on the catalytic activity of the zeolite. The reaction temperature was 823 or 873 K and the contact time was 4.0 g·sec·cm^{-3}. The mother zeolites were ZSM-5-23.3, M-10, Y-5.2, and X-2.1, respectively.

***Figure 2.13** The effect of copper content on NO conversion (Iwamoto et al., 1986)*

The degree of copper exchange is related to the aluminium content (Si:Al ratio) of the zeolites. Thus, for the zeolites shown, 80% exchange in the ZSM-5 has approximately as much copper as 34%, 18% and 7% exchange for mordenite, zeolite-Y and -X respectively. The data in Figure 2.13 indicates that with the same amount of copper (rather than level of exchange),

mordenite has less than half the activity of the ZSM-5 while that of zeolite-Y and -X is negligible.

As displayed by Figure 2.14, Iwamoto *et al.* (1991d) were able to achieve increased selectivity[6] to nitrogen and oxygen with increasing amounts of copper up to a theoretical "150% copper exchange" as calculated by equation (2.10). Thus, even though the copper content was in excess of that required by charge balancing stoichiometry, these data were taken to indicate that the "excess" copper was still catalytically active.

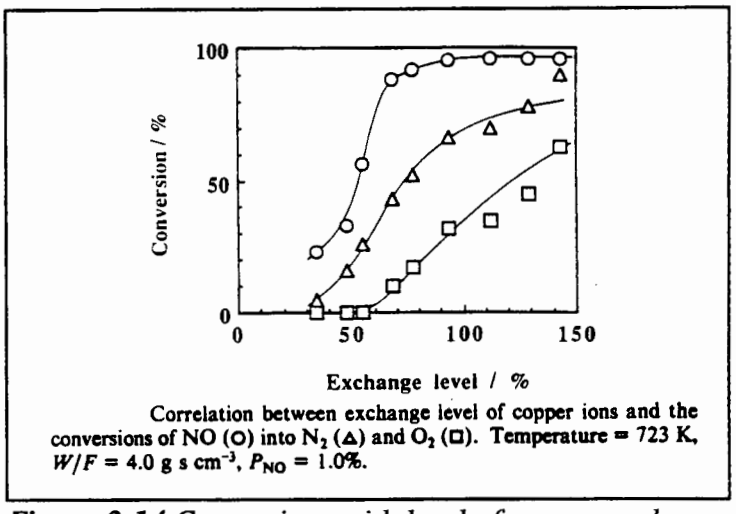

Correlation between exchange level of copper ions and the conversions of NO (O) into N_2 (△) and O_2 (□). Temperature = 723 K, W/F = 4.0 g s cm^{-3}, P_{NO} = 1.0%.

Figure 2.14 Conversions with level of copper exchange (Iwamoto et al., 1991d)

The form and location of these "excess" copper ions and their specific catalytic role has not been elucidated.

2.4.6. THE EFFECT OF Si:Al RATIO

The data in Figure 2.15 led Iwamoto *et al.* (1986) to conclude that the activity per cupric ion exchanged into the zeolite was dependent on the Al content of the base zeolite and independent of the zeolite structure. Furthermore, as already described in Section 2.4.4, Iwamoto (1991a) considered catalytic activity on the basis of copper ions which were deemed *accessible* to NO, as a function of zeolite aluminium content. His calculations indicated higher reaction rates for lower aluminium contents and his results also indicated that the reaction rates over mordenite and ZSM-5 were the same. Hence, zeolite structure was taken to affect only the "effectiveness" or accessibility of copper ions while the activity of the metal ions was considered to be controlled by the zeolite aluminium content.

This dependency on Al content indicates that besides dictating the exchange capacity of a zeolite, the Si:Al ratio of a particular zeolite affects the catalytic activity of the Cu ions. This may perhaps be analogous to the phenomenon that Bronsted acid site strength increases with increasing Si:Al (Barthomeuf, 1991).

[6] Selectivity defined as: Ratio of amount of one product (N_2) to another (NO_2), Smith (1981)

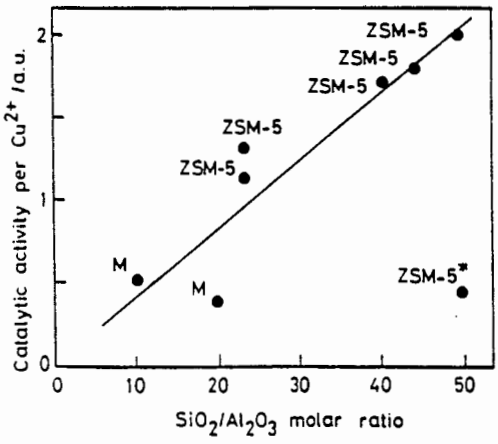

Correlation between the Al content of each mother zeolite and catalytic activity per cupric ion exchanged into the zeolite. The asterisk (*) indicate that only the ZSM-5 zeolite was prepared by using TPA·Br.

***Figure 2.15** Specific activity versus Si:Al ratio (Iwamoto et al., 1986)*

Iwamoto *et al.* (1986) noted that ZSM-5 synthesized with the template TPA-Bromide, yielded a lower specific activity (units not described) than template-free ZSM-5 preparations. The single data point is shown in Figure 2.15. It was suggested that the TPA Bromide or other organic compounds could have altered the distribution and location of aluminium and cation sites.

While data collected by Li and Hall (1991) indicate that the activity of a specific zeolite is a function of copper concentration (discussed in Section 2.4.5.), it is not clear whether this phenomenon was taken into account in obtaining the data shown in Figure 2.15.

Li and Hall (1991) examined the activity of a dealuminated zeolite-Y (Si:Al = 6.6) and unlike Iwamoto *et al.*, suggested that Si:Al ratio was not a controlling factor since its activity was similar to that of zeolite-Y with a Si:Al ratio of 2.5. Indeed some of Li and Hall's data contradicts results obtained by Iwamoto *et al.* (1986, 1991a).

Data obtained by Li and Hall (1991) are shown in Table 2.3. Although Cu-ZSM-5-14-96 had a *lower* Si:Al ratio and 4% more copper than Cu-ZSM-5-26-166, the former yielded a 50% higher rate and turnover frequency.

As calculated by Li and Hall (1991), TOF is an average measure which inherently assumes that all copper ions contained within a zeolite are equally active. Thus, TOF as such, does not explicitly account for the activity of the copper dimers discussed in Section 2.3.4.

That total copper content, as suggested by Li and Hall (1991), and not aluminium content determines the activity of zeolite decomposition catalysts, demands that catalysts have identical copper contents if their activities are to be compared.

Table 2.3 Rates for NO decomposition at 773K and Activation Energies (Li and Hall, 1991)

Catalyst	Rate[b] (mol · NO/g-min)	Cu loading (mol · Cu/g)	TOF × 1000	E_a[c] kcal/mol
Cu-Z-12-140	1.39×10^{-3}	8.2×10^{-4}	28.2	22
Cu-Z-14-96	6.15×10^{-4}	5.1×10^{-4}	20.1	29
Cu-Z-21-114	5.39×10^{-4}	4.2×10^{-4}	21.4	26
Cu-Z-26-166	3.91×10^{-4}	4.9×10^{-4}	13.3	17
Cu-Z-24-76	1.66×10^{-4}	2.5×10^{-4}	5.66	17
Cu-M-5-62	3.52×10^{-5}	7.9×10^{-4}	0.74	17
Cu-Y-2.5-74	1.62×10^{-5}	1.56×10^{-3}	0.17	5
Bulk Co_3O_4[d]	3.05×10^{-6}	—	—	28
Bulk CuO[e]			0.25	8

[b] Moles of NO which have been converted to N_2, i.e., decomposition rates.

[c] The apparent activation energies are for the linear parts of the Arrhenious plots for the lower temperature region.

[d] Data taken from Ref. (*14*) and the inlet pressure of NO was extrapolated to 4% of an atmosphere with the assumption that the reaction was first order to NO.

[e] Data taken from Ref. (*4*). The reaction temperature was 873 K, and the inlet pressure of NO was extrapolated to 4% of an atmosphere based on the first order of NO pressure dependence. Z represents ZSM-5.

2.4.7. THE EFFECT OF TEMPERATURE

Upon initial adsorption onto Cu-ZSM-5, nitric oxide has been found to decompose to nitrogen and oxygen even at room temperature. However, the reaction is not sustained and ceases upon complete adsorption/surface coverage by NO. Iwamoto *et al.* (1986) explained that with initial reaction, the active sites were poisoned by the oxygen produced. This oxygen could only desorb at higher temperatures, thus rendering the sites unavailable for further NO adsorption and decomposition at room temperature. TPD studies on the NO/Cu-ZSM-5 system by Li and Armor (1991) showed that the onset of sustained NO decomposition over Cu-ZSM-5 is approximately 350°C - the temperature at which oxygen begins to desorb from the catalyst.

Li and Hall (1991) found that activity (measured in terms of TOF), increased with temperature, levelling off at temperatures greater than 500°C. The data were repeatable upon lowering and increasing the reaction temperature back up to 550°C, which suggested that no structural damage of the catalyst was incurred.

Iwamoto *et al.* (1991d) achieved maximum selectivity to nitrogen and oxygen around 500°C. Both NO conversion and nitrogen selectivity were found to fall at higher temperatures (Figure 2.16). As with Li and Hall's (1991) data, the decreased activity was not permanent and

was regained on decreasing the reaction temperature. This phenomenon was not well explained and was attributed to a "...reversible change of the structure of active site(s) and/or adsorbability of NO". The presence of nitrous oxide below 400°C, which was described in Section 2.4.3, is visible in Figure 2.16.

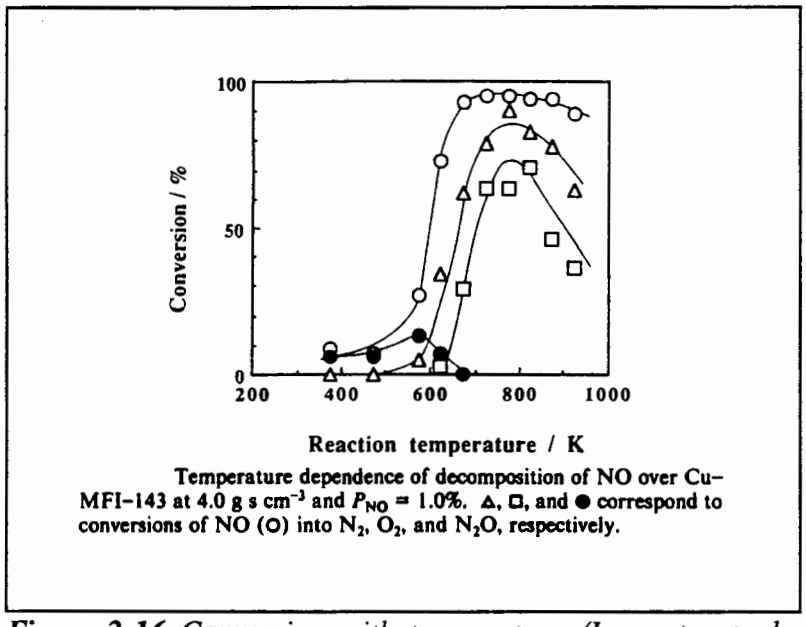

Temperature dependence of decomposition of NO over Cu-MFI-143 at 4.0 g s cm^{-3} and P_{NO} = 1.0%. △, □, and ● correspond to conversions of NO (○) into N_2, O_2, and N_2O, respectively.

Figure 2.16 *Conversion with temperature (Iwamoto et al.,* 1991d)

2.4.8. REACTION KINETICS

Li and Hall (1991) determined a first order rate dependence on NO concentration for temperatures between 350 and 550°C. A negative reaction order was determined for oxygen which was found to be dependent on temperature. The reaction was described by a Langmuir-Hinshelwood rate equation of the form:

$$r = \frac{d[N_2]}{d\tau} = \frac{k[NO]}{1 + K[O_2]^{1/2}} \qquad (2.14)$$

Since the concentration of surface vacancies (reduced sites) was controlled by the rate of spontaneous desorption of O_2, the reaction rate was determined to be limited by the rate of reduction of the catalytic sites (Cu^{2+} -> Cu^{+}) by the desorption of O_2.

The activation energies obtained by Li and Hall (1991) for the reaction over Cu-ZSM-5 (Table 2.3) range between 17 and 29 kcal/mol. With the exception of that for the sample Cu-ZSM-24-76, the activation energies are seen to decrease with an increase in percent copper exchange (the amount of non-stoichiometric or excess copper), irrespective of Si:Al ratio. These data have been reproduced in Table 2.4 and indicate that the "excess" (over 100% exchange)

copper plays a significant role in the reaction mechanism. The influence of copper content on the rate of oxygen desorption is discussed further in Section 2.4.10 which describes the mechanism of the direct decomposition reaction.

2.4.9. THE EFFECT OF WATER AND SO_2

Both water and SO_2 are encountered in flue gas and automotive exhausts and their impact on NO reduction must therefore be considered. Although water has been found to decrease NO conversion, the effect is not permanent and catalytic activity can be regained by excluding water from the reactants (Li and Hall, 1990 and Iwamoto *et al.*, 1991a).

Table 2.4 Activation energies for the direct decomposition reaction over Cu-ZSM-5 (Li and Hall, 1991)

Catalyst	E_a *kcal/mol*
Cu-Z-24-76	*17*
Cu-Z-14-96	*29*
Cu-Z-21-114	*26*
Cu-Z-12-140	*22*

In contrast, the introduction of SO_2 (concentration not given) to Cu-ZSM-5 between 400 and 650°C has been found to poison the activity of the catalyst completely. However, the catalytic activity could be restored by regeneration in a helium stream at 700°C (Iwamoto *et al.*, 1991a; 1991d).

With the use of X-ray absorption near edge spectra (XANES) and Extended X-ray absorption fine structure (EXAFS), Hamada *et al.* (1990b) determined that $CuSO_4$ crystals were not formed upon contact with SO_2 and suggested that the deactivation could have been a result of SO_4^- ions preventing NO adsorption by "surrounding" the copper sites. Upon regeneration of the deactivated catalyst by heating to 700°C, the catalyst was returned to its original state.

In contrast to ZSM-5, Iwamoto (1991a) found that the framework structures of zeolite-Y and mordenite were destroyed by the reaction with SO_2 at elevated temperatures and the catalytic activity could thus not be regenerated. Since the structures of mordenite and ZSM-5 are both based on 5-1 sbus (refer section 2.2.3), a similar destruction of the ZSM-5 framework might be expected. This resistance to SO_2 poisoning presents a clear advantage of ZSM-5 over mordenite and zeolite-Y.

2.4.10. REACTION MECHANISM - COPPER (I) AS THE ACTIVE SITES

Li and Hall (1991) explained that the sustained ability of Cu-ZSM-5 to decompose NO lies in the fact that oxygen produced in the reaction is able to continuously desorb from the active sites at high temperature, renewing sites required for NO decomposition. Electron spin resonance spectroscopy confirmed that a reduction of Cu^{2+} to Cu^+ accompanied this spontaneous

desorption of O_2 from the catalyst. Thus the reaction was based on the oxidation/reduction capacity of copper ions within the zeolite structure.

The catalyst was found to be almost completely oxidised at steady state and thus, although the active sites (Cu^+) amounted to less than 10% of the total zeolite copper content, the presence and number of these Cu^+ centres were maintained at steady state by a balance of oxidation rate and O_2 desorption rate. Evidence of this steady state concentration of Cu^+ was exhibited by the same steady state NO conversion and selectivity to N_2 which was achieved over catalysts which were either pre-reduced (to Cu^+) or pre-oxidized (all copper as Cu^{2+}).

The pre-reduced copper catalyst (Cu^+) was exposed to pulses of NO and initially there was complete selectivity to N_2. With progressive reaction, selectivity to nitrogen decreased to a steady state value while NO conversion remained almost complete. No oxygen was detected downstream and it was considered to have been consumed in the oxidation reaction with NO. Hence, initially the oxygen atoms produced by the decomposition were used to oxidise the catalyst (Cu^+ -> Cu^{2+}) and after saturation, they desorbed as oxygen molecules which reacted with unconverted NO.

Gravimetric studies by Li and Hall (1991) led them to believe that a Cu-ZSM-5 with low copper exchange had lower steady state activities and a lower spontaneous oxygen desorption rate than one with a greater copper concentration. This was supported by Li and Armor (1991), who compared nitric oxide TPD profiles of Cu-ZSM-5 with two different exchange levels. The results indicated that some oxygen from the catalyst with the lower copper concentration desorbed at a higher temperature than the other catalyst. Hence it was suggested that the additional copper contributed to O_2 desorption.

It is suggested here, that this phenomenon could be linked to a distribution of active site strengths. Initial amounts of copper exchanged into the zeolite framework would take up the strongest sites (Barthomeuf, 1991); these would presumably also be the strongest oxygen adsorption sites. Thus, any additional copper would take up the weaker sites and facilitate oxygen desorption and enhance the reaction.

In agreement with Li and Hall, Iwamoto *et al.* (1986) proposed that Cu(I) ions were the catalytically active sites. Carbon monoxide adsorbs selectively and permanently onto Cu^+ at room temperature. Iwamoto *et al.* (1986) observed that nitric oxide decomposition did not occur and NO^- adsorption bands were not observed on a catalyst sample which had been pre-exposed to CO while, in the presence of Cu^+ in the Cu-ZSM-5, the NO^- species were evident.

Iwamoto *et al.* (1986) proposed a reaction cycle, believing that
1) Cu(I) ions are the active sites and
2) NO^- (nitrosyl) species are reaction intermediates.

Adjacent pairs react, yielding nitrogen, oxygen and cupric ions according to:

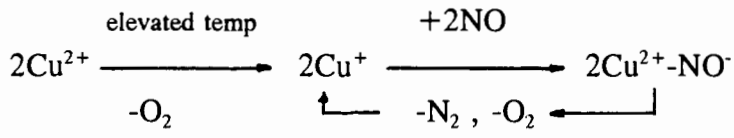

Shelef (1992) questioned this oxidation/reduction cycle and proposed a mechanism based on the active sites consisting of co-ordinatively unsaturated cupric ions in a square planar configuration on which NO molecules are chemisorbed in the gem-dinitrosyl form.

The reaction mechanism remains controversial with Hall and Valyon (1992) conceding that although the mechanism proposed by Shelef may be possible, evidence obtained by Li and Hall (1991) and Valyon and Hall (1992) suggests strongly that a redox mechanism is operative. Hall and Valyon (1992) proposed that the reaction proceeds on single Cu^+ ions by forming first the mononitrosyl then the gem-dinitrosyl which decomposes into N_2 O leaving and oxygen atom behind.

From their infrared studies, Valyon and Hall (1992) suggested that a possible equilibrium exists between the species shown in Figure 2.17 ("*S*" represents a reduced copper site).

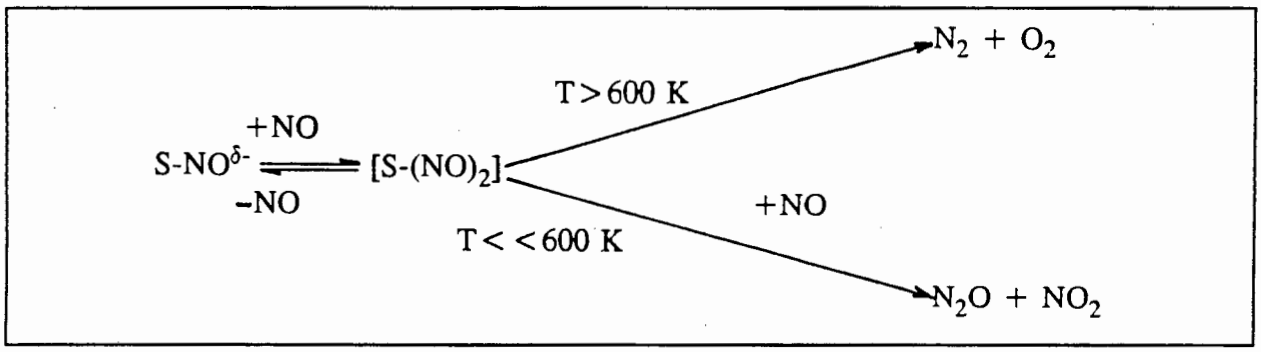

***Figure 2.17** Possible pathways for the decomposition of nitric oxide over Cu-ZSM-5 (Valyon and Hall, 1992)*

Mastikhin and Filimonova (1992) suggested a similar pathway incorporating the disproportionation of nitric oxide to N_2O, NO_2 and N_2O_3. Nitrogen would be formed from the decomposition of N_2O_3 in the following manner:

$$N_2O_3 + NO \rightarrow N_2 + NO_2 + O_2 \qquad (2.15)$$

Li and Armor (1991) suggested from their adsorption studies on Cu-ZSM-5 at 25°C, that NO disproportionates to N_2O and NO_2 with further decomposition of the N_2O to the products, N_2

and O. This oxygen was then available to oxidize the catalyst or react with NO to yield NO_2. Any remaining N_2O desorbed at higher temperatures. No nitrogen dioxide was recorded as a reaction product and it was suggested that any NO_2 formed, did not desorb as NO_2 but decomposed to NO and O at higher temperatures and desorbed as NO and O_2 at about 360°C. The similarity between the TPD profiles of NO and NO_2 suggested that NO_2 was implicated in the decomposition reaction.

It is clear that the mechanism of the direct decomposition remains uncertain. However, Li and Hall (1991), with their data, have presented the most convincing arguments for a mechanism involving the reduction and oxidation of copper ions with the reaction rate limited by the rate of oxygen desorption.

2.4.11. CONCLUDING REMARKS

Inconsistencies are evident in the comparison of the results of the investigations which have been reviewed. The reaction mechanism remains disputed, but a credible interpretation of experimental evidence has been offered. The inquiry into the direct decomposition reaction has revealed that the conversion to nitrogen is intrinsically stoichiometric and the significance of the oxidation reaction to produce nitrogen dioxide has been identified. Also, various aspects of zeolite structure have been explored as potential limiting factors of catalytic activity, yet, a clear understanding of the particular efficacy of Cu-ZSM-5 as a catalyst remains to be achieved. The properties of zeolites which have been noted as possible influences on catalytic activity are:

- Pore size
- Channel configuration
- Si:Al ratio (Aluminium content)
- Location/accessibility of cations at extraframework positions
- Copper content/level of exchange

and should be noted for the forthcoming discussions on the activity of zeolites for the SCR reaction.

The direct, stoichiometric decomposition of nitric oxide to nitrogen and oxygen remains the most attractive route to NOx reduction since it does not require co-reactants and produces no undesired by-products. However, Iwamoto and Hamada (1991c) have conceded that present NO decomposition catalysts (Cu-zeolites) do not have sufficiently high activity for practical implementation. There is little indication that the required 1 to 2 orders of magnitude increase can be achieved. Increasing temperature to enhance the reaction kinetics is not feasible since a decrease in activity occurs above 600°C. It has thus been suggested that the higher reaction rates afforded by the selective catalytic reduction using hydrocarbons are more practical. This process is essentially aimed at automotive NOx control, the reducing agent being supplied by unburnt fuel.

2.5. THE SCR OF NOx WITH HYDROCARBONS OVER ZEOLITES

2.5.1. INTRODUCTION

A number of hydrocarbons have been used as reducing agents for the SCR of NOx. Hamada *et al.* (1990a) and Iwamoto *et al.* (1991b) investigated the use of propane and propene and Sato al (1991) used ethene because it is the predominant hydrocarbon in gasoline and diesel engines.

The reaction products are nitrogen, water, carbon dioxide and carbon monoxide. Using Cu-ZSM-5 and propane as the reducing agent, Iwamoto *et al.* (1991b) did not detect any nitrous oxide as a reaction product in the temperature range 200-600°C. However, Hamada *et al.* (1990a) noted the formation of small amounts of nitrous oxide over H-form zeolites when using propane and propene. This suggests a significant difference in the reaction mechanisms over the two types of catalyst.

Teraoka *et al.* (1992) used ethene as the reducing agent and did not detect any carbon monoxide above 400°C and reported the overall reaction stoichiometry as:

$$2xNO + yC_2H_4 + (3y-x)O_2 \rightarrow xN_2 + 2yCO_2 + 2yH_2O \qquad (2.16)$$

NOx conversions may be diminished by the oxidation of the reducing agent (hydrocarbon), to CO and CO_2, similar to the observed decrease in NOx conversion due to the increase in the catalytic oxidation of ammonia at high temperature (as noted in Section 1.5.2.). While the oxidation of ammonia produces NO, thereby increasing total NOx, the SCR reaction with hydrocarbons is directly affected by a loss of the reducing agent through its preferential consumption by oxidation. Hamada *et al.* (1990a) have observed that besides ammonia, no other reducing agents have been shown to be as selective as hydrocarbons.

In contrast with findings for the direct decomposition reaction, it has been observed for the SCR with hydrocarbons, that Na-ZSM-5 (Hamada *et al.*, 1990a and Sato *et al.*, 1991) and silicalite (Hamada *et al.*, 1990a) offers significant catalytic activity.

2.5.2. THE EFFECT OF ZEOLITE STRUCTURE

Hamada *et al.* (1990a) investigated the use of H-form zeolites using propane and propene as reducing agents. It was found that mordenite was more active than ZSM-5, followed by zeolite-Y. It should however be noted that, the H-mordenite contained more aluminium (Si:Al=10.1) than the ZSM-5 sample (Si:Al=31.4). While investigating these two zeolites with a more comparable number of acid sites, Sasaki *et al.* (1992) found H-ZSM-5 (Si:Al=17) and H-mordenite (Si:Al=10) to have very similar activities.

With the addition of copper, Sato *et al.* (1991) observed that at 250°C (the optimum temperature for both ZSM-5 and mordenite with ethene), the reactivity of copper exchanged zeolites was highest for ZSM-5 followed by mordenite, followed by L-type and ferrierite (Mordenite with a Si:Al ratio of 9.5 (110% exchange) contained more copper than the ZSM-5 which had a Si:Al of 11.7 and only 60% copper exchange). However, the margins in the difference in catalytic activity of the various zeolites were small. The conversion to nitrogen over Cu-ZSM-5 was only 19% greater than Cu-mordenite. This amount is much less significant than the approximately 180% increase in NO conversion using Cu-ZSM-5 rather than Cu-mordenite for the direct decomposition reaction (with same copper content) (refer Figure 2.13 in section 2.3.5). Alternatively, one could consider the two orders of magnitude difference in TOFs between Cu-mordenite and Cu-ZSM-5 recorded in Figure 2.12 from Li and Hall (1991).

These results suggest that zeolite structure/type does not play as significant a role in the SCR with hydrocarbons. When compared with the dependency of the direct decomposition reaction on zeolite type, the relative insensitivity of the SCR reaction to zeolite type is unexpected. Such an insensitivity to zeolite type would immediately suggest a homogeneous *gas phase* reaction rather than a catalytic reaction! However, a close comparison of the conversion data over wide range of catalysts *viz*, silicalite, Na-ZSM-5 and H-zeolite-Y (Hamada, 1990a) indicates otherwise. It would seem that a type of reaction mechanism, distinctly different from that for the direct decomposition reaction exists.

2.5.3. THE EFFECT OF COPPER CONCENTRATION

Sato *et al.* (1991) compared Cu-ZSM-5 with H-ZSM-5 (using ethene) and their data in Figure 2.18 show that they both had similar activity. Again, this result is in direct contrast with that for the direct decomposition catalysts. H-ZSM-5 has been shown to have insignificant activity for the direct decomposition reaction when compared with its copper containing counterpart (Section 2.3.2.).

Notwithstanding this relative insignificance of copper (in comparison to the H-form), Sato *et al.* (1991) investigated the effect of copper concentration on the nitric oxide reduction reaction over ZSM-5. It was found that found that activity increased to an optimum at 100% exchange and decreased slightly with greater copper loading - unlike the effect of excess copper exchange for the direct decomposition reaction (Section 2.4.5). Physical obstruction of the zeolite channels by copper ions is not plausible since the ionic radius of Cu(II) is of the order of 0.073 nm (Lof, 1987) compared with pore diameters of abut 0.55 nm for ZSM-5 (see Section 2.2.3).

Data taken from "Table 1" from Sasaki *et al.* (1992), shows that with propane, H-ZSM-5 is substantially more active than Cu-ZSM-5 for the SCR reaction. Cu-ZSM-5 was found to be very efficient for the "undesirable" oxidation reaction, giving essentially complete conversion of the

hydrocarbon above 300°C. Above 500°C, only carbon dioxide was detected in the reactor effluent, no CO (Iwamoto *et al.*, 1991b). These results suggest that the significance of copper, is dependent of the particular hydrocarbon used.

2.5.4. THE EFFECT OF TEMPERATURE

The effect of reaction temperature (Figure 2.18) observed by Sato *et al.* (1991) is interesting, with different cations yielding similar activities but in very different temperature windows. It would appear that a reactant limitation existed in the case of reaction over Ag-MFI-90[7] which is apparently the most active catalyst among those examined.

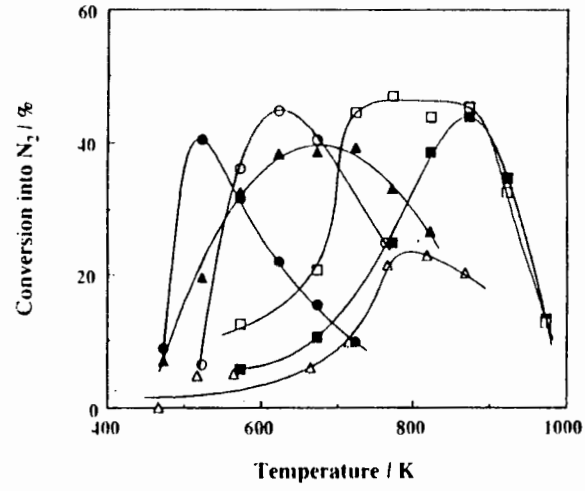

Temperature dependence of the catalytic activities of various cation-exchanged ZSM-5 zeolites and alumina. Catalyst weight, 0.5 g. NO (1000 ppm), C_2H_4 (250 ppm), and O_2 (2%). Total flow-rate, 150 cm^3 min^{-1}. (●) Cu-MFI-102; (○) Co-MFI-90; (■) Zn-MFI-96; (▲) H-MFI-100; (□) Ag-MFI-90; (△) Al_2O_3.

***Figure 2.18** The temperature dependence of various ions on ZSM-5 for the SCR with ethene (Sato et al., 1991)*

In all cases, an optimum temperature exists, above which conversion to nitrogen decreases as a result of the oxidation of the reducing agent (Sato *et al.*, 1991; Iwamoto *et al.*, 1991b).

In comparison with the optimum temperature of 250°C for Cu-ZSM-5 shown in Figure 2.18 where ethene was used, Iwamoto *et al.* (1991b) found the optimum reaction temperature to be around 400°C when propene was used (also Cu-ZSM-5). Although the data is sparse, the

[7]designation: metal - zeolite type - percentage ion exchange

optimum temperature for reduction with propane over Cu-ZSM-5 was in the region of 250°C (Sasaki *et al.*, 1992).

In contrast, Hamada *et al.* (1990a) observed that the use of propane instead of propene increased the optimum reaction temperature over the hydrogen form of ZSM-5. This result would serve to indicate very different mechanisms over the copper and hydrogen forms of ZSM-5. Furthermore, it is clear that the choice of reducing agent, plays a very significant role in the SCR with hydrocarbons.

These optimum temperatures are lower than the operating temperatures of 300-400°C noted for typical metal oxide catalysts (Section 1.7). For this reason, SCR with hydrocarbons is not suitable for high temperature applications.

The relative rates of the SCR and direct decomposition reactions my be compared by considering that Iwamoto *et al.* (1986) used a catalyst mass to flowrate ratio (W/F) of 4 g.s/ml at 450°C to achieve 50% conversion of 4% NO to nitrogen, while in the present case, in the SCR with propane, Hamada *et al.* (1990a) were able to achieve the same conversion with a W/F of 0.96 g.s/ml (at 300°C -clearly, optimum temperatures were different).

2.5.5. THE EFFECT OF OXYGEN

Iwamoto *et al.* (1991b) observed that the reduction of nitric oxide did not take place in the absence of oxygen over Cu-ZSM-5 using propene. However, conversions were found to increase to a maximum at 1% oxygen and decreased at higher concentrations. This could conceivably, have been attributed to the oxidation of the reducing agent at high oxygen concentrations. Although investigating the use of propane over H-ZSM-5, Hamada *et al.* (1991) found that the effect of oxygen was to increase NO conversion to nitrogen from 1% in the absence of oxygen to 18% in the presence of 10% oxygen and unlike Iwamoto *et al.* (1991b), did not observe an optimum or maximum oxygen concentration.

Notwithstanding the disparity in the effect of oxygen concentration, it is clear that oxygen is required for the SCR reaction.

Sasaki *et al.* (1992) proposed that the beneficial effect of oxygen on the SCR reaction is attributed to either:
1) the partial oxidation of the hydrocarbon, or
2) the oxidation of nitric oxide to NO_2.

The enhancing effect of oxygen will be discussed further with reference to the reaction of nitrogen dioxide and the reaction mechanism.

2.5.6. THE EFFECT OF NITROGEN DIOXIDE

Hamada *et al.* (1991) found that NO_2 was reduced to a greater extent than nitric oxide and that this reaction also took place in the absence of oxygen. In the presence of oxygen, conversion was largely independent of its concentration. This suggests that oxygen required in the reaction mechanism can be supplied by nitrogen dioxide.

The increased conversion obtained when using NO_2 led Hamada *et al.* (1991) to propose that nitrogen dioxide was an intermediate in the reduction reaction and they suggested a reaction scheme incorporating the oxidation of nitric oxide. The role of NO oxidation to NO_2 has been proposed in the face of their own evidence which shows that alumina and similarly H-ZSM-5, do not catalyse the oxidation reaction.

2.5.7. THE EFFECT OF SO_2

Upon addition of SO_2, the catalytic activity of Cu-ZSM-5 was diminished but not completely extinguished. The effect of temperature on NO conversion remained the same (Figure 2.19). 300ppm sulphur dioxide resulted in a 15% decrease in conversion to nitrogen at 500°C. The effect was not permanent and original activity was gradually regained upon exclusion of SO_2 from the feed. The mechanism of the deactivation has not been determined (Iwamoto *et al.*, 1991b).

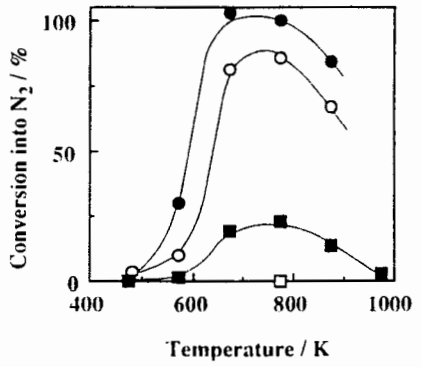

Conversions into N_2 in the $NO+O_2+C_3H_6$ or NO system with or without SO_2. (○) $P_{NO}=530$ ppm, $P_{O_2}=1.0\%$, $P_{C_3H_6}=1000$ ppm, $P_{SO_2}=300$ ppm, $W/F=0.1$ g·s·cm^{-3}, and catalyst: Cu-ZSM-5 (exchange level = 149%). (●) $P_{NO}=500$ ppm, $P_{O_2}=1.0\%$, $P_{C_3H_6}=990$ ppm, $W/F=0.1$ g·s·cm^{-3}, and catalyst: Cu-ZSM-5 (exchange level = 137%). (■) $P_{NO}=1000$ ppm, $W/F=0.3$ g·s·cm^{-3}, and catalyst: Cu-ZSM-5 (exchange level = 152%). (□) $P_{NO}=5500$ ppm, $P_{SO_2}=220$ ppm, $W/F=0.1$ g·s·cm^{-3}, and catalyst: Cu-ZSM-5 (exchange level = 149%).

***Figure 2.19** The effect of SO_2 addition on conversion to N_2 (Iwamoto et al., 1991b)*

2.5.8. REACTION MECHANISM

The reaction mechanism has not been determined, but noting the difference in the results obtained using H-form and copper-form zeolites, Sasaki *et al.* (1992) proposed alternate reaction schemes as follows:

The reaction over H-zeolites was thought to have occurred through the reaction of propane with NO_2 formed from the oxidation of NO in the following way:

$$NO \xrightarrow{+O_2} NO_2 \xrightarrow{+C_3H_8} (C_xH_yO_z) \xrightarrow{+NO_x} N_2 + CO_x + H_2O \qquad (2.17)$$

Because of the high activity for hydrocarbon oxidation, the initial reaction step over Cu-zeolites was proposed as partial oxidation of the hydrocarbon, with subsequent reaction with NO or NO_2 in the following way:

$$C_3H_8 \xrightarrow{+O^*} (C_pH_qO_r) \xrightarrow{+NO\ (or\ NO_2)} N_2 + CO_x + H_2O \qquad (2.18)$$
$$\qquad\qquad\qquad\qquad\qquad\qquad\quad \xrightarrow{+O^*} CO_x + H_2O$$

where O^* represents activated oxygen on the transition metal catalyst.

In a similar way, the effect of oxygen suggested to Montreuil and Shelef (1992) that a partially oxygenated hydrocarbon might be a reaction intermediate. Their investigation with various alcohols, aldehydes, ketones and ethers lent support to this theory.

2.5.9. CONCLUDING REMARKS

The foregoing discussion of SCR with hydrocarbons, reveals a strong dependence on the particular hydrocarbon used and also a distinct difference between the use of the hydrogen or copper form of a zeolite.

While some inconsistencies have been noted, all the work discussed in this section has been published after 1990. Thus, the work in this field is new and incomplete.

Beyond the low operating temperatures of this hydrocarbon process, low selectivities in the consumption of the reducing agent makes this process unsuitable for the oxygen rich environment of furnaces. In addition, the gaseous hydrocarbons are not present in applications such as coal fired boilers, thus, the use of ammonia as a reducing agent is now investigated as a viable means of stationary source NOx reduction.

2.6. THE SCR OF NOx WITH AMMONIA OVER ZEOLITES

2.6.1. INTRODUCTION

The work discussed in this section covers SCR studies conducted as early as 1977 and as recently as 1992. A number of these investigations have been conducted as "field tests", rather than fundamental studies of the reaction mechanism and effects of catalyst composition and catalyst properties.

Earlier work strongly featured the use of zeolite-Y and more recently, mordenite has been studied. Except that which is contained in a 1990 US Patent held by Byrne of Engelhard Corporation, no studies with ZSM-5 have been encountered.

As an indication of the relative scarcity of published work on zeolites, Bosch and Janssen's "Review of the Fundamentals and Technology of Catalytic Reduction of Nitrogen Oxides" published in 1988, refers to only 9 studies of zeolites in comparison to approximately 50 references to vanadium based catalysts and approximately 30 each, of Fe_2O_3 and noble metal catalysts.

These few zeolite studies have been conducted with a number of different catalysts *viz*, H-form, Cu-form, zeolite-Y, mordenite, ZSM-5 and other zeolites, and the experimental conditions varied. Thus, the small body of literature is far from conclusive.

This review of SCR with ammonia maintains as much as possible, the same structure of the review of the direct decomposition reaction covered in Section 2.3. Reaction stoichiometry and the difference between zeolite types are first examined, followed by the effects of framework Si:Al ratio, copper concentration, operating parameters such as temperature and feed gas composition and finally, kinetics and the reaction mechanism are investigated.

2.6.2. REACTION STOICHIOMETRY

Seiyama *et al.* (1977) investigated the reduction of NO with ammonia over Cu-zeolite-Y below 400°C in the absence of oxygen and found that the activity reached a maximum around 120°C, dropping to negligible levels at higher temperatures. Mizumoto *et al.* (1979) noted a significant increase in NO conversion upon co-feeding oxygen and suggested a reaction mechanism different to that described for the oxygen free system. The marked effect on activity even at low temperature can be seen in Figure 2.20.

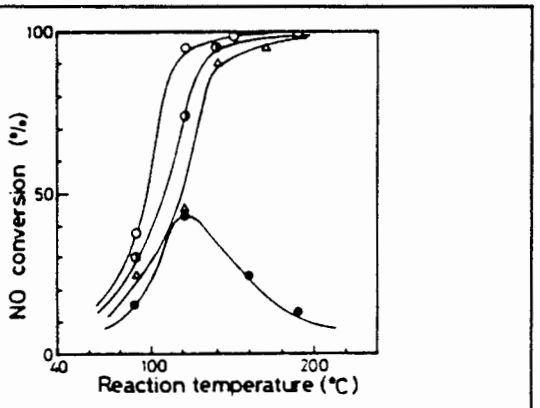

Influence of oxygen on the NO–NH_3 reaction over Cu(II)NaY (64%). SV = 1800 hr^{-1}, p_{NO}, p_{NH_3} = 0.4%, p_{O_2} = 0% (●), 0.3% (△), 2% (◑), 4% (○).

***Figure 2.20** The influence of oxygen on the NO-NH_3 reaction over Cu(II)NaY (Mizumoto et al., 1979)*

In the absence of oxygen, the reaction products of nitrous oxide and nitrogen were observed in a ratio of 1:2 described by the stoichiometry (Mizumoto *et al.*, 1979):

$$4NO + 2NH_3 \rightarrow 2N_2 + N_2O + 3H_2O \qquad (2.19)$$

However, with oxygen as a reactant, nitrogen was observed exclusively - no nitrous oxide was detected (Mizumoto *et al.*, 1979). No evidence of the disproportionation of NO over H-mordenite was observed between 147-407°C by Brandin *et al.* (1989), who suggested that the small and finite amount of nitrous oxide detected, was not a reaction product but was probably adsorbed on the fresh catalyst at room temperature. The disproportionation reaction is described by:

$$4NO \rightarrow N_2O + N_2O_3 \qquad (2.20)$$

and is known to occur over zeolites at ambient temperature and below (Addison and Barrer, 1955; Kasai and Bishop, 1972).

An analysis of the amounts of NO and oxygen consumed and the amount of nitrogen produced by the reaction of NO, NH_3 and oxygen, led Mizumoto *et al.* (1979) to suggest that the overall stoichiometry is:

$$4NO + 4NH_3 + O_2 \rightleftharpoons 4N_2 + 6H_2O \qquad (2.2)$$

which is the reaction describing the SCR of NO.

Unlike the reaction over Cu-zeolite-Y (reaction (2.19)), it is well documented that the presence of oxygen is essential for the SCR of NO over H-mordenite. This has been noted by among others, Brandin *et al.* (1989), Kiovsky *et al.* (1980) and Hirsch (1982).

This oxygen requirement along with an energy balance and an investigation of the effect of varying ammonia to NO feed ratios, led Hirsch (1982) to describe the reaction over H-mordenite with the same stoichiometry proposed by Mizumoto *et al.* (1979) - equation (2.2) above.

In examining the effect of feed oxygen concentration over H-mordenite, Hirsch (1982) observed an increase in NO conversion with oxygen concentration to a maximum at 0.5% oxygen and subsequently determined that this oxygen concentration was limiting (feed NOx=4930 ppm). He correlated O_2 concentration with NO conversion and calculated a theoretical requirement of 1.35% oxygen for complete NO conversion for his particular experimental conditions . This oxygen requirement is far in excess of that demanded by the stoichiometry of reaction (2.2), and was attributed to a rate limitation since the stoichiometry had already been confirmed by way of an energy balance and supported by reactant/product ratios which conformed to the co-efficients of reaction (2.2).

Notwithstanding the small fraction of NO_2 which constitutes NOx emissions from combustion processes, nitrogen dioxide could play an important role in the SCR process. The rate of NO_2 reduction with ammonia was found to be higher than the rate of NO reduction (Brandin *et al.*, 1987), suggesting that higher NOx reduction rates could be achieved if NO was first oxidized to NO_2.

By examining the reactant ratios as well as the heat of reaction, Hirsch (1980) proposed the following stoichiometry for the reduction of nitrogen dioxide with ammonia :

$$6NO_2 + 4NH_3 \rightleftharpoons 7N_2 + 12H_2O \qquad (2.6)$$

The stoichiometry does not include oxygen as a reactant. That oxygen is not required for the reduction of nitrogen dioxide was previously noted by Pence and Thomas (1972). Since NO was found not to be reduced in the absence of oxygen, this reaction of NO_2 with ammonia (without oxygen), led Kiovsky *et al.* (1980) to believe that the role of oxygen was to convert unreactive NO to NO_2. The role of nitrogen dioxide and the reaction mechanism are discussed in Sections 2.6.8. and 2.6.11.

2.6.3. THE EFFECT OF ZEOLITE STRUCTURE

Brown and Wootton (1991), final year Chemical Engineering students at the University of Cape Town, sought to contribute to a systematic analysis of the effects of zeolite pore size, channel structure and other zeolite properties on SCR which, up to that date, had not been seen in available literature.

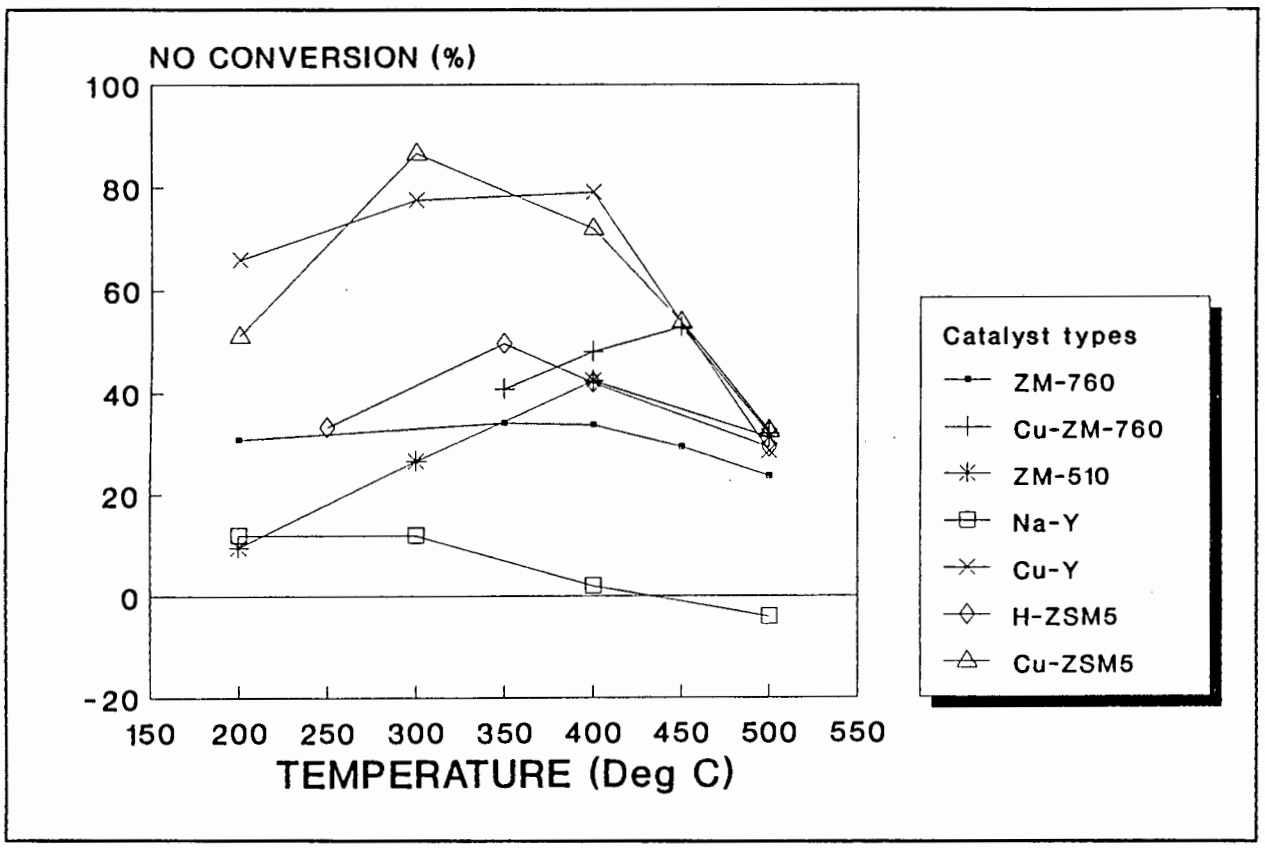

Figure 2.21 Comparison of mordenite, ZSM-5 and zeolite-Y for the SCR reaction with ammonia (Brown and Wootton, 1991)

Their data are displayed in Figure 2.21 which indicates that H-ZSM-5 (Si:Al=46) gave a higher NO conversion than H-mordenite (ZM-760 with Si:Al=60) under similar operating conditions and that Cu-ZSM-5 produced higher NO conversions than Cu-mordenite. Since H-ZSM-5 contained more aluminium (acid sites) than the H-mordenite used, the higher conversions yielded by H-ZSM-5 cannot be considered to indicate that it is more active than mordenite. However, below 400°C, the significantly higher conversion offered by Cu-ZSM-5 over Cu-mordenite may be regarded as an indication of the superiority of ZSM-5 since both zeolites had similar copper contents (by mass). The proposal by Iwamoto *et al.* (1986) that higher Si:Al ratios yield higher activities (see Section 2.4.6.), is not confirmed by these data. The decrease in NO conversion above 450°C and the convergence of 5 of the graphs in Figure 2.21 suggest a limitation due to experimental conditions/procedures rather than being of catalytic significance. Cu-zeolite-Y gave similar conversions to Cu-ZSM-5, but with its high aluminium content, Cu-zeolite-Y had

approximately 12 times the amount of copper contained in the ZSM-5 sample and can therefore be considered to be less effective than ZSM-5 on the basis of copper utilization. These results suggest the following order of activity for the SCR reaction with ammonia:

Cu-ZSM-5 > Cu-mordenite > Cu-zeolite-Y,

which is identical to the order determined for the activity of zeolites for the direct decomposition reaction. Again, the large pores of zeolite-Y suggested that pore size was not a limiting factor and similarly, the one-dimensional channels of mordenite compared with the 3-dimensional pores of zeolite-Y pores, suggested that the pore configuration did not dictate catalytic activity.

Since 1991, Byrne *et al.* (1992) has published a similar comparison of zeolites. Three types of iron (Fe) exchanged zeolites were evaluated. The first was a large pore zeolite with a 3-D pore system and the other two were both medium pore zeolites, one possessing a 2-D and the other, a 1-D pore structure. While Si:Al ratios and metal loadings were not given, the large port, 3-D zeolite gave higher NO conversions than the 1-D zeolite followed by the 2-D medium port zeolite. The higher activity offered by the zeolite with the one-dimensional pore structure over the 2-D structure, suggested that pore structure may not have been the factor which determined catalytic activity.

It should be informative to compare activation energies for reaction over eg. ZSM-5 and mordenite, to examine whether intrinsic differences between these two zeolites exist.

2.6.4. THE EFFECT OF COPPER CONCENTRATION

The catalytically enhancing effect of copper on the H-mordenite has been noted by Nam *et al.* (1988) and Brandin *et al.* (1989). Conversion versus space time data collected by Nam *et al.* for Cu-mordenite at 300°C showed an increase of approximately 24 times over H-mordenite. The increase in NO conversion can be seen in Figure 2.22 .

However, unlike the effect of increased copper concentration for the direct decomposition reaction over Cu-ZSM-5, Nam *et al.* (1978) observed an optimum copper concentration for Cu-mordenite, with activity decreasing at high copper loadings. The optimum occurred at 2.3 wt% copper which corresponded to an exchange of 30% of the initial hydrogen ions. A similar trend was observed by Altomare (1981) - the data are shown in Figure 2.23. It was suggested that the decrease was due to pore plugging at high Cu loadings. Beyond the speculation offered, there was no evidence to support the assumption of pore plugging.

It should be noted that the atomic radius of copper is 0.128 nm (Lof, 1987) and the ionic radii of Cu(I) and Cu(II) are 0.077 and 0.073 nm respectively, in comparison to pore apertures of the order of 0.7 nm for the 12-membered oxygen rings, and 0.57 nm for the 8-membered rings

in mordenite (refer to section 2.2.3.). Thus, pore blockage by copper ions does not seem plausible.

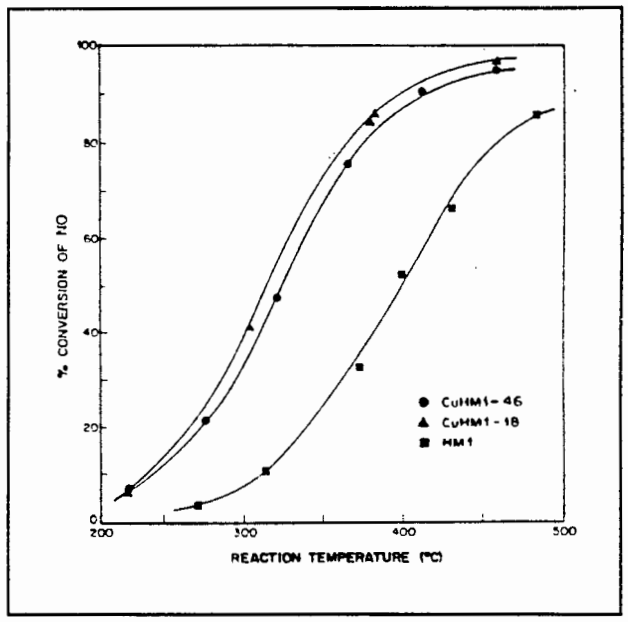

Figure 2.22 The effect of copper addition on NO conversion (Nam et al., 1988)

Investigating ammonia TPD from H-mordenites exchanged with various amounts of copper, Choi *et al.* (1991) observed a strong correlation between the intensity (size) of two ammonia desorption peaks and NO reduction activity. Although catalysts of up to 4.14 wt% (58 mol% exchange) copper were used, cf. optimum of 2.3% recorded by Nam *et al.* (1978), no mention was made of an optimum copper concentration.

In contradiction of their own proposal of an optimum copper concentration, Figure 2.24 with data from Altomare (1981) and Nam *et al.* (1988), displays TOF over Cu-mordenite for similar levels of copper exchange as those shown for the data in Figure 2.23 while no optimum is observed. In addition, reaction rate is seen to decrease with copper exchange and contradicts Choi *et al.*'s (1991) observation that increased copper loading yielded increased ammonia adsorption and increased activity for the SCR reaction.

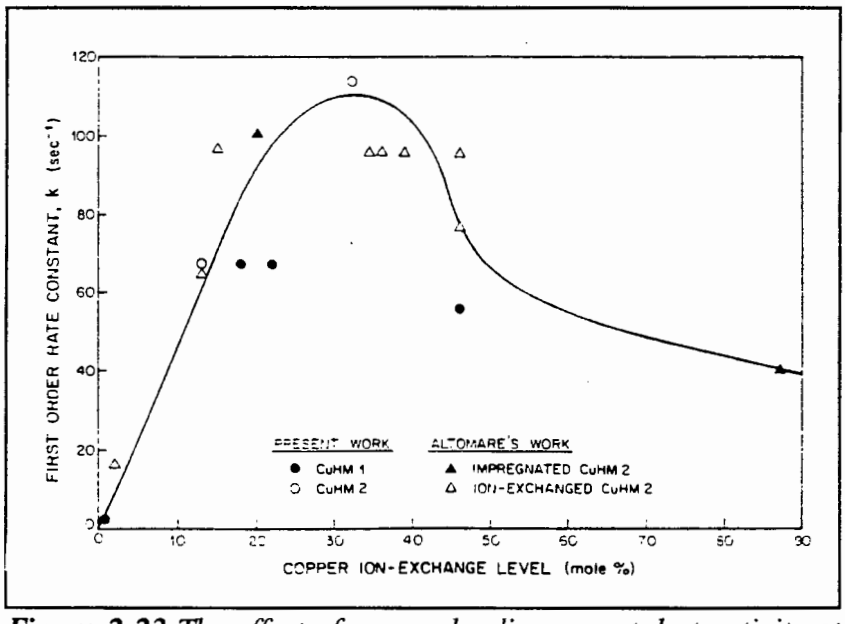

Figure 2.23 The effect of copper loading on catalyst activity at 340°C (Nam et al., 1987)

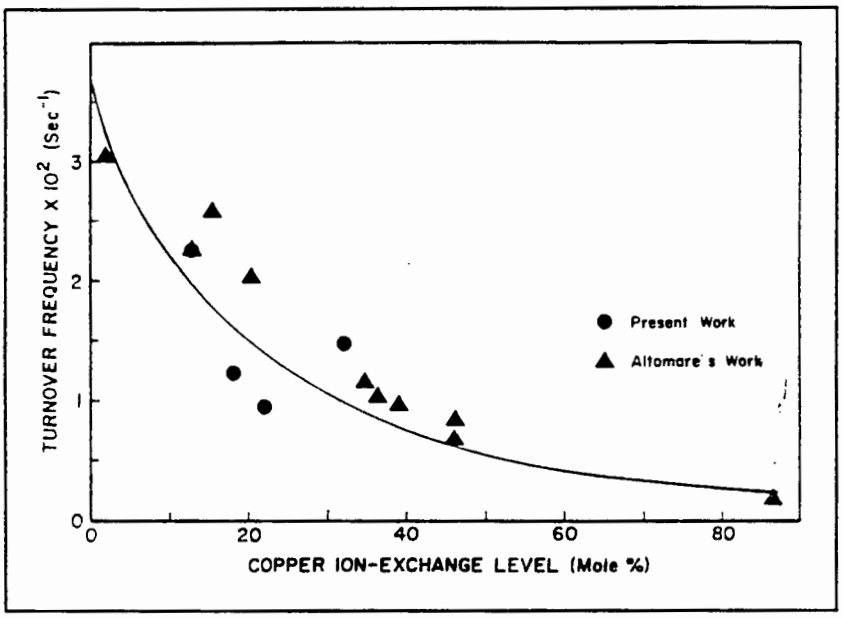

***Figure 2.24** Turnover Frequency of Cu-H-mordenite at 340°C (Nam et al., 1988)*

While preceding paragraphs indicate that the addition of copper to zeolites has been shown to enhance catalytic activity, the evidence of the effect of varying copper concentration is contradictory.

2.6.5. THE EFFECT OF Si:Al RATIO

The effect of Si:Al ratio on copper exchanged catalysts for the direct decomposition reaction was highlighted by Iwamoto *et al.* (1991a), who proposed that zeolite aluminium content dictates the effectiveness of copper ions (refer section 2.3.6.). However, Li and Hall's (1991) results indicated no dependence on aluminium content. While this disparity exists, there is no reason why a similar effect of Si:Al ratio on the direct decomposition reaction, should not be noted in the use of zeolite catalysts for the SCR reaction. Such a study of the effect of Si:Al in different zeolites catalysts for SCR has not been encountered.

If the acid sites are the catalytically active ones, then the discussion of the relationship between Si:Al and number of acid sites in Section 2.2.5, makes it clear that reaction over zeolites will be dependent on framework aluminium content. This dependence was borne by data obtained by Andersson *et al.* (1989), which indicated decreased NO conversion with dealumination of H-mordenite over the entire temperature range examined.

The nature of the active sites is discussed further in Section 2.5.12., which gives some insight into the reaction mechanism.

While no change in calculated activation energies for the SCR reaction was recorded, Andersson *et al.* (1989) found that pre-exponential factors decreased with dealumination of H-mordenite. This was taken to indicate a change in the number of sites but not in the site strengths.

That the number of sites decreases with de-alumination, is consistent with the active sites being associated with the aluminium atoms. However, constant site strengths exhibited by invariant activation energies contradicts Barthomeuf's (1991) maxim that acid site strength increases with increased de-alumination (refer Section 2.2.5). Notwithstanding the disparity in the findings of Li and Hall (1991) and Iwamoto (1991a) on the effect of aluminium content, the evidence offered by Andersson *et al.* does not support Iwamoto's findings which indicate higher activities for higher Si:Al ratios.

2.6.6. THE EFFECT OF TEMPERATURE

The optimum operating temperature for SCR is dictated by the extent of the ammonia oxidation reaction which produces nitric oxide (Nam *et al.*, 1986) according to:

$$4NH_3 + 5O_2 \rightleftharpoons 4NO + 6H_2O \qquad (2.4)$$

This phenomenon is illustrated in Figure 1.6 which shows the optimum operating temperature as being a "trade-off" between the extents of the SCR reaction ((2.2)) and the ammonia oxidation reaction.

Figure 1.10 after Byrne *et al.* (1992) indicates that an attraction of the zeolite used, is the higher maximum operating temperature obtained over the other catalysts shown.

Data recorded by Mizumoto *et al.* (1979) over Cu-Y, indicated the onset of the SCR reaction at temperatures as low as 100°C (Figure 2.20). Above this temperature, complete conversion was rapidly reached under their particular experimental conditions. At higher space velocities, a similarly rapid increase in activity can be observed for both H-mordenite and Cu-mordenite above 150°C in Figure 2.30a (Brandin *et al.*, 1989).

Brandin *et al.* (1989), Haas *et al.* (1989) and Choi *et al.* (1991) all observed a decrease in NO conversion below 400°C over Cu-H-mordenite.

The graph of NO conversion over H-mordenite in Figure 2.30a shows no decrease up to 415°C, the temperature limit of the investigation, and rate constants calculated by Nam *et al.* (1988) for H-mordenites show no decrease up to 540°C, the temperature limit of that study ("Figure 7" by Nam *et al.* (1988)). This evidence would suggest that H-mordenites are able to operate at higher temperatures than their copper containing counterparts. With such scant evidence however, this observation remains unconfirmed.

Brandin *et al.* (1989) examined the ability of H-mordenite to catalyse ammonia oxidation. Below 427°C (the highest temperature studied), no nitric oxide was observed as a reaction product and no nitrogen dioxide or nitrous oxide were detected, nitrogen was the only product. The stoichiometry of this oxidation reaction is:

$$4NH_3 + 3O_2 \rightleftharpoons 2N_2 + 6H_2O \qquad (2.3)$$

No other such studies of the ammonia oxidation reaction were described in conjunction with the SCR investigations.

In their study of a vanadia-alumina catalyst, Nam *et al.* (1986) noted that the activation energy for the oxidation of ammonia to nitric oxide (53.9 kcal/mol) was four times higher than the activation energy for the NO reduction reaction which was 12.8 kcal/mol. A similar comparison for zeolite catalysts has not been seen. Williamson *et al.* (1975) determined an activation energy of 36.7 kcal/mol for the ammonia oxidation reaction over Cu(II)Na-Y.

It seems that a study of the kinetics of these catalytic ammonia oxidation reactions is required in order to gain a better understanding of the optimum/maximum temperatures attainable. Such a study should suggest why higher operating temperatures may be obtained over the zeolite such as those used by Byrne *et al.* (1992), in comparison with the noble metal and vanadium based catalysts (Figure 1.10).

2.6.7. REACTION KINETICS

The SCR reaction over Cu-H-mordenite has been described as a first order irreversible process by Eng (1977), Ganti (1980) and Altomare (1981) and confirmed by Nam *et al.* (1988), with a zero order dependence on ammonia and oxygen concentration.

The activation energy (E_a)of the SCR reaction over mordenites was calculated to be 12.9 kcal/mol, irrespective of copper concentration (Nam *et al.*, 1988). This can be compared to 17.0 kcal/mol calculated by Eng (1977) over Cu-H-mordenite, 12.8 kcal/mol calculated by Ganti (1980), 16.3 kcal/mol obtained by Altomare (1981) - all postgraduate research projects carried out at the University of Massachusetts - and 11.9 kcal/mol obtained by Ham *et al.* (1992).

The constant activation energies obtained by Nam *et al.* (1988) irrespective of copper concentration, is in direct contrast with the data recorded for the direct decomposition reaction over Cu-ZSM-5 (Table 2.3), which reveal a dependence of E_a on percentage copper exchange. On the basis of the location and strengths of the active copper sites, it would be expected that similar observations (trends) be noted for the use of Cu-zeolites for the SCR reaction. The data in the same table also indicate that mordenite and ZSM-5 had similar activation energies, and

it is therefore expected that ZSM-5 should yield a similar activation energy to that over mordenite.

Nam *et al.* (1988) also found that the activation energies for the SCR of NO over H-mordenite and Cu-mordenite were the same, which suggested that the active sites were similar and similar mechanisms were operative.

2.6.8. THE ROLE OF NITROGEN DIOXIDE AND THE EFFECT OF NO:NOx RATIO

While the rate of nitrogen dioxide reduction is greater than that of nitric oxide reduction (Brandin *et al.*, 1989), Odenbrand *et al.* (1987) observed that equimolar NO-NO_2 mixtures gave a higher conversion than either NO or NO_2 alone and patented a process based on this finding. The high activity can be seen in Figure 2.25 over H-mordenite (312°C), both with and without oxygen in the feed. It is important to note that the NH_3:NOx ratio was 1.5, indicating that the reaction/s were not limited by ammonia. A lower than expected NO_2 conversion would prevail in the case where the ammonia present in the feed was less than that demanded by the stoichiometry:

$$6NO_2 + 8NH_3 \rightleftharpoons 7N_2 + 12H_2O \qquad (2.6)$$

which describes the reduction of nitrogen dioxide with ammonia, which differs from the 1:1 NH_3:NO ratio required by the reduction of nitric oxide (reaction (2.2)).

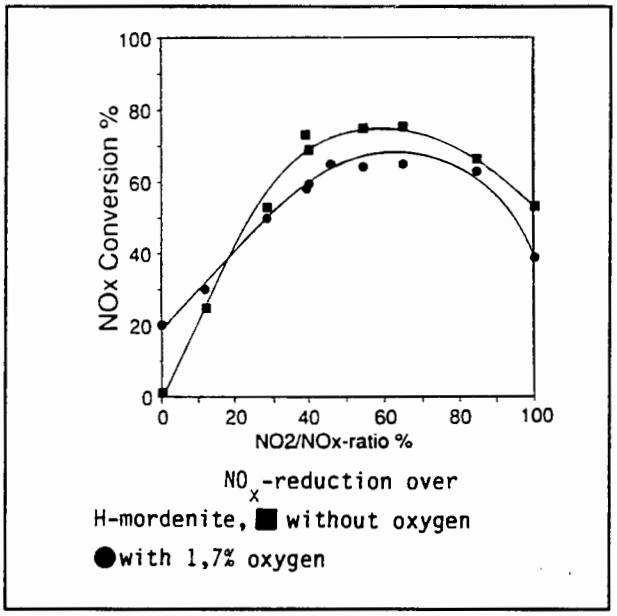

Figure 2.25 *The effect of NO_2:NOx ratio (Brandin et al., 1989)*

According to Active-Site Theory (Levenspiel, 1972), the shape of the two graphs in Figure 2.25, is representative of a classical dual-site reaction controlled by reaction rate rather than reactant adsorption or product desorption. The reaction scheme is shown in Figure 2.26, which suggests that NO and NO_2 react together rather than in the two separate reactions (2.2) and (2.6).

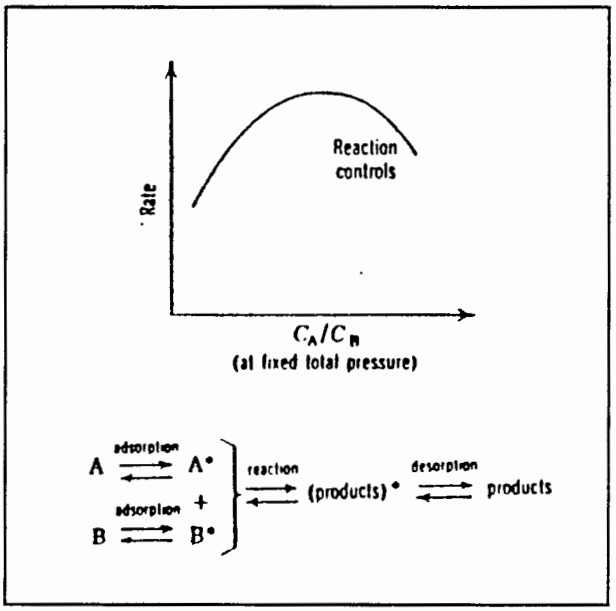

Figure 2.26 *Characteristics of a dual-site reaction (Levenspiel, 1972)*

Hirsch (1982) also investigated the effect of NO_2:NOx feed ratio over H-mordenite in the absence of oxygen and noted a similar increase in NOx conversion with increasing amounts of nitrogen dioxide. For mole ratios of NO_2:NO less than 1:1, conversions showed a linear

response. He observed that two moles of NOx were converted for every mole of NOx present in the feed and proposed a stoichiometry of the form:

$$NO + NO_2 + 2NH_3 \rightleftharpoons 2N_2 + 3H_2O \qquad (2.7)$$

which he considered was equivalent to equation (2.2) if it was recognized that nitrogen dioxide would at high temperature, dissociate into nitric oxide and oxygen by the reaction:

$$NO_2 \rightleftharpoons NO + \frac{1}{2}O_2 \qquad \Delta H = 5.65*10^4 \text{ J/mol } NO_2 \qquad (2.21)$$

That NO_2 decomposes to give NO and oxygen does not seem well founded. It stands to reason that if nitrogen dioxide decomposes to nitric oxide prior to reaction with ammonia, the stoichiometry for the reaction of NO_2 and ammonia should be identical to that described by reaction (2.2). It would be important, to compare the activation energy for the catalytic decomposition of NO_2 and the NO_2/NH_3 reaction (2.6), to determine whether NO_2 would preferentially decompose, rather than react with ammonia.

Kiovsky *et al.* (1980) examined the effect of increasing NO_2:NOx ratios (from 0.5 to 0.92) in the presence of oxygen and water, and observed a continuous increase in NOx conversion. This result contradicts the trend shown in Figure 2.25 taken from Brandin *et al.* (1989). Furthermore, the increase in NOx conversion is not explained by the stoichiometries described in the preceding paragraphs. Firstly, higher NO_2 than NO feed concentrations were used, which defies the 1:1 NO to NO_2 ratio described by reaction (2.7). Since NO would be the limiting reactant, an increase in conversion is not expected. Secondly, since total NOx and the NH_3:NOx ratio were kept constant at 1:1 (rather than 1.3 required by reaction (2.6)), ammonia would be the limiting species, and again, an increase in NOx conversion would not be expected. Although water was shown to decrease conversions, it was not noted as having altered the reaction mechanism.

These studies emphasize the significant role of NO_2 in Selective Catalytic Reduction of NOx and also expose the gaps which exist in the understanding of its catalytic function and use.

2.6.9. THE AMMONIA TO NITRIC OXIDE RATIO

Investigating the optimum NH_3:NOx ratio for NOx mixtures, Hirsch (1982) determined a monotonic increase in this ratio from 1 for a pure NO feed to 1.3 for a pure NO_2 feed (Figure 2.27). The linear trend suggests that the two reactions (2.2) and (2.6) occurred in parallel.

The investigation of reaction (2.7) by Hirsch (1982), took place in the absence of oxygen and in their review paper, Nakatsuji and Miyamoto (1991) also recorded this stoichiometry as being relevant to an oxygen free environment. This condition is supported by the data in Figure 2.27 which suggest that this reaction stoichiometry (reaction (2.7)) does not describe the reduction of NOx in an oxygen containing environment, since the optimum NH_3:NOx ratios for NOx mixtures is greater than the 1:1 ratio implicit in the stoichiometry of equation (2.7).

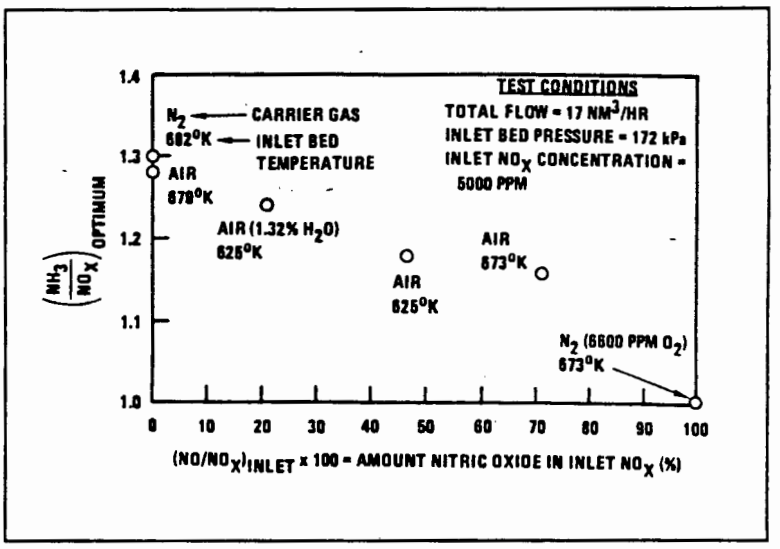

Figure 2.27 The effect of NOx composition on the optimum NH_3:NO_x mole ratio (Hirsch, 1982)

This data also does not support the following stoichiometry:

$$8NO + 4NO_2 + 12NH_3 + O_2 \rightleftharpoons 12N_2 + 18H_2O \qquad (2.22)$$

presented by Nakatsuji and Miyamoto (1991) as the relevant reaction of nitric oxide and nitrogen dioxide in the presence of oxygen, which prescribes an overall NH_3:NOx ratio of 1:1. (Equation (2.22) is the corrected form of equation (2.8) in Section 2.1.)

Yet again, these studies reveal an incomplete understanding of factors affecting the selective reduction of NOx.

2.6.10. THE EFFECT OF WATER AND SO_2 ON THE REACTION

Water and sulphur dioxide are present in flue gas and SO_2 has been noted as a catalyst poison (section 1.7.). Thus, the effect of both of these species on zeolites must be examined if they are to be employed as SCR catalysts.

Using H-mordenite, Hirsch (1982) found that the presence of 1.3% water vapour in the carrier gas had no effect on NOx reduction at a reaction temperature of 350°C (Feed [NO]=5000 ppm). Kiovsky *et al.* (1980) however, recorded a 15% decrease in NOx conversion upon addition of 10% water to the feed at 300°C (Feed [NO]=2500ppm). This inhibition decreased with increasing temperature and was negligible at 400°C.

While these results reveal little or no effect on NO conversion, hydrothermal stability of zeolites must be considered. Zeolites are formed under high temperature and/or pressure in the presence of water. When exposed to these conditions under which they were formed, zeolites tend to a more stable and less porous phase. Thus, over long time periods and extreme conditions, many zeolites will lose their original structure (Dyer, 1988). Byrne *et al.* (1992) showed that after 73 days of hydrothermal ageing at 600°C with 10% water in nitrogen, NO conversion (at 550°C) over a zeolite catalyst (ZNX[8]) was decreased by only 10%.

Catalyst deactivation by SO_2 has been shown to be a function of temperature (Mizumoto *et al.*, 1979; Choi *et al.*, 1991; Ham *et al.*, 1992). No deactivation was observed over Cu-H-mordenite at temperatures above 300°C (Figure 2.28) irrespective of SO_2 concentration (Ham *et al.*, 1992). These workers proposed that the deactivation at low temperature was due to the formation of ammonium salts which caused pore blockage. It was suggested that with similar sulphur contents, catalysts at higher temperatures were not deactivated because the ammonium salts were deposited deep within the pores by the process of capillary condensation, permitting access to the zeolite channels. Ham *et al.* (1992) suggested that the ammonium salts formed could be ammonium sulphate ($(NH_4)_2SO_4$) and/or ammonium bisulphate (NH_4HSO_4).

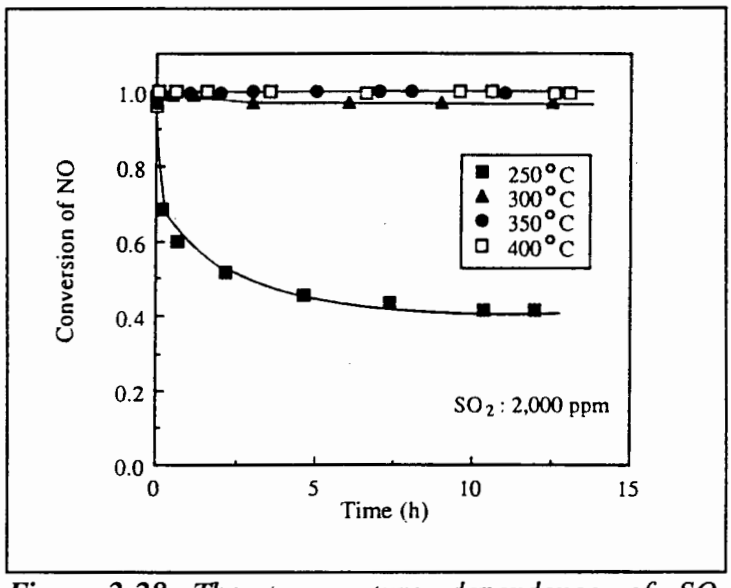

***Figure 2.28** The temperature dependence of SO_2 deactivation on NO conversion for CuHM (Ham et al., 1992)*

The concepts of pore filling and pore blocking are illustrated in Figure 2.29.

In contrast to pore blockage, Mizumoto *et al.* (1979) observed destruction of the Cu-Na-zeolite-Y framework subsequent to exposure to SO_2. It was suggested that SO_2 was catalytically

[8] ZNX™ - Engelhard Corporation, N.J., U.S.A.

oxidized to SO_3 which reacted with NH_3, water and the zeolite framework to yield $(NH_4)_3Al(SO_4)_3$.

While catalytic activity was severely reduced by the effect of SO_2, it was not totally eliminated. The remaining activity was attributed to the ability of remaining copper ions and cupric sulphate to catalyse the reaction. In support of this, the residual activity of the poisoned catalyst was estimated to be of the same order as that of an alumina supported cupric sulphate catalyst (Kasaoka *et al.*, 1975 as cited by Mizumoto *et al.*, 1979).

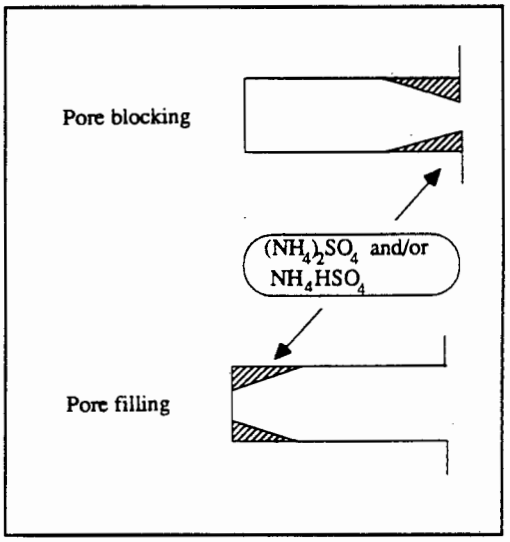

***Figure 2.29** Pore blockage and pore filling (Ham et al., 1992)*

Albeit with a different zeolite, Choi *et al.* (1991) used X-ray absorption near edge spectra (XANES) to investigate the state of copper on mordenite which had been exposed to SO_2 as a reactant, and showed that $CuSO_4$ was not formed. The sulphate species were not conclusively identified and it was suggested that deactivation was a consequence of copper ions which were simply "surrounded" by sulphate ions.

The destruction of the framework as described for zeolite-Y, has not been described in other studies which have been reviewed here. It is well known that zeolite-Y has a low tolerance to mineral acids (Dyer, 1988). The framework aluminium is readily leached and hydrolysed to hexacoordinated species (cf. $(NH_4)_3Al(SO_4)_3$ in which aluminium is also hexacoordinated). Zeolites such as mordenite and ZSM-5 with higher Si:Al ratios possess greater resistance to acid attack (Dyer, 1988), and it is suggested here, that this phenomenon could be an indication that such chemical attack by SO_2 would be less likely in mordenite and ZSM-5.

Byrne (1990) patented the use of iron and/or copper containing zeolites possessing a 3-dimensional structure and pores of at least 7 Angstroms and cited ultrastable zeolite-Y (USY), Beta and ZSM-20 as satisfying these criteria. He suggested that the large pores offered greater resistance to sulphur poisoning in comparison with small to medium pore zeolites eg ZSM-5, by preventing physical blockages and/or diffusional resistance caused by the competitive adsorption of the reactants. He also noted a claim in a Japanese Patent[9] that dealumination of mordenites to Si:Al ratios greater than 12, enhances resistance to poisoning by SO_3 and sulphuric acid mist. This resistance of mordenite to acid attack has already been noted above.

In summary, it appears that resistance to SO_2 poisoning is affected by zeolite type and aluminum content as well as pore size (to prevent physical blockage).

[9]Japanese Patent Publication (Kokai) NO. 51-69476.

2.6.11. REACTION MECHANISM

Having investigated the use of H-mordenites, Kiovsky *et al.* (1980) proposed Bronsted acids as the active sites. The mechanism envisaged nitrogen dioxide as the reactive species which was produced from the *gas* phase oxidation of nitric oxide in the presence of oxygen - this being the rate limiting step. NO_2 would then adsorb on the catalyst surface and react with ammonium ions formed from the chemisorption of ammonia on the acid sites, producing nitrous oxide and water with the nitrous oxide further decomposing to nitrogen and oxygen.

This mechanism is questionable when the kinetics and thermodynamics of the NO oxidation reaction to NO_2 are considered. The homogeneous gas phase reaction of nitric oxide and oxygen is slow. In addition, the reaction rate is known to be inversely proportional to temperature and it is also thermodynamically limited above 490°C (refer to section 2.1.). In contrast, the equilibrium constants calculated for the SCR reaction (shown in Figure 2.1) indicate that the decomposition of nitric oxide is favoured to temperatures well over 1300°C and the SCR reaction has been shown to proceed at temperatures up to 600°C (Byrne, 1992).

Brandin *et al.* (1989) examined the ability of H-mordenite, Cu-mordenite and Fe-mordenite to catalyse the NO oxidation reaction. When one compares Figure 2.30a and b, it can be seen that the rate of the catalytic oxidation reaction measured in terms of NO conversion (H-mordenite) is lower than the rates of the SCR reaction obtained under similar conditions. With the SCR reaction, NO conversion is seen to increase at temperatures above 300°C in Figure 2.30a, while in Figure 2.30b, NO_2 production decreases above this temperature. It is also obvious that copper exchanged mordenite had little activity for the oxidation reaction, but catalysed the SCR reaction efficiently. Thus, even if the oxidation reaction was a catalytic one, the rate of the reaction is slower than the SCR reaction, and this evidence serves to contradict the reaction mechanism proposed by Kiovsky *et al.* (1980). Furthermore, the proposed mechanism does not produce the stoichiometry confirmed by Hirsch (1982) and generally accepted as appropriate for the SCR of NO or NO_2.

According to the mechanism proposed by Brandin *et al.* (1989), Lewis acids are the catalytically active sites. These would be dehydroxylated Bronsted sites and exchanged polyvalent metal cations. The distinct relationship which they determined between Si:Al ratio and catalytic activity supports this.

Nam *et al.* (1988) observed that while the measured activation energy remained the same for all mordenites irrespective of copper content, the frequency factors for various samples of H-mordenite and Cu-mordenite varied. Copper containing catalysts had higher pre-exponential factors than unexchanged mordenites and indicated a change in the number of active sites on the copper mordenites but no change in site strengths. The electronic structures of copper and hydrogen ions are different and one would expect the sites strengths to differ. In addition, by

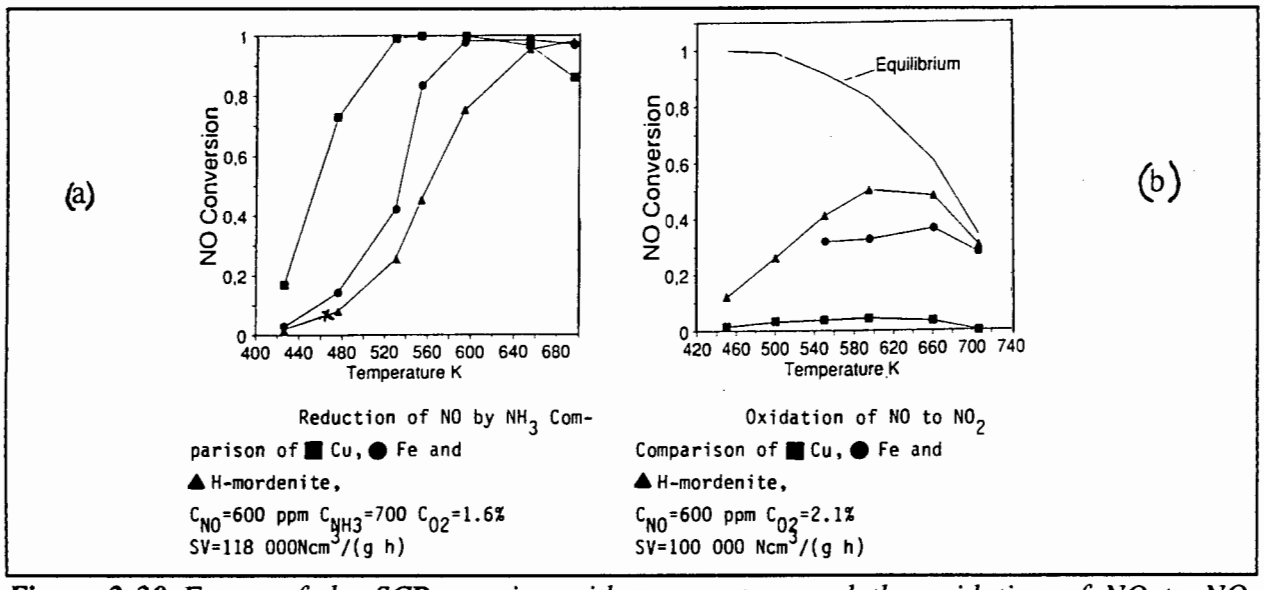

***Figure 2.30** Extent of the SCR reaction with temperature and the oxidation of NO to NO_2 (Brandin et al. , 1989)*

charge balancing, one copper(II) ion replaces two protons, resulting in fewer "active sites" rather than more. Clearly, the mechanism and nature of the active sites is not well understood.

While the SCR of nitric oxide does not take place in the absence of oxygen, NO_2 and NOx mixtures are reduced without oxygen. Brandin *et al.* (1989) interpreted this observation in a mechanism in which the initial step involves two molecules. When NO_2 is present, it replaces oxygen in this initial step. It was proposed that the high electron affinity of nitrogen dioxide (3.91 eV), resulted in the oxidation of NO by NO_2 (see below) rather than oxygen (0.45 eV), even in the presence of oxygen in NO-NO_2 mixtures. This suggestion however, fails to explain why NOx conversions in Figure 2.25 are lower in the presence of 1.7% oxygen. This slight drop in the presence of oxygen was also recorded by Hirsch (1980).

Brandin *et al.* (1989) proposed the following steps for the initial oxidation of NO in a mechanism for the reduction of NO:

$$NO + O_2 \rightarrow NO^+ + O_2^- \qquad (2.23)$$
$$NO + NO_2 \rightarrow NO^+ + NO_2^-$$

Such a reaction involving NO and NO_2 simultaneously, is consistent with the inverted parabolic shape of Figure 2.25 and Figure 2.26 which is predicted from Active-Site Theory (refer Section 2.6.8.).

Brandin *et al.* (1989) suggested that the reactants, NO and NO_2 were ionized as described in equations (2.23) above, in a similar way to the ionization of water on a dehydroxylated zeolite, and formed surface bonded nitrites and nitrates. Lewis acid sites were required for this initial

NO oxidation which was the rate limiting step. With ammonia as a reactant, the final reaction products, nitrogen and water resulted from the decomposition of ammonium nitrite/nitrate formed by adsorption of ammonia on a neighbouring Bronsted acid.

Mizumoto *et al.* (1979) proposed the following mechanism for the SCR reaction over Cu-zeolite-Y:

$$\begin{aligned}
&Cu^{2+}(NH_3)_n + NO \rightarrow \\
&[Cu^{2+}(NH_3)_nNO] \rightarrow \\
&Cu^{+}(NH_3)_m + N_2 + H_2O + (n-m-1)NH_3 + H^{+}(ads). \\
&Cu^{+}(NH_3)_m + \frac{1}{4}O_2 + H^{+}(ads) \rightarrow \\
&Cu^{2+}(NH_3)_m + \frac{1}{2}H_2O. \\
&Cu^{2+}(NH_3)_m + (n-m)NH_3 \rightarrow Cu^{2+}(NH_3)_n
\end{aligned} \qquad (2.24)$$

resulting in the overall stoichiometry:

$$NO + NH_3 + \frac{1}{4}O_2 \rightarrow N_2 + \frac{3}{2}H_2O \qquad (2.25)$$

This mechanism interprets the reaction as one involving the reduction/oxidation of copper, but unlike that for the direct decomposition reaction, copper (II) ions are seen to be the active "sites" rather than copper (I) ions. The mechanism differs from that proposed by Brandin *et al.* (1989) by describing the formation of an ammonium-NO complex on a single site rather on two separate sites. It is also interesting to note in the use of copper ion exchanged catalyst, that protons (H^{+}_{ads}) are described by the mechanism - perhaps equivalent to Bronsted acids. A rate limiting step was not identified.

These two mechanisms proposed by Brandin *et al.* (1989) and Mizumoto *et al.* (1979) are seen to be distinctly different and mutually exclusive.

Choi *et al.* (1991) investigated Cu-mordenite under reaction conditions using X-ray absorption spectroscopy, and suggested that the active copper species contained both ammonia and NO. Although determined under different reaction conditions to those employed by Williamson and Lunsford (1976), (higher temperature and presence of oxygen), their results suggested similar

structures. Williamson and Lunsford proposed that a square planar $[Cu(NH_3)_4]^{2+}$ complex was the reactive species.

2.6.12. CONCLUDING REMARKS

Similar to the finding for the use of zeolites for the direct decomposition reaction, Cu-ZSM-5 has been found to be more active than Cu-mordenite and Cu-zeolite-Y. Again, the particular efficacy of Cu-ZSM-5 has not been revealed. In the remainder of the foregoing review of the work on SCR with ammonia over zeolites, in both H-form and copper ion exchanged form, a number of inconsistencies have been highlighted *e.g.*, the effect of copper concentration and reaction stoichiometry. Also, a reaction mechanism has been disputed in this review. It is apparent that these aspects of SCR with zeolites demand clarification.

This section completes the review of zeolites for the catalytic reduction of nitrogen oxides. It was the intention of this project to compare the effectiveness of copper oxide and zeolites for the SCR reaction, and that which follows, is a discussion of the use of copper oxide for this purpose.

2.7. THE SCR OF NITRIC OXIDE OVER COPPER OXIDE USING AMMONIA

2.7.1. INTRODUCTION

The use of copper oxide as a simultaneous SOx/NOx sorbent and catalyst has been described in Section 1.8. Copper sulphate formed by the reaction of CuO and SO_2, has been found to be a more effective NOx catalyst than CuO (Kiel *et al.*, 1992), and consequently, NOx reduction studies have emphasized the use of copper sulphate rather than CuO as a SCR catalyst. This reason has probably contributed to the little which has been published on the use of CuO for the SCR of NO with ammonia. The dearth of published work is confirmed by Kiel *et al.* (1992) who recently reported that "explicit kinetic data on the SCR of NO by ammonia over CuO or $CuSO_4$ catalysts under dilute gas conditions and in the presence of oxygen are 'very scarce'". The information which is recorded below was obtained from one reference, that by Kiel *et al.* (1992). The catalyst was copper oxide supported on 1.5mm diameter porous silica spheres.

2.7.2. RESULTS OF PARAMETRIC STUDIES

While nitrogen was the predominant product of the reduction of nitric oxide, small amounts of nitrous oxide were formed with the amounts increasing with temperature above 200°C. This is shown in Figure 2.31. The production of nitrous oxide has not been noted as a product of SCR

over zeolites (in the presence of oxygen) and is thus a significant observation (Refer to Section 2.6.2.).

The optimum reaction temperature can be seen to be 350°C (Figure 2.31). The inclusion of 10% water in the feed was found to decrease NO conversion by 10% and increase the optimum reaction temperature by 50°C (Feed [NO]=1000 ppm). These observations were not explained.

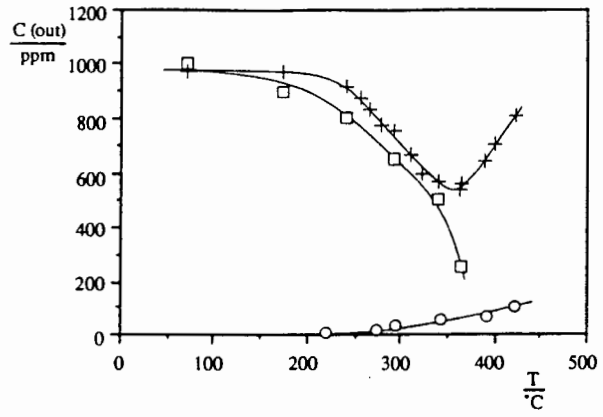

Nitric oxide (+), ammonia (□) and nitrous oxide (○) concentrations at the fixed-bed gas outlet as a function of the bed temperature for fresh np(5.7) catalyst particles containing CuO only.

***Figure 2.31** The extent of NO reduction with temperature over CuO (Kiel et al., 1992)*

In the use of copper oxide at high temperature, it should be noted that CuO is converted to Cu_2O at about 900°C (Masterton and Slowinski, 1977) and the use of cuprous oxide has not been addressed in the literature examined.

Kiel *et al.* (1992) determined that for NO and NH_3 concentrations of 250-1000 ppm, the dependence of the rate of the SCR reaction was first order in NO and zero order in ammonia concentration, supporting 'the observations for zeolite catalysts.

An activation energy of 16 kcal/mol was determined and compared with 10 kcal/mol obtained by Fukuzawa and Ishihara (1979) over $CuO/CuSO_4$ on Bauxite. It was suggested that the lower activation energy could have been derived from data affected by pore diffusion. The intrinsic rate constant calculated by Kiel *et al.* (1992) for CuO below 330°C was:

$$k_r = 9.2*10^6 \exp(-\frac{68*10^3}{RT}) \qquad \frac{m^3}{m_{cat}^3\ s} \qquad (2.26)$$

This activation energy is not markedly different to the activation energies noted for the SCR reaction over zeolites (cf 11-17 kcal/mol). It is interesting to note this in light of the significant difference in the form in which copper appears in the two catalysts; as mobile ions stabilized

within a zeolite framework in one instance and in clusters of discrete particles of an ionic oxide (Masterton and Slowinski, 1977) in the other instance. It is obvious that the mechanisms proposed for reaction over zeolites (which invoke adjacent active sites and "adsorbed" protons and other surface species) do not extend to the reaction over copper oxide. A mechanism for the SCR reaction over copper oxide has not been encountered.

When comparing the rate constants obtained by Kiel *et al.* (1992) over CuO with those for nitric oxide reduction over V_2O_5-TiO_2 (Figure 2.32), it is apparent that the rates over the latter are approximately three orders of magnitude greater than those obtained over copper oxide.

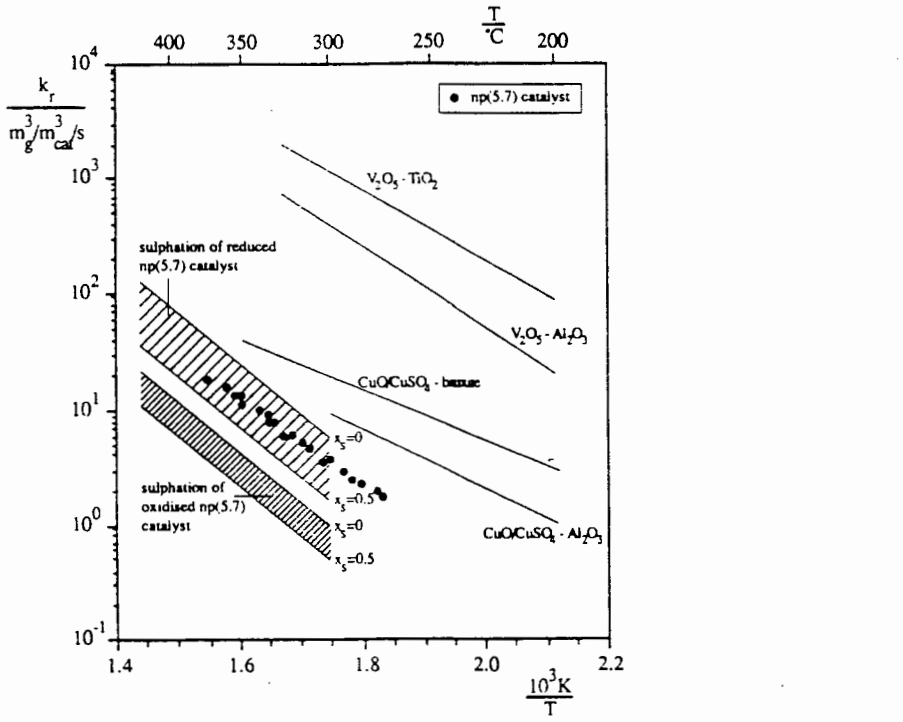

Comparison of experimental values of the intrinsic reaction rate constant k_r for the np(5.7) catalyst with literature data given by Wong and Nobe [18] for 10 wt.-% V_2O_5 on TiO_2 or Al_2O_3 catalysts, and with data given by Fukuzawa and Ishihara [19] for CuO/$CuSO_4$ on bauxite or Al_2O_3 catalysts. Also shown are modified reaction rate constants for sulphation of the reduced and the oxidised catalyst, according to eqns. (17) and (18) respectively, with the sulphation degree x_s ranging from 0 to 0.50.

***Figure 2.32** Comparison of SCR rate constants (Kiel et al., 1992)*

The catalyst mass to flowrate ratios which were required to obtain the indicated conversions in the investigation of the reactions and catalysts reviewed, are listed in Table 2.5 to offer insight to the relative reaction rates.

The feed NO concentration and the W/F ratio required for a similar conversion (100%) of the direct decomposition reaction as the SCR reactions, reveal the marked difference in reaction rates. When Iwamoto *et al.*'s (1991b) data are compared with those recorded by Choi *et al.* (1991), the rate of the SCR reaction with the hydrocarbon can be seen to be lower than the

reaction with ammonia. Finally, the amount of copper oxide catalyst used by Kiel *et al.* (1992) was more than double the mass of Cu-mordenite used by Choi *et al.* (1991) (while conversion is 50%, feed [NO] was doubled). These are rough guidelines only - copper loadings of the catalysts should also be considered.

***Table 2.5** Comparison of catalyst weight to flowrate ratios used for catalytic NO reduction*

Reaction	*Catalyst*	*Feed [NO] (ppm)*	*W/F (g.s/ml)*	*Maximum conversion(%)*	*Reference*
Direct decomposition	*Cu-ZSM-5*	*40000*	*4*	*100*	*Iwamoto (1986)*
SCR - propene	*Cu-ZSM-5*	*500*	*0.1*	*100*	*Iwamoto (1991b)*
SCR - ammonia	*Cu-mordenite*	*500*	*0.031*	*100*	*Choi et al. (1991)*
SCR - ammonia	*CuO*	*1000*	*0.075*	*50*	*Kiel et al. (1992)*

2.7.3. CONCLUDING REMARKS

The review of only one paper on the use of copper oxide for SCR indicates the scarcity of work in this field. Whether further work on CuO is warranted should be assessed by the value of copper oxide as a SCR catalyst in comparison with zeolites and other catalysts in view of the low reaction rates (in comparison with V_2O_5 catalysts). Thus copper oxide must offer significant advantages over vanadium based catalysts if it is to be used as a SCR catalyst - these advantages are envisaged in its use in high temperature applications combined with particulate removal.

This section concludes the review of the literature on the catalytic reduction of nitrogen oxides and a synthesis of the knowledge gained from the literature study is now presented.

2.8. CONCLUSION TO LITERATURE REVIEW

The objectives of the literature review were to:

1) gain an understanding of reaction kinetics and mechanism, response to operating parameters
2) describe the factors which influence and dictate catalytic activity
3) describe catalyst selection criteria such as intrinsic activity and optimum operating temperatures.

With respect to these objectives, the following findings are noted:

1) The reaction mechanisms for the direct decomposition reaction and the SCR reactions have not been conclusively determined. In particular, the use of nitrogen dioxide has been shown prominently, but its catalytic role remains uncertain.

2) Although disparities exist in the findings, two particular factors have been noted as being significant to the use of zeolites for catalytic NOx reduction. They are, copper content and aluminium content.

   Cu-ZSM-5 has been shown to be more active than Cu-mordenite and Cu-zeolite-Y for the direct decomposition reaction and experimental evidence suggests that the same order of activity pertains to the SCR reaction. An understanding of the superiority of ZSM-5 to other zeolites remains incomplete. While accessibility of active sites within the zeolites has been considered, most experimental evidence suggests that the zeolite pore diameters and the pore configurations are not limiting factors. Since these structural differences seem not to verify the superiority of ZSM-5 over the other zeolites, it is suggested here that chemical rather than physical properties of Cu-ZSM-5 be investigated.

3) SCR with ammonia has been shown to be more effective than SCR with hydrocarbons, which in turn yields higher reaction rates than the direct decomposition reaction. Also, the comparison of catalysts has revealed that zeolites offer higher reaction rates than copper oxide for the SCR with ammonia. While these rates may be lower than those which may be achieved with vanadia based catalysts, these catalysts may be employed at higher temperatures. The zeolites in particular, have shown potential for high temperature applications.

The catalytic activity offered by copper oxide indicates that the zeolite framework is not a pre-requisite for catalytic reduction of NOx. A direct comparison of the use zeolites and copper oxide has not been encountered and thus, the advantages of copper oxide and zeolites respectively, have not been enumerated. The experimental program which will be described in Chapter 3, attempts to accomplish this, by investigating the extent of the SCR reaction over these catalysts under similar operating conditions.

3. EXPERIMENTAL PROCEDURES

3.1. EXPERIMENTAL PROGRAM

The objectives of the experimental program, as outlined in Chapter 1, were to investigate copper doped ZSM-5, silicalite and a fibrous aluminosilicate for catalytic NOx reduction.

Silicalite was chosen as a support for copper doping because it has the same three- dimensional pore structure as ZSM-5 while not possessing the ion exchange capability of the zeolite (see Section 2.3.3-ZSM-5 structure). An amorphous fibrous aluminosilicate filter material doped with copper, was investigated as a potential NOx removal catalyst to be applied in a high temperature multi-functional flue gas cleaning system.

The three catalysts were synthesized and an experimental rig was built in order to investigate the two NOx reduction reactions of interest:
1) the decomposition reaction and
2) the selective catalytic reduction reaction with ammonia.

The direct decomposition reaction over Cu-ZSM-5 was investigated because of its significance as a desirable NOx removal technique. This investigation also sought to validate the experimental technique by attempting to duplicate seminal results published in the literature (Iwamoto *et al.* (1986, 1991a,c,d) and Li and Hall (1990, 1991)).

Although a considerable amount of work on the direct decomposition reaction has been published, the literature review contained in Chapter 2 shows that little has been published on the use of Cu-ZSM-5 and copper oxide as SCR catalysts. Thus, copper doped ZSM-5, silicalite and ceramic filter material are investigated as SCR catalysts and their catalytic activities compared with that of Cu-ZSM-5 for the direct decomposition reaction.

The experimental parameters investigated were:
1) Reaction temperature
2) Feed gas composition
3) Gas flowrate

Synthesis and characterization of the catalysts are described below. The layout of the experimental rig is presented, the analytical tools, their commissioning and use and the operating procedures are also described.

3.2. CATALYST SYNTHESIS

3.2.1. SYNTHESIS OF Na-ZSM-5

The ZSM-5 catalyst was prepared in the Department of Chemical Engineering at the University of Cape Town following a procedure based on the patent by Argauer and Landolt (1972). For an intended Si:Al ratio of 60, the following synthesis mixture was stirred at 160°C and 9 MPa for 3 days (Table 3.1):

Table 3.1 *Na-ZSM-5 synthesis mixture*

NaOH	*2.29g*
Tetrapropylammonium Bromide	*31.43g*
Water	*120.00g*
Ludox	*39.82g*
$Al(OH)_3$	*0.338g*

The templating agent, tetrapropylammonium-Bromide (TPA-Br) was removed by calcining in nitrogen for 6 hours (60 ml/min) followed by treatment in air for an additional 6 hours (60 ml/min) at 500°C. The sodium form of ZSM-5 remains after the organic template has been removed.

The sodium ions of the detemplated catalyst were then exchanged with copper in a liquid phase ion exchange procedure which is described below.

3.2.2. SYNTHESIS OF SILICALITE

The silicalite was also synthesized at the University of Cape Town. The procedure was based on the method patented by Dwyer and Jenkins (1976) with the following synthesis mixture (Table 3.2) held at 153°C and 350 kPa for 3 days:

Table 3.2 *Silicalite synthesis mixture*

TPA-Br	*31.2 g*
NaOH	*2g*
Water	*200g*
Ludox	*38.2g*

The organic template was removed by heating, using the same procedure described for ZSM-5.

3.2.3. FIBROUS ALUMINOSILICATE

The ceramic filter material was obtained from Cerel Ltd, U.K. It is a fibrous amorphous aluminosilicate compacted into a form referred to as a candle, with the aid of a proprietary organic binder which must be removed before use. Its chemical composition is shown in Table 3.3. and the material is thermally stable to 1000°C.

Table 3.3 Composition of aluminosilicate filter candle after firing (Cerafil - Technical Data brochure, 1991, Cerel Ltd)

SiO_2	*52.2% w/w*
Al_2O_3	*47.8% w/w*

The filter candle was crushed into a powder (212μm < particles < 75μm) to obtain a form similar to the powdered ZSM-5 and silicalite. Prior to copper impregnation, the powder was calcined in air at 550°C for 12 hours to remove the binding agent.

3.2.4. COPPER DOPING PROCEDURE

Zeolite ion-exchange procedure

The sodium ions in Na-ZSM-5 may be exchanged in a liquid medium ion exchange procedure as described Section 2.3.7. The ions will be located at extra framework sites. However, as noted in the discussion of zeolites in Chapter 2, only two extraframework sites have been isolated in ZSM-5 and the location of excess (non-stoichiometric) copper which has been noted in the literature, has not been determined.

Na-ZSM-5 (25g) was stirred and refluxed at 100°C for 2 hours in 1250 ml of 0.0080M copper nitrate solution. The salt solution was filtered and the catalyst thoroughly flushed with distilled water over a vacuum filter and oven dried at 80°C overnight.

The volume of salt solution was determined by a 50:1 volume to catalyst mass ratio which was used in preliminary ion exchange studies with zeolite-Y and mordenite. Although Li and Hall (1990), Hamada *et al.* (1990), Li and Armor (1991) and others have carried out ion exchange of ZSM-5 at room temperature, the exchange time and temperature used in the present study were maintained for consistency with early ion exchange investigations.

The molar copper content of the exchange solution was 12 times the molar aluminium content of the catalyst and again, was a practice carried through from preliminary ion exchange investigations. The aluminium content of ZSM-5 was 33.9 μmol/g and 12 times this amount required 10.2 mmol Cu in 1250 ml of exchange solution for 25 grams of catalyst resulting in an desired salt solution concentration of approximately 0.008 M. This concentration is similar to the 10-11 mmol/l used by Iwamoto *et al.* (1991d).

Incipient wetness impregnation

Silicalite and the fibrous aluminosilicate cannot be ion exchanged because they do not possess that characteristic property of zeolites. Catalytically active species are introduced to these non-zeolitic materials by impregnation. Incipient wetness impregnation involves spraying a catalyst support with a liquid medium containing the desired catalytic material and subsequent drying to leave it on the support (Twigg, 1989).

Copper oxide is obtained after calcination of copper nitrate. $Cu(NO_3)_2.3H_2O$ loses its water of hydration at 26°C (van der Grift *et al.*, 1990), melts at 114.5°C (Perry and Green, 1984) and decomposes at 170°C with the release of HNO_3 (Perry and Green, 1984), leaving copper oxide.

In order to impregnate silicalite and the fibrous aluminosilicate, 50 ml of 0.025M copper nitrate solution was poured over 2.5 grams of the powder on a vacuum filter and immediately placed in an oven at 80°C and left to dry overnight. The impregnation procedure was then repeated once more. The concentration of the salt solution was dictated by the desire to obtain an equivalent concentration of copper to that achieved by ion exchange.

Silicalite (initially white) immediately took on the obvious blue colour of the copper nitrate solution upon contact with the liquid. This dramatic colour change was taken to indicate that the copper species were well distributed within the silicalite, having been drawn into the pores by capillary forces (Maatman and Prater, 1957). The distribution of impregnated copper species is discussed further under "Catalyst Characterization" in Section 3.3.

The same impregnation procedure applied to the filter material did not produce a significant copper loading. This was observed by the absence of blue coloration (cf silicalite impregnation) and quantified by atomic absorption spectroscopy. Unlike the silicalite, the filter material was non-porous and copper impregnation would have been limited to the outer surfaces of the ceramic fibres.

Because of the inability to impregnate the filter material with the incipient wetness technique described, a blend of copper oxide and powdered ceramic filter was prepared. A mass of 0.0490 g of Baker technical grade copper(II) oxide and 1.9921 g of the powdered ceramic filter

were physically combined. Thus, the distribution of copper was unlike that which was produced within the pores of silicalite.

This amount of CuO was chosen to match the copper content of Cu-silicalite. Details of catalyst composition will be presented in the next section.

3.3. CATALYST CHARACTERIZATION

The following techniques were employed for the characterization of the catalysts used:

Powder x-ray diffraction (XRD)
X-ray fluorescence (XRF)
Atomic absorption spectroscopy (AAS)
Scanning electron microscopy (SEM)
Temperature programmed reduction (TPR)

3.3.1. X-ray Diffraction

Powder X-ray diffraction was used to confirm that the synthesized materials were indeed ZSM-5 and silicalite. As described in Section 2.3.3, ZSM-5 and silicalite are isostructural. Diffraction patterns for Na-ZSM-5 and silicalite (Figure 3.1 and Figure 3.3) were compared with the simulated pattern for ZSM-5 in von Ballmoos' (1984) compilation of zeolite XRD patterns (Figure 3.2). The largest peaks for ZSM-5 are listed in Table 3.4 and can be indentified in the diffraction patterns shown in Figure 3.1 and Figure 3.3. Although the resolution of the peaks (recorded with 2θ scanning intervals of 0.1°) is poor compared with the simulated diffraction pattern (2θ intervals of 0.01°), the similarity in peak positions and relative intensities may be taken to indicate that both synthesized materials exhibited the characteristic ZSM-5 structure.

Table 3.4 Relative intensities of the 8 largest peaks for ZSM-5 (taken from von Ballmoos, 1984)

2 theta	I_{rel}
7.92	*52.3*
7.94	*47.5*
8.87	*35.0*
23.1	*100.0*
23.26	*78.4*
23.68	*36.7*
23.91	*53.7*

The similarity of the diffraction patterns for Na-ZSM-5 and Cu-ZSM-5 (Figure 3.1) indicated that ion exchange did not alter the zeolite framework structure. Similarly, there was no evidence of structural change upon impregnation of silicalite with copper nitrate (Figure 3.3).

The diffraction data were obtained with a Philips X-ray diffractometer using Cu-K_α radiation. The voltage was 40kV, with a current of 30 mA, a time constant of 1 second. 1° slits and aluminium and perspex holders were used.

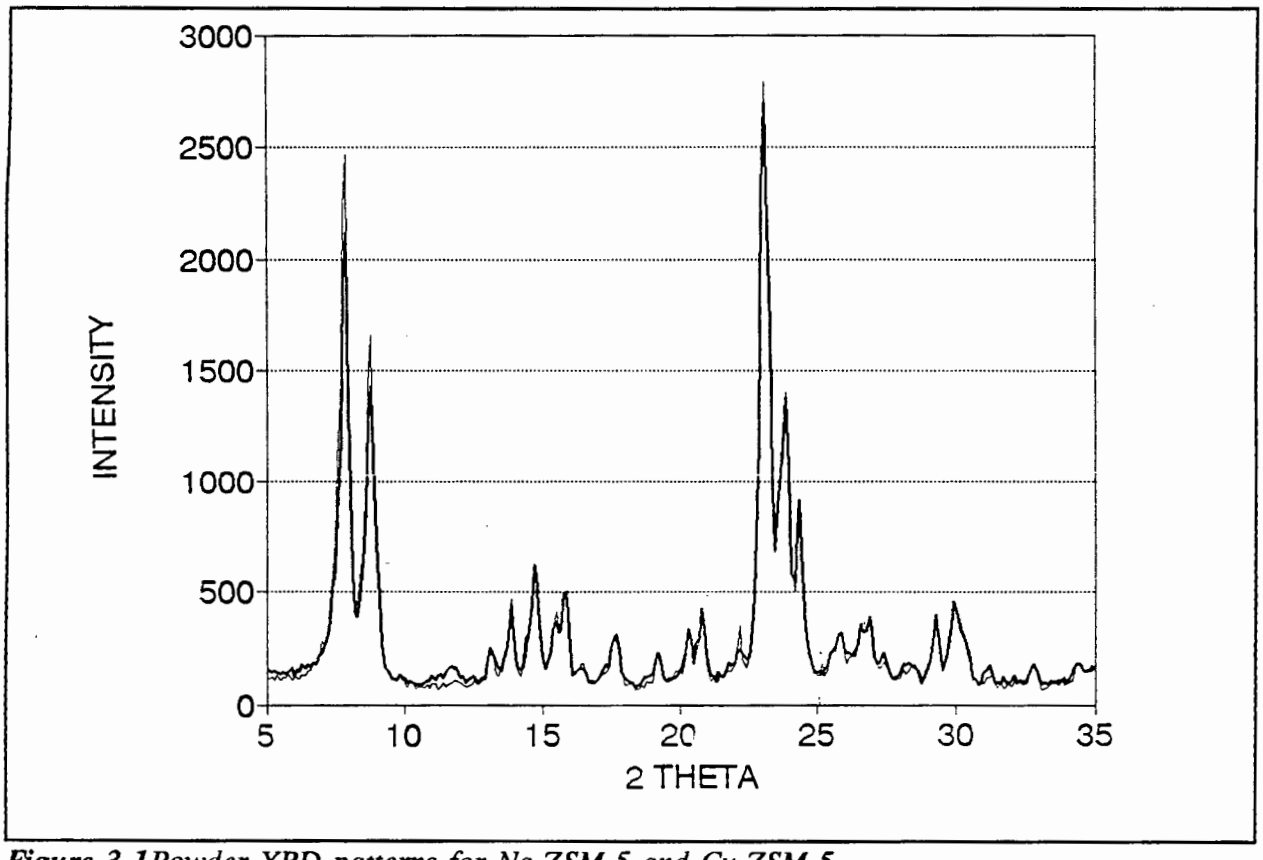

Figure 3.1Powder XRD patterns for Na-ZSM-5 and Cu-ZSM-5

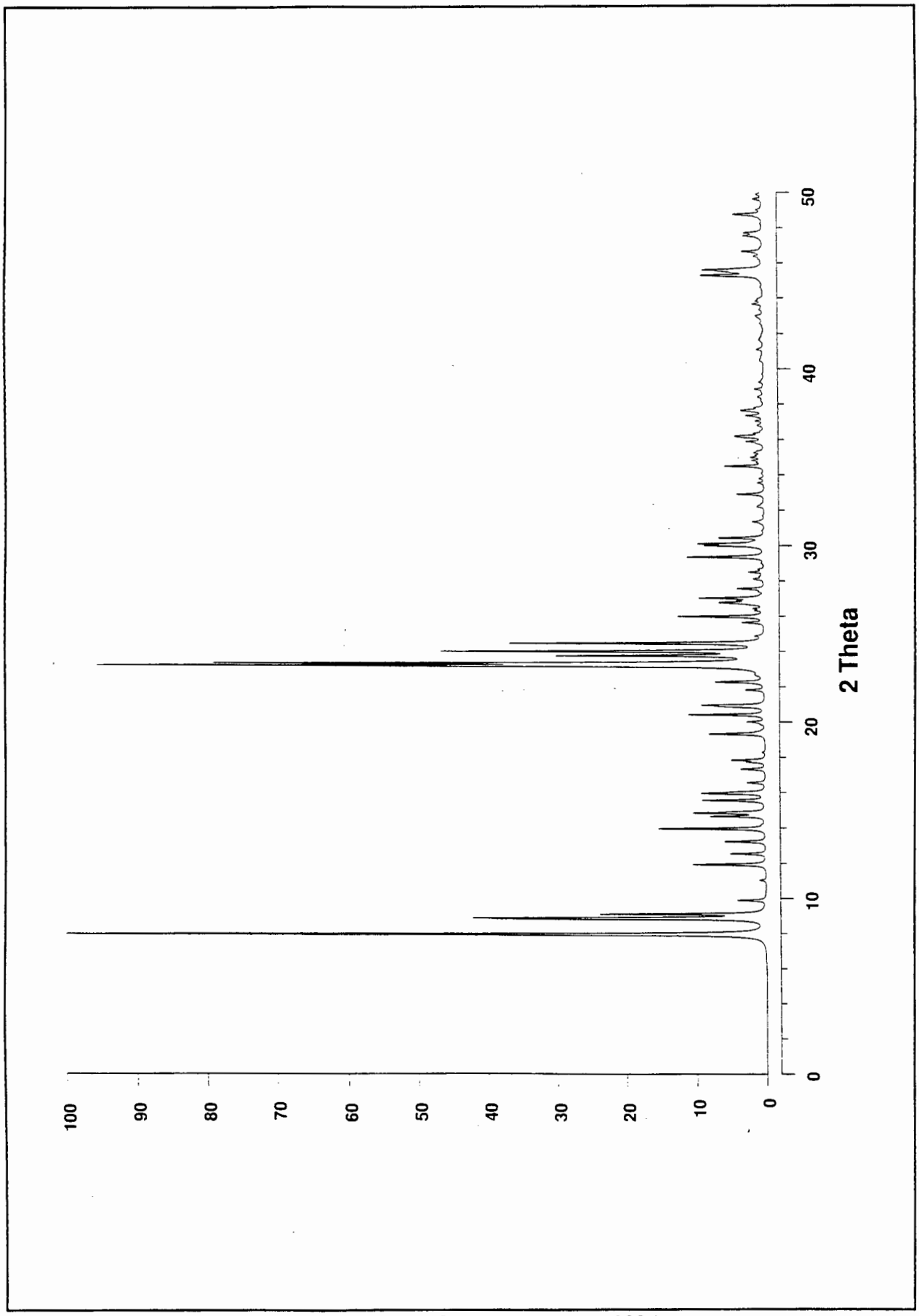

Figure 3.2 Simulated XRD pattern for ZSM-5 (Von Ballmoos, 1984)

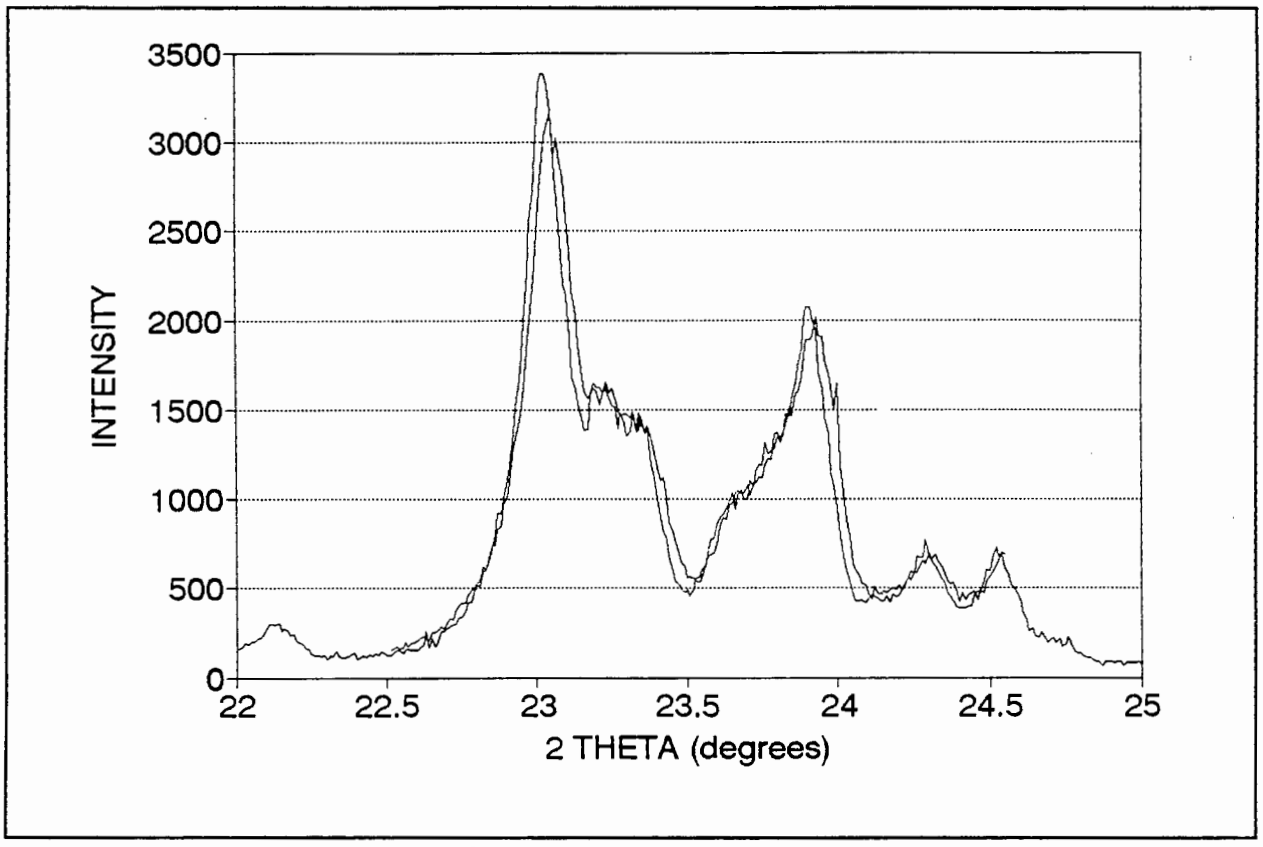

***Figure 3.3** Powder XRD patterns for silicalite and copper nitrate impregnated silicalite*

3.3.2. CHEMICAL ANALYSIS - XRF AND AAS

The Na-ZSM-5 was synthesized with an intended Si:Al of 60. Actual Si:Al was determined by chemical analysis carried out by *Mintek - Analytical Science Division* using X-ray fluorescence spectroscopy (XRF) for SiO_2 and Al_2O_3. The results are listed in Table 3.5. Na-ZSM-5 was found to have a Si:Al ratio of 43 and analysis of Cu-ZSM-5 confirmed that the ion exchange procedure did not cause any dealumination.

Atomic absorption spectroscopy (AAS) was used by *Mintek* for sodium and copper analysis. The copper content of Cu-ZSM-5 and Cu-silicalite were confirmed using AAS at the Department of Chemical Engineering-UCT and the results were within 7% of those obtained by *Mintek*. These results are also listed in Table 3.5 The copper loading per gram of material is given on a "wet" basis - untreated catalyst with adsorbed water. The copper fraction of the CuO/filter mix was calculated directly from the mass of each component added.

The copper content of the ion-exchanged ZSM-5 equates to a theoretical 111% exchange according to the charge relationship between copper(II) and the aluminosilicate framework described by equation (2.10).

Table 3.5 Chemical Analysis of catalysts used

CATALYST	*Si:Al*	*Cu:Al*	*Na:Al*	*(2Cu+Na):Al*	*Cu loading (mmol/g)*	*Cu loading (% w/w)*
Na-ZSM-5	*43*	*0.0*	*1.31*	*1.31*	-	-
Cu-ZSM-5	*46*	*0.55*	*0.24*	*0.80*	*0.19*	*1.13*
Cu-Silicalite	-	-	-	-	*0.07*	*0.45*
CuO/filter mix	-	-	-	-	*0.08*	*0.51*

3.3.3. Scanning Electron Microscopy

Scanning electron micrographs of Na-ZSM-5 and silicalite are shown in Figure 3.4 and Figure 3.5. These photographs reveal that the size of the ZSM-5 crystallites are approximately 2 microns while those of the silicalite are approximately 10 microns. The silicalite displays a greater degree of surface crystallinity than ZSM-5. It should be remembered that the two materials possess the same pore structure.

ZSM-5 can be seen to form agglomerates while the silicalite crystals are essentially independent. By virtue of their small size, the agglomeration of ZSM-5 crystallites into large clusters may possibly be attributed to electrostatic forces.

3.3.4. TEMPERATURE PROGRAMMED REDUCTION (TPR)

Temperature programmed reduction is a method of characterizing the susceptibility of metal ions to reduction in a dynamic environment. This information is pertinent to the use of Cu-zeolites for NOx reduction in the light of the redox mechanisms which have been proposed for both the decomposition reaction and the SCR reaction. TPR also provides information on the dispersion of the metal species and metal/support interaction (Van der Grift *et al.*, 1990).

TPR processes are sensitive to experimental conditions (heating rate, gas flowrate, catalyst mass and reducing gas concentration) and reduction profiles are best interpreted in conjunction with profiles recorded for standard reference compounds under the same operating conditions. Gentry *et al.* (1979) determined that a 1% increase in hydrogen concentration resulted in a decrease of approximately 10°C in the reduction peak temperature, T_m. Similarly, an increase in gas flowrate lowered the temperature peak since lower conversions resulted in higher residual H_2 concentrations. A decrease in T_m of 15-30°C was observed upon increasing the reductant flowrate from 10 to 20 ml/min.

In addition to studying the redox behaviour of metal oxides, TPR has been used to "fingerprint" commercial catalysts, and under select conditions in systems such as ion exchanged zeolites, it has been used to obtain kinetic and mechanistic data. A review of the TPR of metal oxides has been published by Hurst, Gentry, Jones and McNicol (1982).

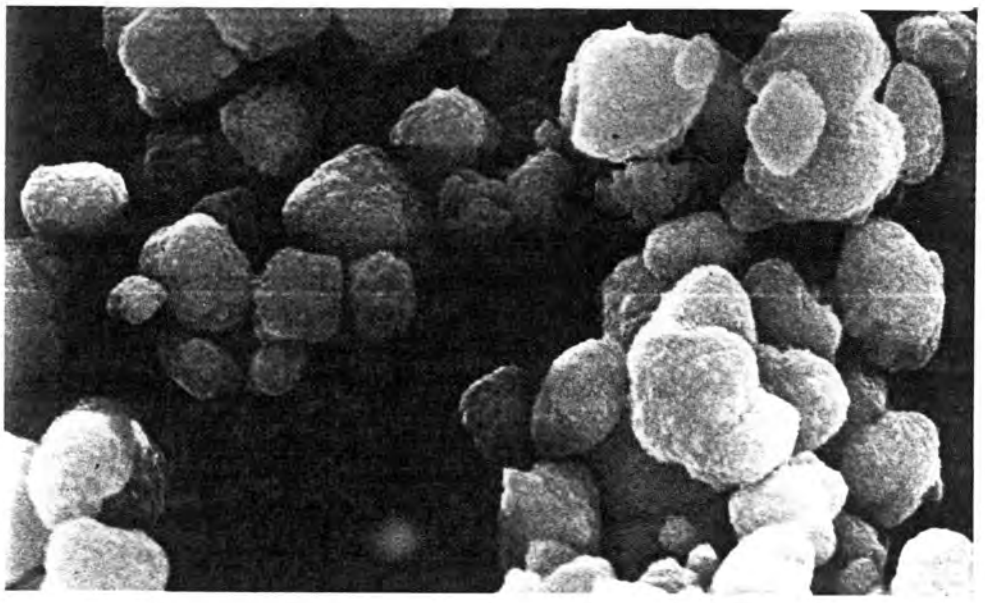

Figure 3.4 Micrograph of Na-ZSM-5 (magnification: 5.6x10⁴)

5μm: ⟵——————⟶

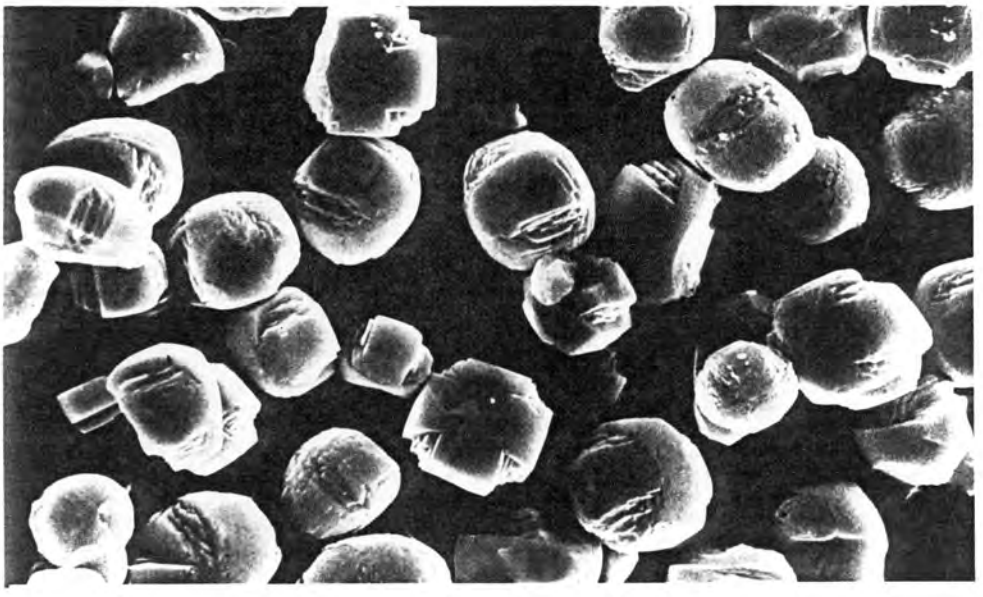

Figure 3.5 Micrograph of silicalite (magnification: 0.695x10⁴)

20μm: ⟵——————⟶

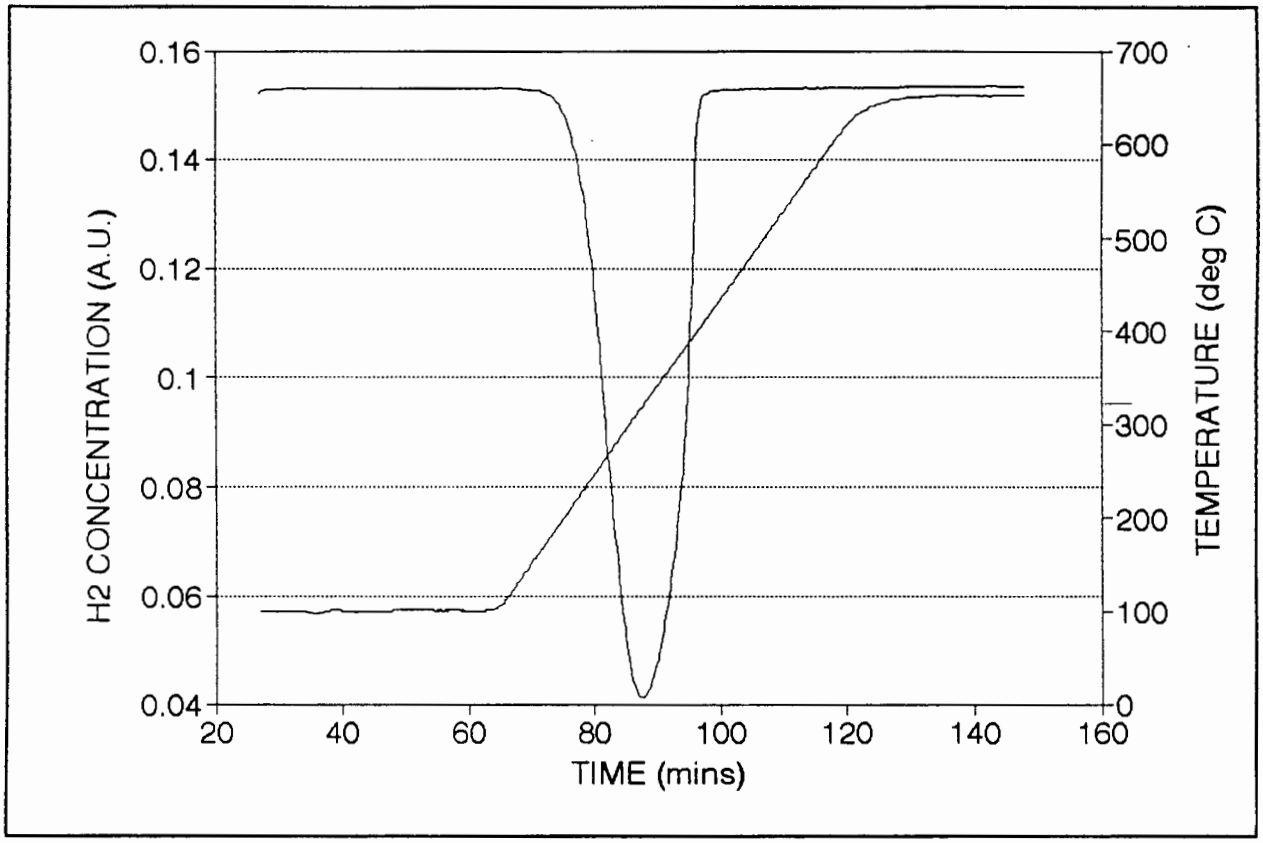

Figure 3.6 TPR - CuO

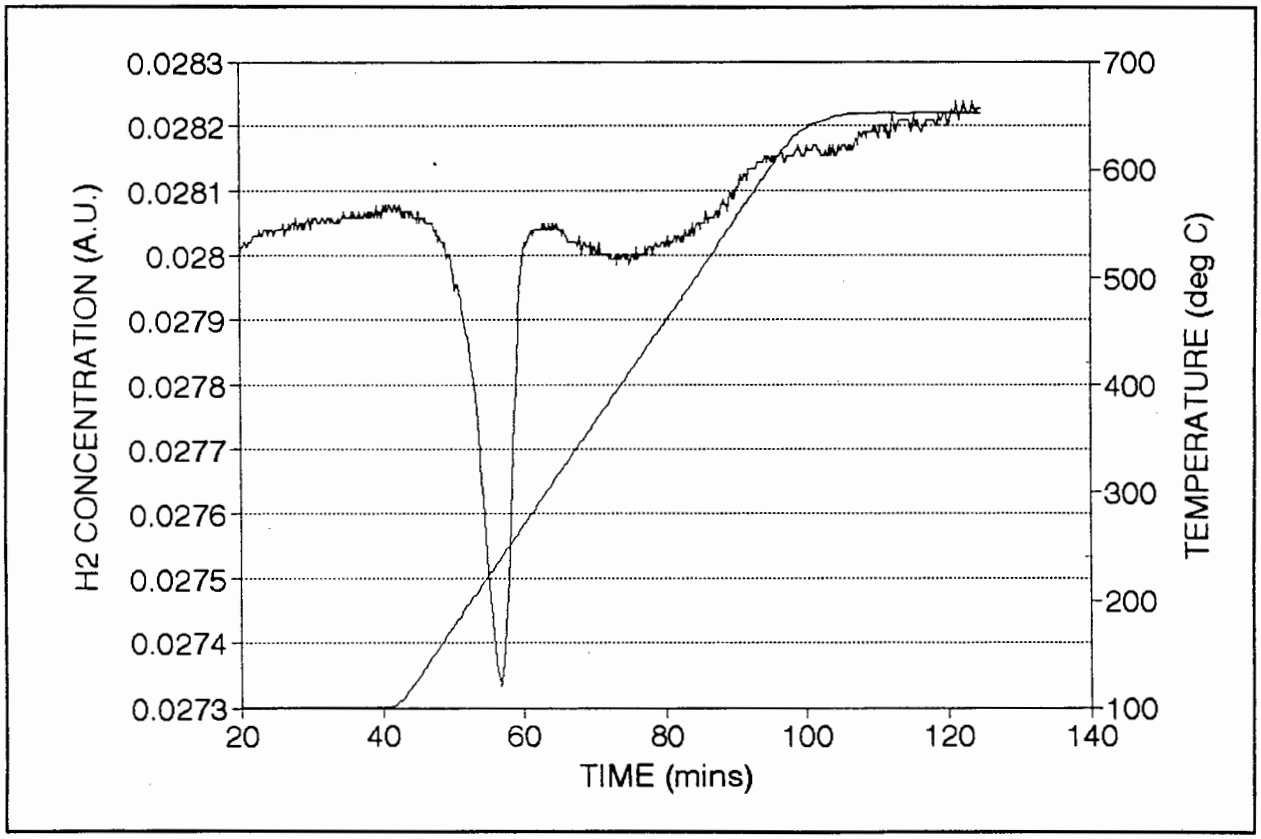

Figure 3.7 TPR - Imp Si

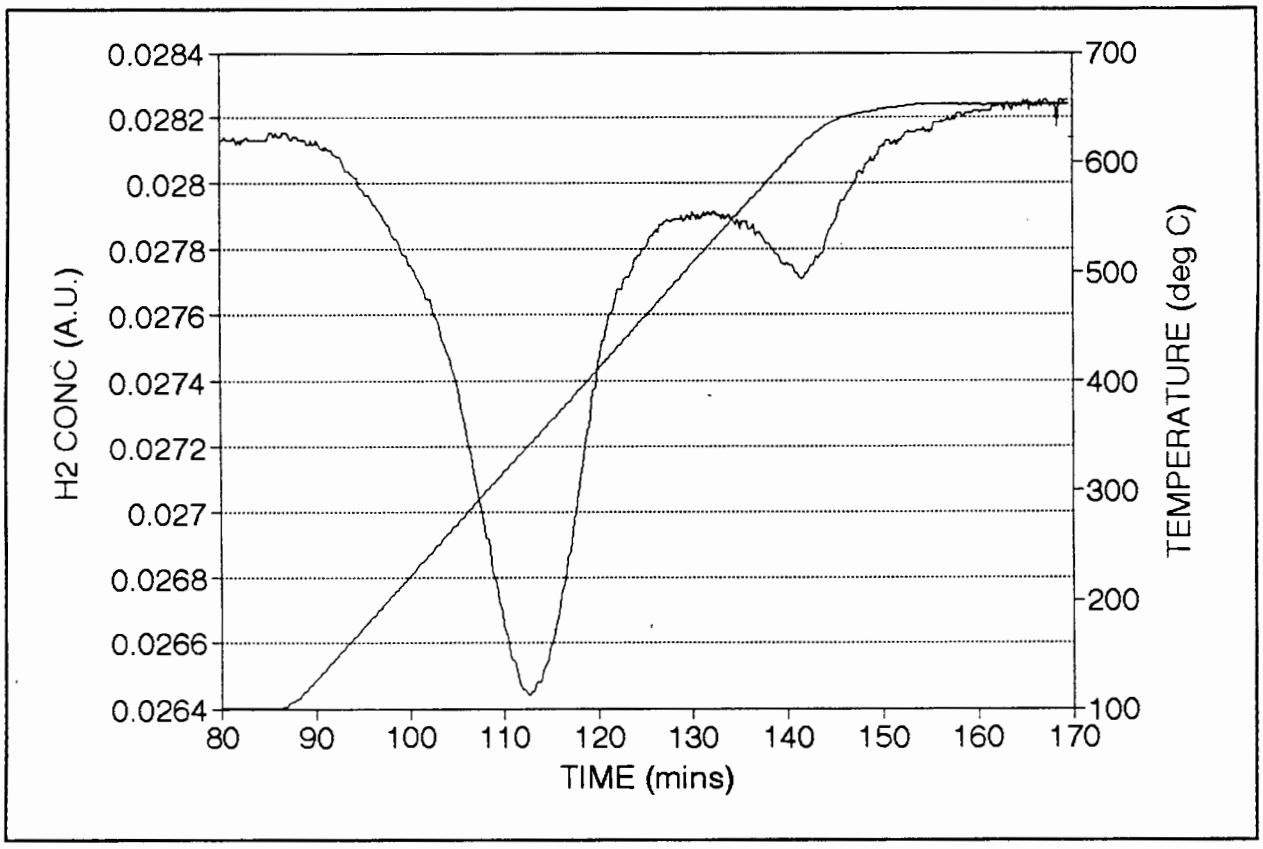

Figure 3.8 TPR - Cu-ZSM-5

The reaction for the reduction of a bulk oxide such as CuO has been described as (Hurst *et al.*, 1982):

$$CuO + H_2 \rightarrow Cu + H_2O \qquad (3.1)$$

while the reaction with metal ions exchanged into a zeolite framework has been proposed as (Uytterhoeven, 1978):

$$Cu^{2+} + H_2 \rightarrow Cu^0 + 2H^+ \qquad (3.2)$$

It is believed that the protons reacts with the zeolite lattice to produce hydroxyl groups (Beyer *et al.*, 1976).

The reduction profiles of bulk, unsupported CuO powder, impregnated silicalite and Cu-ZSM-5 are displayed in Figure 3.6, Figure 3.7 and Figure 3.8 and relevant data is listed in Table 3.6. The details of the procedure and operating conditions are detailed in Appendix 3.

Gentry *et al.* (1981) found the TPR of CuO to be a single reduction process and the single reduction peak for CuO is evident in Figure 3.6. The peak temperature, T_m for bulk CuO is

Table 3.6 Results of TPR of copper catalysts

	T_m	H_2 consumption mmol H_2/g	Copper content mmol Cu/g
CuO	*319*	*12.33*	*12.57*
Cu-ZSM-5	*341*	*0.382*	*0.178*
CuO-Silicalite	*238*	*0.143*	*0.071*

14°C lower than that obtained by Gentry *et al.* (1981) and may be accounted for by a difference in experimental conditions. In the present study, a lower H_2 concentration and temperature ramping rate and a greater catalyst mass were used.

The peak temperature for the reduction of the copper supported on silicalite (Figure 3.7) was 81°C lower than that of the bulk oxide and was similar to the result obtained by Robertson *et al.* (1975). They observed that T_m for CuO supported on silica was lowered by about 70°C and gave a broader reduction profile than bulk copper oxide - the support had acted purely as a dispersing agent, thereby promoting reduction.

Van der Grift *et al.* (1990) found that calcination of an impregnated porous silica support in 10% oxygen at 427°C did not yield a well dispersed CuO catalyst; T_m was the same as for bulk CuO. Thus, the low T_m obtained for copper doped silicalite in the first TPR profile in the present study suggests that silicalite is a suitable support for impregnation and that the impregnation procedure used, produces a well dispersed CuO catalyst. Unsupported CuO gave a broader peak than the impregnated silicalite because far more material was used (refer to Table 3.6).

The stability of copper ions exchanged into the ZSM-5 structure is evident in the greater resistance to reduction which can be seen in the high T_m (341°C) in Figure 3.8, when compared with CuO. The peak temperature for Cu-ZSM-5 at 341°C co-incides with the temperature at which spontaneous oxygen desorption occurred on Cu-ZSM-5 which was investigated by Li and Armor (1991). While this could confirm the mechanism of the decomposition reaction (refer to discussion on oxygen desorption in Section 2.4.7), this co-incidence may be entirely fortuitous, resulting from the combination of the particular catalyst mass, hydrogen concentration and flowrate and temperature programming rate employed.

The ZSM-5 reduction profile in Figure 3.8 showed two reduction peaks. While Gentry *et al.* (1979) observed two distinct reduction process in Cu-zeolite-Y, this was not expected for ZSM-5. The two reduction peaks for zeolite-Y were attributed to the reduction of supercage and sodalite cage ions respectively and the framework structure of ZSM-5 is quite different to the caged framework of zeolite-Y. The TPR of Cu-ZSM-5 was repeated on two other occasions.

Although both of these runs were not entirely successful, they did not show any evidence of a second peak. These results of TPR of Cu-ZSM-5 were considered not to be of great significance to this project and it was therefore decided that this uncertainty should not be pursued further.

The hydrogen consumption by the reduction of the bulk unsupported copper oxide (Table 3.6) corresponded to that described by the stoichiometry of equation (3.1). However, the amount of reductant consumed in the reaction with Cu-ZSM-5 and the supported CuO was one half of that predicted by the stoichiometry of equation (3.2) and (3.1) respectively. Since the copper contents of the catalysts were confirmed, the disparity between copper loading and the TPR result suggest that complete reduction did not occur and Cu^{2+} was reduced to Cu^{+} but not to Cu^{0}. This suggestion was not confirmed.

TPR of a CuO/aluminosilicate fibre mix was not performed since it was considered that this sample (with the exception of containing less copper oxide) was identical to that of the bulk, unsupported copper oxide. Copper oxide powder was simply blended (physically) with particles of the fibrous aluminosilicate. Thus, in contrast with the copper species introduced to silicalite by incipient wetness impregnation, the size and form of the unsupported copper oxide particles were unaltered.

While inconsistencies have been noted and have been left unresolved, the use of TPR was not intended as an integral technique for this project. TPR was used only as a means of verifying copper dispersion on silicalite and the work with ZSM-5 was essentially an exploratory exercise. However, it is suggested here that TPR could be a powerful investigative tool and should be investigated further. If the reduction processes from Cu(II) to Cu(I) to Cu(0) can be identified with TPR, an in-situ reduction subsequent to the SCR reaction may provide an insight to the state of the copper containing catalyst under reaction conditions.

3.4. DESCRIPTION OF EXPERIMENTAL RIG

A schematic arrangement of the experimental rig is shown in Figure 3.9. The reactants were mixed and fed through 1/4" OD stainless steel tubing to a glass reactor enclosed within a heating block. The reactor products were then piped to a gas chromatograph for analysis. In addition, a NOx chemiluminescence analyzer was employed for the investigation of the SCR reaction with an ammonia scrubber and water trap upstream of the analyzer.

Calibration and process gas included 3.8% NO and 1.1% NO in helium, 1.0% ammonia in helium and high purity helium from *Fedgas*. Synthetic air (21% O_2 - 79% N_2) and high purity oxygen were supplied by *Air Products*.

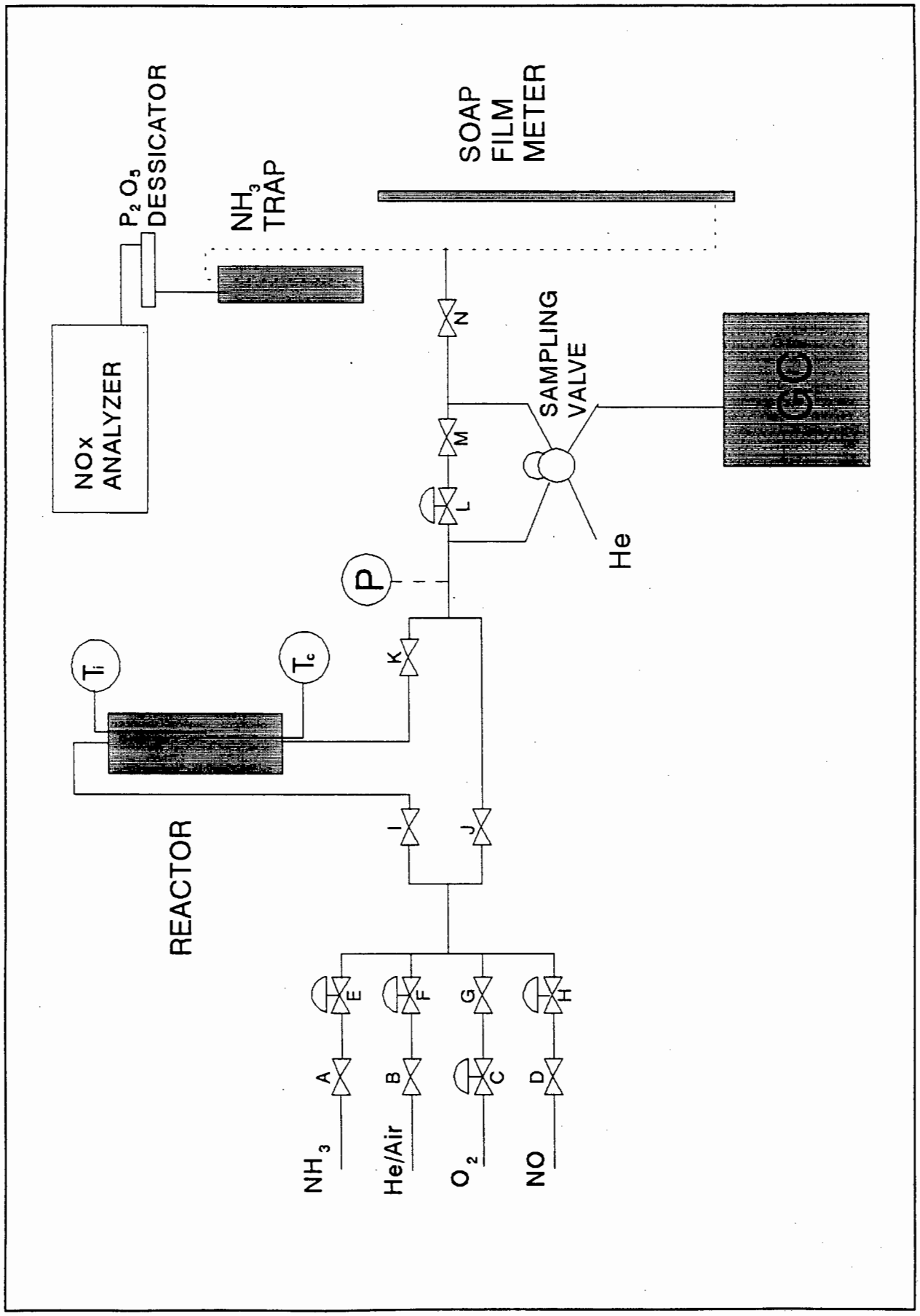

Figure 3.9 Schematic of Experimental Rig

With the aid of a soap-film meter and a stopwatch, the desired feed compositions were blended by manual adjustment of the three "Nupro" fine metering valves (C,E,H). Air for calcination and helium for purging the system were controlled by the same purge rotameter (F) since the two gas sources were always used independently of each other.

The array of Whitey ball valves (identified in Figure 3.9 as I, J and K) was configured to allow gas flow down through the reactor or to bypass it.

The furnace was manufactured in the Department of Chemical Engineering at UCT and consisted of four tubular Kanthal heating rods embedded in brass filings and encased in a stainless steel cover. The cylindrical shell was split vertically and was hinged at the side, allowing visual inspection of the contents of the reactor without having to withdraw the reactor from the heating block.

The glass reactor consisted of a 12 mm OD, 8 mm ID soda glass tube 45 cm long. The glass had a softening temperature of approximately 580°C and dictated the upper temperature limit of experiments. This tube was connected to the 1/4" stainless steel tubing by 1/2" Swagelok fittings on each end, sealed to the glass tube with teflon seals.

The desired mass of catalyst powder was supported on a bed of glass wool, in turn supported on a tubular glass insert. To monitor catalyst bed temperature, a chromel-alumel thermocouple (type K), was passed through this short glass insert and through the glass wool packing, allowing the thermocouple tip to be positioned in direct contact with the catalyst.

Reactor temperature was controlled by a "Unitemp" PID controller with an average bed temperature variation of 5°C in 530°C. A steel sleeve separated the temperature controlling thermocouple and the glass reactor. Heating rate under full power was approximately 30°C/min.

The gas sampling system is also shown in Figure 3.9. The reactor product line is split in two immediately upstream of an open/closed ball valve (M) and a needle valve (L). The arm leading to the GC sampling valve was a 56 cm length of 1/8" OD stainless steel tubing while the line leading from the ball valve remains 1/4" in diameter and carries that gas which bypasses the GC sampling valve. The pressure gauge was used to monitor the sample loop pressure which had to be kept constant in order to achieve uniform gas sample size. The sampling valve was a 6-port device with a 250 μl sample loop.

The location of the NOx analyzer relative to the reactor is depicted in Figure 3.9. The gas flow taken downstream of valve "N", was bubbled through a phosphoric acid bath to remove ammonia, then passed through phosphorous pentoxide to dry the gas prior to analysis.

3.5. DESCRIPTION OF ANALYTICAL TECHNIQUES AND PROCEDURES

It was intended originally that a NOx chemiluminescence analyzer would be used for determining nitric oxide consumption and a wet chemical method be used for quantifying ammonia. While these two methods would have sufficed for the SCR investigation, an additional analytical technique was required for the study of the decomposition reaction since ammonia was not involved, and nitrogen and oxygen were the relevant product species to be observed. Gas chromatography was selected as a suitable quantitative method for these gases.

The NOx chemiluminescence analyzer was available for only a short time and preliminary efforts at quantifying ammonia by absorption and back titration were not successful (and will be discussed in section 3.5.3.). Consequently, gas chromatography was employed as a sole quantitative technique for the complete analysis of the gases during the direct decomposition study.

The equipment used and the analytical procedures employed will now be discussed.

3.5.1. GAS CHROMATOGRAPHY

A Varian 'Series 1400' gas chromatograph originally fitted with an FID was customized with the installation of a thermal conductivity detector (TCD). The TCD was a Gow-Mac model 10-952 Micro TC Cell fitted with gold plated filaments and had an internal volume of 0.14 ml. A Gow-Mac model 40-200 Power Supply Control Unit was employed in conjunction with the TCD and a Varian 4270 Integrator was used for data collection and analysis.

Helium was used as the carrier gas and was passed through a 3Å molecular sieve upstream of the GC to remove any water.

Column selection

The GC oven and its peripheral equipment described above are able to accommodate only a single column for gas separation, demanding that the analysis of nitrogen, oxygen, ammonia, nitric oxide, ammonia, nitrogen dioxide, nitrous oxide and water be effected with a single column.

Although many workers have used gas chromatography for the determination of oxygen, nitrogen, nitrous oxide and nitric oxide[10], few have employed this technique for the determination of nitrogen dioxide. Having scoured the NOx reduction literature, it was found that only one group used gas chromatography for the analysis of NO_2. Moretti *et al.* (1974) were able to separate the SCR products using two ovens and two columns (Chromosorb 102 with 10% tetrahydroxy-ethyl-ethylen-diamine and 5A) with detection limits of 1000 ppm for NH_3 and 500 ppm for N_2, O_2, NO, NO_2 and N_2O.

Hecker and Bell (1981) were able to analyze the products of NO reduction studies with three columns (Chromosorb 106, Chromosorb 103 and 5A) and two ovens. Although their detection limits lay between 10-35 ppm for each of NO, NH_3, N_2, N_2O, CO and CO_2, in the presence of CO, NO concentrations below 600 ppm could not be resolved.

As already described, the equipment available only made provision for a single oven and a single column.

In a novel application, Wilhite and Hollis (1968) recommended the use of 8 feet of Porapak Q in series with 8 feet of Porapak R for the separation of a likely Martian atmosphere (including: oxygen, nitrogen, nitric oxide, nitrous oxide, water, ammonia and nitrogen dioxide, all the gases of present interest), using a temperature ramping rate of 12°C/min. No detection limits were mentioned.

Such a column was fabricated and tested using the same temperature ramping rate and carrier gas flowrate but the desired separations could not be achieved. It was found that the ammonia, NO_2 and water peaks spread severely and tailed. Moreover, water and nitrogen dioxide were not separated.

Alternative analytical techniques were sought for the determination of ammonia and NO_2 and it was decided to pursue the separation of only nitrogen, oxygen and nitric oxide with gas chromatography. A standard for N_2O was not available and it was therefore not conclusively identified or quantified.

Li and Hall (1990) made use of eight feet of 5Å molecular sieve for the separation of nitrogen, oxygen and nitric oxide at room temperature but it was found here, that on a home-made column, nitric oxide was not eluted below 50°C. It was eluted however, upon raising the column temperature to 100°C.

---

[10] Amirnazmi *et al.* (1973), Moretti *et al.* (1974), Clay and Lynn (1975), Peters and Wu (1977), Seiyama *et al.* (1977), Bauerle *et al.* (1978), Tagaki-Kawai *et al.* (1980), Hecker and Bell (1981), Kato *et al.* (1981), Mahaligam *et al.* (1981), Powell and Nobe (1981), Hardee and Hightower (1984), Mizumoto *et al.* (1979), Iwamoto *et al.* (1991d), Hamada *et al.* (1991)

While the Porapak Q/Porapak R column was able to separate these three gases, six metres of Porapak Q alone yielded a superior resolution of nitrogen, oxygen and nitric oxide separation and this column was finally chosen for use in the remainder of this investigation. Elution times were significantly shorter than those on the 5Å column and separation could be effected at room temperature, removing the need for any temperature programming with its attendant complication of chromatogram base line drift.

Process gas selection

The NO concentrations of 3.8% and 1.1% used in this investigation, were far higher than would occur in combustion flue gases (approx. 1000ppm) and most studies of the SCR reaction have typically been carried out using concentrations of 300-1000 ppm. Noting the concentration dependence of rate equations, it was considered that reaction kinetics would be affected by the feed concentrations, but that the reaction mechanism would remain unaffected. Consequently, the concentrations were not unsuitable for the "effect studies" to be carried out.

3.8% NO in helium (ordered as 4%) was obtained and used in the investigation of the decomposition reaction since Li and Hall (1990, 1991) and Iwamoto *et al.* (1986) used 4% NO in helium in their studies. 1.1% NO/helium which was to be blended with ammonia, was used in the investigation of the SCR reaction.

GC is not as sensitive to NOx as a chemiluminescent analyzer, and the high NO concentrations would make it easier to use GC for its detection (detection limits have already been discussed).

In order to approximate authentic flue gas compositions, some workers have used NOx in nitrogen as a feed mixture. In all of these cases, catalytic activities were measured in terms of NOx conversions using NOx analyzers. Although theoretically possible, the use of GC to quantify the amount of nitrogen produced in the NOx reduction reactions in the presence of a nitrogen carrier gas would be profoundly difficult because the carrier would be in such large excess. Hence, in the present study, helium was chosen as an inert carrier for nitric oxide.

Quantitative determination by GC

Using the Porapak Q column, sampled gas concentrations were calculated by relating chromatogram peak areas to molar gas compositions. Since thermal conductivities vary for different gases, TCD response (peak area) is not identical for all gases. Thus, in order to make quantitative determinations, detector "response factors" are required. Dietz (1967) recorded these factors for many gases but none are listed for nitrogen oxides.

The weight response factors listed in the first column of Table 3.7 were taken from Dietz (1967) and were defined as (TCD response relative to benzene)*(molar mass of separated gas). Molar response factors were then calculated by dividing the weight factors by the molar mass and are shown in the second column of Table 3.7. The final column in this table reflects the molar response factors relative to nitrogen. The weight factors were converted to molar values to facilitate determination of gas compositions on a volume/molar basis, assuming the ideal gas law to be applicable under ambient conditions.

Table 3.7 TCD response factors (1st column only taken from Dietz, 1967)

Species	*Wt factor*	*Molar factor *10²*	*Molar factor relative to N_2*
Ar	*0.95*	*2.378*	*0.99*
CO	*0.67*	*2.393*	*1.00*
CO_2	*0.915*	*2.080*	*0.87*
H_2O	*0.55*	*3.056*	*1.28*
N_2	*0.67*	*2.393*	*1.00*
NH_3	*0.42*	*2.471*	*1.03*
O_2	*0.80*	*2.500*	*1.04*

Response factors for nitrogen, oxygen and nitric oxide for the present experimental system were determined by separately recording the chromatogram peak area counts for a number of samples of NO, synthetic air (79% N_2, 21% O_2) and high purity oxygen which had been diluted with helium. Area counts were correlated with theoretical gas compositions determined by gas flowrate measurements. The response of all three gases was linear over the concentration ranges of interest and the relative molar response factors were calculated to be:

$$NO : N_2 : O_2 = 1.16 : 1 : 1.02$$

using synthetic air as the source of nitrogen and oxygen (calculation procedure, data and graphs shown in Appendix 2).

The factor of 1.02 for oxygen relative to nitrogen compares well with 1.04 calculated from Dietz's results (Table 3.7). The relative factor for nitric oxide seemed a bit high in comparison to the listed factors but since this could not be compared directly with a documented source, the above factors were used.

To determine sample compositions, a peak area count was firstly obtained for a known NO concentration. Following that, oxygen and nitrogen concentrations were calculated by direct proportion, using the relative factors listed above. Typical calculations are shown in Appendix 2.

This sampling method is valid since the gas sample is always taken at the same temperature and pressure using a constant volume sample loop i.e., constant sample size.

The column was cleared periodically by maintaining it at 200°C overnight (maximum temperature for Porapak Q is 275°C) under flowing helium and at the same time, the TCD block was raised to 300°C.

A typical chromatogram is shown in Appendix 2. The integrated areas were determined from peak base to peak base, allowing for baseline drift..

The GC operating data and parameters used are listed in Table 3.8

***Table 3.8** GC operating data and parameters*

Column: 6 metres of 60/80 mesh porapak Q in 1/8" OD stainless steel tubing (self packed)	
Carrier gas:	*Helium*
Carrier gas flowrate:	*30 ml/min*
Column temperature:	*20°C*
TCD temperature:	*120°C*
Filament current:	*200 mA*
Amplifier gain:	*1*
Current attenuation:	*1*
Component residence times:	N_2 - *1.37 minutes*
	O_2 - *1.44 minutes*
	NO - 1.60 minutes
INTEGRATOR PARAMETERS	
Peak threshold:	*29*
Peak width:	*4*
Attenuation:	*1*

Oxidation of NO to NO_2 on the column.

Amirnazmi *et al.* (1973) cited a number of problems inherent in the use of GC for the separation of oxygen and nitric oxide: oxidation of NO on the column, disproportionation of NO to NO_2 and N_2O in the presence of oxygen, gas phase oxidation of nitric oxide to NO_2 and extreme tailing of the NO peak.

To minimize the oxidation of NO on the column, Amirnazmi *et al.* (1973) took two measures. In order to separate the nitric oxide and oxygen rapidly, 2 feet of Porapak Q were packed ahead of 4 feet of molecular sieve 5Å. In addition, the column was prepared using the method described by Dietz (1968) wherein the column was intentionally saturated with NO_2 to inhibit the oxidation reaction.

In the present study, analysis of a mixture of nitric oxide and oxygen with the Porapak Q column showed far less NO than the theoretical composition of the sample. For example, a blend of 0.48% NO and 1.83% oxygen was found to result in an integrated NO peak representing only 0.23% NO. While it has already been described that NO_2 was not quantified directly by GC, a mass balance calculated with the remaining NO and oxygen supported the assumption that NO_2 was produced. Upon ramping the temperature of the column to 150°C, a peak was observed where NO_2 was expected.

It is unreasonable to suspect that this NO_2 formation was occurring as an oxidation reaction prior to sampling since the residence time of the gas stream from the point of mixing NO with oxygen to the GC sampling valve was less than 3 seconds. This was further refuted by two tests:
1) the gas was passed through an ethanol bath at -38°C to condense any NO_2 (BP 21.3°C, Perry and Green, 1984)
2) verification with chemiluminescent NOx analyzer.

1) Cold trap
The amount of NO_2 removed by the cold trap should result in a proportional increase in the TCD response to the remaining NO. This was not observed. In fact, a further decrease in measured NO concentration was noted. This was attributed to the extended residence time within the extra length of piping to and from the cold trap, in this instance, allowing the oxidation of NO to take place prior to gas sampling.

2) NOx analyzer
NO/O_2 mixtures similar to those analyzed by GC were blended and fed to the NOx analyzer. With oxygen concentrations as high as 25%, the oxidation of NO to NO_2 was less than 11% with a tube residence time of 3 seconds. Thus it was not possible that as much as 60% NO conversion as indicated by the GC results, was occurring upstream of the GC.

An attempt was made to employ the technique used by Dietz (1968) to inhibit NO oxidation by saturating the Porapak Q with NO_2. This was not successful. Upon introducing a sample to the column, accumulated oxygen, nitrogen and nitric oxide were immediately eluted from the column.

3.5.2. NOx ANALYSIS BY CHEMILUMINESCENCE

Use was made of a Beckman Model 955 Chemiluminescence NOx Analyzer which has the capability of measuring NO and NOx over five concentration ranges from 25 to 10 000 ppm with a claimed linearity of 1% over each concentration range. Such an instrument is ideal for quantifying NOx since it is selective, robust and unlike GC, provides the capability of continuous on-line detection.

This technique relies on the reaction of nitric oxide with ozone to give NO_2. Approximately 10% of the nitrogen dioxide molecules produced in this reaction are initially in an electronically excited state.

$$NO + O_3 \rightarrow NO_2^* + O_2$$
$$NO_2^* \rightarrow NO_2 + h\nu$$

Photon emissions accompanying the return to a stable state are directly proportional to the feed NO concentration and a quantitative measurement is thus made in comparison with a known standard. In order to obtain a total NOx reading with a gas containing NO_2 as well as NO, the sample is first passed over a molybdenum catalyst (Kato *et al.*, 1981) which quantitatively reduces any nitrogen dioxide to nitric oxide before the sample is reacted with ozone.

High purity oxygen was used as a source for the ozone generator with a feed rate of approximately 1 litre per minute as recommended in the operating manual when using NOx concentrations above 2500 ppm.

It has been recommended by Kato *et al.* (1981) that should ammonia be present in the gas sample, it should be removed before entering the NOx analyzer. It was found that the ammonia reduced NOx over the catalytic converter in the analyzer and resulted in erroneous NOx readings. In the present work, it was found that this indeed, was the case. This occurred when the instrument was in "NOx" mode which required that the gas sample be directed to the molybdenum catalyst to obtain a combined reading for NO and NO_2. It was also recommended that water be removed to prevent the formation of ammonium nitrate and to prevent deposition on the windows and mirrors within the instrument thereby altering the effectiveness of the analyzer. In the "NO" (only) mode, the presence of ammonia does not affect the concentration of NO as recorded by the analyzer since the gas sample is not passed through the molybdenum catalyst.

In the present system, ammonia was removed by sparging the gas stream through a 28% w/w phosphoric acid solution and water was removed subsequently by passing the gas through a bed of phosphorous pentoxide.

Notwithstanding the NO source concentration being higher than the maximum readable concentration on the analyzer, the nitric oxide was used as a "span" or calibration gas; all measurements being made relative to this. Upon dilution which was required, the nitric oxide concentration fell into a range suitable for use with the analyzer. The analyzer was calibrated in the 0 - 10 000 ppm range, with the supplied gas spanned to give a reading of 5 000 ppm and all readings were taken relative to this calibration value.

A sample pressure of 1 psi was used, giving a theoretical sample flow of 60 ml/min to the reaction chamber.

The accuracy of the analyzer was tested by measuring the NO and NOx concentrations of various known gas compositions. Instrument readings and the theoretical gas composition of the blended gas mixture (as determined by flowrate measurements) were within 4% of each other which indicated that the instrument was suitable for use.

The nitric oxide-helium mixtures were analyzed as 3.8% and 1.1% by Fedgas with claimed accuracies of 2% of the stated concentration. These figures were not subsequently confirmed in any way.

Fractional NO conversion was calculated by:

$$1 - \frac{[NO]_{bypass}}{[NO]_{reactor}} \qquad (3.4)$$

where "bypass" signifies the concentration of NO in the stream which bypasses the reactor (feed concentration) and "reactor" represents the composition of the reactor product.

3.5.3. ANALYSIS OF AMMONIA

As described in Section 3.5.1 (Column Selection), GC was not used to quantify ammonia in this project. The use of GC for ammonia analysis has been described in the literature, however, it is not a trivial application, typically requiring two- and three-column systems and temperature ramping (Moretti *et al.*, 1974; Hecker and Bell, 1981).

In the present experimental program, attempts were made to quantify ammonia with solution chemistry but none were particularly successful. Two analytical techniques were applied, back titration after absorption into an acidic solution and direct measurement with an ammonia gas sensing electrode.

Various concentrations of H_2SO_4 (0.1 - 1.0 N) were used to absorb ammonia prior to back-titration with sodium hydroxide. Gas was sparged through a sintered glass disc to produce fine

bubbles to enhance mass transfer and to obtain complete absorption. In another configuration, to eliminate any gas loss through incomplete absorption, a predetermined volume of acid was displaced from a vessel by the ammonia containing gas. The trapped gas was then shaken up with the remaining acid, to obtain complete absorption. Both methods yielded inconsistent results which indicated between 40 and 70% of the theoretical amount of ammonia in the span gas (1.0%) as supplied and certified by *Fedgas*. Because of the pressure drop encountered, use of the sparger introduced a procedural difficulty in flowrate measurements. If flowrates are to be measured downstream of the sparger, clearly, a closed system is required to prevent any gas loss prior to the flowrate measurement.

The low concentrations of ammonia presented a difficulty to the acid-base titration technique. In order to obtain significantly high concentrations for confident measurements, a large volume of gas is required. Low gas flowrates are desired in order to ensure complete absorption into the liquid medium (using sparger). However, the use of low flowrates is thwarted by the practical desire of obtaining sufficiently large gas volumes in a reasonable time period. In addition, large volumes of base are required for the back titration.

It has been shown that titration was not able to confirm the concentration of the supplied ammonia stock gas. Further, it is suggested that the use of this quantitative procedure is unsuitable for SCR work because of the formation of nitric acid from the reaction of nitrogen dioxide (formed from NO and oxygen) and water according to the stoichiometry (Kirk-Othmer, 1981):

$$3NO_{2(g)} + H_2O_{(l)} \rightharpoonup 2HNO_{3(aq)} + NO_{(g)} \qquad (3.5)$$

In addition, nitrous acid is formed with the following stoichiometry (Ebbing, 1984):

$$NO_{(g)} + NO_{2(g)} + H_2O_{(l)} \rightharpoonup 2HNO_{2(aq)} \qquad (3.6)$$

In an investigation to confirm the inappropriateness of acid-base titration for quantifying ammonia in this work, NO and oxygen were bubbled through a water bath and the pH was monitored. The pH was seen to decrease in accordance with the formation of acid species as described above.

An attempt was than made to obtain direct concentration measurements with a Corning ammonia selective electrode. While not designed as a gas phase measuring instrument, the supplier of the electrode suggested that it could be employed in this fashion, on condition that the membrane was kept moist. The instrument was found to be unsuitable for gas phase measurements - erroneous and inconsistent readings were recorded. The electrode was then used to monitor the concentration of ammonia in a liquid bath into which gas was constantly absorbed. The response of the electrode was found to be too slow to make such continuous measurements. In a

continuous application, the electrode would be suitable for recording fluctuations about a mean concentration but could not be used to monitor the increasing concentrations encountered here. In the next attempt at employing the electrode, it was used to make discrete readings of ammonia which had been absorbed into a known volume of an acid solution over a fixed time period. This too, was unsuccessful - inconsistent readings were recorded. Although without experimental evidence to this effect, it is suggested that NO may have caused interference and consequently produced erroneous measurements. It was revealed that the sensitivity of ion selective electrodes in general, demanded great care in their use[11].

A few methods of ammonia analysis which have been described in the literature are:

- NOx/NH_3 chemiluminescence analyzer with *Matheson-Kitagawa* NH_3 detection tubes (Nam *et al.*, 1986)
- Spectrophotometric methods: Nessler's reagent (Kiel *et al.*, 1992) and "indophenol blue" (Mizumoto *et al.*, 1979)
- Infra-red spectrophotometry (Hirsch, 1982)

Other workers (*e.g.*, Kiovsky *et al.* (1980), Choi *et al.* (1991)), did not make ammonia measurements but relied on the knowledge of feed concentrations to calculate data such as NO:NH_3 ratios, and monitored the extent of the SCR reaction through NOx conversions.

Dräger[12] tubes for ammonia in the concentration range 0.05 to 10 vol.% were used for occasional measurements. The reaction of ammonia with bromophenol blue indicator produced a violet coloration along the linearly calibrated tube which provided a direct indication of ammonia concentration by visual inspection (standard deviation 10-15%). The tubes were used in conjunction with a pump which administered a constant volume of gas which was to be analyzed.

Use of the tubes to confirm the concentration of ammonia delivered and certified as 1.0% by Fedgas, indicated a concentration of 0.87%. The implications of this result are discussed in Section 4.2.7, in conjunction with the results of the experimental runs.

In the experimental work to be described in Chapter 4, NO conversion (NOx analyzer) and nitrogen measurements from GC were used to follow the extent of the SCR reaction.

---

[11] Professor K. Koch, Analytical Chemistry, University of Cape Town (Private communication).

[12] Drägerwerk Aktiengesellschaft Lübeck, Federal Republic of Germany.

3.5.4. OPERATING PROCEDURE

The following procedure was observed in the execution of a typical experimental run (additional details are presented thereafter):

1. Weigh desired amount of catalyst powder
2. Dismantle reactor, rinse (with water) and dry to remove any traces of previous catalysts used
3. Create catalyst bed support by inserting glass wool into reactor tube and packing against the inner glass sleeve
4. Pour measured catalyst mass on top of glass wool plug and re-assemble reactor
5. Introduce synthetic air flow at 30 ml/min (down flow) for calcining (open valves "I" and "K" and close "J" in Figure 3.9)
6. Heat reactor to 520°C and maintain for at least 4 hours
7. Upon completion of calcination, divert gas flow from reactor (ie to bypass by opening "J" and closing "I" and "K") and terminate air flow
8. Remove air supply line and connect helium source to valve "B" (Figure 3.9)
9. Set required flowrates: NO or NO, NH_3 and oxygen by using a soapfilm meter and stopwatch, manually adjusting needle valves "E", "C" and "H" as required.
   Adjust valve "L" to obtain pressure of 10 kPa upstream of "L" for constant GC sample pressure
10. Switch off all reactant gases by closing valves "A", "G" and "D" and still in "bypass mode" introduce helium flow to purge all manifolds and passages
11. Switch helium flow from bypass to the reactor, purging reactor of calcination air
12. Adjust controller set point to obtain desired reactor temperature under helium flow and allow to settle (at least 1 hour)
13. Sample helium flow (passing through reactor) to observe any air leaks and address leaks as they arise.
14. Switch off helium flow by shutting valve "B"
15. Turn on pre-adjusted NH_3, O_2 and NO flows in order (valves "A", "C", "D")
16. Start stopwatch to monitor time on-stream
17. Sample gas with using GC or other technique at desired time intervals.
18. Shut off gas supplies in same order as they were turned on and switch furnace off if desired

If reactor temperature is to be changed using the same charge of catalyst, helium is first used to purge the reactor and flow system before the reactor is allowed to attain its new setpoint temperature. Similarly, if flowrates are to be adjusted, helium is first used to purge the reactor of remaining reactants and products. New gas flows are then be established individually (on bypass) and the new gas composition introduced when required.

GC alone was used for analysis of the direct decomposition reaction while, in addition to this, the NOx analyzer was used in the investigation of the SCR reaction.

Gas sampling procedure for GC

While investigating the direct decomposition reaction, the entire gas stream was directed through the GC sampling valve since the flowrates were low (30 ml/min). This was done by closing ball valve "M" in Figure 3.9. When higher flowrates were used in the SCR investigation (1000-1800ml/min), a representative gas sample was forced to pass through the sample loop by maintaining a pressure of 10 kPa in the sample delivery line. This was obtained by manually adjusting valve "L" (with "M" open) while the pressure was monitored on a 0-250 kPa gauge as indicated in Figure 3.9. With a pressure of 10 kPa upstream of the sampling valve, a gas flowrate of 84 ml/min was obtained through the sampling loop. This relates to a residence time of 0.94 seconds from the tee piece ahead of "L" to the sampling point. The remainder of the gas stream bypassed the sampling line and with a total feed rate of 1 litre per minute, to a total residence time less than 3 seconds from the reactor outlet to the sampling point was obtained. This configuration was designed to allow the pressure in the reactor to closely approach ambient conditions. Thus, the system was operated at essentially atmospheric pressure.

Operation at constant pressure avoided errors in flow and feed composition in the absence of mass flow controllers. In addition, the delivery pressure from each of the gas cylinders was set at 300 kPa, chosen as a sufficiently high pressure to minimize flowrate changes upon altering the manifold pressure when blending two or more gases. The error between total flowrates as a sum of individual flow measurements and a reading of the combined flows was typically less than 1.5%. Preliminary efforts to control gas flow using purge rotameters were unsuccessful and necessitated the use of finer needle valves and a soap film meter.

In obtaining and analysing a gas sample, the sampling valve was turned to admit the sample to the column and left in this position until nitrogen, oxygen and nitric oxide had been eluted (1.7 minutes). Only after complete elution was the sampling valve turned to its original position. This was done to eliminate "spikes" appearing in the chromatogram.

Catalyst bed packing/pressure drop considerations

It was found that both the silicalite and CuO/filter mix had a high packing density which resulted in high pressure drops across packed beds of 0.5 g. In contrast, a 1 g packed bed of ZSM-5 with a tapped height of approximately 3.5 cm did not hinder gas flow significantly. When low flowrates were used (30 ml/min), the difference between gas flowrate through the

reactor and on "bypass" was less than 4% and when higher flowrates were used (> 1000 ml/min) the difference was of the order of 5%.

The difference in physical association of the silicalite and ZSM-5 may be observed in the scanning electron micrographs displayed in Figure 3.4 and Figure 3.5 which show that the silicalite particles are essentially discrete while the ZSM-5 crystallites can be seen to form agglomerates. The difference in packing was obvious to the naked eye, with a packed bed of ZSM-5 permeated by visible channels as a result of the agglomeration. It has already been suggested that electrostatic forces were responsible for this phenomenon.

In order to overcome the excessive pressure drop and near complete flow restriction caused by the packing density of silicalite and CuO/filter mix, less catalyst was used and the powders were dispersed in wads of glass wool which were then inserted into the reactor. Specific details of the runs are described in Chapter 4 and are listed in Appendix 5.

Catalyst pre-treatment/calcination

In-situ calcination of ZSM-5 (steps 5 and 6 of run procedure) was carried out to remove chemisorbed water and any remaining organics (eg template). Silicalite impregnated with copper nitrate was calcined to produce the desired catalyst, CuO brought about by the thermal decomposition of the salt (refer Section 3.2.4.)

Verification that the copper on the ZSM-5 was indeed ion exchanged and was not present in the form of copper oxide after calcination (and reaction) could be obtained from the colour of the catalyst. At 500°C, Cu-ZSM-5 was greyish but returned to a blue colour upon cooling to room temperature, while the impregnated silicalite was visibly and permanently blackened (CuO).

3.5.5. REACTOR AND CATALYST SUPPORT SUITABILITY

As part of the commissioning of the experimental rig, the suitability of the thermocouple which was in direct contact with the reactants, was investigated. The thermocouple was found not to impart any catalytic activity.

In a separate exercise, the suitability of glass wool[13] was examined. Again, no catalytic activity was observed.

[13]Technical grade, "UniTEK" low lead glass wool by SaarChem (PTY) LTD

Ceramic filter material (undoped) was examined for any catalytic activity at 450°C, by loading the reactor with 0.5 gram of the powder. Essentially no nitrogen was recorded as a reaction product and the ceramic filter material could be considered as catalytically inactive for the SCR reaction.

Having commissioned the rig and its associated analytical equipment and established suitable operating practices, the investigation of the reactions/catalysts was initiated. The results of the study will now be presented and discussed.

4. RESULTS AND DISCUSSION

As described in Chapter 1, the objectives of the experimental program were to evaluate two catalysts *viz*, Cu-ZSM-5 and CuO for the catalytic reduction of nitric oxide. The preparation of these catalysts and the experimental rig have been described in Chapter 3 and results of the reaction studies are now presented in the order in which they were carried out: the decomposition reaction followed by the selective reduction with ammonia.

Each experimental run has been numbered sequentially and the operating parameters, product analysis details and calculated data are listed in Appendix 4 and 5.

4.1. THE DIRECT DECOMPOSITION OF NITRIC OXIDE

4.1.1. INTRODUCTION

The decomposition reaction was studied with the intention of duplicating published results in an attempt to validate the experimental procedures employed. This was done by investigating the decomposition of NO (3.8% in helium) over copper ion exchanged ZSM-5. The operating parameters which were varied were reaction temperature and NO feed composition, and the results were compared with those published by Li and Hall (1991) and Iwamoto *et al.* (1986).

4.1.2. THE EFFECT OF TEMPERATURE

NO conversion and nitrogen production with temperature

Total NO conversion and conversion to nitrogen are plotted in Figure 4.1 as a function of temperature. The terms are defined as:

$$\text{Fractional NO conversion:} \quad \frac{[NO]_i - [NO]_o}{[NO]_i} \qquad (4.1)$$

$$\text{Fractional Conversion to } N_2\text{:} \quad \frac{\text{moles of } N_2 \text{ produced}}{\text{moles of NO in feed}} \qquad (4.2)$$

Both NO conversion and conversion to nitrogen are seen to increase with temperature, and notwithstanding the visible scatter for the data recorded at the highest temperatures, these data suggest a decrease in catalytic activity above 500°C. The form of these two graphs is not unlike that displayed in Figure 2.16 for NO conversion and conversion to nitrogen, taken from Iwamoto *et al.* (1991d).

The presence of product(s) other than nitrogen is indicated by the values of NO conversion to nitrogen in Figure 4.1, which are less than the maximum value of 50% as calculated by Equation (4.2) in accordance with the stoichiometry of the direct decomposition reaction (Equation (2.11)). The discussion of the direct decomposition in Chapter 2, revealed that these products would be nitrogen dioxide and below 400°C, nitrous oxide. The oxidation of NO to NO_2 was discussed in Section 2.4.3 and Section 3.5.1.

The graph of NO conversion to nitrogen indicates onset of significant nitrogen production above 350°C. This temperature co-incides with the temperature at which oxygen desorbs from Cu-ZSM-5 (Li and Armor, 1991) and confirms Li and Hall's (1991) proposal that the rate limiting step in the decomposition reaction is the desorption of oxygen (the reaction product), which is required in order to renew active sites for further reaction.

Similar to the findings of both Iwamoto *et al.* (1991d) and Li and Hall (1991), the activity of the catalyst was completely "reversible" over the entire temperature range examined and showed no permanent deactivation at temperatures above 500°C. It should also be noted that Iwamoto *et al.* (1986) observed no deactivation in a run which extended over 30 hours.

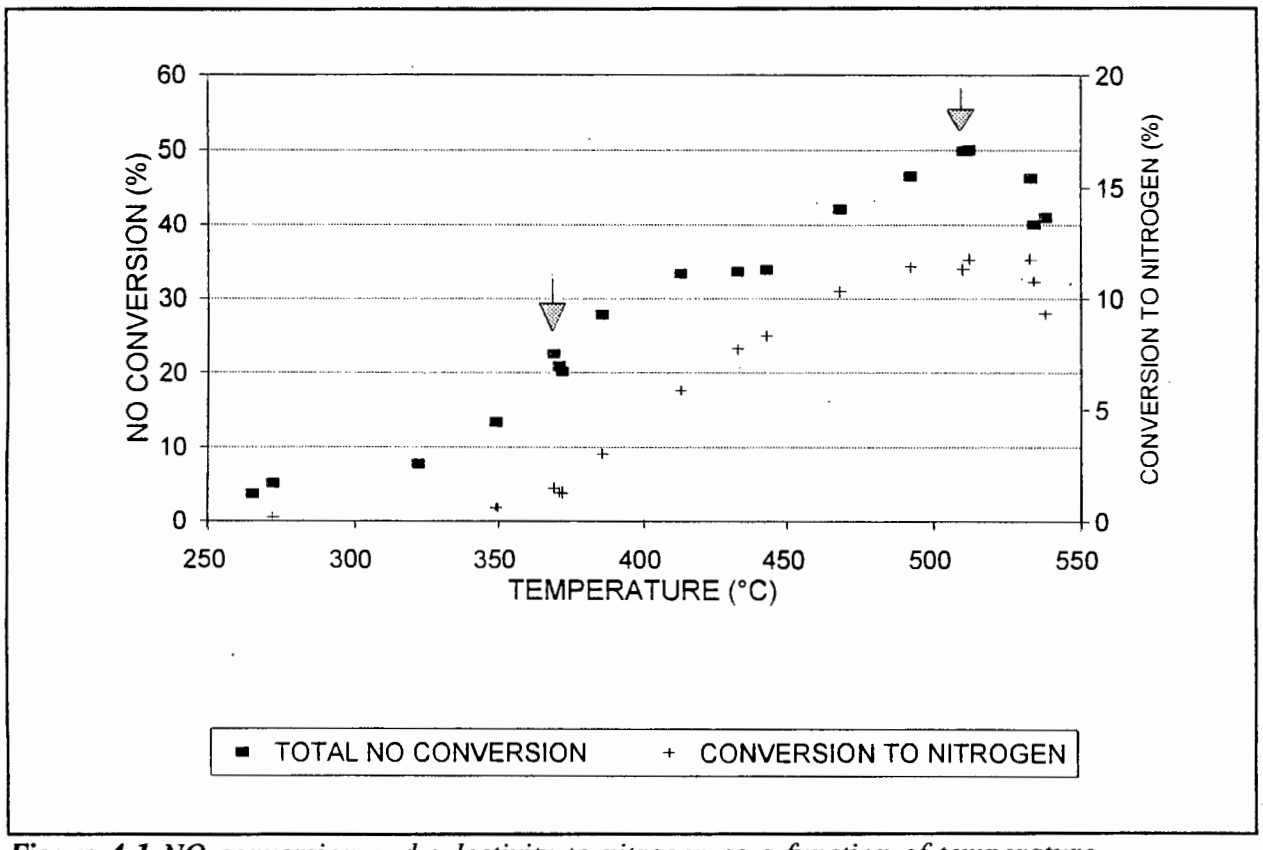

Figure 4.1 *NO conversion and selectivity to nitrogen as a function of temperature (Arrows indicate "repeat" runs)*

Reaction rates as a function of temperature

In order to calculate an activation energy of reaction and to allow a comparison to be made with Li and Hall's (1991) data, turnover frequencies (TOF) were calculated from the amounts of nitrogen produced by the direct decomposition reaction. The turnover frequency is defined as: the number of NO molecules converted per copper ion per second or alternatively, according to the stoichiometry of the decomposition reaction, as twice the number of nitrogen molecules produced per copper ion per second. These TOFs are plotted against the inverse of temperature to produce an Arrhenius Plot in Figure 4.2.

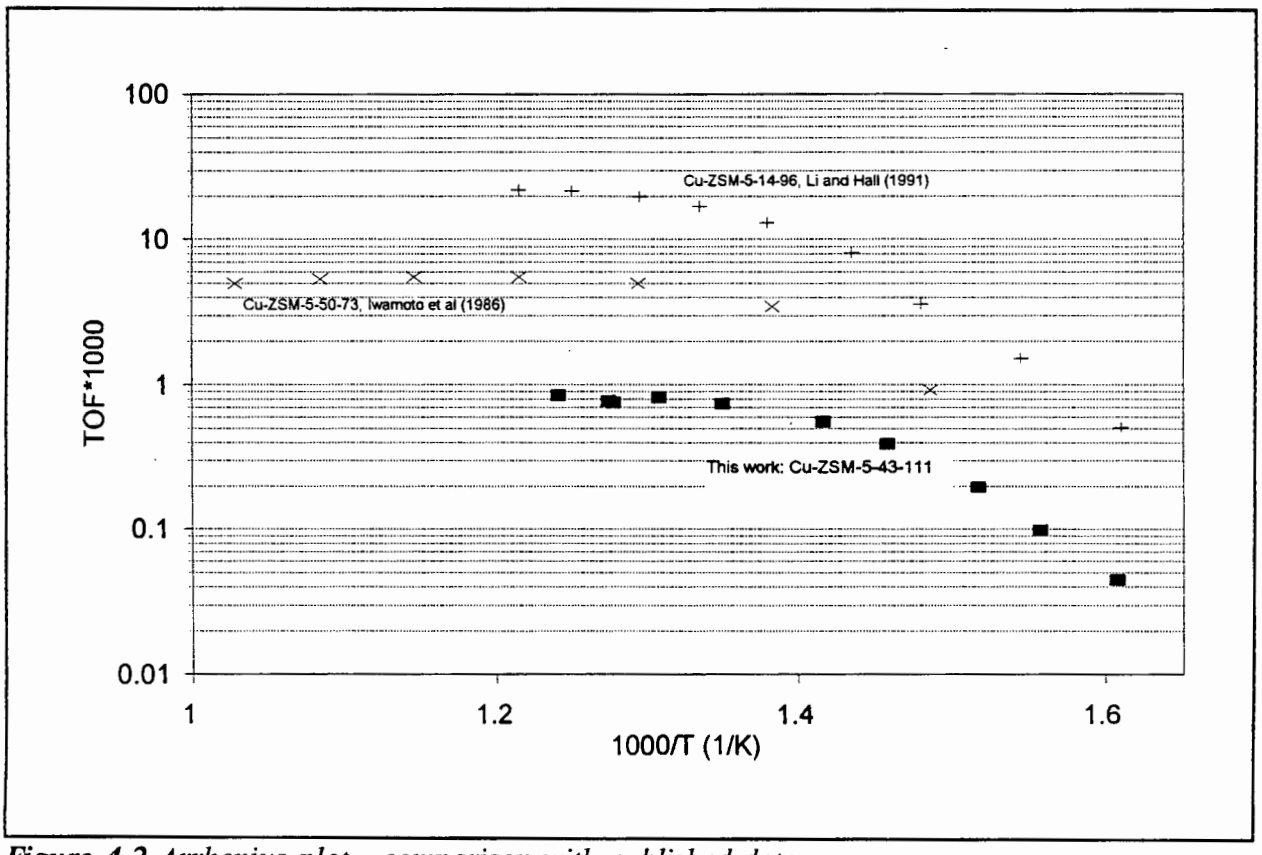

***Figure 4.2** Arrhenius plot - comparison with published data*

In Figure 4.2, the data are compared with those obtained by Li and Hall with Cu-ZSM-5-14-96 and Iwamoto *et al.*[14] (1986) with Cu-ZSM-5-50-73. While the graphs are similarly shaped, the TOFs are an order of magnitude lower than those obtained Li and Hall and are also lower than those obtained by Iwamoto *et al.*

[14] TOFs calculated using data read from "Figure 2"-Iwamoto *et al.* (1986). Calculation shown in Appendix 4.

Two explanations are offered for the lower TOFs recorded in the present work:

1) Catalyst preparation - In the use of a ZSM-5 sample which had been prepared with the templating agent TPA-Br, Iwamoto *et al.* (1986) observed a four fold decrease in specific activity compared with ZSM-5 which had been synthesized using a template-free method (refer Figure 2.15).

2) Copper content - Li and Hall (1991) observed a strong dependence of TOF on total copper content. Data in Table 2.3 taken from Li and Hall (1991), shows Cu-ZSM-5-14-96 with 0.51 mmol Cu/g yielding a turnover frequency four times higher than Cu-ZSM-5-24-76 with 0.25 mmol Cu/g, which is closer to the amount of copper used in the present study (see Table 4.1 below).

   Because of the dependence of TOF on total copper content observed by Li and Hall, it was suggested in Chapter 2, that in order to compare two catalysts, they should both contain (ideally) identical amounts of copper. This is however, not easily achieved in practice.

Table 4.1 *Comparison of rates for nitric oxide decomposition at 500°C and activation energies*

Catalyst	*Cu loading (mol. Cu/g)*	*TOF*1000*	E_a *(kcal/mol)*	
Cu-ZSM-5-14-96	$5.1*10^{-4}$	*20.1*	*29*	*(Li and Hall, 1991)*
Cu-ZSM-5-46-111	$1.9*10^{-4}$ *(wet)*	*0.87*	*29*	*(This work)*

Unlike Li and Hall (1991), who used 20-50 mg of catalyst and obtained conversions of the order of 4-8%, a catalyst mass of 1 gram yielded theoretical NO conversions[15] of up to 27% (at 512°C) in the present study. At such high conversions, the differential conditions employed by Li and Hall (1991) were not attained. TOFs calculated using data at high conversions would reflect an average rate across the catalyst bed which would have been subjected to a significant reactant concentration gradient, resulting in lower observed average reaction rates.

[15] This is a "theoretical" NO conversion, back-calculated by considering the amount of NO required (by reaction stoichiometry) to produce the amounts of nitrogen recorded by GC i.e., NO consumed in oxidation to NO_2 is not included (calculations shown in Appendix 4).

Table 4.2 The effect of feed flowrate on reaction rate

RUN#	*TEMP. (°C)*	*FEED FLOWRATE (ml/min)*	*NO CONV. TO N_2 (%)*	*1000*TOF*
20	*510*	*24.3*	*27*	*0.75*
33	*503*	*92.3*	*15*	*1.50*

While a theoretical NO conversion of 27% was recorded for Run# 32 (as listed in Appendix 4) at 512°C, runs carried out at lower temperatures eg. Run# 22 at 322°C, gave conversions below 10%. In these cases of low conversion, differential conditions may be assumed and the TOFs obtained in the present study may be directly compared with Li and Hall's data. At these low temperatures, the TOFs recorded in the present investigation remain an order of magnitude lower than those obtained by Li and Hall. The TOFs are also lower than those calculated from Iwamoto *et al.*'s (1986) data, which were recorded under conditions of essentially complete NO conversion. This clearly indicates that the reaction rates recorded in this study, are lower than those obtained by Li and Hall and Iwamoto *et al.*

Activation energy of the decomposition reaction

The slope of the Arrhenius plot (Figure 4.2) represents an activation energy for the reaction. The log of the TOFs below 400°C increase linearly with temperature and the reaction rates were considered to be in a regime of kinetic control. Linear regression of these data yielded an activation energy of 29 kcal/mol (r^2= 0.990) for the decomposition reaction (Calculation shown in Appendix 4).

This result falls on the upper limit of the 17-29 kcal/mol range obtained by Li and Hall (1991) for a number of samples of copper exchanged ZSM-5 (Table 2.4) and corresponds with the activation energy calculated for their Cu-ZSM-5-14-96.

4.1.3. THE EFFECT OF VARYING NO FEED CONCENTRATION

To complement the comparison of the present work with Li and Hall's results, the dependence of the reaction rate on NO concentration was investigated. While maintaining a constant reactant flowrate, turnover frequencies were obtained with various NO feed concentrations which were achieved by diluting the stock 3.8% NO in helium, with additional helium.

The data which were collected at 500°C, are presented in Figure 4.3. Linear regression of the data produced a slope of 1.2 (r^2 = 0.979) (Data and regression results shown in Appendix 4).

Li and Hall (1991) examined the dependence of the NO decomposition rate on NO partial pressure over Cu-ZSM-5-26-166 between 350 and 550°C and obtained reaction orders in the range 0.9 to 1.1. The first order dependence (1.2) obtained in the current work by linear regression of the data plotted in the same way as that done by Li and Hall, compares favourably with the results obtained by them.

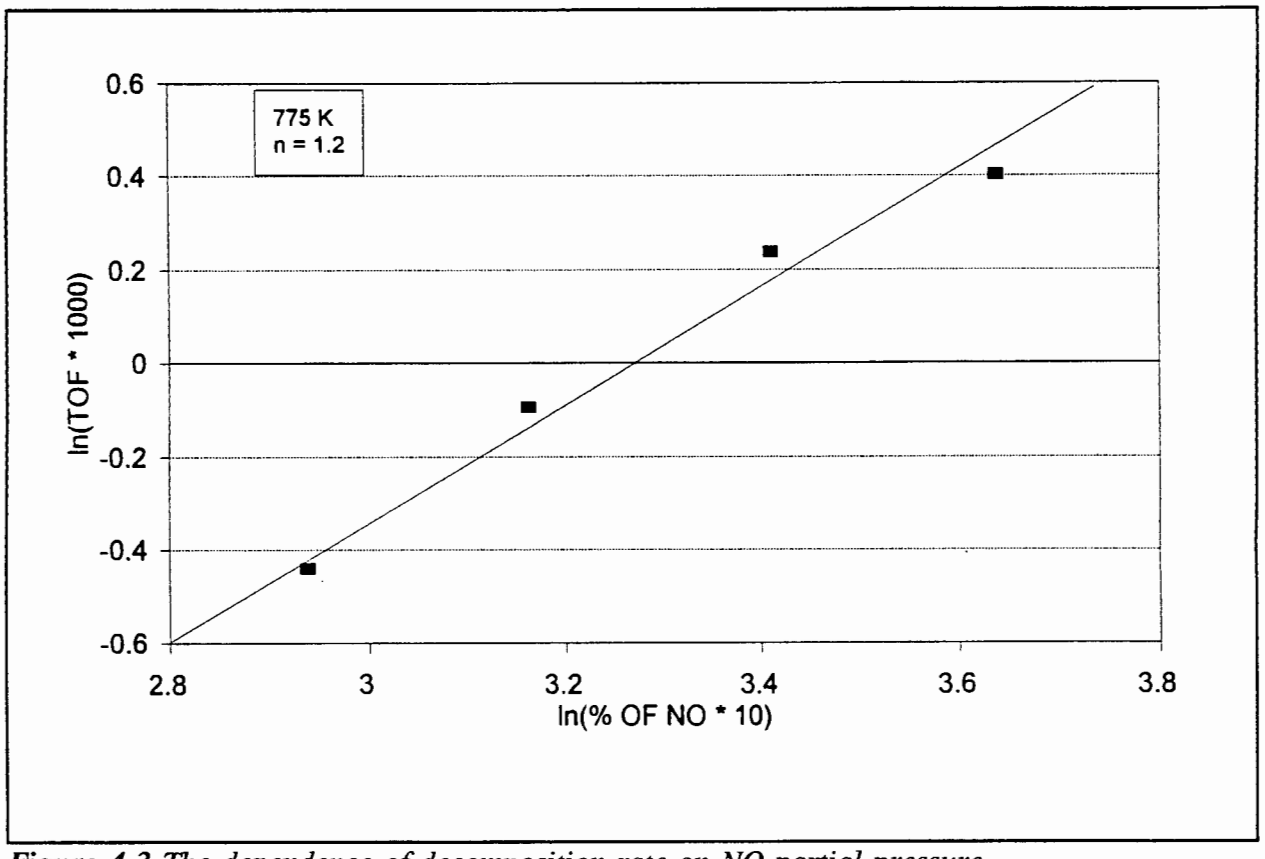

Figure 4.3 The dependence of decomposition rate on NO partial pressure

4.1.4. MASS BALANCE CONSIDERATIONS

Prior to recording a chromatogram for the reactor effluent, a sample of the feed gas was analyzed with the reactants bypassing the reactor. This was done in order to reconcile the mass balance, accounting for any nitrogen or oxygen present in the feed. The amount of nitrogen produced in the reaction was then calculated by difference between the amount recorded as reactor product and any nitrogen which might have been recorded in the feed.

While above 400°C, the catalytic decomposition of nitric oxide is intrinsically stoichiometric (Li and Hall, 1990), the homogeneous gas phase oxidation of nitric oxide to nitrogen dioxide must be accounted for. As indicated by Figure 2.16 from Iwamoto *et al.* (1991d), below 400°C, nitrous oxide is produced and this must also be considered in the calculation of a mass balance.

Since nitrous oxide was not quantified in the present investigation (see Section 3.4.1), mass conservation was verified by considering only two possible reactions:
1) the direct decomposition reaction (equation (2.11))
2) the oxidation to NO_2 (equation (2.12))

The total amount of nitric oxide converted (as recorded by GC) was compared with a theoretical NO consumption. This theoretical NO consumption was obtained by considering the sum of the amounts of nitric oxide which were required to produce nitrogen and nitrogen dioxide according to the stoichiometries of equation (2.11) and equation (2.12). The amount of nitrogen produced in the reaction, was recorded by GC and since no oxygen product was observed, it was considered to have been entirely consumed in the oxidation with unconverted NO to produce NO_2 (as per equation 2.12).

For runs carried out below 400°C, large discrepancies were encountered in the reconciliation of recorded (GC) and theoretical NO consumption figures (calculated according to the assumptions described above). However, at higher temperatures, differences of less than 10% were obtained. The difference between recorded and theoretical NO conversions are listed in Table 4.3 as percentages (calculations shown in Appendix 4).

As an example, on the basis of a constant volume gas sample, GC data indicated a total consumption of 0.77% NO for Run# 23 carried out at 372°C in which only 0.05% nitrogen was produced. According to the stoichiometries of reactions (2.11) and (2.12), the theoretical NO required to produce this amount of nitrogen (0.05%) and the amount of nitrogen dioxide associated with 0.05% oxygen (ie. 0.1% NO_2), is 0.2% NO. This value represents 26% of the actual nitric oxide consumption (0.77%) as recorded by GC, yielding a discrepancy or "error" of 74%.

Table 4.3 *Discrepancy between actual and theoretical NO conversion*

RUN#	*TEMP (°C)*	*ERROR (%)*
22	*322*	*55*
23	*372*	*74*
24	*400*	*10*
25	*433*	*7*
26	*468*	*2*
27	*492*	*2*
28	*533*	*-2*

In the runs labelled 22 to 28 in Table 4.3, as the reaction temperature increased from 322 to 533°C, the discrepancy in the mass conservation calculation fell below 10% at Run# 24 which was recorded at 400°C and decreased to 2% at higher temperatures.

It is suggested that the "missing" nitrogen (unaccounted for by the two reactions: direct decomposition and oxidation reaction) was consumed in the formation of nitrous oxide at temperatures below 400°C. While the presence of nitrous oxide was not monitored, these data and the explanations offered for the discrepancy in the "mass balance" carried out, do not contradict the observation of nitrous oxide production below 400°C as noted by Iwamoto *et al.*

(1991d) and the absence of nitrous oxide at higher temperatures as noted by Li and Hall (1991) and Li and Armor, 1992) - refer Section 2.4.3.

4.1.5. REACTOR RESPONSE

Figure 4.4 and Figure 4.5 shows nitrogen peak area counts taken at five minute intervals for two separate sets of runs executed at various temperatures. The data shown in Figure 4.4 were obtained using a fresh catalyst sample and the run at 500°C was the first experimental run performed after calcination. The data in Figure 4.5 were obtained the following day, using the same batch of catalyst which had been left overnight in a static environment. Out of the three runs shown, the run at 369°C (filled squares) was the first to be executed.

In both figures, the data represented by filled squares show a marked decrease in nitrogen production within 20 minutes of contact with the feed gas flow while the remaining graphs do not show this trend.

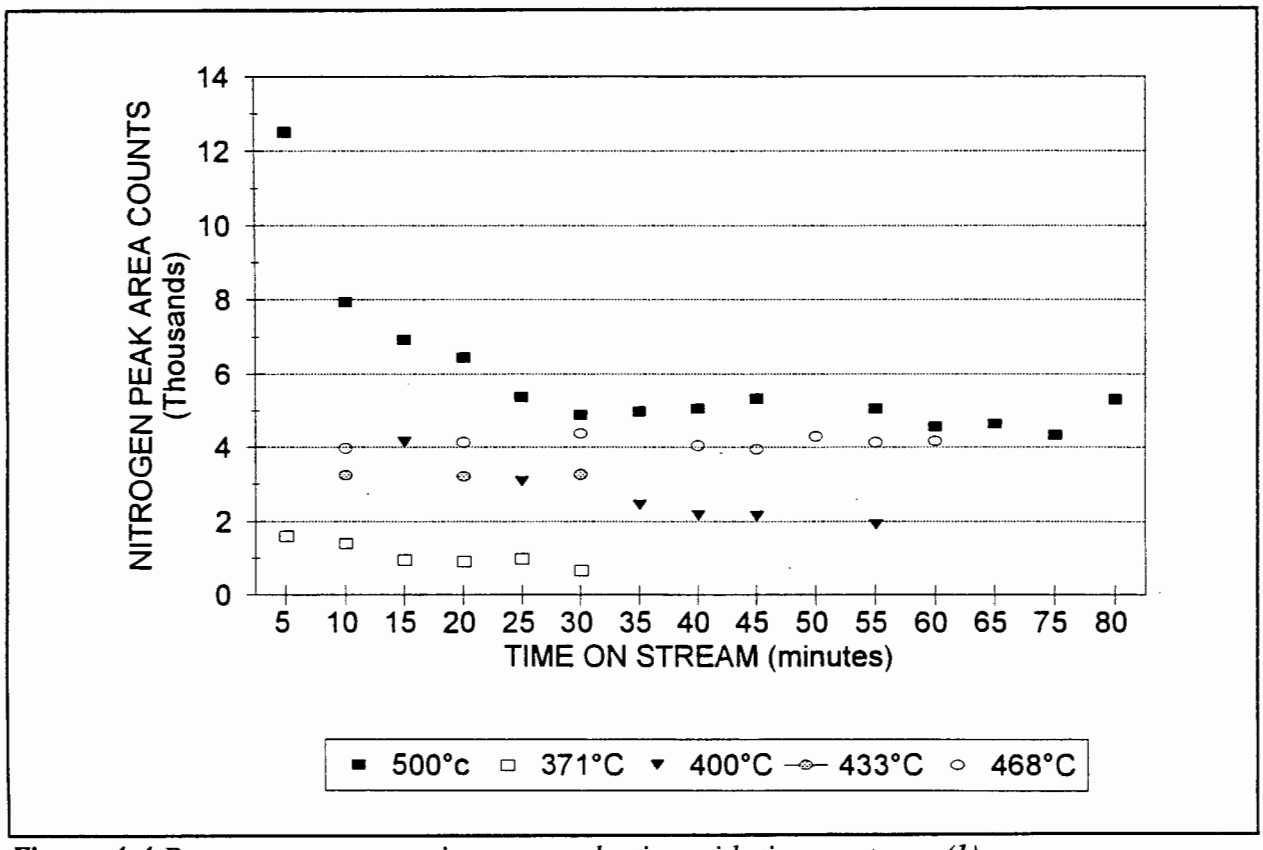

Figure 4.4 Reactor response - nitrogen production with time onstream(1)

Such a trend was observed by Li and Hall (1990), whose data show attainment of steady state within 20 minutes (Figure 4.6). The same trend (decreasing nitrogen production on approach

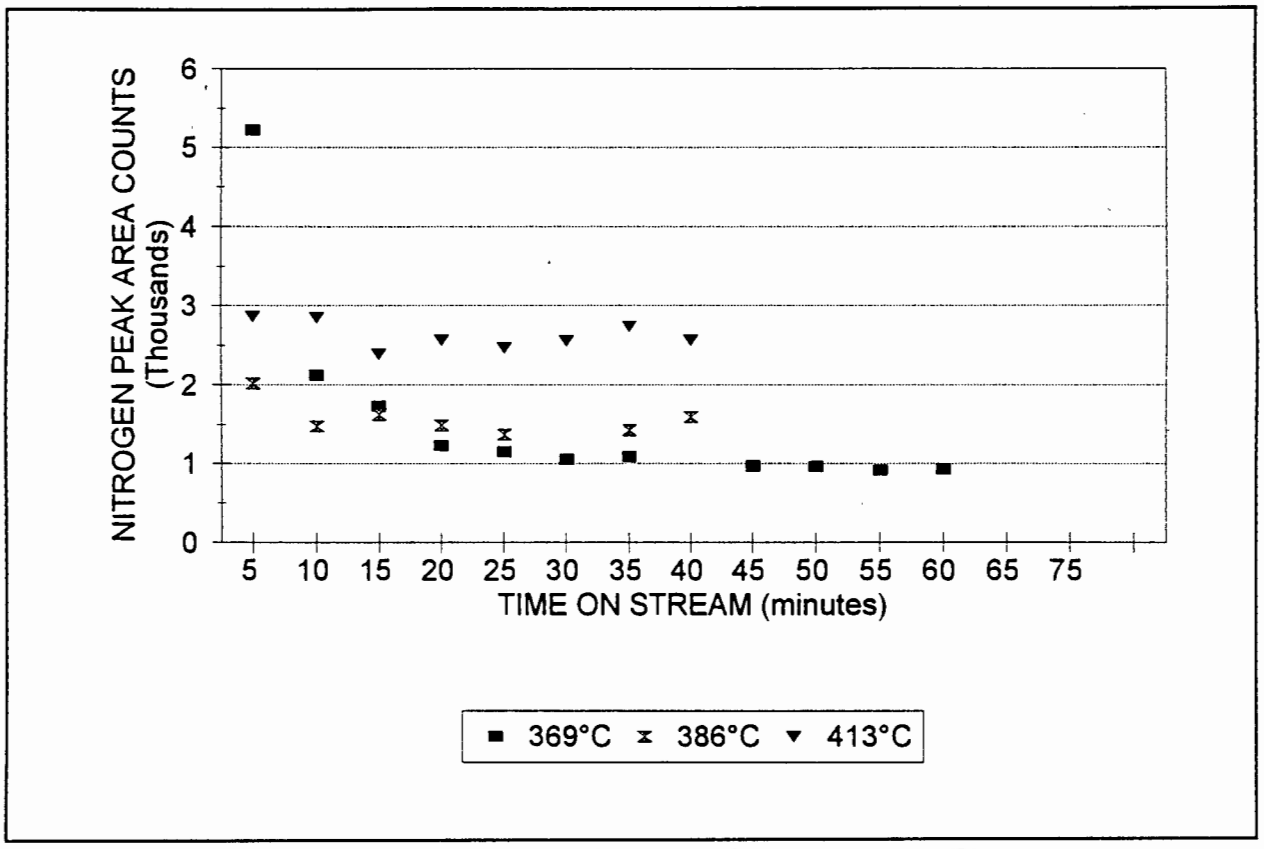

***Figure 4.5** Reactor response - nitrogen production with time onstream(2)*

to steady state) was observed in the "pulse experiments" carried out by Li and Hall (1991) shown in Figure 4.7.

The sharp decrease in nitrogen production in the two runs discussed above (filled squares in Figure 4.4 and Figure 4.5), suggests an approach to an equilibrium or steady state for the active sites, as suggested by Figure 4.7. As described in the operating procedures listed in Section 3.5.4, the catalyst bed was purged with helium between consecutive runs. It is suggested that the equilibrium for the active sites was maintained over the 1 hour intervals between the consecutive runs carried out at different temperatures, but was not maintained overnight; the state of the active sites reverted to that of the freshly calcined catalyst. It is not unreasonable to suggest that the active monovalent copper ions (at equilibrium) were re-oxidized by air (oxygen) which diffused into the catalyst bed overnight while the reactor was not purged with helium.

The data shown in Figure 4.4 and Figure 4.5 clearly indicate when steady state was reached and "steady state values" used to calculate TOFs were obtained by averaging the data typically collected after 20 minutes on stream.

In order to determine the consistency of the data, the readings at 371°C were duplicated twice, with one of the points being recorded after an interval of six days. The repeat runs are indicated

with arrowheads in Figure 4.1. A reading at 510°C was also duplicated well, certifying the repeatability of the data.

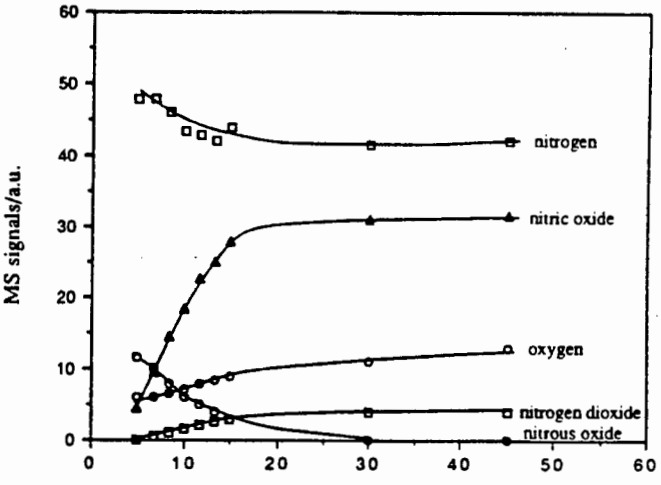

Mass spectroscopy signals of the product stream of NO decomposition reaction over Cu–ZSM-5-26–166 at 773 K and a contact time of 1 s. The background signals of O_2 and N_2 were 4 and 16 (arbitrary units), respectively. Shown are the uncorrected data. The instrument used was not calibrated for sensitivity, and so the data are presented as arbitrary units (au).

***Figure 4.6** Product spectrum with reaction time (Li and Hall, 1990)*

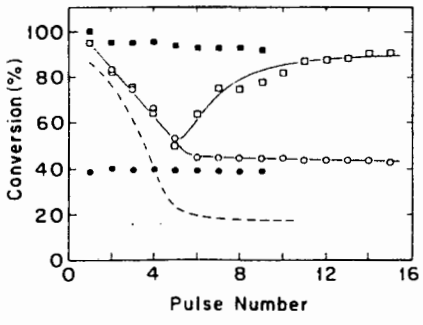

Pulsed experiments for NO decomposition over Cu-ZSM-5-26-166. (□) represents the conversion of NO (the disappearance of NO) over a reduced sample pulsed at 773 K. (○) the conversion to N_2 over the reduced sample pulsed at 773 K, (■) the conversion of NO over an oxidized sample pulsed at 773 K, and (●) the conversion to N_2 over the oxidized sample pulsed at 773 K. The dashed line shows the conversion to N_2 over the reduced sample when pulsed at 623 K.

***Figure 4.7** Pulse experiments for NO decomposition (Li and Hall, 1991)*

4.1.6. SUMMARY OF FINDINGS

This investigation of the direct decomposition of nitric oxide over Cu-ZSM-5 has revealed the following findings:

- Response to temperature qualitatively similar to observations of Iwamoto *et al.* (1986, 1991a,c,d), Li and Hall (1990, 1991).
- TOFs lower than those obtained by Li and Hall (1991) and those calculated using data obtained by Iwamoto *et al.* (1986)
- An activation energy of 29 kcal/mol
- First order rate dependence on NO partial pressure
- An ability to duplicate an E_a and order of reaction with respect to NO, published by Li an Hall (1991)
- Additional information is required for complete mass balance calculation (N_2O and NO_2)

This ability to produce the data and results described above, verified the suitability of the equipment and experimental procedures. With this confidence, the next experimental phase was initiated - the investigation of the selective catalytic reduction of NO with ammonia.

4.2. THE SELECTIVE CATALYTIC REDUCTION OF NO WITH AMMONIA

4.2.1. INTRODUCTION

One of the aims of the present experimental phase was to examine the feasibility of employing copper doped amorphous aluminosilicate fibres for NOx removal. Underlying the selection of this ceramic filter fibre is the belief that the reduction of NOx and particulate removal from flue gases may be effected simultaneously. However, the inability to impregnate the non-porous aluminosilicate fibres with copper nitrate has already been noted in Chapter 3. A physical blend of copper oxide powder and the aluminosilicate fibres was investigated as an alternative. In this physical mixture, copper oxide is considered to be in an *un*supported form which is unlike the copper oxide which is well dispersed throughout, and "supported" on the large surface area presented by the micro-porous silicalite structure.

Both copper oxide and Cu-ZSM-5 have been shown to be catalytically active but little has been published on the use of either of these catalysts for SCR. Hence, this experimental program sought to compare the catalytic activities of supported and unsupported copper oxide with Cu-ZSM-5.

The investigation of SCR was carried out in two stages. The first phase was a parametric study which set out to determine suitable experimental conditions to be used; the effects of reaction temperature, oxygen feed concentration and gas flowrate on the SCR reaction were studied. In addition, ammonia oxidation and the reaction of NO and ammonia were investigated. The results of these investigations are covered in Sections 4.2.2 to 4.2.8. Cu-ZSM-5 was the catalyst used in all the experiments described in these sections. Having established appropriate experimental conditions, the second investigative phase was to evaluate the performance of the various copper doped aluminosilicates as SCR catalysts. These experiments are discussed in Sections 4.2.9 and 4.2.10.

4.2.2. AMMONIA OXIDATION OVER Cu-ZSM-5

The oxidation of ammonia is significant because the extent of NO formation by the reaction:

$$4NH_3 + 5O_2 \rightleftharpoons 4NO + 6H_2O \qquad (2.4)$$

dictates the maximum operating temperature for SCR processes (refer Section 1.5.2.). While the formation of nitric oxide takes place through the above reaction, nitrogen may also be formed from the oxidation of ammonia with the stoichiometry:

$$4NH_3 + 3O_2 \rightleftharpoons 2N_2 + 6H_2O \qquad (2.3)$$

The oxidation of ammonia was investigated in the temperature range 300-550°C (Figure 4.8). Up to 550°C, only nitrogen was recorded as a reaction product. Above 350°C, nitrogen production increased linearly with temperature. These results were obtained with the use of GC for gas analysis.

Should nitric oxide have been formed from the oxidation of ammonia, it would have reacted with oxygen on the GC column to produce nitrogen dioxide which could not be monitored (explained in Section 3.5.1). If any NO was produced in the temperature range investigated, it was not present in quantities sufficiently large to be detected by GC (after reaction with oxygen). Thus, although the gas analysis did not present conclusive evidence that no nitric oxide was produced, the linear increase in nitrogen production (Figure 4.8) suggests that no reaction other than that to nitrogen occurred - a change in product selectivity eg. due to increased production of nitrogen dioxide with increasing temperature, would have been evident as a change in the slope of the graph.

That nitrogen alone was recorded as the product of the ammonia oxidation reaction is similar to the result obtained by Brandin *et al.* (1989), who found no evidence of oxidation to nitric oxide over H-mordenite up to 430°C. The lack of nitric oxide observed in the present work, suggests that Cu-ZSM-5 is suitable for use as a SCR catalyst up to at least 520°C, the maximum

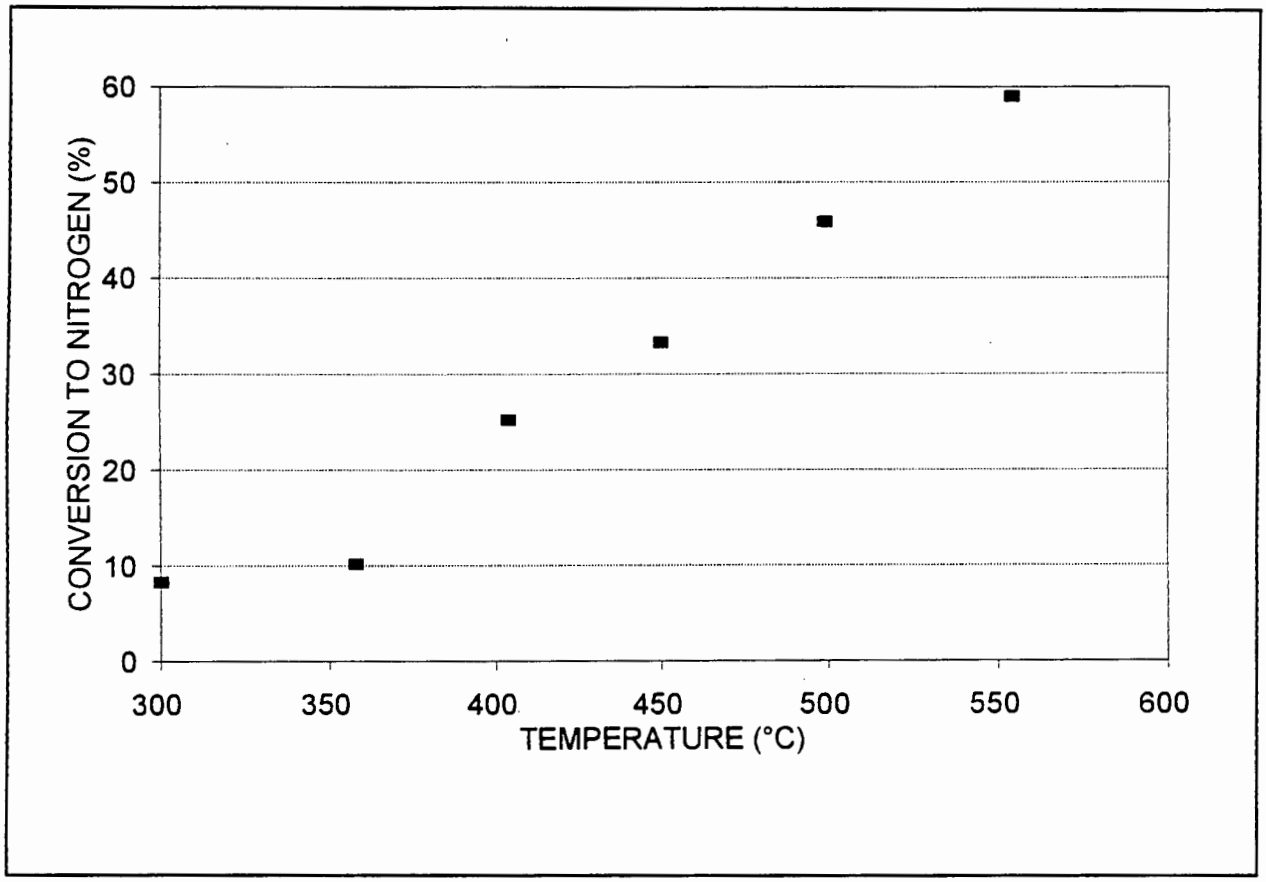

***Figure 4.8** The oxidation of ammonia - [NH_3]= 0.5%, [O_2]= 1.7%*

temperature investigated. This observation of little or no nitric oxide production from ammonia oxidation at such high temperatures confirms the suitability of ZSM-5 as a catalyst for use at higher temperatures than conventional SCR catalysts.

"Empty bed runs" were conducted: Ammonia and oxygen were passed through the reactor without any catalyst present (185-506°C). No decrease in oxygen concentration was observed (by GC) and similarly, no nitrogen production was observed (data shown in Appendix 5). Therefore, unlike the "Thermal DeNOx" process (Lyon, 1975) employed above 1000°C, at these temperatures, the ammonia oxidation reaction is catalytic.

4.2.3. THE AMMONIA-NO REACTION OVER Cu-ZSM-5

The ability of Cu-ZSM-5 to catalyse the ammonia-nitric oxide reaction (in the absence of oxygen) was examined in the temperature range 300-540°C. The reaction stoichiometry has been described by Mizumoto *et al.* (1979) as:

$$4NO + 2NH_3 \rightarrow 2N_2 + N_2O + 3H_2O \qquad (2.19)$$

This reaction was studied to allow a comparison to be made with the SCR reaction (reaction (2.2)) which takes place in the presence of oxygen. Mizumoto *et al.* (1979) demonstrated that the rate of the SCR reaction is greater than that of reaction (2.19).

With a catalyst mass to flowrate ratio (W/F) of approximately 0.062 g.s/ml, the amount of nitrogen produced as a percentage of the feed NO, increased from 2% at 300°C to 18% at 540°C. These conditions and results are noted to allow a comparison to be made with the investigation of the SCR reaction.

Since nitrous oxide was not monitored, the 2:1, N_2:N_2O product ratio could not be investigated.

4.2.4. THE EFFECT OF TEMPERATURE ON THE SCR REACTION

Recall that the stoichiometry of the SCR of nitric oxide is:

$$4NO + 4NH_3 + O_2 \rightleftharpoons 4N_2 + 6H_2O \qquad (2.2)$$

The effect of temperature on this reaction over Cu-ZSM-5 is shown in Figure 4.9. The data were obtained with a feed oxygen concentration of 1.7% (chosen arbitrarily). The two graphs depict NO conversion and the amount of nitrogen produced (nitrogen concentration in the reactor product stream). Both increase with temperature up to 500°C above which a decline is observed. NO conversion was determined with the NOx chemiluminescence analyzer while the amount of nitrogen produced was recorded with GC.

When compared with NO conversion over Cu-Mordenite c.f. Brandin *et al.* (1989), Choi *et al.* (1991) and Nam *et al.* (1992), the optimum for reduction over Cu-ZSM-5 occurs at a higher mean temperature. The conversion versus temperature profile compares well with that obtained by Byrne (1990) over Cu-Beta, which shows an optimum at approximately 460°C.

The decrease in NO conversion above 500°C is reminiscent of the decrease in nitrogen produced by the direct decomposition reaction above 500°C. The common feature of these two reaction systems, Cu-ZSM-5, suggests that this "optimum" temperature is characteristic of the catalyst (since it is not dictated by thermodynamics). However, it would seem that the similarity is

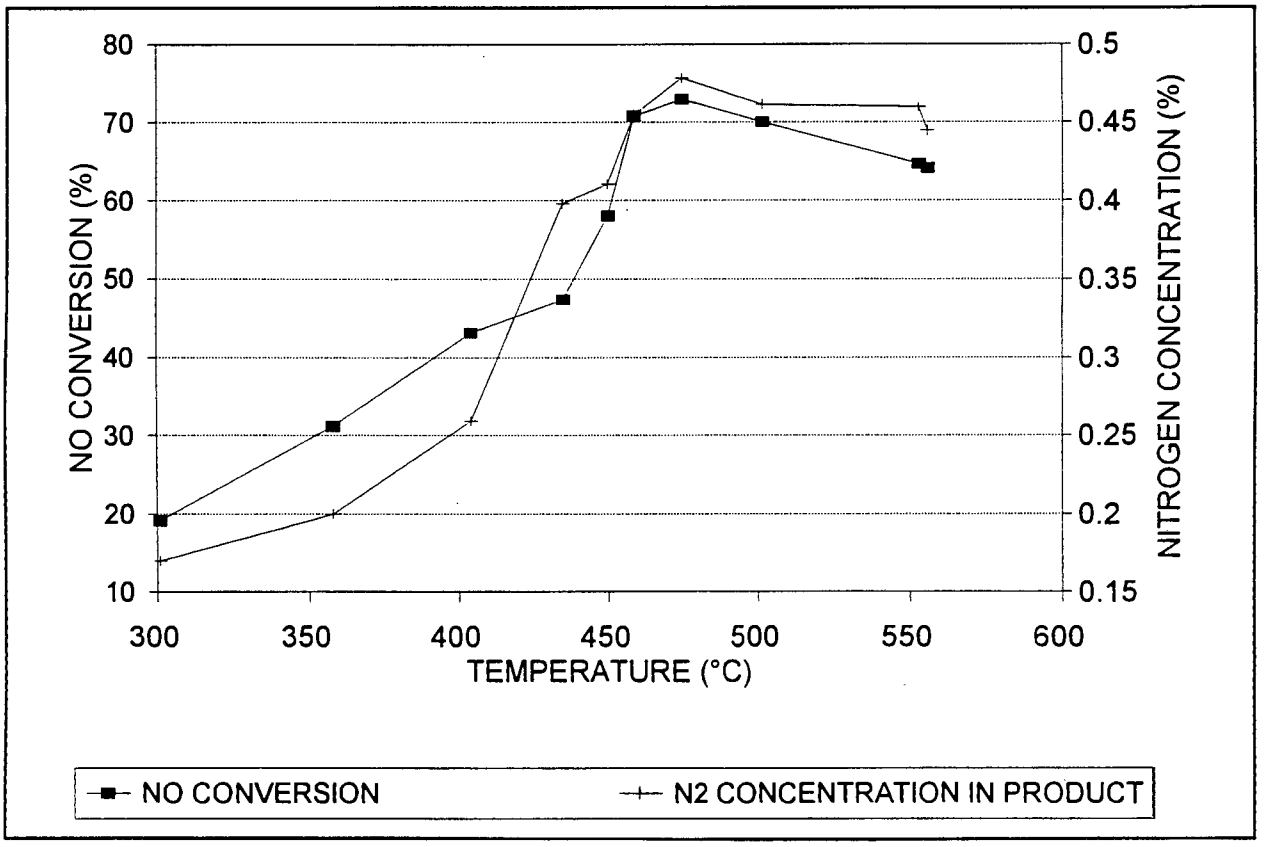

Figure 4.9 NO conversion and nitrogen produced from the SCR reaction

fortuitous, since the same optimum temperature was obtained by Byrne (1990) over Cu-Beta.

In Figure 4.9, the NO conversion graph lies above the nitrogen concentration graph at temperatures below 420°C, while above this temperature, their positions are reversed. This would suggest that there was a change in the rate of nitrogen production - a change in product selectivity. However, NO_2 has not been observed as a product of the SCR reaction and Mizumoto *et al.* (1979) observed that nitrogen was the only product of the SCR reaction over Cu-Y (also no nitrous oxide was detected). It is thus suggested that this observed trend which suggests a "selectivity change" is due to experimental error and that nitrogen is the only reaction product to be considered below the "optimum" NO conversion temperature; above which, NO may be formed from the oxidation of ammonia reaction (refer to Figure 1.5, section 1.6.2.1).

The difference between the rate of the SCR reaction (reaction (2.2)) and the ammonia/nitric oxide reaction (reaction (2.19)) in the absence of oxygen, may be seen by comparing the amount of nitrogen produced as a percentage of feed NO at a similar W/F ratio: 90% was obtained for the SCR reaction at 500°C compared with 18% at 540°C for reaction in an oxygen free environment.

4.2.5. THE EFFECT OF OXYGEN CONCENTRATION

The effect of feed oxygen concentration was investigated and the results are shown in Figure 4.10. NO conversion and the amount of nitrogen produced in the SCR reaction, increased with oxygen concentration and reached a maximum at 3% oxygen. Since the feed NO concentration was 0.5%, this amount of oxygen is far in excess of that demanded by the stoichiometry of the SCR reaction (equation (2.2)).

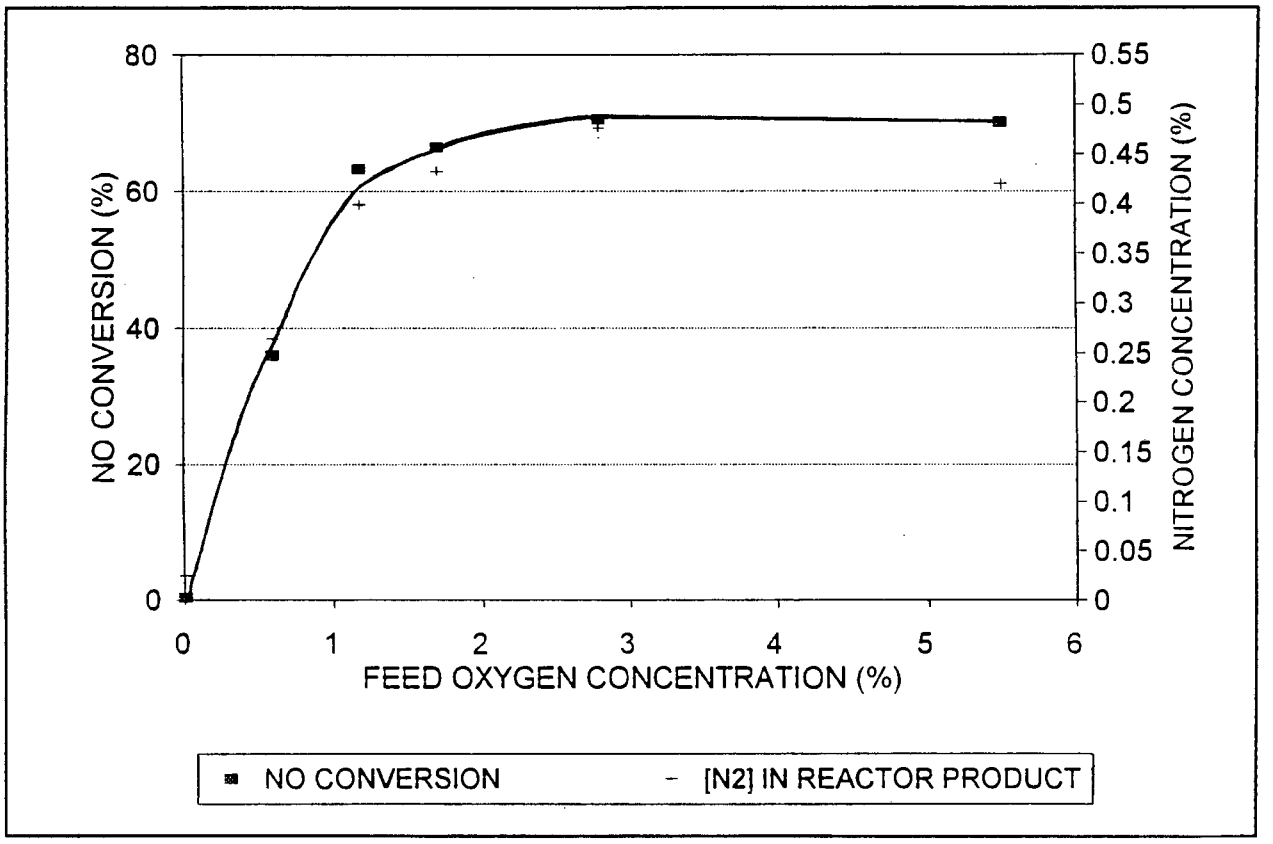

***Figure 4.10** Oxygen dependence of the SCR reaction.*

Hirsch *et al.* (1982) observed a similar dependence on oxygen concentration in his investigation of the SCR reaction over H-mordenite and assigned the dependency to a rate limitation rather than a stoichiometric requirement. Further explanations for this oxygen dependency were not offered. It should however be noted, that the oxygen concentration in typical flue gases are of the order of 7%, and thus, with NOx levels of approximately 1000 ppm which are generated in combustion processes, oxygen would normally not be a limiting factor.

It should be noted that above 3% oxygen, the maximum extent of NO conversion was achieved - ammonia was the limiting reactant (data shown in Table A5.1).

4.2.6. THE EFFECT OF FEED FLOWRATE

Nam *et al.* (1988) observed a pseudo-first order dependence of reduction rate on NO concentration. This was obtained by plotting the log of unconverted nitric oxide against space time according to the rate equation:

$$-\frac{dC_{NO}}{dt} = kC_{NO} \qquad (4.1)$$

which, yields upon integration:

$$k = -\frac{1}{\tau}\ln(1-X_{NO}) \qquad (4.2)$$

In order to investigate this relationship in the present study, feed composition and reaction temperature (455°C) were kept constant while feed flowrates were increased from 12.0 ml/sec to 37.5 ml/sec. The data were plotted as $\log(1-X_{NO})$ against space time (Figure 4.11), according to equation (2.4) and a linear relationship was expected.

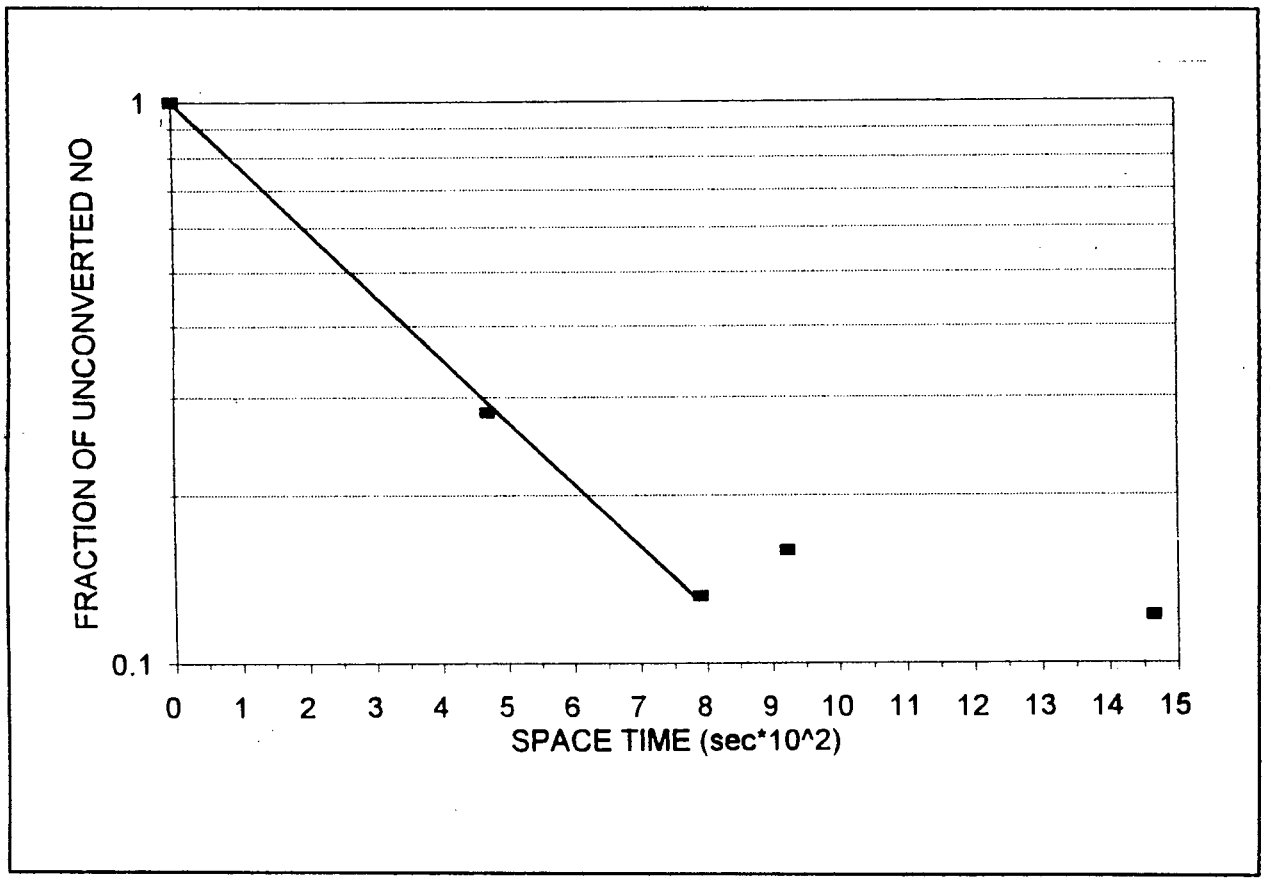

Figure 4.11 The first order functionality of the SCR reaction over Cu-ZSM-5

The above flowrates correspond to space velocities of 24 500 to 76 500 h^{-1} respectively and are equivalent to W/F ratios of 0.088 and 0.028 g.s/ml. These W/F ratios may be compared with those used for the decomposition reaction which are of the order of 2 and 4 g.s/ml, indicating a (approximately) two orders of magnitude difference in reaction rates.

In Figure 4.11, the three datapoints at the lowest space times show a linear form (r^2= 0.937), similar to the first order dependence observed by Nam *et al.* (1988) over Cu-H-Mordenite, while at higher residence times, higher conversions are not observed, the fraction of unconverted NO[16] remains constant.

The data obtained at the highest space times in Figure 4.11 indicate a reactant limitation which is attributed to complete consumption of ammonia. This is evident in the data recorded for Runs 95 and 96 (Table A5.1) in which the amount of nitrogen produced is seen to equal the amount of ammonia in the feed and the theoretical feed composition calculations indicate ammonia as the limiting reactant.

4.2.7. EXAMINATION OF SCR REACTION STOICHIOMETRY

With the use of "Dräger tubes" for ammonia analysis, the amounts of ammonia converted (Run# 87 and Run# 135) were compared with the amounts of nitrogen produced by the SCR reaction. On both occasions, these two values were within 3% of each other. Thus, although a complete mass balance was not obtained in conjunction with nitric oxide conversion, the data do not contradict the 1:1 nitric oxide to ammonia ratio as described by the accepted stoichiometry of the SCR reaction (equation 2.2).

As described in Section 3.5.3, the use of the Dräger tubes indicated an ammonia stock concentration of 0.87% rather than the 1.0% as certified by *Fedgas*. The results of the above examination of the reaction stoichiometry are based upon a conversion *i.e.*, ammonia readings were taken of the feed gas and the reactor effluent and a fractional conversion was obtained. Hence, assuming that the indicator tubes "under-read" consistently, the verification of the stoichiometry may be considered valid.

Further evidence of the 1:1 ammonia to nitrogen ratio is presented by the data in Table 4.4 which shows that the amount of nitrogen produced by the SCR reaction over the 80°C range, correspond to the amounts of ammonia in the feed (maximum conversion reached, complete ammonia consumption - ammonia limiting).

---

[16]Unconverted NO = (Moles NO in feed) - (Moles N_2 produced) according to stoichiometry of the SCR reaction (equation 2.2).

Table 4.4 Conversion/Temperature data for the SCR reaction

Run#	Temperature	Feed Composition			Product composition
		N_2	NH_3	O_2	N_2
	°C	(%)	(%)	(%)	(%)
81	475	0.55	0.49	1.70	0.48
82	502	0.55	0.49	1.70	0.49
83	553	0.55	0.49	1.70	0.49

4.2.8. REACTOR RESPONSE - TIME TO STEADY STATE

The extent of reaction as monitored by the amount of nitrogen produced with time, is shown in Figure 4.12 which clearly indicates that steady state was achieved within 5 minutes. This rapid attainment of steady state upon contact with the reactants is unlike that observed for the direct decomposition reaction (Figure 4.4 and Figure 4.5) in which the approach to steady state was marked by a decrease in nitrogen production from a high initial value (Refer Section 4.1.6).

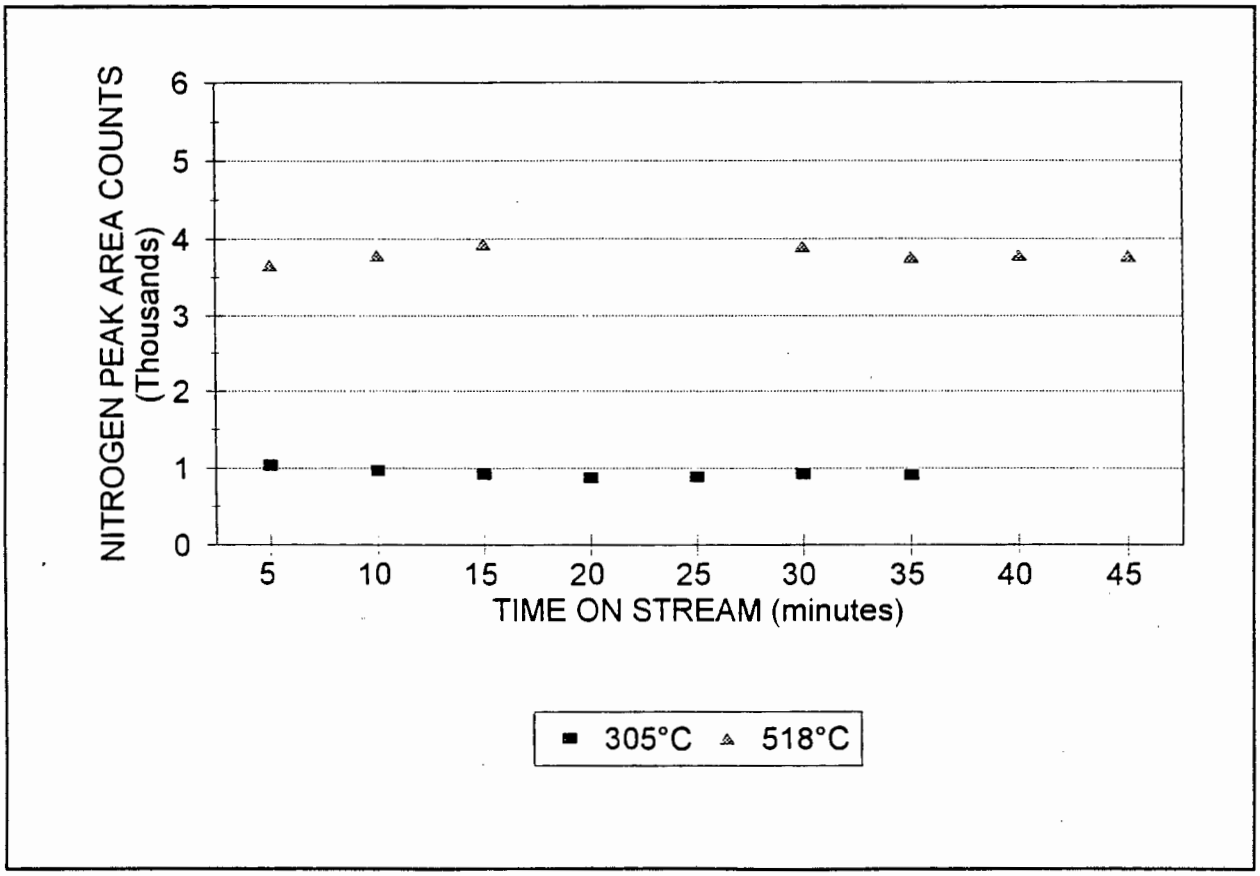

Figure 4.12 Reactor response

Evidence of the exothermicity of the SCR reaction was observed by an increase in catalyst bed temperature upon feeding the reactants to the reactor. A one hour lag time prior to gas sampling was introduced for all SCR experiments to allow the reactor temperature to reach a steady state. As recorded in Section 3.4, temperature fluctuations of approximately 3°C were observed about the mean reactor temperature. For consistency, gas samples were taken only at the maximum temperature reached in any temperature cycle.

4.2.9. PRELIMINARY INVESTIGATION OF CuO AS A SCR CATALYST

Having explored a number of operating parameters, the next experimental phase was to compare Cu-ZSM-5 and CuO as SCR catalysts. Catalyst masses of 1g were used in the parametric studies of Cu-ZSM-5 already described, and in order to avoid complete conversion, less catalyst was used in subsequent runs. The results of these preliminary CuO runs with 0.5g (rather than 1g) of impregnated silicalite and CuO/filter are shown in Figure 4.13. These results are displayed as TOFs and are compared with the data obtained for the SCR reaction over 1g of Cu-ZSM-5 (Runs 75-87). Repeat runs for Cu-ZSM-5 are also shown in Figure 4.13.

An Arrhenius plot (Figure 4.2) was used to compare the direct decomposition data with that obtained by Li and Hall (1991) and in order to calculate activation energies for the SCR reaction, this method was maintained to evaluate the SCR catalysts under investigation. Turnover frequency is defined as the number of nitrogen molecules converted per second, per copper atom contained in the catalyst bed, and by the stoichiometry of reaction (2.2), this number is the same as the number of molecules of nitric oxide converted per second, per copper atom. All TOFs calculated in this experimental program made use only of data derived from gas chromatography *i.e.*, nitrogen production data.

Using the same feed flowrate (18 ml/s), the impregnated silicalite gave higher TOFs than the larger bed (1g) of Cu-ZSM-5 and unsupported copper oxide gave rates comparable with Cu-ZSM-5.

The impregnated silicalite catalyst sample contained 0.035 mmol of copper in total, compared with 0.20 mmol contained in 1.054 g of Cu-ZSM-5. Considering that 75% of maximum NO conversion was obtained with the silicalite, it would have been expected that ZSM-5 would have produced the maximum NO conversion. It is suggested that incomplete conversion was recorded for the ZSM-5 sample because of channelling and bypassing which occurred in the large catalyst bed (bed depth 3.5 cm). Such channels were visible to the eye as a result of the agglomeration of the ZSM-5 crystallites described in Section 3.5.4 (Catalyst bed packing). A similar problem was not encountered with silicalite because it was dispersed with glass wool (also described in Section 3.5.4. Because of the high packing density of silicalite, an undiluted bed of 0.5g of silicalite was found to restrict the gas flow, hence the bed had to be expanded).

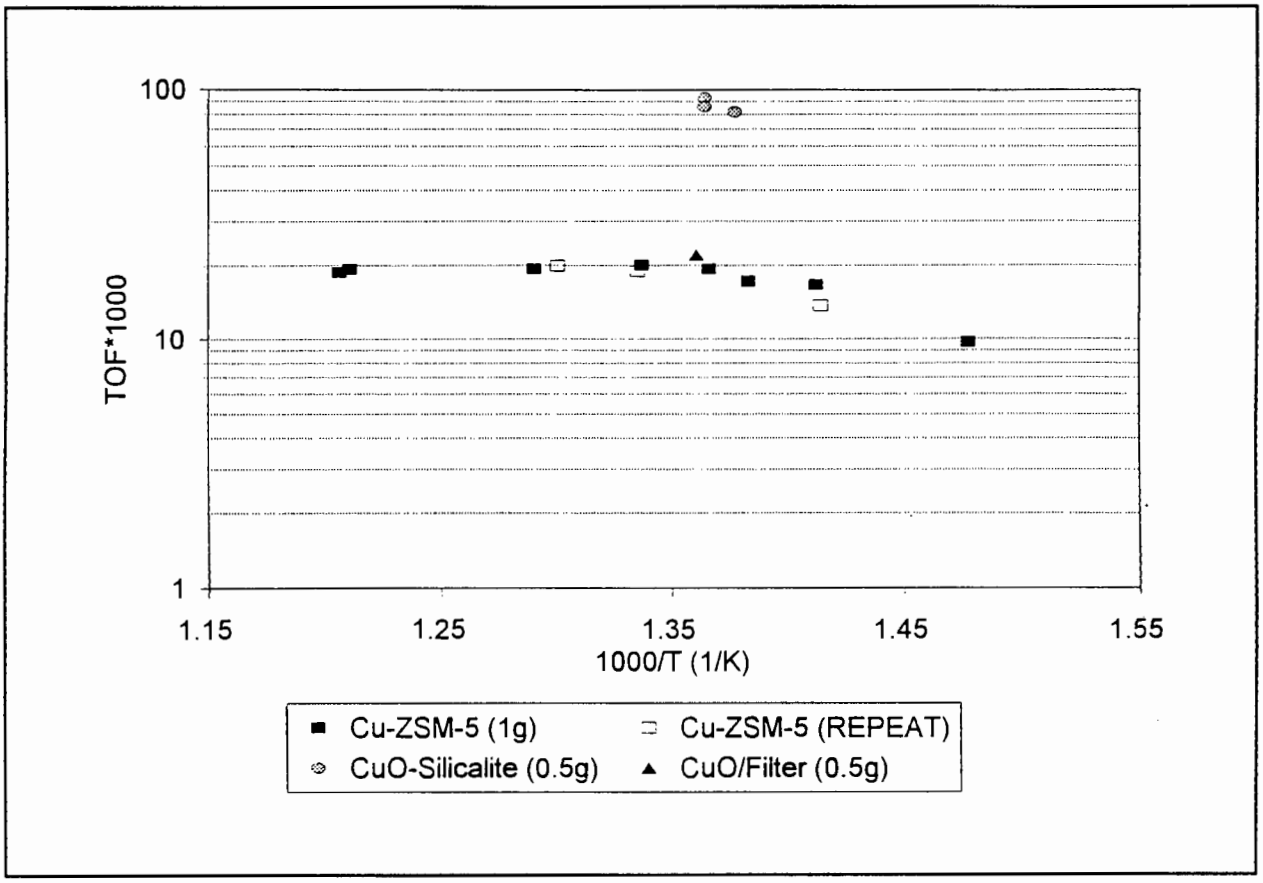

Figure 4.13 Preliminary comparison of CuO and Cu-ZSM-5

TOF as it is used under the present non-differential reactor conditions, is an average nitrogen production rate for the entire catalyst bed. The TOF for ZSM-5 was lower than that obtained for silicalite because the amount of nitrogen was averaged over a greater amount of copper. That 1g of ZSM-5 produced as much nitrogen as only half the mass of silicalite, should not be taken as a direct indication of the greater intrinsic activity of the copper oxide catalyst because of the channelling described above. Thus, in order for the TOFs to be used as significant indicators of reaction rates/activity, no limitations other than that of the reaction kinetics should be present.

In order to avoid reactant limitation (maximum conversion), catalyst mass was further decreased from 0.5 to 0.1g in subsequent runs and in order to use such small quantities of catalyst while maintaining bed volumes sufficiently large to avoid reactant bypassing, the catalyst was embedded in a plug of glass wool. As previously described, this was formed by dispersing small amounts of catalyst powder on tufts of glass wool which were then stamped into the glass reactor to form a continuous plug. In this way, bed heights of the order of 2 cm were obtained, offering good gas flow distribution. As described in Section 3.5.5, the glass wool did not impart any catalytic activity.

4.2.10. COMPARISON OF Cu-ZSM-5 AND CuO AS SCR CATALYSTS

Cu-ZSM-5

Data from the investigation of the SCR reaction over 0.116g of Cu-ZSM-5 are displayed in Figure 4.14. The Arrhenius plot shows a linear relationship between TOF and temperature. In spite of using only 0.116 g of ZSM-5, feed flowrates had to be increased at higher reaction temperatures, to avoid maximum NO conversion. The high conversions were noted by the amounts of nitrogen produced, which approached the amounts of NO and ammonia in the feed (The data can be seen in Appendix 5). Flowrates of 8.8 ml/s to 49.0 ml/s were employed and corresponded to space velocities of 12 600 and 70 100 h^{-1} respectively.

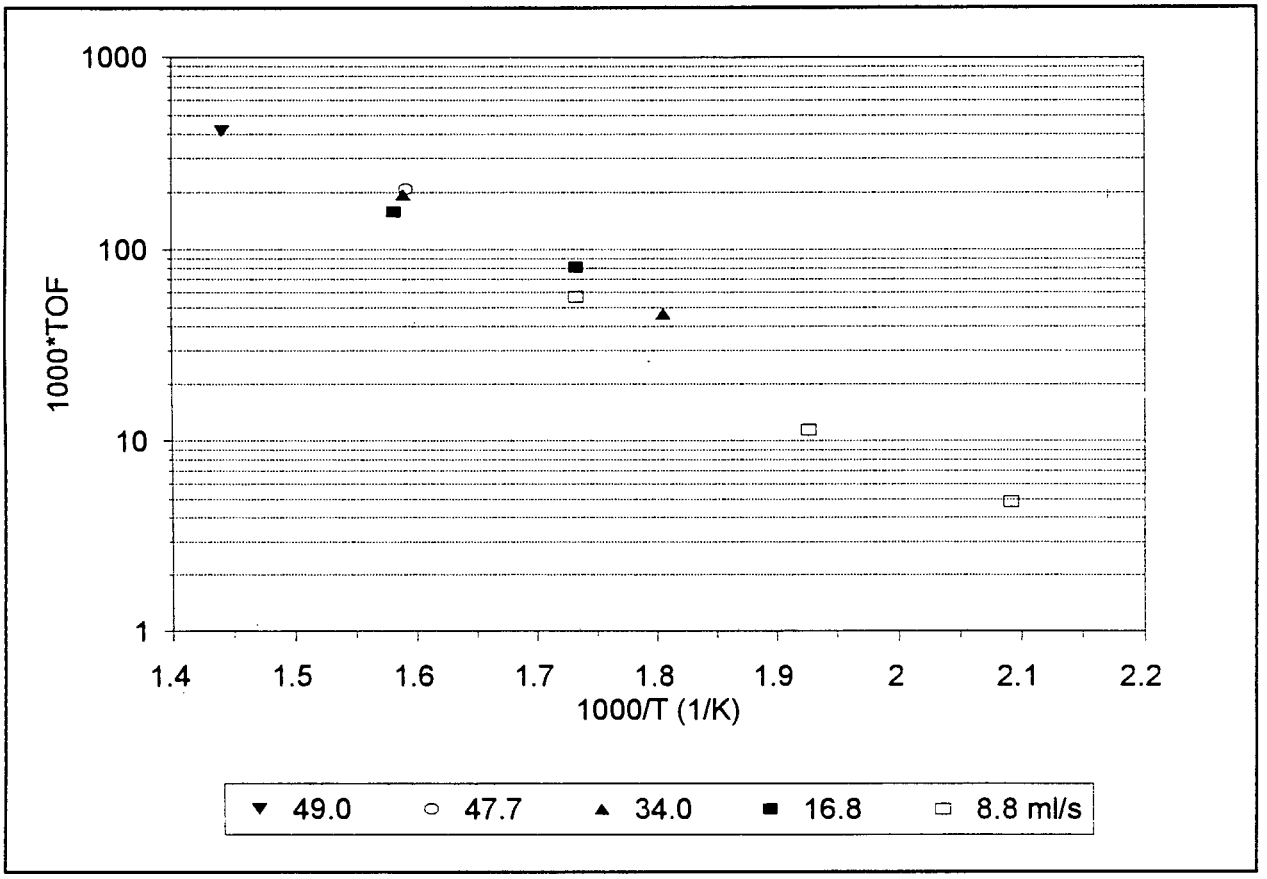

Figure 4.14 Arrhenius Plot for SCR reaction over Cu-ZSM-5

The linearity of the Arrhenius plot suggests that the reaction rate was limited by kinetics in the temperature range investigated. The change in flowrate affected the TOF by affecting the concentration gradient across the catalyst bed. TOF is seen to increase with increasing flowrate as residence time and conversion decrease (higher residual (and average) NO concentrations within reactor, yielding higher reaction rates according to rate dependency on reactant concentration). Although noticeable, the differences between the three data points collected at

different flowrates at 350°C were not sufficiently large to render the data unsuitable for calculation of an activation energy for the reaction.

The foregoing discussion of the effect of conversion (concentration gradients across catalyst bed) on TOF reveals that differential conditions (low conversions) should be maintained throughout the temperature range over which data is collected in order to calculate an activation energy.

Linear regression of the data plotted in Figure 4.14 yielded an activation energy of 14 kcal/mol (r^2 = 0.980) for the SCR reaction over Cu-ZSM-5.

An oxygen concentration of 3% was used in these runs - a concentration above the limit where oxygen concentration was found to be limiting under the present conditions (refer to Figure 4.10).

CuO - supported and unsupported

Characterization of impregnated silicalite indicated that a high copper dispersion was obtained, and having established in preliminary runs that copper oxide was suitably active, the significance of copper dispersion was examined by comparing in more detail, copper oxide which had been supported on silicalite and bulk copper oxide which was physically mixed with crushed aluminosilicate fibres.

The data for Cu-ZSM-5 shown in Figure 4.14 are re-plotted in Figure 4.15 along with results obtained for impregnated silicalite and the CuO/ceramic fibre blend which shows that Cu-ZSM-5 is the most active catalyst, followed by CuO on silicalite and the blend of CuO/amorphous aluminosilicate fibres.

While a mass of 0.1116g of silicalite was used with a flowrate of 16.5 ml/s, preliminary runs indicated that the CuO/aluminosilicate fibre mix was less active, and in order to obtain significant conversion, the mass of this catalyst was doubled to 0.2120 g. Employing a similar flowrate and reactor temperature, the impregnated silicalite was found to produce almost three times the amount of nitrogen as that produced by the 0.2120g of the copper doped aluminosilicate fibres. Thus, in order to obtain higher conversions, the feed flowrate was decreased from 16.5 ml/s to 7.7 ml/s in the investigation of the CuO/fibrous aluminosilicate mix. This is a clear indication of the lower activity offered by the CuO/filter compared with impregnated silicalite.

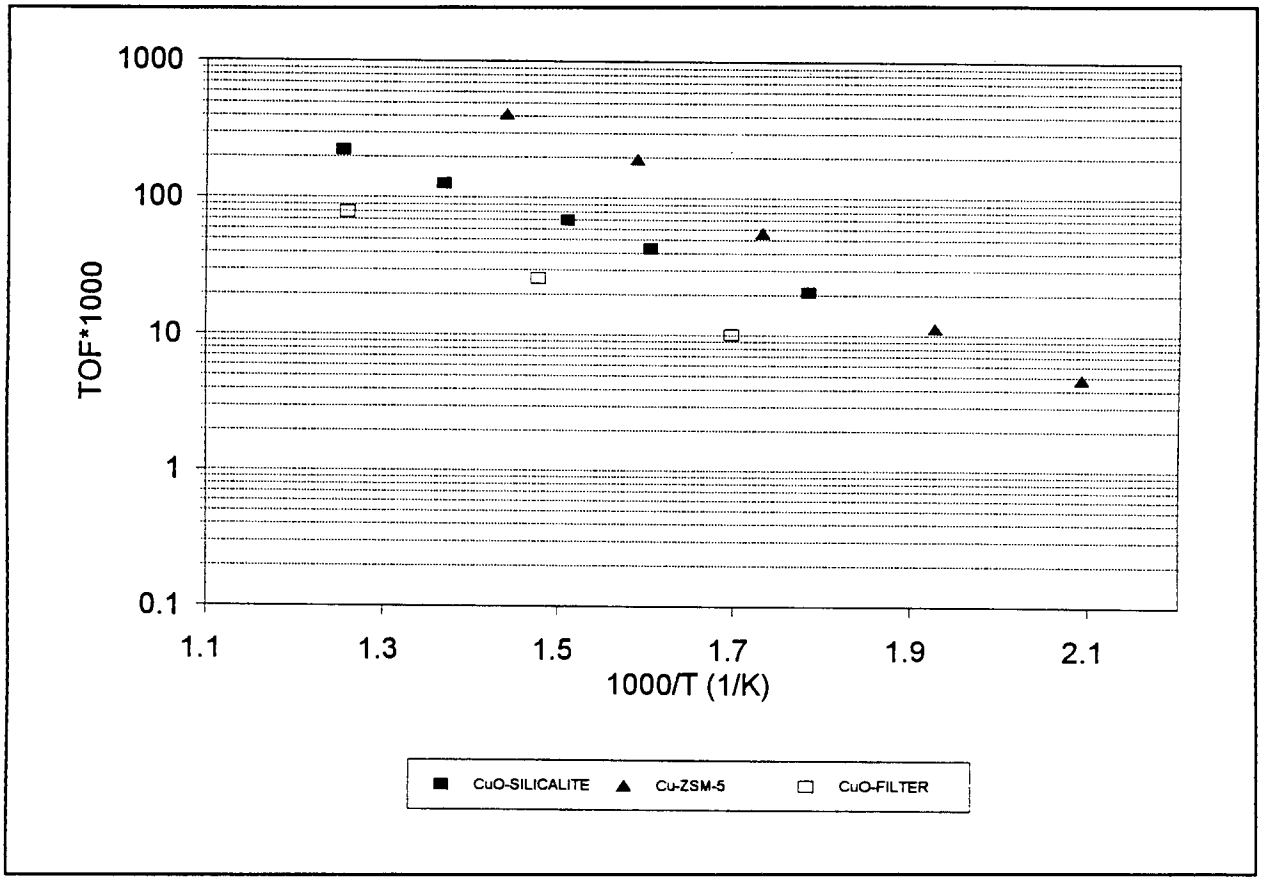

Figure 4.15 Comparison of supported, unsupported CuO and Cu-ZSM-5

Independent of the magnitude of TOFs, the slopes of the Arrhenius plots yield activation energies. Linear regression of the three graphs in Figure 4.15 gave the following activation energies:

14 kcal/mol for Cu-ZSM-5 (r^2= 0.980) and
9 kcal/mol for impregnated silicalite (r^2= 0.999) and
9 kcal/mol for copper oxide mixed with the fibrous aluminosilicate (r^2=0.998).

The activation energy for reaction over Cu-ZSM-5 may be compared with those obtained by Eng (1977), Ganti (1980), Altomare (1981), Nam *et al.* (1988) and Ham *et al.* (1992) for Cu-mordenite, which range from 11.9 to 17.0 kcal/mol. This suggests that Cu-mordenite and Cu-ZSM-5 have similar catalytic sites. The similarity of the activation energy between Cu-ZSM-5 and Cu-mordenite was expected, considering Li and Hall's (1991) results which presented the same activation energy for ZSM-5 and mordenite for the direct decomposition reaction (refer Section 2.5.7).

The activation energies calculated for copper oxide on silicalite and with the filter material is lower than the 16.2 kcal/mol obtained by Kiel *et al.* (1992) but is similar to the 10.0 kcal/mol recorded by Fukuzawa and Ishihara (1979) over $CuO/CuSO_4$ on bauxite.

It is significant to note that the activation energies obtained for supported (impregnated silicalite) and unsupported (physical mixture of CuO and aluminosilicate fibres) copper oxide were the same. It was expected, and confirms that the catalytic sites were the same in both cases. The higher TOFs recorded for the impregnated silicalite over the physical CuO/filter mix, would have been afforded by the greater dispersion of the copper species throughout the highly porous structure of silicalite.

For the purpose of comparison, a reaction rate constant was calculated for supported copper oxide, in the same way as that done by Kiel *et al.* (1992). This was obtained by considering the first order dependence on the rate described by:

$$r = k_r C_{NO} \tag{4.3}$$

Further, assuming plug flow and reaction rates determined by kinetics, an "intrinsic" rate constant was calculated according to the equation:

$$k_r = - \frac{U_g}{(1-\epsilon)L} \ln\left[\frac{C_{NO_{(out)}}}{C_{NO_{(in)}}}\right] \tag{4.4}$$

where U_g represents the superficial gas velocity ($m.s^{-1}$), L is the catalyst bed height (m) and ϵ is the bed voidage. Concentration is expressed in ($mol.m^{-3}$).

Using data from Run# 115 for impregnated silicalite at 287°C, a rate constant of 38 $(m_g)^3.(m_{cat})^{-3}.s^{-1}$ was calculated. An estimated voidage of 0.9 is not very accurate and therefore, undue significance should not be placed on the numerical accuracy of the rate constant - the rate constant was obtained only as an indication of its order of magnitude (Data and calculation shown in Appendix 5). This rate constant calculated for Run# 115 is shown in Figure 4.16, superimposed on Figure 2.32 taken from Kiel *et al.* (1992) and reveals that the rate constant obtained in the present study is higher than those obtained by Kiel *et al.* for copper oxide on silica but is similar to those described by Fukuzawa and Ishihara (1979) for CuO on Bauxite.

The TOF calculated for Cu-ZSM-5 was compared with those obtained by Nam *et al.* (1988) which are shown in Figure 2.24. The TOFs are defined in the same way: moles on NO converted per second per mole of copper ions. The Arrhenius plot for ZSM-5 in Figure 4.15 indicates a TOF of approximately 0.1 while the data in Figure 2.24 (Nam *et al.*, 1988) gives TOFs of the order of 0.01 at 340°C. This difference may be attributed to the concentration of nitric oxide used; 0.5% compared with 0.05% used by Nam *et al.* (1988). The difference in TOFs is commensurate with the first order dependence of reaction rate on NO feed concentration. On the basis of this comparison, Cu-ZSM-5 and Cu-mordenite are seen to have similar activities.

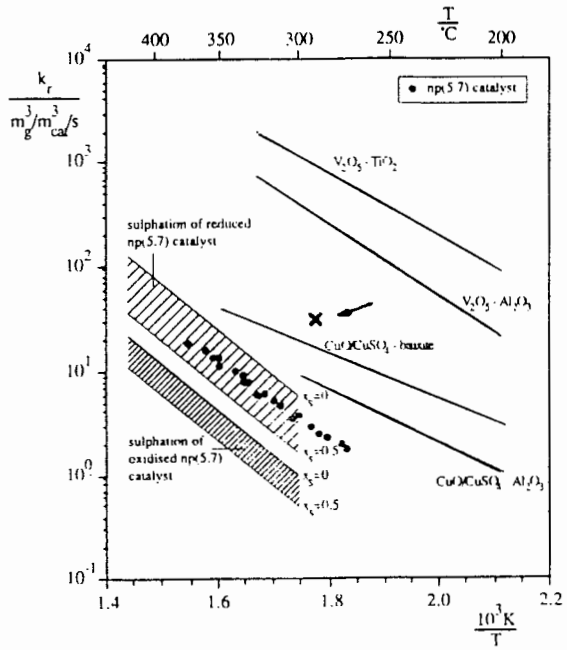

Comparison of experimental values of the intrinsic reaction rate constant k_r for the np(5.7) catalyst with literature data given by Wong and Nobe [18] for 10 wt.-% V_2O_5 on TiO_2 or Al_2O_3 catalysts, and with data given by Fukuzawa and Ishihara [19] for $CuO/CuSO_4$ on bauxite or Al_2O_3 catalysts. Also shown are modified reaction rate constants for sulphation of the reduced and the oxidised catalyst, according to eqns. (17) and (18) respectively, with the sulphation degree x_s ranging from 0 to 0.50.

***Figure 4.16** Comparison of rate constants for SCR of NO over various catalysts (Kiel et al., 1992)*

4.2.11. SUMMARY OF FINDINGS

- Ammonia oxidation below 540°C was catalytic with no evidence of nitric oxide produced.
- As recorded in literature, the rate of nitric oxide reduction with ammonia (NO and NH_3 only) is lower than the rate of the SCR reaction which includes oxygen as a reactant.
- Rate dependence on oxygen feed concentration was observed. Under the conditions used, a dependence was noted below 3% oxygen in the feed.
- Reaction rate: first order dependency on NO concentration as described in literature.
- Ammonia consumption measurements confirmed preferred stoichiometry for SCR reaction over Cu-ZSM-5.
- Catalyst activity ranking: Cu-ZSM-5 > CuO-silicalite > CuO/aluminosilicate fibre.
- Rates of SCR reaction (TOF) three orders of magnitude greater than the direct decomposition reaction (Cu-ZSM-5).
- Reaction rate constant calculated for CuO comparable to published rates for CuO.

- Activation energies for SCR reaction:

Cu-ZSM-5:	14 kcal/mol
CuO-Silicalite:	9 kcal/mol
CuO/filter:	9 kcal/mol

  which are comparable to published results.
- Dispersion of CuO on silicalite affected only the reaction rate and not the mechanism of the reaction - indicated by same activation energy for both CuO catalysts.
- Cu-ZSM-5 and CuO suitable for use up to the temperature limit of this study, 550°C, with no decrease in conversion as a result of ammonia oxidation to nitric oxide.

In terms of experimental procedures, it is recommended that differential conditions be used in order to avoid maximum conversion dictated by a reactant limitation. It is also suggested that for greater accuracy in the calculation of data such as activation energies which require that data be collected over a wide temperature range, the objective should be to maintain constant conversion levels at all temperatures. However, this is admittedly a time consuming task which requires many more runs than were carried out in the present investigation.

The significance of these findings is described in Chapter 5, in which conclusions are drawn and recommendations are made with respect to the employment of copper doped aluminosilicate barrier filters for simultaneous high temperature flue gas cleaning.

5. CONCLUSIONS AND RECOMMENDATIONS

The following conclusions have been drawn from the review of the literature on catalytic NOx reduction and the results of this experimental program. This study details the direct decomposition reaction and the selective catalytic reduction (SCR) reaction over copper ion exchanged ZSM-5 and supported and unsupported copper oxide.

1. An activation energy of 29 kcal/mol was obtained for the nitric oxide decomposition reaction over Cu-ZSM-5 and a reaction rate dependence of 1.2 on NO partial pressure was observed at 500°C. Both results compare well with those published by Li and Hall (1991) (17-29 kcal/mol and 1.1 respectively). Through the ability to duplicate these data, the experimental system and procedures used in the present study were considered to be valid.

2. The experimental investigation of the direct decomposition reaction sought only to verify the catalytic activity of Cu-ZSM-5 and was not intended as a detailed study of the mechanism. A review of work published in this field, essentially covered by three groups: W.K. Hall *et al*, Y. Li *et al* and M. Iwamoto *et al*, exposed a number of uncertainties which were not addressed by this experimental program. These include:
   i) an explanation for diminished activity at temperatures beyond 500°C,
   ii) the location/state/utility of non-stoichiometric (excess) copper within the zeolite pore structure
   iii) conflicting interpretations of the reaction mechanism
   iv) whether Si:Al ratio is a significant parameter for catalyst activity (beyond dictating exchange capacity) or whether absolute copper loading dictates activity.

   Admittedly, answers to these questions are not trivial. While to date, ZSM-5 has been shown to be the most active catalyst for the decomposition reaction, it is not sufficiently active for commercial application. Thus, a better understanding of the mechanism of this reaction may allow more active catalysts to be developed to effect this, the most attractive NO removal technique.

3. Besides catalysing the direct decomposition reaction, Cu-ZSM-5 is an active catalyst for the SCR of nitric oxide with ammonia, suitable for use up to at least 550°C, the temperature limit of this study. The high temperature operating window is similar to that observed for a number of transition metal exchanged zeolites. These zeolites may be used at higher temperatures than vanadium pentoxide based catalysts and lead the way forward to the development of NOx removal systems able to operate at high temperature.

4. Turnover frequencies for the SCR reaction were three orders of magnitude greater than those measured for the direct decomposition reaction. This disparity clearly illustrates the unacceptably low rates of the direct decomposition reaction and verifies the question of its commercial viability.

5. To prevent reactant limitations and concentration gradients within packed beds, low conversions should be used. Having suggested this, time consuming "trial and error" is required to establish suitable operating parameters. While differential conditions may be desired, they are not easily applied since sensitive and accurate analytical instruments are required. The experimental program has shown that gas analysis is not a trivial exercise. A suitable method of ammonia analysis is required. Further, because of the propensity for oxidation, it is recommended that investigations employing nitric oxide should not be attempted without the use of a chemiluminescence analyzer or a similarly sensitive and selective instrument if a complete mass balance is required.

6. The significance of oxygen for the SCR reaction is apparent when comparing the extent of the catalytic NO/NH_3 reaction with the $NO/NH_3/O_2$ reaction. Under similar operating conditions, the former was found to give only 15% NO conversion while the latter achieved 65% conversion. For the SCR reaction, there was an obvious rate dependence on oxygen concentration (below 3%) even though oxygen was present in an amount greater than that required by reaction stoichiometry. This phenomenon cannot be fully explained from an assessment of the literature and data at hand. However, such an oxygen dependence was noted by Hirsch (1982), who attributed it to a rate limitation rather than a stoichiometric limitation. Under typical furnace operating conditions, flue gas contains 4-7% oxygen, and approximately one fifth of the 0.5% NO concentration used in this study. Thus, in commercial applications, oxygen would not be a limiting factor.

7. Cu-ZSM-5 was found to catalyse the oxidation of ammonia to nitrogen only - no nitric oxide was detected. This result is similar to that recorded Brandin *et al* (1989).

   Nitric oxide conversion versus temperature profiles characteristically show an optimum, with decreased conversion at higher temperatures. This has been attributed to the oxidation of ammonia to nitric oxide. However, this explanation may not be immediately acceptable considering the evidence of nitrogen production from ammonia oxidation over zeolites (and not nitric oxide) observed in this study and by Brandin *et al* (1989). Although ammonia and oxygen react readily, when in the presence of nitric oxide, they will preferentially react with NO according to the stoichiometry of the SCR reaction, at least at the temperatures covered in this study. Thus, a more extensive investigation of the relative rates of the two reactions i.e., ammonia oxidation and SCR, is required and should be studied at sufficiently high temperatures to discern their individual characteristics.

8. Atomic absorption spectroscopy confirmed the visual observation of insignificant copper loading on the non porous ceramic filter material under the same conditions used to impregnate silicalite. Thus other methods of incorporating copper with the aluminosilicate fibres should be investigated. TPR indicated that a high copper oxide dispersion on silicalite was obtained and suggests that a similarly high dispersion may be achieved with the

ceramic fibres if copper can be successfully impregnated (perhaps by including copper oxide during synthesis).

9. The same activation energy (9 kcal/mol) was calculated for the SCR reaction over supported (CuO-silicalite) and unsupported (CuO/aluminosilicate fibre) copper oxide, which confirmed that the catalyst was in the same form in both cases and that the same reaction mechanism was operative. This activation energy is similar to the value of 10 kcal/mol obtained by Fukuzawa and Ishihara (1979) but is lower than 16 kcal/mol calculated by Kiel *et al* (1992).

   While the activation energy did not change, impregnated silicalite gave higher TOFs than the CuO/filter mix and bulk unsupported CuO under the same conditions, emphasizing the significance of dispersion of the active species.

10. The activation energy for the SCR reaction over Cu-ZSM-5 was calculated to be 14 kcal/mol and compares well with the results obtained by Nam *et al* (1992) and other workers who have recorded values in the range 12.8 to 17.0 kcal/mol for Cu-Mordenite. No such activation energy for the reaction over Cu-ZSM-5 was available for comparison. That the activation energy for these two copper ion exchanged zeolites are so similar suggests that similar active sites are encountered. In contrast, the difference in activation energies for CuO and the zeolites indicates distinct dissimilarity of the active sites with different reaction mechanisms occurring over the ion exchanged and impregnated materials.

11. The literature review shows that little has been published on SCR with zeolites and copper oxide. The reaction mechanism, including reaction intermediates and the effect of oxygen has yet to be determined. That NO_2 (formed by the gas phase reaction of nitric oxide and oxygen) and not NO is the reactive species, as suggested by Kiovsky *et al* (1980) seems unconvincing. Similarly, the use of NO_2 as a feed constituent has not been clarified. While an equimolar NO:NO_2 feed ratio has been shown to give a reaction rate higher than either NO or NO_2 individually, no convincing explanations have been offered.

12. In the temperature range investigated in this study (200-550°C), the activity of CuO supported on silicalite approached that of Cu-ZSM-5. The relative cost of CuO over a copper containing zeolite makes the former an attractive catalyst to investigate. The TOFs reveal no drop in the SCR reaction rate over CuO up to 550°C while a slight decrease in NO conversion is noted for ZSM-5 above 500°C, suggesting that CuO may be suitable for use at temperatures higher than ZSM-5. This requires further investigation. However, the activity of CuO should be kept in perspective by comparing reaction rate constants over CuO with vanadium based catalysts (as presented by Kiel *et al*, 1992) - those for CuO being three orders of magnitude lower.

In summary, it has been shown that a high copper oxide dispersion was obtained over silicalite which yielded the same activation energy as unsupported copper oxide. The post-synthesis copper impregnation technique did not alter the form of the active species on silicalite (evident by the activation energy) but gave reaction rates higher than unsupported copper oxide, emphasizing the importance of a high dispersion. Thus, in the quest for a catalytically active particulate filter, attention should be given to achieving a suitably high dispersion of copper on such a fibrous aluminosilicate, perhaps by including copper during synthesis.

REFERENCES

Altomare, C. 1981.
M.S. Thesis., University of Massachusetts, cited by Nam *et al.* (1988).

Ambs, W.J. and Flank, W.H. 1969.
J.Catal., **14**, 118. as cited by McDaniel and Maher (1976)

Amirnazmi, A., Benson, J.E. and Boudart, M. 1973.
Oxygen Inhibition in the Decomposition of NO on Metal Oxides and Platinum.
J. Catal., **30**, 55-65.

Andersson, L.A.H., Brandin, J.G.M. and Odenbrand, C.U.I. 1989.
Selective catalytic reduction of NOx over acid-leached mordenite catalysts.
Catalysis Today, **4**, 173-185.

Argauer and Landolt. 1972.
U.S. Patent 3 702 886.

Barthomeuf, D. 1991.
Acidity and Basicity in Zeolites in *Catalysis and Adsorption by zeolites*, Öhlmann, G. *et al.* (eds) Amsterdam: Elsevier.

Beyer, H., Jacobs, P.A. and Uytterhoeven, J.B. 1976.
J. Chem. Soc., Faraday I, **72**, 674 as cited by Hurst *et al.* (1982)

Boer, F.P., Hegedus, L.L., Gouker, T.R. and Zak, K.P. 1990.
Controlling power plant NOx emissions.
Chemtech, **May**, 312-319.

Bosch, H., and Janssen, F. 1988.
Catalytic Reduction of Nitrogen Oxides - A Review on the Fundamentals and Technology.
Catalysis Today, **2**, 369-532.

Bosman. 1987.
Summarizing world atmospheric sulphate deposition load with special reference to the South African Eastern Transvaal Highveld - Department of Water Affairs as cited by Petrie *et al.* (1992).

Bosman. 1990.
The impact of atmospheric sulphate deposition on surface water quality in the Eastern Transvaal Highveld - First IUPPA regional conference on air pollution, National Association for Clean Air as cited by Petrie *et al.* (1992).

Brandin, J.G.M., Andersson, L.A.H. and Odenbrand, C.U.I. 1989.
Catalytic reduction of nitrogen oxides on mordenite - Some aspects of the mechanism. *Catal. Today*, **4**, 187-203.

Breck, D.W. 1984.
Zeolite Molecular Sieves - Structure, Chemistry and use. Florida: Robert E Krieger.

Bremer, H., Morke, W., Schodel, R. and Vogt, F. 1973.
Adv. Chem. Ser., **121**, 249. as cited by McDaniel and Maher (1976).

Brown, A. and Wootton, T. 1991.
NOx Removal - Catalytic processes for the removal of nitrogen oxides from combustion gases.
Report for CHE425C - Chemical Engineering Project, Department of Chemical Engineering, University of Cape Town.

Byrne, J.W. 1990.
Method for Reduction of Nitrogen Oxides with Ammonia using Promoted Zeolite Catalysts.
U.S. Patent number 4 961 917,

Byrne, J.W., Chen, J.M. and Speronello, B.K. 1992.
Selective Catalytic Reduction of NOx using Zeolitic Catalyts for High Temperaure Applications.
Catal. Today, **13**, 33-42.

Chang, R., Sawyer, J., Lips, H., Bedick, R. and Dellfield, R. 1986.
The Testing and Evaluation of Ceramic Filter Fabrics in *Gas Cleaning at High Temperatures*, The Institution of Chemical Engineers Symposium Series No. 99. pp 177-191.

Choi, E.Y., Nam, I.S., Kim, Y.G., Chung, J.S and Nomura, M. 1991.
An x-ray absorption study of copper ion exchanged H-mordenite for selective catalytic reduction of NO by ammonia.
J. Molecular Catalysis, **69**, 247-258.

Davis, M.E. 1991.
Zeolites and Molecular Sieves: Not Just Ordinary Catalyts.
Ind. Eng. Chem. Res., **30**, 1675-1683.

Dean, A.M., DeGregoria, A., Hardy, J.E., Hurst, B. and Lyon, R.K. 1985.
U.S. Patent 4 507 269 as cited by Lyon, R.K. and Hardy, J.E. (1986)

Dietz, R.N. 1968.
Anal. Chem., **40**, 1576 as cited by Amirnazmi *et al.* (1973).

Dietz, W.A. 1967.
Response Factors for Gas Chromatographix Analyses.
J. of G.C., **Feb**, 68-71.

Dwyer, F.G. and Jenkins, E.E. 1976.
U.S. Patent 3 941 871.

Dyer, A. 1988.
An introduction to zeolite molecular sieves. Bath: John Wiley & Sons.

Els. 1987.
Emission inventory - indentification of sources, quanitification of emission factors in Eastern Transvaal Highveld. Report C/85/13 as cited by Petrie *et al.* (1992).

England, C and Corcoran, W.H. 1975.
The Rate and Mechanism of the Air Oxidation of Parts-per-Million Concentrations of Nitric Oxide in the Presence of Water Vapour.
Ind. Eng. Chem., Fundam., **14**(1), 55-63.

Fenimore, C.P. 1971.
Formation of nitric oxide in premixed hydrocarbon flames - 13th Int. Symp. on Combustion, 1970, The Combustion Institute, Pittsburgh, 1971, as cited by Bosch and Janssen (1988).

Fenimore, C.P. 1972.
Formation of nitric oxide from fuel nitrogen in ethylene flames.
Combust. Flame, **19**, 289 as cited by Bosch and Janssen (1988).

Gentry, S.J., Hurst, N.W. and Jones, A. 1979.
Temperature Programmed Reduction of Copper Ions in Zeolites.

J. Chem. Soc., Faraday Trans. I, **75**, 1688-1699.

Gentry, S.J., Hurst, N.W. and Jones, A. 1981.
Study of the Promoting Influence of Transition Metals on the Reduction of Cupric Oxide by Temperature Programmed Reduction.
J. Chem. Soc., Faraday Trans. I, **77**, 603-619.

Glick, H.S., Klein, J.J. and Squire, W. 1957.
J. Phys. Chem., **27**, 850 as cited by Bosch and Janssen (1988).

Haas. J., Steinwandel, J. and Plog, C. 1989.
Metal-Doped Zeolites for Selective Catalytic Reduction of Nitrogen Oxides in Combustion Gas in *Zeolites as Catalysts, Sorbents and Detergent Builders*, Karge, H.G. and Weitcamp, J. (eds), Amsterdam: Elsevier.

Hall, W.K. and Valyon, J. 1992.
Mechanism of NO decomposition over Cu-ZSM-5.
Catalysis Letters, **15**, 311-315.

Ham, S.W., Choi, H., nam, I.S. and Kim, Y.G. 1992.
Deactivation of Copper-ion-exchanged Hydrogen-Mordenite-type Zeolite Catalyst by SO_2 for NO reduction by NH_3.
Catalysis Today, **11**, 611-621.

Hamada, H., Kintaichi, Y., Sasaki, M., Ito, T. and Tabata, M. 1990a.
Applied Catalysis, **64**, L1-L4.

Hamada, H., Matsubayashi, N., Shimada, H., Kintaichi, Y., Ito, T. and Nishijima, A. 1990b.
XANES and EXAFS Analysis of Copper Ion-Exchanged ZSM-5 Zeolite Catalyst used for Nitrogen Monoxide Decomposition.
Catalysis Letters, **5**, 189-196.

Hamada, H., Kintaichi, Y., Sasaki, M., Ito, T. and Tabata, M. 1991.
Selective reduction of nitrogen monoxide with propane over alumina and HZSM-5 zeolite - Effect of oxygen and nitrogen dioxide intermediate.
Applied Catalysis, **70**, L15-L20.

Harms, S.M. 1987.
The oligomerization of propene over nickel oxide silica alumina.
M.Sc Dissertation, University of Cape Town, 1987.

Hecker, W.C. and Bell, A.T. 1981.
Gas Chromatographic Determination of Gases Fromed in Catalytic Reduction of Nitric Oxide.
Anal. Chem., **53**, 817-820.

Hirsch, P.M. 1982.
Selected Conversion of NOx by Catalytic Reduction with Ammonia.
Environmental Progress, **1**(1), 24-29.

Hurst, N.W., Gentry, S.J., Jones, A. and McNicol, B.D. 1982.
Temperature Programmed Reduction.
Catal. Rev.-Sci. Eng., **24**(2), 233-309.

Iwamoto, M., Furukawa, H. and Kagawa, S. 1986.
Catalytic Decomposition of Nitric Monoxide over Copper Ion-Exchanged Zeolites in New Developments in Zeolite Science and Technology; Murakami, Y., Iijima, A. and Ward, J.W. (eds), Amsterdam: Elsevier, pp 943-949.

Iwamoto, M. 1990.
Catalytic Decomposition of Nitrogen Monoxide in *Future opportunities in Catalytic and separation technology - Studies in Surface Science and Catalysis Vol 54.*, Misono, M., Moro-oka,Y., Kimura, S. (eds) Amsterdam: Elsevier.

Iwamoto, M. 1991a.
Copper Ion-exchanged Zeolites as Active Catalysts for Direct Decmposition of Nitrogen Monoxide in *Chemistry of Microporous Crystals - Proceedings of the International Symposium on Chemistry of Microporous Crystals*, Tokyo, June 26-29, 1990, Tokyo: Kodansha Ltd pp 327-334.

Iwamoto, M., Yahiro, H., Shundo, S., Yu-u, Y. and Mizuno, N. 1991b.
Influence of sulfur dioxide on catalytic removal of nitric oxide over copper ion-exchanged ZSM-5 zeolite.
Applied Catalysis, **69**, L15-L19.

Iwamoto, M., and Hamada, H. 1991c.
Removal of nitrogen monoxide from Exhaust gases through novel catalytic processes.
Catalysis Today, **10**, 57-71.

Iwamoto, M., Yahiro, H., Tanda, K., Mizuno, N., Mine, Y. and Kagawa, S. 1991d.
Removal of Nitrogen Monoxide through a Novel Catalytic Process. 1. Decomposition on Excessively Copper Ion Exchanged ZSM-5 Zeolites.

J. Phys. Chem., **95**, 3727-3730.

Kagawa, S., Furukawa, H. and Iwamoto, M. 1980.
Proc. 7th. Inter. Congr. Catal., 1406 as cited by Iwamoto, M. (1991a)

Kiovsky, J.R., Koradia, P.B. and Lim, C.T. 1980.
Evaluation of a New Zeolitic Catalyst for NOx Reduction with NH_3.
Ind. Eng. Chem. Prod. Res. Dev., **19**, 218-225.

Kirk Othmer Encyclopedia of Chemical Technology. 1981.
Third ed. John Wiley and Sons.

Kucherov, A.V. and Slinkin, A.A. 1986.
Introduction of transition metal ions in cationic positions of high-silica zeoiltes by a solid state reaction. Interaction of copper compousds with H-mordenite or H-ZSM-5.
Zeolites, **6**, 175-180.

Li, Y. and Armor, J.N. 1991.
Temperature-programmed desorption of nitric oxide over Cu-ZSM-5.
Appl. Catal., **76**, L1-L8.

Li, Y. and Armor, J.N. 1992.
Catalytic decomposition of nitrous oxide on metal exchanged zeolites.
Applied Catalysis B: Environmental, **1**, L21-L29.

Li, Y. and Hall, W.K. 1990.
Stoichiometric Catalytic Decomposition of Nitric Oxide over Cu-ZSM-5 Catalysts.
J. Phys. Chem., **94**(16), 6145-6148.

Li, Y. and Hall, W. K. 1991.
Catalytic Decomposition of Nitric Oxide over Cu-Zeolites.
J. Catal., **129**, 202-215.

Lyon, R.K. 1975.
U.S. Patent 3,900,559.

Lyon, R.K. and Hardy, J.E. 1986.
Discovery and Development of the Thermal DeNOx Process.
Ind. Eng. Chem. Fundam., **25**, 19-24.

Lyon, R.K. 1987.

Thermal DeNOx.
Environ. Sci. Technol., **21**(3), 231-236.

Maatman R.W. and Prater, C.D. 1957
Ind. Eng. Chem., **49**, 2 as cited by Harms (1987).

Masterton, W.L. and Slowinski, E.J. 1977.
Chemical Principles., 4th edition. London: Holt-Saunders.

Mastikhin, V.M. and Filimonova, S.V. 1992.
^{15}N Nuclear Magnetic Resonance Studies of the NO-O_2-NH_3 Reaction over ZSM-5 Zeolites.
J. Chem. Soc. Farady Trans., **88**(10), 1473-1476

McDaniel, C.V. and Maher, P.K. 1976.
Zeolite stability and Ultrastable zeolites in *Zeolite Chemistry and Catalysis*, edited by Rabo, J.A., ACS Monograph 171, Washington D.C.

Mizumoto, M., Yamazoe, N. and Seiyama, T. 1979.
Effects of Coexisting Gases on the Catalytic Reduction of NO with NH_3 over Cu(II) NaY.
J. Catalysis, 59, 319-324.

Montgomery, T.A., Samuelson, G.S. and Muzio, L.J. 1989.
JAPCA, **39**, 721. as cited by Kiel *et al.* (1992).

Montreuil, C.N. and Shelef, M. 1992.
Applied Catalysis B: Environmental, **1**, L1-L8.

Moretti, E., Leofanti, G., Andreazza, D., Giordano, N. 1974.
Gas Chromatographic Separation of Effluent from the Ammonia Oxidation Reaction: O_2, N_2, N_2O, NO_2, NH_3 and H_2O.
J. Chromatographic Science, **12**, 64-66.

Mortier. W.J. 1982.
Compilation of extra framework sites in zeolites, London: Butterworth.

Muzio, L.J., Teague, M.E., Kramlich, J.C., Cole, J.A., McCarthy, J.M. and Lyon, R.K. 1989.
JAPCA, **39**, 287. as cited by Kiel *et al.* (1992).

Nakajima, F. 1991.

Air Pollution Control with Catalysis - Past, Present and Future.
Catal. Today, **10**, 1-20.

Nakatsuji, T. and Miyamoto, A. 1991.
Removal Technology for Nitrogen oxides and Sulfur Oxides from Exhaust Gases.
Catalysis Today, **10**, 21-31.

Nam, I.S., Eldridge, J.W. and Kittrell, J.R. 1986.
Model of Temperature Dependence of a Vanadia-Alumina Catalyst for NO Reduction by NH_3: Fresh Catalyst.
Ind. Eng. Chem. Prod. Res. Dev. **25**, 186-192.

Nam, I.S., Eldridge, J.W. and Kittrell, J.R. 1988.
Nitric Oxide Reduction by Ammonia on Copper Exchanged Hydrogen Mordenite in *Catalysis 1987, Studies in surface science and catalysis Vol. 38*, edited by Ward, J.W., Amsterdam: Elsevier, pp 589-600.

Necker, P. 1985.
Survey on measurements to reduce NOx in Europe in *NOx symposium*, Rentz, O., Iszle, F., and Weibel, M. eds, Internationale Betriebserfahrungen, Karlsruhe as cited by Bosch and Janssen (1988).

Nicolaides, C.P., Wapiennik, M., Weiss, K.I.G., van den Akker, H., van Zalk, B. and Wielaard, P. 1991.
Alkali metal cation exchange of HZSM-5 and the catalytic properties of the alkalized zeolites.
Applied Catalysis, **68**, 31-39.

Odenbrand, C.U.I., Andersson, L.A.H., Brandin, J.G.M. and Järås, S. 1989.
Dealuminated mordenites as catalysts in the oxidation and decomposition of nitric oxide and in the decomposition of nitrogen dioxide: characterization and activities.
Catalysis Today, **4**, 155-172.

Paplawsky, W.J. and Pence, D.T. 1989.
Bench-scale studies on the use of metal-exchanged synthetic mordenite for the simultaneous removal of nitrogen oxide (NOx) and sulfur oxide (SOx) from simulated flue gases.
NTIS Report# DE89 004063, from Energy Res. Abstr., **14**(5).

Pence, D.T. and Thomas, T.R. 1972.

Proceedings of the AEC Pollution Control Conference, CONF-721030, as cited by Hirsch, P.M. (1980).

Perry's Chemical Engineers' Handbook. 1984.
Chief editors: R.H. Perry and D. Green, Sixth Edition, McGraw-Hill.

Petrie, J.G., Burns, Y.M. and Bray, W. 1992.
Air pollution - Chapter 17 in *Environmental Management in South Africa*, edited by Fuggle , R.F. and Rabie, M.A. Cape Town: Juta & Co. 1992, p. 417 - 455.

Pruce, L. 1981.
Reducing NOx emissions at the burner, in the furnace and after combustion.
Power, **1**, 33 as cited by Bosch and Janssen (1988).

Sato, S., Yu-u, Y., Yahiro, H., Mizuno, N. and Iwamoto, M. 1991.
Cu-ZSM-5 zeolite as highly active catalyst for removal of nitrogen dioxide from emission of diesel engines.
Applied Catal., **70**, L1-L5.

Sasaki, M., Hamada, H., Kintaichi, Y. and Ito, T. 1992.
Role of oxygen in selective reduction of nitrogen monoxide by propane over zeolite and alumina-based catalysts.
Catalysis Letters, **15**, 297-304.

Seiyama, T., Arakawa, T., Matsuda, T., Takita, Y. and Yamzoe, N. 1977.
Catalytic Activity of Transition Metal Ion Exchanged Y Zeolites in the Reduction of Nitric Oxide with Ammonia.
J. Catal., **48**, 1-7.

Schoonheydt, R.A., Vandamme, L.J., Jacobs, P.A. and Uytterhoeven, J.B. 1976.
Chemical, Surface and Catalytic Properties of Non-Stoichiometrically Exchanged Zeolites.
J. Catal., **43**, 292-303.

Shelef, M. 1992.
On the mechanism of nitric oxide decomposition over Cu-ZSM-5.
Catalysis Letters, **15**, 305-310.

Siddiqi, A.A. and Tenini, J.W. 1981.
Nitrogen oxides (NOx) controls in review.
Hydrocarbon Process., Int. Ed., **60**, 115 as cited by Bosch and Janssen (1988).

Sienko, M.J. and Plane, R.A. 1979.
Chemistry: Principles and applications, Tokyo: McGraw-Hill, 1979, p. 338.

Sigal, I.Ya. 1983.
The development and aims of investigations to study the conditions of formation of nitrogen oxides in furnace processes.
Thermal Engineering, **30**, 499 as cited by Bosch and Janssen (1988).

Smith, J.M. 1981.
Chemical Engineering Kinetics, Third Edition. Singapore: McGraw-Hill.

Smith, J.M and Van Ness, H.C. 1987.
Introduction to Chemical Engineering Thermodynamics, Fourth ed, Singapore: McGraw-Hill.

Speronello, B.K., Byrne, J.W. and Chen, J.M. 1990.
Zeolite catalysts and their use in reduction of nitrogen oxides.
European Patent, number 0 393 905 A2.

Suzuki, N., Nishimura, K. and Tokunaga, O. 1980.
J. Nucl. Sci. Technol., **17**, 822 as cited by Bosch and Janssen (1988).

Teraoka, Y., Ogawa, H., Furukawa, H. and Kagawa, S. 1992.
Influence of cocations on catalytic activity of copper ion-exchanged ZSM-5 zeolites for reduction of nitric oxide with ethene in the presence of oxygen.
Catalysis Letters, **12**, 361-366

Twigg M.V. 1989.
Catalyst Handbook, London: Wolfe, p. 42.

Tyson, P.D., Kruger, F.J., Louw, C.W. 1988.
S.A.. National Scientific Programmes, Report No 150, 1-122.

Uytterhoeven, J.B. 1978.
Acta Phys. Chem., **24**, 53 as cited by Hurst *et al.* (1982).

Valyon, J. and Hall, W.K. 1992.
An Infrared Study of an Active NO Decomposition Catalyst.
Private communication to J.G. Petrie from W.K.Hall.

Van Hooff, J.H.C. and Roelofsen, J.W. 1991.
in *Introduction to Zeolite Science and Practice*, van Bekkum, H., Flanigan, E.M. and Jansen, J.C. (eds) , Amsterdam: Elsevier, pg 251.

Von Ballmoos, R. 1984.
Collection of simulated XRD powder patterns for zeolites, Butterworth Scientific Ltd.

Wellburn, A.R. 1985.
The effects of NOx on vegetation, in: "Air Quality Guidlines", Consultation on ecological effects of air pollutants, Neukirchen, Austria, June 1985 as cited by Bosch and Janssen (1988).

Wilhite, W.F., and Hollis, O.L. 1968.
The use of Porous-Polymer Beads for Analysis of the Martian Atmosphere.
J. Gas Chromatography, **6**(Feb), 84-88.

Winter, E.R.S. 1971.
The catalytic decomposition of nitric oxide by metallic oxides.
J. Catal., **22**, *158* as cited by Bosch and Janssen (1988).

Williamson, W.B. and Lunsford, J.H. 1976.
Nitric Oxide Reduction with Ammonia over Cu(II)Y Zeolites.
J. Phys. Chem., **80**(24), 2664-2671.

Woolery, G.L., Alemang, L.B., Dessau, R.M. and Chester, A.W. 1986.
Zeolites, **6**, 14. as cited by Li and Hall (1991).

Zeldovich, J. 1946.
Oxidation of nitrogen in combustion and explosion.
Compt. Rend. Acad. Sci. USSR, **51**, 217 as cited by Bosch and Janssen (1988).

APPENDIX 1 - THERMODYNAMIC ANALYSIS

The equilibrium constants shown in Figure 2.1, 2.2 and 2.3 were calculated according to the method described by Smith and Van Ness (1987) using data taken from Table 4.1, "Heat capacities of gases in the ideal-gas state" and Table 4.4, " Standard heats of formation at 25°C".

ΔH°_{298} and ΔG°_{298} were calculated for each of the reactions listed below. The equilibrium constants at 298.15 K were then obtained using :

$$\ln K = \frac{\Delta G^\circ}{RT}$$

The value of J was obtained by substituting known values into the equataion:

$$\frac{\Delta H^\circ}{R} = \frac{J}{R} + (\Delta A)T + \Delta\frac{B}{2}T^2 - \Delta\frac{D}{T}$$

which allowed I to be calculated using known values at 298.15 K in the equation:

$$\ln K = -\frac{J}{RT} + \Delta A \ln T + \frac{\Delta B}{2}T + \frac{\Delta D}{2T^2} + I$$

Having established the value of the constant I, this equation was used again, to calculate the equilibrium constants at temperatures other than at 298.15K. The method and a sample calculation are shown in "Example 15.5", on page 510 in Smith and Van Ness: *Introduction to Chemical Engineering Thermodynamics*, Fourth Edition, published by McGraw Hill Book Company.

The stoichiometries for which the equilibrium constants were calculated are listed below and the data used in the calculations are shown overleaf in Figure 4.16 and Figure 4.16 .

1. $6NO + 4NH_3 = 5N_2 + 6H_2O$
2. $8NO + 2NH_3 = 5N_2O + 3H_2O$
3. $4NO + 4NH_3 + O_2 = 4N_2 + 6H_2O$
4. $4NO + 4NH_3 + 3O_2 = 4N_2O + 6H_2O$
5. $2NO + O_2 = 2NO_2$
6. $6NO_2 + 8NH_3 = 7N_2 + 12H_2O$
7. $NO_2 + NO + 2NH_3 = 2N_2 + 3H_2O$
8. $2NO_2 + 4NH_3 + O_2 = 3N_2 + 6H_2O$
9. $2NO_2 = N_2O_4$
10. $4NH_3 + 3O_2 = 2N_2 + 6H_2O$
11. $2NH_3 + 2O_2 = N_2O + 6H_2O$
12. $4NH_3 + 5O_2 = 4NO + 6H_2O$
13. $2NO = N_2 + O_2$
14. $2NO_2 = N_2 + 2O_2$

Table A1.1 Data used in the calculation of equilibrium constants

RXN	ln K	(J/R)	I	Δ A	Δ B*1E3	Δ D*1E-5	ΔH_{298} (J/mol)	ΔG_{298} (J/mol)
1	736.21	-217513.550	-8.3356	2.586	-4.189	1.586	-1807968	-1824932
2	332.5	-115814.330	-69.5284	2.798	-0.652	-4.017	-944984	-824216
3	666.38	-195694.910	-4.3040	2.441	-4.030	1.801	-1627468	-1651832
4	498.23	-157703.660	-48.5353	3.355	-2.558	-1.617	-1299268	-1235032
5	28.43	-14087.136	-15.5717	-0.449	0.626	-1.385	-114140	-70480
6	1177.63	-327309.760	42.1340	6.084	-9.779	7.972	-2732016	-2919124
7	318.97	-90803.885	5.6331	1.445	-2.328	1.593	-756664	-790676
8	568.11	-159789.126	15.2962	2.745	-4.497	3.401	-1332828	-1408252
9	2.049	-7783.201	-33.0223	1.696	-0.133	-1.203	-57200	-5080
10	526.72	-152057.617	3.7545	2.151	-3.712	2.231	-1266468	-1305632
11	221.32	-66530.998	-9.1792	1.304	-1.488	0.261	-551184	-548616
12	387.05	-108420.330	11.8145	1.861	-3.394	2.661	-905468	-959432
13	69.83	-21818.644	-4.0300	0.145	-0.159	-0.215	-180500	-173100
14	41.4	-7731.508	11.5417	0.594	-0.785	1.170	-66360	-102620

Table A1.2 ln K at various temperatures

TEMPS:	100	200	300	400	500	600	700	800 (°C)
	26.799	21.135	17.447	14.856	12.934	11.453	10.276	9.318 (1/K)
RXN								(1/T*1E4)
1	589.6784	466.6696	386.6349	330.3973	288.7100	256.5659	231.0179	210.2186
2	255.8466	191.4272	149.5102	120.0777	98.2870	81.5115	68.2038	57.3928
3	534.4867	423.7801	351.7559	301.1492	263.6363	234.7106	211.7199	193.0016
4	392.9031	304.4691	246.9461	206.5501	176.6284	153.5769	135.2737	120.3883
5	19.1408	11.2746	6.1237	2.4895	-0.2111	-2.2962	-3.9537	-5.3023
6	956.3548	770.8423	650.257	565.577	502.828	454.450	415.998	384.688
7	257.6723	206.2520	172.8154	149.3291	131.9230	118.5027	107.8361	99.1512
8	460.1512	369.6130	310.7502	269.4085	238.7707	215.1485	196.3726	181.0838
9	-2.5773	-6.4263	-8.8922	-10.5931	-11.8282	-12.7598	-13.4832	-14.0579
10	424.0986	337.9965	281.9933	242.6482	213.4842	190.9954	173.1192	158.5629
11	176.6548	139.1719	114.7956	97.6757	84.9915	75.2157	67.4494	61.1295
12	313.7119	252.2143	212.2321	184.1487	163.3335	147.2816	134.5199	124.1256
13	55.1934	42.8911	34.8806	29.2498	25.0754	21.8569	19.2996	17.2186
14	36.0526	31.6165	28.7569	26.7603	25.2865	24.1531	23.2534	22.5209

APPENDIX 2 - CALCULATION OF TCD RESPONSE FACTORS

A typical chromatogram and data recorded by the integrator are in shown in Figure A2.1. The three peaks observed, correpsond to: nitrogen, oxygen and nitric oxide respectively.

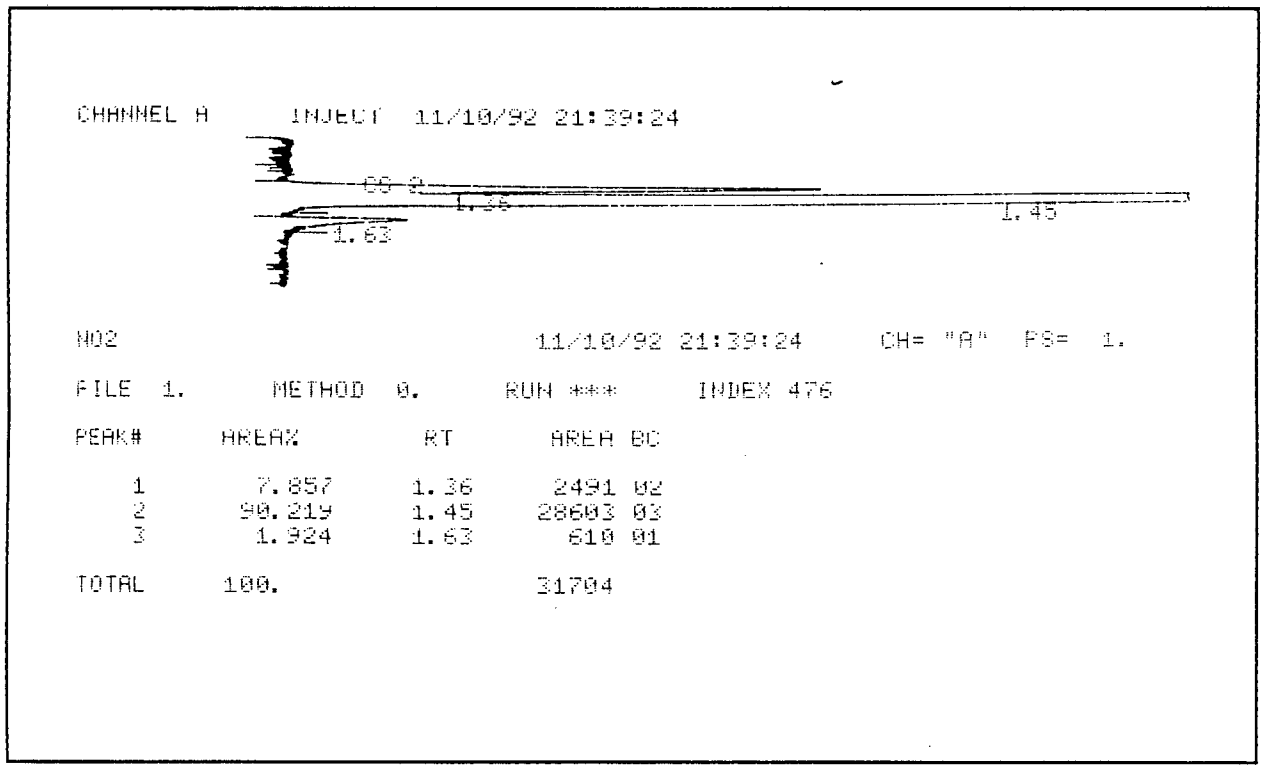

Figure A2.1 Typical chromatogram and integrator output

The linearity of the TCD response in the range of gas concentrations used, is shown in Figure A2.2.

As described in Chapter 3, because of the difference in thermal conductivities of various gases, TCD response factors are required to relate integrated peak area counts to actual gas compositions. Response factors were calculated by obtaining an average peak area count for a set of readings of one particular gas composition, from which a slope was calculated by assuming a zero area count in the absence of the gas (zero concentration). The response factors could also have been calculated by obtaining area counts for a number of different gas compositions, followed by linear regression of these data. However, the method used here was less time consuming, requiring gas of only one concentration. This method was valid because of the linearity of the TCD response to all three gases which has already been confirmed.

The method of calculation is shown below in Table A2.1. The response factor is calculated as the inverse of the slope of the "peak area vs concentration" graph. As an example: 9569 area counts represent 1.1% v/v NO, hence $1.1495*10^{-4}$ % NO is represented by a single area count. Thus, the composition of NO in any gas sample may be obtained by multiplying the peak area count obtained for that component, by this response factor (since sample pressure and hence sample volume (size) remains constant). A similar calculation is performed for nitrogen and oxygen and the response factors are shown (Table A2.1) relative to that obtained for nitrogen. These ratios which are less cumbersome than the actual values of the response factors, were used to facilitate calculations.

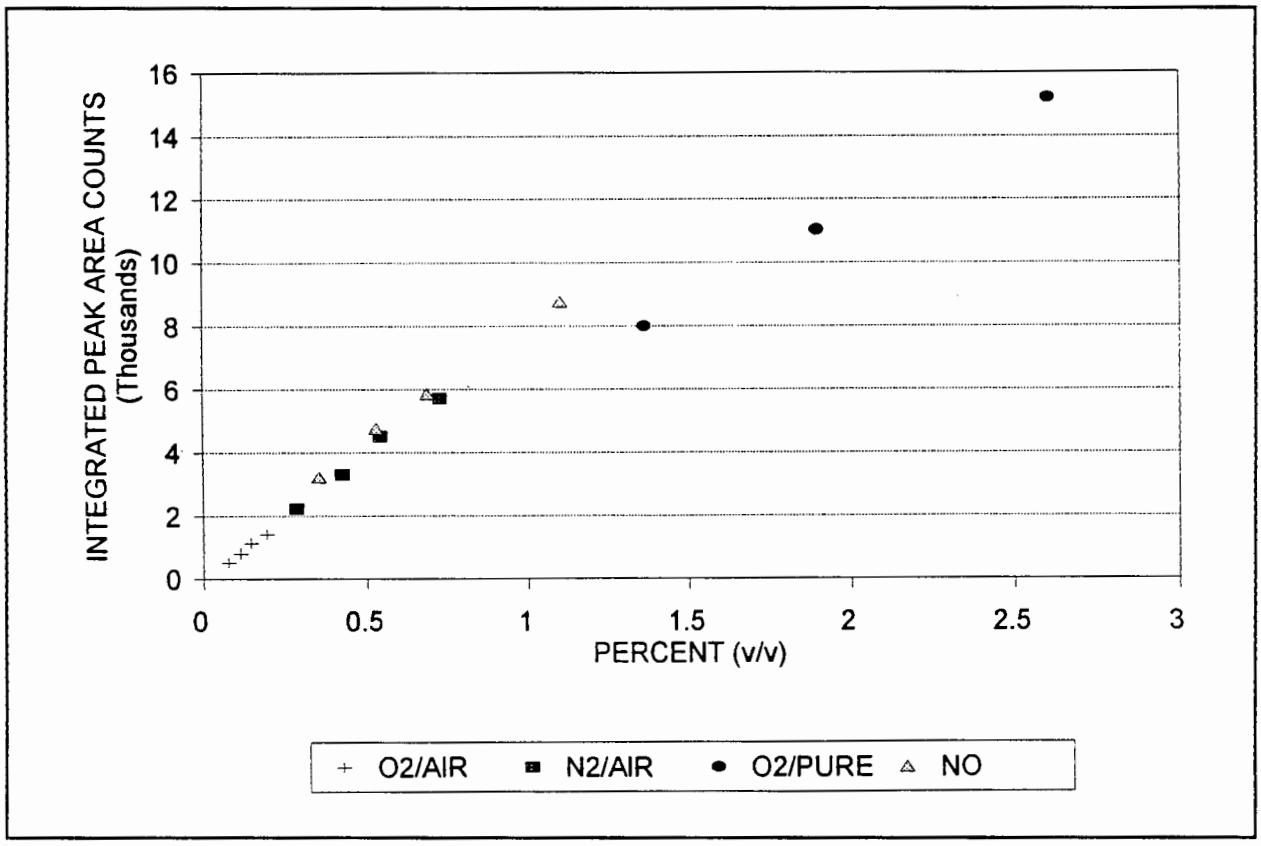

Figure A2.2 Linear response of TCD to gas concentrations

Table A2.1 Calculation of TCD response factors for NO, N_2 and O_2

Component	*NO*	*N_2*	*O_2*
Peak area counts	*9433*	*44707*	*11572*
	9609	*44358*	*11567*
	9267	*44853*	*11729*
	9516	*44651*	*11744*
	9930	*44679*	*11697*
	9601	*44254*	*11539*
	9625		
Average	*9569*	*44584*	*11641*
Std Deviation	*204*	*228*	*92*
Theoretical composition (%) (from flowrate measurements)	*1.1*	*4.7*	*1.25*
*Response factor * 10^4*	*1.150*	*1.054*	*1.074*
Ratio with respect to N_2	***1.10***	***1.00***	***1.02***

APPENDIX 3 - CATALYST CHARACTERIZATION DATA

Table A3.1 *Chemical analysis of catalysts by* Mintek

	Al_2O_3	SiO_2	*Cu*	*Na*	
Cu-ZSM-5	*1.64*	*89.6*	*1.13*	*0.18*	
Impregnated silicalite		*< 0.30*	*95.7*	*0.45*	*415ppm*
(Al_2O_3 and SiO_2 by XRF and Cu and Na using AAS)					

TPR operating data

Catalyst mass:	0.5	g
Calcination Heating rate:	10	°C / min in nitrogen
Calcination temperature:	530	°C
Calcination time:	2	hours
Settling/Adsorption temperature:	100	°C
Temperature programming rate:	10	°C / min in 5% H_2 in Nitrogen
Maximum temperature:	650	°C

APPENDIX 4 - DIRECT DECOMPOSITION REACTION DATA

All experimental data pertaining to the direct decomposition reaction are shown in Table A4.1. Sample calculations are given below.

Calculation of gas composition from GC data

Example: Run #27

3.8% NO = 30782 area counts.
Hence, one area count represents: 3.8% / 30782 = $1.235*10^{-4}$ % NO

Relative molar factors: N_2:NO:O_2 = 1 : 1.15 : 1.02. Hence,
nitrogen peak of 4538 counts represents: 4538 * $1.235*10^{-4}$ / 1.15 = 0.487% nitrogen in feed.

Calculation of TOF

Example: Run#27 at 492°C

Catalyst	Cu-ZSM-5
Mass	1.0171 g
Copper content	1.13% w/w
Feed N_2 content	0.05% v/v
Effluent N_2 content	0.485% v/v
Difference	0.435%
Total flowrate (NTP)	26.2 ml/min (20°C)
Avogadro's number	$6.022*10^{23}$ molecules per mole
Assume ideal gas volume	= nRT/P = 1(mol) * 8.314 (J/mol.K) * 293 (K) / 101330 (Pa)
	= 24.04 ml/mmol
Rate of nitrogen production	= 0.435% / 100 * 26.2 (ml/min) / 60 (s/min)
	= $1.900*10^{-3}$ (ml N_2/s)
	= $1.900*10^{-3}$ (ml/s) / 24.04 (ml/mmol)
	= $7.904*10^{-5}$ (mmol N_2/s)
	= $7.904*10^{-8}$ (mol N_2/s) * $6.022*10^{23}$ (molecules/mol)
	= $4.760*10^{16}$ (N_2 molecules/second)

Copper content = 1.13% / 100 * 1.0171 (g cat)
= 0.0115 (g Cu)
= 0.0115 (g Cu) / 63.546 (g/mol)
= $1.809*10^{-4}$ (mol Cu)
= $1.809*10^{-4}$ (mol Cu) * $6.022*10^{23}$ (molecules/mol)
= $1.089*10^{20}$ (molecules of Cu)

TOF defined as twice the number of nitrogen molecules produced per second per copper ion = number of nitric oxide molecules converted per second per copper ion.

TOF = 2*[$4.760*10^{16}$ (N_2 molecules/s) / $1.089*10^{20}$ (molecules of Cu)]
= 2*[$4.760*10^{-4}$ (N_2 molec/Cu.s)]
= $8.74*10^{-4}$

Conservation of mass calculation

Run #27 at 492°C

Measured by GC:	N_2 produced	0.435%
	O_2 produced	0.00%
	NO consumed	1.77%

Theoretical O_2 produced: 0.435% (from N_2 produced - stoichiometry: $2NO = N_2 + O_2$)

Theoretical NO consumed in decomposition reaction (from stoichiometry)
0.87%

Since no oxygen was recorded as a reaction product, assume all oxygen consumed in the oxidation reaction with NO - stoichiometry: $2NO + O_2 = 2NO_2$.

Theoretical NO consumed in oxidation reaction (from oxidation stoichiometry)
0.87%

Theoretical total NO consumption (0.87% in decomposition + 0.87% in oxidation reaction)
1.74%

cf actual consumption: 1.77% as measured by GC

Error: 2%

NITRIC OXIDE DECOMPOSITION DATA PLOTTED IN FIGURE 4.3 "COMPARISON OF ARRHENIUS PLOTS"

Data taken from "figure 2", Iwamoto *et al* (1986)
W/F = 4 g.s/ml. Assume catalyst = 4 grams, then flowrate = 60 ml/min

TEMP °C	NO CONVERSION (%)	N2 SELECTIVITY (%)	1000*TOF	1000/T
400	58	22	0.923	1.49
450	95	50	3.437	1.38
500	96	72	5.001	1.29
550	98	78	5.530	1.22
600	98	78	5.530	1.15
650	98	75	5.318	1.08
700	98	70	4.963	1.03
Taken from "Figure 2"			0.51	1.61
from Li and Hall (1991)			1.52	1.55
(Cu-ZSM-5-14-96)			3.60	1.48
			8.03	1.44
			12.99	1.38
			16.88	1.34
			19.74	1.30
			21.70	1.25
			21.92	1.22

Calcuation of TOFs with data taken from Iwamoto *et al.*, (1986) - run at 400°C

NO flowrate = 4% of 60 ml/min

N_2 flowrate = 0.04 * (60 ml/min) / (60 s/min) * 0.58 * 0.22

= 0.0051 ml/s

= (0.0051 ml/s) / ((22.4 ml/mmol) * (293 K / 273 K)) * (6.022*10^{23} molecules/mol) * (10^{-3} mol/mmol)

= 1.279*10^{17} molecules of N_2 produced per second

[Cu] Iwamoto *et al.*, (1986) used Cu-ZSM-5-50-73
Cu-ZSM-5-46-111 used in this study has 0.19 mmol Cu/g
hence, by direct proportion:
(46/50) * (73% / 111%) * (0.19 mmol Cu/g)
= 0.115 mmol Cu/g in Cu-ZSM-5-50-73
= $(0.115*10^{-3}$ mol/g) * 4 g * $(6.022*10^{23}$ ions/mol)
= $2.770*10^{20}$ Cu ions

1000*TOF = 2 * ($1.279*10^{17}$ molecules of N_2 per second) /
($2.770*10^{20}$ Cu ions) * 1000
= 0.923

TABLE A4.1. - DATA FROM INVESTIGATION OF DIRECT DECOMPOSITION

	RELATIVE MOLAR RESPONSE				
N2	1	CATALYST	Cu-ZSM-5		
O2	1.02	MASS	1.0171	g	
NO	1.15	BED DEPTH	3.5	cm	
		SPACE VELOCITY	819	per hr (at 24 ml/min NTP)	

RUN #	TEMP (°C)	FEED: PEAK AREA COUNT N2	O2	NO	FEED [NO] (%)	PRODUCT: PEAK AREA COUNT N2	O2	NO	PRODUCT COMPOSITIO (ACCORDING TO GC) N2(%)	O2(%)	NO(%)	PRODUCED (ACCORDING TO GC) N2(%)	O2(%)	CONSUMED NO(%)	BALANCE ERROR (%)	ACTUAL NO CONV. (%)	CONV. TO N2 (%)	THEORET. NO CONV. (%)	FEED FLOWRATE (ml/min)	TOF*1000	1000/T (1/K)
20	510	897	0	30782	3.8	4909	0	15410	0.53	0.00	1.90	0.43	0.00	1.90	9	50	11	27	24.3	0.7518	1.28
21	265	897	0	30782	3.8	484	0	29625	0.05	0.00	3.66	-0.04	0.00	0.14	224	4	0		24.3		1.86
22	322	484	0	30782	3.8	796	0	28367	0.09	0.00	3.50	0.03	0.00	0.30	55	8	0	6	24.3		1.68
23	372	484	0	30782	3.8	943	0	24551	0.10	0.00	3.03	0.05	0.00	0.77	74	20	1	18	24.3	0.0860	1.55
24	400	484	0	30782	3.8	2340	0	23643	0.25	0.00	2.92	0.20	0.00	0.88	10	23	5	13	26.2	0.3745	1.49
25	433	484	0	30782	3.8	3243	0	20418	0.35	0.00	2.52	0.30	0.00	1.28	7	34	8	18	26.2	0.5568	1.42
26	468	484	0	30782	3.8	4150	0	17815	0.45	0.00	2.20	0.39	0.00	1.60	2	42	10	21	26.2	0.7398	1.35
27	492	484	0	30782	3.8	4538	0	16438	0.49	0.00	2.03	0.44	0.00	1.77	2	47	11	24	26.2	0.8181	1.31
28	533	484	0	30782	3.8	4646	0	16523	0.50	0.00	2.04	0.45	0.00	1.76	-2	46	12	23	26.2	0.8399	1.24
29	369	380	0	31888	3.8	936	0	24683	0.10	0.00	2.94	0.06	0.00	0.86	73	23	2	20	23.8	0.0985	1.56
30	386	380	0	31888	3.8	1498	0	22987	0.16	0.00	2.74	0.12	0.00	1.06	56	28	3	22	23.8	0.1981	1.52
31	413	380	0	31888	3.8	2539	0	21243	0.26	0.00	2.53	0.22	0.00	1.27	29	33	6	22	24.2	0.3889	1.46
32	512	380	0	31888	3.8	4683	0	15930	0.49	0.00	1.90	0.45	0.00	1.90	6	50	12	27	24.2	0.7752	1.27
33	349	373	0	32650	3.8	608	0	28272	0.06	0.00	3.29	0.02	0.00	0.51	81	13	1	12	26.4	0.0450	1.61
34	371	373	0	32650	3.8	878	0	25818	0.09	0.00	3.00	0.05	0.00	0.80	74	21	1	18	26.4	0.0967	1.55
35	272	268	0	33294	3.8	336	0	31547	0.03	0.00	3.60	0.01	0.00	0.20	86	5	0	5	27.7	0.0134	1.83
36	443	117	0	32760	3.8	3263	0	21636	0.33	0.00	2.51	0.32	0.00	1.29	2	34	8	17	27.0	0.6143	1.40
37	534	147	0	33106	3.8	4240	0	19848	0.42	0.00	2.28	0.41	0.00	1.52	-7	40	11	19	26.5	0.7762	1.24
38	538	400	0	32744	3.8	3931	0	19399	0.40	0.00	2.25	0.36	0.00	1.55	8	41	9	22	26.5	0.6770	1.23
EFFECT OF FEED CONCENTRATION																					
39	503	268	0	32630	3.8	2501	0	23985	0.25	0.00	2.79	0.23	0.00	1.01	10	26	6	15	92.3	1.4977	1.29
40	503	0	0	26287	3.0	1914	0	19745	0.19	0.00	2.27	0.19	0.00	0.75	-2	25	6	12	92.3	1.2700	1.29
41	503	0	0	22075	2.7	1407	0	16756	0.15	0.00	2.01	0.15	0.00	0.64	8	24	6	13	91.2	0.9624	1.29
42	503	0	0	19364	2.4	1311	0	15210	0.14	0.00	1.86	0.14	0.00	0.51	-10	21	6	10	91.2	0.9103	1.29
43	503	0	0	17388	1.9	1020	0	13911	0.10	0.00	1.51	0.10	0.00	0.38	-2	20	5	10	93.2	0.6439	1.29

Amount of nitrogen produced = Product [N2] - Feed [N2] (Valid since sample volume is constant)
NO consumed = 3.8% (feed concentration) - NO in product
Error in "Mass balance". Calculation described in Section 4.1.5. and sample calculation shown in Appendix 4.
Total NO conversion = 1- ((NO in product)/(NO in feed))
Conversion to Nitrogen = (Nitrogen produced) / (NO in feed)
Theoretical NO conversion described in Section 4.1.2. - Sample calculation shown in Appendix 4.
Turnover Frequency described in Section 4.1.2. and sample calculation shown in Appendix 4.

Table A4.2 Calculation of activation energy and order of reaction for NO

CALCULATION OF REACTION ORDER
WITH RESPECT TO NO PARTIAL PRESSURE
(DECOMPOSITION REACTION)

RUN #	ln(%NO*10)	Ln(TOF*1000)
33	3.64	4.039E-01
34	3.41	2.390E-01
36	3.16	-9.393E-02
37	2.94	-4.402E-01

Regression Output:

Constant	-3.99003
Std Err of Y Est	0.067114
R Squared	0.978546
No. of Observations	4
Degrees of Freedom	2
X Coefficient(s)	**1.222027**
Std Err of Coef.	0.127946

CALCULATION OF Ea
FOR DECOMPOSITION REACTION
LINEAR REGION OF ARRHENIUS PLOT
(BELOW 400°C)

RUN #	LN(TOF)	1/T
30	-8.527	1.517E-03
31	-7.852	1.458E-03
38	-10.008	1.608E-03
39	-9.244	1.553E-03

Regression Output:

Constant	13.59661
Std Err of Y Est	0.116319
R Squared	0.989527
No. of Observations	4
Degrees of Freedom	2
X Coefficient(s)	-14671.1
Std Err of Coef.	1067.234

-14671.1*-8.314 = 121976 J/mol
29.1 kcal/mol

APPENDIX 5 - SCR DATA

The folowing sample calculations describe the data which are shown in Table A5.1 and A5.2.

Theoretical feed composition calculated from flowrates

Example: Run# 75

Feed flowrates:		Stock gas compositions:	
NO	8.00 ml/s	NO	1.1%
NH_3	8.82 ml/s	NH_3	1.0%
O_2	0.31 ml/s	O_2	100%
TOTAL	17.13 ml/s		

Blended gas composition:

NO	8 / 17.13 * 1.1 = 0.51%
NH_3	8.82 / 17.13 * 1.0 = 0.52%
O_2	0.31 / 17.13 * 100 = 1.81%

NO concentration from NOx analyzer

1.1% NO/He span gas read as "5000" ppm on analyzer scale

Example: Run# 75

Reading:	2200 ppm
Hence, actual concentration:	2200 / 5000 * 1.1% = 0.48% NO in feed

Calculation of NO conversion

Example: Run# 75
(1 - outlet/inlet) * 100 = (1 - 1780/2200) * 100 = 19% NO conversion

Feed and product composition as measured by GC

Method identical to that shown in APPENDIX 2.

Calculation of TOF

Method similar to that shown in APPENDIX - 4 for direct decomposition reaction.
Exception: By stoichiometry, number of N_2 molecules produced = number of NO molecules consumed.

Example: Run# 75

N_2 produced	0.18% (Difference between N_2 recorded as product and N_2 in feed)
Flowrate	17.1 ml/s
Catalyst	Cu-ZSM-5
Catalyst mass	1.054 g
[Cu]	1.13% w/w
Gas volume	24.04 ml/mmol
Avogadro's No	6.022e23

N_2 produced = 0.18% * 17.1 (ml/s) / 24.04 (ml/mmol) * 1E-3 (mol/mmol) * 6.022E23 molec/mol
= 7.71E17 molecules N_2 produced per sec

Cu content = 1.054 g * 1.13% / 63.546 {g Cu/mol) * 6.022E23
= 1.129E20 Cu ions

1000*TOF = 7.71E17 / 1.129E20 * 1000
= 6.83

Calculation of space velocity

Example: Run# 95

Catalyst bed depth	3.5 cm
Bed volume (V)	$\pi D^2/4$ * H = 3.14159 * 0.8^2 / 4 * 3.5
	= 1.8 ml
Space velocity	= Q_f/V
	= 12 (ml/s) / 1.76 (ml) * 3600 (s/hr)
	= 24000 h^{-1}

Calculation of estimated rate constant for SCR reaction over copper oxide

Run# 115 at 287°C.

Feed [NO]	(C_{in})	0.50%
Product [N_2]		0.10% therefore, according to reaction (2.2) stoichiometry
Product [NO]	(C_{out})	0.50% - 0.10% = 0.40%
Catalyst mass		0.1116g
Bed depth	(L)	4 cm = 0.04 m
Feed Flowrate		16.5 ml/s at 20°C
		= 16.5 (ml/s) * (287+273)/273
		= 33.85 ml/s at 287°C
Reactor area	$(\pi D^2)/4$	= $\pi(0.8\ cm)^2/4$
		= 0.503 cm^2 hence:
Superficial velocity (U_g)		(33.85ml/s) / (0.503 cm^2)
		= 67.3 cm/s
		= 0.673 m/s

Voidage estimation (ϵ)

Using a measuring cylinder, 0.484 grams gave a tapped bulk volume of approximately 0.9 ml which gives (0.9) / (0.484) = 1.86 ml/g of silicalite.

0.1116 grams would then occupy a volume of 1.86 ml/g * 0.1116 g = 0.21 ml. However, this bed was expanded with glass wool to a total bed volume of 2 ml. Hence, the catalyst volume as a fraction of this total volume in 0.21 / 2 = 0.105. Hence an estimated voidage of 0.9.

$k_r = - U_g * \ln (C_{out}/ C_{in}) / ((1-\epsilon)L)$ = - 0.673 * (-0.223) / ((1-0.9)*0.04))

= 37.5

TABLE A5.1 - DATA FOR THE INVESTIGATION OF THE SCR REACTION (I): PARAMETRIC STUDIES

CATALYST: Cu-ZSM-5

1.1% NO at 10 kPa = 8795 AREA COUNTS
NO CORRECTION FACTOR: 1.251E-04 N2:NO:N2 = 1:1.09:1.03

RUN #	TEMP (°C)	FEED FLOWRATES NO (ml/s)	NH3 (ml/s)	O2 (ml/s)	He (ml/s)	TOTAL (ml/s)	THEORETICAL FEED COMPOSITION NO (%)	NH3 (%)	O2 (%)	NOx ANALYZER FEED [NO] (ppm)	CALC [NO] (%)	PROD. [NO] (ppm)	NO CONV. (%)	FEED ANALYSIS - GC AREA COUNTS N2 (counts)	O2 (counts)	NO (counts)	PRODUCT ANALYSIS - GC AREA COUNTS N2 (counts)	O2 (counts)	NO (counts)	FEED COMPOSITION (from GC) N2 (%)	O2 (%)	NO (%)	PRODUCT COMPOSITI (from GC) N2 (%)	O2 (%)	NO (%)	N2 PROD. (%)	O2 CONS. (%)	CAT MASS (WET) (g)	1000* TOF	1000/T	(ACTUAL N2) / (THEORET N2)	NH3 CONV TO N2 (%)	[NO] FROM NOx ANALYZER (%)	NH3 CONV TO NO (%)
AMMONIA OXIDATION																																		
60	300	-	8.8	0.3	8.7	17.8	-	0.50	1.74	0	-	10	-	0	14533	0	313	13692	0	0.00	1.72	0.00	0.04	1.62	0.00	0.04	0.10	1.054	1.420	1.745	0.54	7	0.0022	0
61	358	-	9.1	0.3	9.2	18.6	-	0.49	1.67	0	-	10	-	0	15200	0	377	13784	0	0.00	1.80	0.00	0.04	1.63	0.00	0.04	0.17	1.054	1.784	1.585	0.39	9	0.0022	0
62	404	-	9.1	0.3	9.2	18.6	-	0.49	1.67	0	-	5	-	0	17132	0	935	14558	0	0.00	2.02	0.00	0.11	1.72	0.00	0.11	0.30	1.054	4.424	1.477	0.53	22	0.0011	0
63	432	-	9.2	0.3	8.4	17.9	-	0.51	1.84	0	-	110	-	0	14910	0	1123	12892	0	0.00	1.76	0.00	0.13	1.52	0.00	0.13	0.24	1.054	5.125	1.418	0.81		0.0242	5
64	434	-	9.2	0.3	8.2	17.7	-	0.52	1.87	0	-	110	-	0	15231	0	1359	12239	0	0.00	1.80	0.00	0.16	1.45	0.00	0.16	0.35	1.054	6.112	1.414	0.66		0.0242	5
65	450	-	9.2	0.3	8.5	18.0	-	0.51	1.78	0	-	55	-	0	15187	0	1290	12012	0	0.00	1.79	0.00	0.15	1.42	0.00	0.15	0.38	1.054	5.900	1.383	0.59	29	0.0121	2
66	455	-	9.2	0.3	8.2	17.7	-	0.52	1.87	0	-		-	0	16961	0	2651	12166	0	0.00	2.00	0.00	0.30	1.44	0.00	0.30	0.57	1.054	-	1.374	0.81			
67	499	-	9.2	0.3	8.5	18.0	-	0.51	1.78	0	-	420	-	0	14805	0	1778	10325	0	0.00	1.75	0.00	0.20	1.22	0.00	0.20	0.53	1.054	8.132	1.295	0.58	40	0.0924	18
68	554	-	9.2	0.3	8.5	18.0	-	0.51	1.78	0	-	15	-	0	14656	0	2284	9394	0	0.00	1.73	0.00	0.26	1.11	0.00	0.26	0.62	1.054	10.446	1.209	0.63	51	0.0033	1
AMMONIA/NO REACTION																																		
69	300	8.0	8.8	-	-	16.8	0.52	0.52	-	2420	0.53	2450	-	0	0	3243	257	0	2982	0.00	0.00	0.41	0.03	0.00	0.37	0.03	0.00	1.054	-	-				
70	358	7.5	9.1	-	-	16.5	0.50	0.55	-	2190	0.48	2120	3	0	0	4125	108	0	4178	0.00	0.00	0.52	0.01	0.00	0.52	0.01	0.00	1.054	-	-	0.94			
71	390	7.5	9.1	-	-	16.5	0.50	0.55	-	2080	0.46	2050	1	0	0	3862	157	0	3752	0.00	0.00	0.48	0.02	0.00	0.47	0.02	0.00	1.054	-	-	3.02			
72	470	9.4	9.2	-	-	18.6	0.56	0.49	-	2500	0.55	2320	7	0	0	4794	525	0	4543	0.00	0.00	0.60	0.06	0.00	0.57	0.06	0.00	1.054	-	-	1.81			
73	482	9.4	9.2	-	-	18.6	0.56	0.49	-	2600	0.57	2210	15	0	0	4660	594	0	4213	0.00	0.00	0.58	0.07	0.00	0.53	0.07	0.00	1.054	-	-	0.98			
74	540	9.4	9.2	-	-	18.6	0.56	0.49	-	2600	0.57	2200	15	0	0	4840	848	0	3923	0.00	0.00	0.61	0.10	0.00	0.49	0.10	0.00	1.054	-	-	1.36			
SCR REACTION																																		
75	301	8.0	8.8	0.3	-	17.1	0.51	0.51	1.81	2200	0.48	1780	19	0	14103	1447	1564	13158	1588	0.00	1.67	0.18	0.18	1.56	0.20	0.18	0.11	1.054	6.823	1.742	1.83			
76	358	7.5	9.1	0.3	-	16.8	0.49	0.54	1.84	2050	0.45	1410	31	0	15614	1696	1743	14501	1359	0.00	1.85	0.21	0.20	1.71	0.17	0.20	0.13	1.054	7.470	1.585	1.31			
77	404	7.5	9.1	0.3	-	16.8	0.49	0.54	1.84	1900	0.42	1080	43	0	16379	1572	2428	14634	1130	0.00	1.94	0.20	0.28	1.73	0.14	0.28	0.21	1.054	10.406	1.477	1.32			
78	435	9.5	9.1	0.3	-	18.8	0.55	0.48	1.70	2510	0.55	1320	47	0	14881	1929	3471	13031	1001	0.00	1.76	0.24	0.40	1.54	0.13	0.40	0.22	1.054	16.653	1.412	1.52			
79	450	9.5	9.1	0.3	-	18.8	0.55	0.48	1.70	2300	0.51	965	58	0	12259	1648	3580	10692	903	0.00	1.45	0.21	0.41	1.26	0.11	0.41	0.19	1.054	17.176	1.383	1.28			
80	459	9.6	9.2	0.3	-	19.1	0.55	0.48	1.73	2400	0.53	700	71	0	12820	1936	3964	10536	541	0.00	1.52	0.24	0.45	1.25	0.07	0.45	0.27	1.054	19.281	1.366	1.17			
81	475	9.4	9.2	0.3	-	18.9	0.55	0.49	1.70	2400	0.53	650	73	0	13179	2056	4171	11665	958	0.00	1.56	0.26	0.48	1.38	0.12	0.48	0.18	1.054	20.043	1.337	1.20			
82	502	9.4	9.2	0.3	-	18.9	0.55	0.49	1.70	2400	0.53	720	70	0	12327	2002	4278	11064	948	0.00	1.46	0.25	0.49	1.31	0.12	0.49	0.15	1.054	20.558	1.290	1.28			
83	553	9.4	9.2	0.3	-	18.9	0.55	0.49	1.70	2410	0.53	850	65	0	12327	2002	4266	10654	1103	0.00	1.46	0.25	0.49	1.26	0.14	0.49	0.20	1.054	20.500	1.211	1.38			
84	556	9.5	9.2	0.3	-	19.0	0.55	0.48	1.74	2400	0.53	860	64	0	12259	1648	3877	10632	765	0.00	1.45	0.21	0.44	1.26	0.10	0.44	0.19	1.054	18.710	1.206	1.26			
85	434	9.3	9.1	0.3	-	18.7	0.55	0.49	1.71	2400	0.53	1300	46	-	-	-	2736	12259	1137	-	-	-	0.31	1.45	0.14	0.31	-	1.0016	13.718	1.414	1.25			
86	476	9.3	9.1	0.3	-	18.7	0.55	0.49	1.71	2400	0.53	805	66	-	-	-	3769	10785	810	-	-	-	0.43	1.27	0.10	0.43	-	1.0016	18.898	1.335	1.19			
87	496	9.3	9.2	0.3	-	18.8	0.54	0.49	1.70	-	-	-	-	-	-	-	3918	8799	503	-	-	-	0.45	1.04	0.06	0.45	-	0.9933	19.915	1.300	DRAGER TUBES: NH3 CONSUMED = 0.4			
EFFECT OF OXYGEN CONCENTRATION																																		
88	476	9.3	9.1	0.0	-	18.4	0.56	0.49	0.00	2510	0.55	2500	0	-	-	-	221	0	4313	-	-	-	0.03	0.00	0.54	0.03	-	1.0016	1.089	1.335				
89	476	9.3	9.1	0.3	-	18.7	0.55	0.49	1.71	2400	0.53	805	66	-	-	-	3769	10785	810	-	-	-	0.43	1.27	0.10	0.43	-	1.0016	18.898	1.335				
90	477	9.3	9.1	0.2	-	18.6	0.55	0.49	1.18	2610	0.57	960	63	-	-	-	3480	6419	1060	-	-	-	0.40	0.76	0.13	0.40	-	1.0016	17.355	1.333				
91	471	9.3	9.1	0.1	-	18.5	0.55	0.49	0.59	2500	0.55	1600	36	-	-	-	2305	1775	2432	-	-	-	0.26	0.21	0.30	0.26	-	1.0016	11.427	1.344				
92	481	9.3	9.1	0.5	-	18.9	0.54	0.48	2.80	2310	0.51	680	71	-	-	-	4148	19908	480	-	-	-	0.48	2.35	0.06	0.48	-	1.0016	21.031	1.326				
93	477	9.3	9.1	1.1	-	19.5	0.53	0.47	5.50	2010	0.44	600	70	-	-	-	3664	42502	371	-	-	-	0.42	5.02	0.05	0.42	-	1.0016	19.108	1.333				
94	472	9.6	9.3	1.1	-	20.0	0.53	0.47	5.31	1910	0.42	650	66	-	-	-	4158	41845	392	-	-	-	0.48	4.95	0.05	0.48	-	1.0016	22.252	1.342				
EFFECT OF FEED FLOWRATE																															BED DEPTH	3.5 cm		
95	444	5.9	5.7	0.5	-	12.0	0.54	0.47	4.00	2150	0.47	600	72	-	-	-	4102	30420	149	-	-	-	0.47	3.60	0.02	0.47	-	1.054	12.546	1.395	BED VOLUME	1.8 cm^3		
96	454	10.8	10.6	0.9	-	22.3	0.53	0.47	4.09	2180	0.48	600	72	-	-	-	4039	31497	177	-	-	-	0.46	3.72	0.02	0.46	-	1.054	22.896	1.376	24576	SPACE VELOCITY (1/hr)		
97	455	18.7	17.2	1.6	-	37.5	0.55	0.46	4.16	2210	0.49	875	60	-	-	-	3447	31328	450	-	-	-	0.40	3.70	0.06	0.40	-	1.054	32.892	1.374	45550			
98	454	9.3	9.0	0.8	-	19.1	0.54	0.47	3.93	2150	0.47	655	70	-	-	-	3937	28892	341	-	-	-	0.45	3.41	0.04	0.45	-	1.054	19.119	1.376	76674			
																															39023			

TABLE A5.2 - DATA FOR THE INVESTIGATION OF THE SCR REACTION (II): COMPARISON OF Cu-ZSM-5 AND CuO

CATALYSTS AS LISTED

1.1% NO at 10 kPa = 8795 AREA COUNTS
NO CORRECTION FACTOR: 1.251E-04 N2:NO:N2 = 1:1.09:1.03

RUN #	TEMP (°C)	FEED FLOWRATES NO (ml/s)	NH3 (ml/s)	O2 (ml/s)	He (ml/s)	TOTAL (ml/s)	THEORETICAL FEED COMPOSITION NO (%)	NH3 (%)	O2 (%)	NOx ANALYZER BYPASS (ppm)	CALC [NO] (%)	RX (ppm)	NO CONV (%)	FEED ANALYSIS - GC AREA COUNTS N2 (counts)	O2 (counts)	NO (counts)	PRODUCT ANALYSIS - GC AREA COUNTS N2 (counts)	O2 (counts)	NO (counts)	FEED COMPOSITION (from GC) N2 (%)	O2 (%)	NO (%)	PRODUCT COMPOSITIO (from GC) N2 (%)	O2 (%)	NO (%)	N2 PROD. (%)	O2 CONS. (%)	CAT MASS (WET) (g)	1000* TOF	1000/T
CuO-SILICALITE (preliminary)																														
100	453	9.3	9.1	0.3	-	18.7	0.55	0.49	1.71	2600	0.57	1500	42	-	-	-	3224	10076	726	-	-	-	0.37	1.19	0.09	0.37	-	0.499	81.608	1.3774
101	453	9.3	9.1	0.3	-	18.7	0.55	0.49	1.71	2500	0.55	1600	36	-	-	-	-	-	-	-	-	-	-	-	-	-	-	0.499	-	-
102	460	9.1	9.2	0.3	-	18.7	0.54	0.49	1.71	2210	0.49	1400	37	-	-	-	2560	11280	1145	-	-	-	0.29	1.33	0.14	0.29	-	0.3461	93.078	1.3643
103	460	6.5	6.4	0.2	-	13.1	0.54	0.49	1.83	2400	0.53	1390	42	-	-	-	3356	12085	1352	-	-	-	0.39	1.43	0.17	0.39	-	0.3461	85.813	1.3643
CuO/FILTER (preliminary)																														
104	455	9.2	9.2	0.3	-	18.7	0.54	0.49	1.66	2080	0.46	1620	22	-	-	-	1297	11806	1262	-	-	-	0.15	1.40	0.16	0.15	-	0.5058	9.048	1.3736
105	462	9.4	9.1	0.3	-	18.9	0.55	0.48	1.64					0	12071	1596	1957	11961	1590	0.00	1.43	0.20	0.22	1.41	0.20	0.22	0.01	0.5013	13.915	1.3605
106	462	9.4	9.1	0.3	-	18.9	0.55	0.48	1.64					0	12071	1596	3096	11391	994	0.00	1.43	0.20	0.36	1.35	0.12	0.36	0.08	0.5013	22.013	1.3605
107	462	9.4	9.1	-	-	18.6	0.56	0.49	0.00					0	0	3918	1125	0	2826	0.00	0.00	0.49	0.13	0.00	0.35	0.129	0.000	0.5013	7.8677	1.3605
Cu-ZSM-5 (preliminary)																														
108	457	9.1	9.2	0.3	-	18.6	0.54	0.49	1.77					0	12802	1036	3739	8450	812	0.00	1.51	0.13	0.43	1.00	0.10	0.43	0.51	0.495	37.731	1.3699
109		9.1	9.2	0.0	-	18.3	0.55	0.50	0.00					0	0	4135	2239	0	3091	0.00	0.00	0.52	0.26	0.00	0.39	0.26	0.00	0.495	-	-
CuO unsupported																														
110	481	9.2	9.2	0.3	-	18.8	0.54	0.49	1.76					-	-	-	3269	11162	880	-	-	-	0.38	1.32	0.11	0.38	-	0.017	13.696	1.3263
111	462	9.2	9.2	0.0	-	18.4	0.55	0.50	0.00					0	0	4002	2801	0	1416	0.00	0.00	0.50	0.32	0.00	0.18	0.321	0.000	0.017	-	-
										BED DEPTH		4.0 cm																		
CuO-SILICALITE										BED VOLUME		2.0 cm^3																		
112		0.0	0.0	0.5	10.2	10.7	0.00	0.00	4.68	19122	SPACE VELOCITY (1/hr)			-	42958	-	-	-	-	-	5.08	-	-	-	-	-	5.077	0.1116	-	-
113		-	8.4	0.5	0.0	8.9	0.00	0.94	5.63	15900				-	55328	-	-	-	-	-	6.54	-	-	-	-	-	6.539	0.1116	-	-
114	524	7.3	8.4	0.5	-	16.2	0.50	0.52	3.09	29006				452	27317	940	2725	26293	655	0.05	3.23	0.12	0.31	3.11	0.08	0.261	0.121	0.1116	222.39	1.2547
115	287	7.5	8.5	0.5	-	16.5	0.50	0.51	3.16	29472				677	25891	865	886	25481	908	0.08	3.06	0.11	0.10	3.01	0.11	0.024	0.048	0.1116	20.777	1.7857
116	350	7.5	8.5	0.5	-	16.5	0.50	0.51	3.16	29472				677	25891	865	1111	25424	895	0.08	3.06	0.11	0.13	3.00	0.11	0.050	0.055	0.1116	43.144	1.6051
117	389	7.5	8.5	0.5	-	16.5	0.50	0.51	3.16	29472				618	26082	994	1310	24986	870	0.07	3.08	0.12	0.15	2.95	0.11	0.079	0.130	0.1116	68.792	1.5106
118	422	7.5	8.5	0.5	-	16.5	0.50	0.51	3.16	29472				618	26082	994	1690	24557	762	0.07	3.08	0.12	0.19	2.90	0.10	0.123	0.180	0.1116	106.57	1.4388
119	457	8.0	8.5	0.5	-	17.0	0.52	0.50	3.12	30438				286	-	-	1520	25166	899	0.03	-	-	0.17	2.97	0.11	0.142	-	0.1116	126.7	1.3699
120	348	8.0	8.4	0.5	-	17.0	0.52	0.50	3.13	30367				257	26456	988	540	25175	960	0.03	3.13	0.12	0.06	2.98	0.12	0.032	0.151	0.1116	28.988	1.6103
121	145	4.0	4.3	0.3	-	8.6	0.51	0.50	3.26	15380				360	24983	1102	671	24623	1109	0.04	2.95	0.14	0.08	2.91	0.14	0.036	0.043	0.1116	16.135	2.3923
122	200	4.0	4.3	0.3	-	8.6	0.51	0.50	3.26	15380				360	24983	1102	643	24277	1104	0.04	2.95	0.14	0.07	2.87	0.14	0.032	0.083	0.1116	14.682	2.1142
123	254	4.0	4.3	0.3	-	8.6	0.51	0.50	3.26	15380				360	24983	1102	816	24367	1007	0.04	2.95	0.14	0.09	2.88	0.13	0.052	0.073	0.1116	23.657	1.8975
124	405	4.1	4.4	0.3	-	8.7	0.52	0.50	3.21	15631				225	24617	1002	1241	23872	1046	0.03	2.91	0.13	0.14	2.82	0.13	0.117	0.088	0.1116	53.569	1.4749
125	405	8.0	8.5	0.5	-	17.1	0.52	0.50	3.11	30528				345	25586	1134	809	24655	1126	0.04	3.02	0.14	0.09	2.91	0.14	0.053	0.110	0.1116	47.78	1.4749
										BED DEPTH		5.0 cm																		
Cu-ZSM-5										BED VOLUME		2.5 cm^3																		
126	205	4.1	4.4	0.3	-	8.8	0.51	0.50	3.18	12605	SPACE VELOCITY (1/hr)			379	23647	965	616	23776	1048	0.04	2.79	0.12	0.07	2.81	0.13	0.027	-	0.116	4.8258	2.0921
127	246	4.1	4.4	0.3	-	8.8	0.51	0.50	3.18	12605				379	23647	965	938	23532	1082	0.04	2.79	0.12	0.11	2.78	0.14	0.064	0.014	0.116	11.382	1.9268
128	304	4.1	4.4	0.3	-	8.8	0.51	0.50	3.18	12605				379	23647	965	3156	23426	613	0.04	2.79	0.12	0.36	2.77	0.08	0.319	0.026	0.116	56.546	1.7331
129	304	7.3	9.0	0.5	-	16.8	0.48	0.53	3.03	24093				-	-	-	2079	23779	800	-	-	-	0.24	2.81	0.10	0.239	-	0.116	80.914	1.7331
130	359	7.3	9.0	0.5	-	16.8	0.48	0.53	3.03	24093				-	-	-	4044	23405	281	-	-	-	0.46	2.77	0.04	0.464	-	0.116	157.39	1.5823
131	401	7.3	9.0	0.5	-	16.8	0.48	0.53	3.03	24093				-	-	-	4128	23079	435	-	-	-	0.47	2.73	0.05	0.474	-	0.116	160.66	1.4837
132	281	14.4	18.6	1.0	-	34.0	0.47	0.55	2.91	48687				0	24436	1227	590	22886	1155	0.00	2.89	0.15	0.07	2.70	0.14	0.068	0.183	0.116	46.403	1.8051
133	356	14.4	18.6	1.0	-	34.0	0.47	0.55	2.91	48687				0	24436	1227	2463	22415	744	0.00	2.89	0.15	0.28	2.65	0.09	0.283	0.239	0.116	193.71	1.5898
134	355	20.5	25.8	1.4	-	47.7	0.47	0.54	2.98	68297				0	24505	1102	1879	22001	887	0.00	2.90	0.14	0.22	2.60	0.11	0.216	0.296	0.116	207.3	1.5924
135	421	20.8	26.7	1.4	-	49.0	0.47	0.55	2.84	70130				0	23794	1309	3653	21019	668	0.00	2.81	0.16	0.42	2.48	0.08	0.419	0.328	0.116	413.84	1.4409
																										NH3 bal:0.43%				
										BED DEPTH		2.5 cm																		
CuO/FILTER										BED VOLUME		1.3 cm^3																		
136	520	7.7	8.9	0.5	-	17.2	0.50	0.52	2.97	49188	SPACE VELOCITY (1/hr)			-	-	-	1114	21485	1116	-	-	-	0.13	2.54	0.14	0.128	-	0.212	54.374	1.261
137	253	3.1	4.3	0.3	-	7.7	0.44	0.56	3.88	22173				-	-	-	396	29102	877	-	-	-	0.05	3.44	0.11	0.045	-	0.212	8.713	1.9011
138	316	3.1	4.3	0.3	-	7.7	0.44	0.56	3.88	22173				-	-	-	458	30072	1206	-	-	-	0.05	3.55	0.15	0.053	-	0.212	10.077	1.6978
139	404	3.1	4.3	0.3	-	7.7	0.44	0.56	3.88	22173				-	-	-	1190	29611	1031	-	-	-	0.14	3.50	0.13	0.137	-	0.212	26.183	1.4771
140	456	3.1	4.3	0.3	-	7.7	0.44	0.56	3.88	22173				-	-	-	2477	28226	685	-	-	-	0.28	3.34	0.09	0.284	-	0.212	54.5	1.3717
141	521	3.1	4.3	0.3	-	7.7	0.44	0.56	3.88	22173				-	-	-	3588	27842	582	-	-	-	0.41	3.29	0.07	0.412	-	0.212	78.945	1.2594

Table A5.3 Calculation of activation energies for reaction over Cu-ZSM-5 and CuO

CuO ON SILICALITE

RUN #	ln(1000*TOF)	1000/T
114	5.404	1.25
115	3.034	1.79
116	3.765	1.61
117	4.231	1.51
119	4.842	1.37

Regression Output:

Constant		10.9849
Std Err of Y Est		0.03741
R Squared		0.99876
No. of Observations		5
Degrees of Freedom		3
No. of Observations		5
X Coefficient(s)	-4.47104	3
Std Err of Coef.	0.09078	

CALCULATION OF Ea:

-4.47104*-8.314*1000 = 37172 J/mol

8.9 kcal/mol

Cu-ZSM-5

RUN #	ln(1000*TOF)	1000/T
126	1.574	2.09
127	2.432	1.93
128	4.035	1.73
129	4.393	1.73
130	5.059	1.58
132	3.837	1.81
133	5.266	1.59
134	5.334	1.59
135	6.025	1.44

Regression Output:

Constant		16.555
Std Err of Y Est		0.21938
R Squared		0.97984
No. of Observations		9
Degrees of Freedom		7
X Coefficient(s)	-7.16586	
Std Err of Coef.	0.38853	

CALCULATION OF Ea:

-7.16586*-8.314*1000 = 59577 J/mol

14.2 kcal/mol

CuO-FILTER

RUN #	ln(1000*TOF)	1000/T
138	2.310	1.70
139	3.265	1.48
141	4.369	1.26

Regression Output:

Constant		10.2547
Std Err of Y Est		0.06655
R Squared		0.99791
No. of Observations		3
Degrees of Freedom		1
X Coefficient(s)	-4.69515	
Std Err of Coef.	0.21472	

CALCULATION OF Ea:

-4.69515*-8.314*1000 = 39035 J/mol

9.3 kcal/mol